CONTRIBUTION OF SOIL WATER AND GROUNDWATER TOWARDS TRANSPIRATION OF TREE SPECIES IN THE GHAAP PLATEAU

by

CINISANI MFAN'FIKILE TFWALA

A thesis submitted in accordance with the requirements for the degree of

Doctor of Philosophy

Faculty of Natural and Agricultural Sciences

Department of Soil, Crop and Climate Sciences

University of the Free State

Bloemfontein, South Africa

Promoter: Prof. L. D. van Rensburg

Co-promoter: Dr P.C. Zietsman

June, 2018

TABLE OF CONTENTS

LIST OF TABLES

LIST OF FIGURES

DECLARATION

I declare that the thesis hereby submitted by me for the degree of Doctor of Philosophy at the University of the Free State is my own independent work and has not been previously submitted by me at another University or Faculty. I furthermore cede copyright of the thesis in favour of the University of the Free State.

Cinisani M. Tfwala

Signature……

Date: June, 2018

Place: Bloemfontein, South Africa.

ACKNOWLEDGEMENTS

- First and foremost, I thank God for the opportunity and ability to undertake my studies up to this level. It is surely by His grace. To Him be all the glory.
- My heartfelt gratitude goes to my promoter, Professor L. D. van Rensburg for patiently and diligently guiding me throughout the study period. I could not ask for better.
- My co-promoter Dr P.C. Zietsman for your readiness to help and guidance is appreciated.
- Professor C.C. du Preez and all staff in the Soil Crop and Climate Sciences Department, especially Mrs R. Van Heerden, Dr J. van Tol, Dr J. Barnard, E. Yokwane, G. Madito, S. Van Stade, C. Kotoyi, D. Wessels, V. van Straaten, N. Badenhorst, D. Olivier and F. Scheepers, are thanked for all forms of assistance provided.
- Special thanks to: Professor R. Schall, Dr Z. Bello, Dr P. Dlamini, Dr G. Bosman, Dr S. Mosea, N. Radebe, K. Makhanya, L. van Westhuizen, P. Tharaga, A. Mengistu, N. Els, Dr B. Kuenene, Dr A. Van Aardt, B. Mabuza, Dr W. Tesfuhuney, Dr S. Mavimbela, N. Mjanyelwa, J. Dlamini, R. Masvodza, O. Chichongue, I. Gura, J. Edeh and A. Bothma for their valuable inputs.
- Kolomela Mine is greatly acknowledged for funding my studies and provision of field experiment sites. Mr I. Gous and the entire environment section team at Kolomela Mine are thanked for their assistance during experimental field work.
- The South African Weather Services for providing us with weather data and the South African Agricultural Research Council for ETo information.
- Hydra Sensor Technologies International Ltd is acknowledged for supplying the HydraSCOUT capacitance probes used in this research.

- The Electronics Department of the University of the Free State is acknowledged for setting up the lysimeter facility at Kenilworth Experiment Farm.
- I thank the Government of Swaziland for granting me study leave to pursue my studies.
- Special thanks to my colleagues at the Department of Agricultural Research and Specialists Services of the Ministry of Agriculture for their support and encouragement.
- My wife Gugu, my daughters Siyandiswa and Sinenkhosi, you have always been my source of inspiration.
- Entire family members, especially my grandmother and my father who unfortunately are both late, my sisters and brothers for the continuous support and encouragement through my entire academic journey. You all have been the best.

NOTIFICATION

The chapters of this thesis are presented as stand-alone publications. Each chapter comprises a specific experiment related to the main objective of the study. Repetitions, especially on the literature reviews may occur since there is no section on the general literature search. Chapter 3, Chapter 4 and Chapter 7 are already published in Physics and Chemistry of the Earth (doi:org/10.1016/j.pce.2018.09.003), Climate Risk Management (doi:org/10.1016/j.crm.2017.04.004) and Agricultural Water Management (doi:org/10.1016/j.agwat.2018.01.005) journals, respectively. Chapter 6 has been accepted for puplication in Pedosphere.

LIST OF ABBREVIATIONS

AE	absolute error
AI	aridity index
ARC	Agricultural Research Council
AW	available water
BCI	Bayesian credibility intervals
BP	base plate
CHPV	compensation heat pulse velocity
DAI	drought area index
DBH	diameter at breast height
DLL	drained lower limit
DUL	drained upper limit
ENSO	El Niño Southern Oscillation
ET	evapotranspiration
FDR	frequency domain reflectometry
GD	Gumbel distribution
GEV	generalized extreme value
HS	HydraSCOUT
IDF	intensity-duration-frequency
IPCC	International Panel on Climate Change
LD	lower door
LS	lower segment
MAE	mean absolute error
MAP	mean annual precipitation
MAT	mean annual air temperature
MBE	mean bias error
MDI	maximal data information
NW	North-west
PDSI	Palmer drought severity index
RAI	rainfall anomaly index

RMSE	root mean squared error
SAR	sodiun adsorbtion ratio
SAWS	South African Weather Services
SD	standard deviation
SE	standard error
SPEI	standardized precipitation-evapotranspiration index
SPI	standardized precipitation index
TDP	thermal dissipation probe
TDR	time domain reflectometry
THD	thermal heat dissipation
UD	upper door
US	upper segment

ABSTRACT

Transpiration (T) by trees is a major route through which water from soils and groundwater aquifers re-enter the hydrologic cycle. It is therefore crucial to accurately quantify tree water use, with a full understanding of their environmental conditions, especially under the context of climate change. The ultimate aim of this study was to quantify T for selected indigenous tree species in an arid environment dominated by mining activities, and further partition it into soil water and groundwater. This involved a series of studies including a global review of whole tree water use, precipitation analysis, methods and instruments validation experiments prior to lysimeter and field tree T measurements.

A meta-analysis was carried out on published whole tree water use studies with the aim of assessing the effects of morphological traits [height (H) and stem diameter at breast height (DBH)] and environmental controls [mean annual precipitation (MAP), mean annual air temperature (MAT) and elevation above sea level (Z)] on tree T at global scale. The study also aimed to analyse the techniques used for T measurement. The study revealed that log transformed T (ln T) was positively and significantly correlated with H ($r_s = 0.55$) and DBH ($r_s = 0.62$) at $P < 0.1$. A weak positive correlation was also found between ln T and MAP ($r_s = 0.16$) at $P < 0.1$. The results further showed that 82% of the studies published during the period (1970 to 2016), used thermodynamic methods to measure T. It was concluded that the physiological traits play a pivotal role in whole tree water use, and hence should be incorporated in modelling T in forest ecosystems.

Long-term precipitation data (1918-2014) was analysed with the aim of i) understanding the occurrence, severity and duration of droughts, ii) getting insights of the interannual variability of precipitation and iii) estimating precipitation intensities and their uncertainties for a range of

storm durations (0.125-6 hrs) and return periods (2-100 years). Calculation of the Standardized Precipitation Index (SPI) showed that more droughts, which lasted for at most 2 years, occurred since the 1990s; these were all moderate droughts with SPI between -1.03 and -1.46, except for the 1992 drought at Groblershoop which was severe (SPI = 1.74). Fitting of the precipitation data to a non-parametric spline smoother revealed that the total annual rainfall followed a secular pattern of fluctuations over the years, while the number of rainfall days and extreme rainfall events were essentially stable. Using the Generalized Extreme Value (GEV) distribution, the estimated extreme precipitation intensities for the plateau ranged from 4.2 mm hr^{-1} for 6 hours storm duration to 55.8 mm hr^{-1} for 0.125 hours at 2 years return period. At 100 year return period, the intensity ranged from 13.3 mm hr^{-1} for 6 hours duration to 175.5 mm hr^{-1} for the duration of 0.125 hours. The uncertainty ranged from 11.7% at 2 years return period to 58.4% at 100 years return period. These results can be integrated into policy formulation for the design of ecosystem water balance management as well as stormwater and flood management infrastructures.

A procedure of transplanting grown trees into lysimeters to study their water use was developed and implemented on four indigenous trees (*Vachelia karoo, Olea Africana, Sersia lancea* and *Ziziphus mucronata*). These trees were sampled together with 1.2 m^3 soil monolith using the locally designed sampler. Three years after transplanting, the water use ranged between 7 and 14 L day^{-1}, which was within the range for other similar trees of the same size growing under natural conditions. Accompanying this transplanting were calibrations of a newly developed HydraSCOUT (HS) capacitance soil water measuring probe and the compensation heat pulse velocity (CHPV) sap flow measurement technique. For the HS probe, the aim was to compare laboratory and field developed calibration equations for the estimation of volumetric soil water

content (θv) on the soils of the tree sampling sites. Laboratory equations estimated θv better (RMSE=0.001 m^3 m^{-3} - 0.015 m^3 m^{-3}) than field calibration equations (RMSE=0.004 m^3 m^{-3} - 0.026 m^3 m^{-3}). The HS probe was confirmed as a good candidate for θv measurement. Against pre-calibrated loadcells, the accuracy of the CHPV technique to estimate water use of the sampled trees was established. Good agreement indices between CHPV and load cells were obtained across species (D = 0.778-1.000, RMSE = 0.001-0.017 L hr^{-1}, MAE < 0.001 L hr^{-1} and MBE = -0.0007-0.0008 L hr^{-1}). It was concluded that the CHPV method can accurately measure tree water use, and therefore can be useful for water resources management in forested areas.

The total T of the trees in the lysimeters measured by the CHPV method was partitioned into groundwater and soil water using a water balance approach. The daily soil water depletion was measured using the HS capacitance probe while the groundwater depletion was measured from a graduated water supply bucket. The contribution of groundwater towards T amongst all the investigated trees ranged from 31% when the top soil was wet to 97% when the top soil was dry. The contribution of soil water ranged from 3% when the top soil was dry to 69% soon after irrigation. It was concluded that trees switch to source water from different pools depending on availability. The water balance approach was shown to be a good method for determining the water source for trees.

Field experiments were conducted in the arid Northern Cape Province of South Africa and aimed to i) assess the trends of T for selected tree species (*Vachellia erioloba, Vachellia karoo, Boscia albitrunca* and *Z. mucronata*) across a range of soil water content conditions and ii) partition the total T of the selected tree species into soil water and groundwater. The soil water content within the upper 0.5 m soil profile ranged from 11 mm during the dry season to 20 mm during the wet season, and was monitored using DFM capacitance probes. The deeper soil layer (0.5-1.2 m) was

generally wetter compared to the top layer with water content of up to >30 mm during the wet season. Measured using the CHPV method, the water use ranged from 6 L day^{-1} on *Z. mucronata* during the dry season to 125 L day^{-1} on *V. erioloba* in summer. The largest (diameter at breast height = 460 mm) *V. erioloba* tree in the experiment was not responsive to seasonal variations of soil water availability as it constantly used about 80 L day^{-1} throughout the year. Diurnal patterns of water use did not cause any concurrent changes on the soil water depletions within the top 1.2 m soil profile, which indicated that the trees sourced water from deeper pools. It was concluded that the water use of trees was inclined to the seasonal variations, which however was not the case in old trees. Almost all the water transpired by trees in the study area was sourced from groundwater reserves. It was recommended that tree water use studies should be extended to other species for comprehensive catchment tree water use calculations to inform water budgets.

Keywords: global whole tree water use, precipitation analysis, tree transplanting procedure, HydraScout capacitance probe calibration, compensation heat pulse velocity calibration, groundwater transpiration, soil water transpiration, tree water use in arid environments

1. Main introduction

1.1 Motivation

Water is the most significant natural resource on earth. Evapotranspiration (ET) from forests, groundwater fluxes and streamflows are key factors influencing the water cycle (Evaristo et al., 2015). The transpiration (T) component of ET, especially from forests contributes significantly to the flux of water from the earth's surface to the atmosphere (Dawson, 1996). At the core of ecohydrological (ecology and hydrology) investigations is the notion of the interdependent interactions between vegetation and the environment (Newman et al., 2006). Ascertaining the temporal and spatial variations of key components of these interactions such as precipitation, groundwater fluxes and vegetation are necessary for management of water resources, especially to meet food and fibre requirements for the ever increasing human population (FAO, 2002).

According to the International Panel on Climate Change (IPCC), the amount, duration and distribution of precipitation is expected to vary going into the 21st century (IPCC, 2014). Impacts of these climatic changes are expected to be worse in fragile water limited environments where the occurrence of precipitation is highly erratic (Zhou et al., 2013). The present study area (Kolomela mine) falls within the arid climatic classification (Thornthwaite, 1948). Groundwater recharge from precipitation in arid areas ranges from 1-5 mm yr^{-1} (De Vries et al., 2000), yet deep rooted trees also source water from the saturated zone (Canadell et al., 1996; Zhou et al., 2013), which means that the net groundwater recharge by precipitation might even be smaller. On the vegetation, changes induced mainly by development across the globe are extremely rapid. For instance, Myers (1993) reported global deforestation at rates of up to 30 ha per minute. These alterations are in turn significant on the global water flux via T. Even though the interactions of various disciplines within the earth and biological sciences have been studied for many years, our understanding of the

interdependencies of the disciplines is far from complete. For accurate quantification of the variations within each of the components and effects on other components, acquisition of observational and experimental data sets is required; which in turn requires suitable methods and techniques of measurement to collect such data.

Sap flow techniques have been used to determine tree water use by many researchers (Swanson and Whitfield, 1981; Grainier, 1987; Green et al., 2003). However, sap flow methods do not determine the source of water used by the trees. The source of water is mainly determined through analysis of the relationships of stable isotopes of hydrogen and/or oxygen from plant tissues and the different sources (Graig, 1961; Dawson and Ehleringer, 1991; Shadwell and February, 2017). However, this requires expensive laboratory equipments which are not available in many laboratories in South Africa, and also involves complicated procedures. Soil water content measurements have also been widely used to establish plant water use (Hillel, 1998). In the present study, a combination of continuous transpiration and soil water content measurements were employed to comprehend the water use patterns of selected dominant tree species. This was preceded by a series of studies including an overview of previous global tree water use, local climate (precipitation) analysis and preparatory studies on calibrations of instruments for soil water content measurements and the compensation heat pulse velocity (CHPV) sap flow measurement equipment.

In addition to the fact that the present study area is arid, which makes it more vulnerable to the effects of climate change (Zhou et al., 2013); the major economic activity in the area and surroundings is open cast mining. Open cast mining exerts an undesirable effect on the environment as it normally requires a constant drawdown of the water table. The depression of the water table is not limited to the centre of operation but may extend to several kilometres outwards (Libisci et al., 1982). To fully understand the effects of the continuous drawdown of groundwater within the study area and put in place adequate mitigation

measures, it is imperative to quantify specific hydrological processes such as tree transpiration and determine their dependence on groundwater reserves. This is especially so in areas such as the present study area where endangered and protected trees such as *Vachellia erioloba* (formerly *Acacia erioloba*) and *Bocia albitrunca* (National Forest Act, 1998) form part of the dominant tree species.

1.2 Objectives

The main objective of the study was to determine the amounts of groundwater and soil water that contribute to meet the total transpiration requirements of trees across the year. This objective was achieved through a series of independent, but overarching studies with specific objectives as outlined below.

Chapter 2: "**Global whole tree water use: effects of tree morphology and environment"**

Objective: A desktop study was conducted to;

i) assess the influence of tree size (height (H), stem diameter at breast height (DBH) ≈ 1.5 m from the ground), mean annual precipitation (MAP), mean annual air temperature (MAT) and elevation above sea level (Z) on tree transpiration at the global scale.

ii) establish the trends of tree transpiration measurement techniques.

Chapter 3: "**Drought dynamics and interannual rainfall variability on the Ghaap plateau, South Africa, 1918-2014"**

Objective: A desktop study was conducted to determine the occurrence and severity of droughts and interannual rainfall variability trends in the Ghaap plateau, Northern Cape Province, South Africa.

Chapter 4: "Precipitation intensity-duration-frequency curves and their uncertainties for Ghaap plateau"

Objective: A desktop study was conducted to estimate the precipitation intensities and their uncertainties (lower and upper limits) for durations of 0.125, 0.25, 0.5, 1, 2, 4 and 6 hrs and return periods of 2, 10, 25, 50 and 100 years in the Ghaap plateau, Northern Cape Province, South Africa using the Generalized Extreme Value (GEV) distribution.

Chapter 5: "**A new *in situ* procedure for sampling indigenous tree – soil monoliths to study water use in lysimeters"**

Objective: to develop a procedure for sampling already grown trees for water use analysis in lysimeters.

Chapter 6: "**Laboratory versus field calibration of HydraSCOUT probes for soil water measurement"**

Objectives:

i) to develop calibration equations for the HydraSCOUT probe for selected soils under laboratory and field conditions.

ii) to evaluate the performance of both sets of calibration equations for estimating volumetric soil water content for the selected soil types.

Chapter 7: "**Calibration of heat pulse velocity technique for measuring transpiration of selected indigenous trees of South Africa"**

Objective: to evaluate the accuracy of the CHPV method in quantifying tree transpiration for selected tree species.

Chapter 8: A soil water balance approach to partition tree transpiration into soil water and groundwater

Objective: to partition transpiration of indigenous trees under shallow water table conditions into groundwater and soil water using the water balance approach.

Chapter 9: "**Transpiration dynamics and water sources for selected indigenous trees under varying soil water content"**

Objectives:

i) to assess the trends of transpiration for selected tree species across a range of soil water content conditions and

ii) to partition the total transpiration of the selected tree species growing in arid environments dominated by open cast mining activities into soil water and groundwater.

1.3 Background of selected tree species

The reclaiming of soil fertility and the general productivity of land in Africa has been one of the major challenges for sustaining land productivity. This problem has been particularly on the extreme in the arid and semi-arid areas of the continent, where the exotic tree species used to revitalize lands in the high rainfall areas have been unsuccessful. The management and cultivation of indigenous trees has been viewed as a key solution for the low rainfall areas (Barnes et al., 1997). This calls for intensified efforts towards research on prominent indigenous trees in different localities. A brief description of each of the trees which were investigated in this study, whose images are shown in Figure 1.1, and their characteristics and uses summarised in Table 1.1, is as follows:

1.3.1. Camel thorn

Camel thorn (*V. erioloba*), formerly known as *A. erioloba,* is an African species and is under the very large acacia genus. The name camel thorn was a mistranslation of the tree's Afrikaans name "kameeldoring" which means giraffe thorn. To emphasize the originality and spread of the tree in the Southern African region, camel thorn has local names in many languages of the region; mpatsaka (Sotho), mokala (Tswana), kameeldoring (Afrikaans), camel thorn (English), umwhohlo (Ndebele) and mogohlo (Sepedi) among many other vernacular names (Barnes et al., 1997; Seymour and Milton, 2003).

Camel thorn, sometimes referred to as the "king of trees" or "keystone tree" in the desert, is commonly a habitant of deep sandy soils in arid to semi-arid environments and is the typical tree species of the dry Kalahari (Steenkamp et al., 2008). The major adaptive mechanism of camel thorn to such environments is through its extensive root system, with a maximum depth of up to 60 m, which enables the tree to source water from deeper reserves (Canadell et al., 1996; Smit, 1999; Seymour and Milton, 2003). Literature reveals that camel thorn can live for as long as between 250 and 300 years (Barnes et al., 1997; Seymour and Milton, 2003).

1.3.2 Black karee

The black karee tree (*Sersia (Rhus) lancea*) is also called bastard willow or karoo tree in English; umhlakotshane in Xhosa; karee, rooikaree or taaibos in Afrikans; inhlokoshiyane in Zulu and mothlothlo, mokalabata or mohlwehlwe in N. Sotho. The tree grows in a wide variety of habitats, but favours rivers and streams.

1.3.3 Buffalo thorn

Buffalo thorn (*Ziziphus mucronata*) is also called buffelsdoring in Afrikaans, umphafa in Xhosa, umphafa, umlahlankosi, or isilahla in Zulu, umlahlabantfu in Swati, mphasamhala in Tsonga, mokgalo in Tswana, mokgalô in N. Sotho and mutshetshete in Venda (Immelman et al., 1973). The tree grows in a variety of habitats, from deserts to forests. Buffalo thorn is also richly known for cultural beliefs. The Zulu people refer to it as the 'Tree of Life' with the zigzag pattern of the branches representing one's journey through life, and the straight and hooked thorns representing the decisions which one has to make at crossroads.

1.3.4 Sweet thorn

Sweet thorn (*Vachelia karoo*) is one of the common acacia species in the Southern part of Africa. The tree has been named several times before being given the current name. In 1768, it was named *Mimosa nilotica*, and the most recent two names are *Acacia incoflagrabilis* and *Acacia natalitia*. The tree also has an array of local names in the region some of which include; soetdoring (Afrikaans) umnga (Xhosa) umunga (Zulu, Shangane and Venda), mooka (Sotho), mukana, moshawoka (Tswana) and mooka, mookana (N. Sotho). The tree is widely distributed across South Africa and extends towards the south more than any of the acacia species (Immelman et al., 1973; Carr, 1976).

1.3.5 Shepherd's tree

The shepherd's tree (*Bocia albitrunca*) is also called white stem in English, witgatboom, witstam and matoppie in Afrikaans, umfithi in Zulu, motlopi in Tswana, mohlopi in N. Sotho and muhvombwe in Venda (Immelman et al., 1973). The tree is usually found in hot, dry woodland and bushveld in rocky or sandy places. The tree has many uses and as such has

itself the title as ‘tree of life’ especially for people living in dry areas. Local culture forbids its destruction in such areas.

1.3.6 Wild olive

Wild olive (*Olea europaea* subsp. *africana*) is also called olienhout in Afrikaans, mohlware in N. Sotho and S. Sotho, umnquma in Zulu, Xhosa and Swati, mutlhwari in Venda and motlhware in Tswana. The tree is distributed all over Africa and also found in Mascarene Islands, Arabia, India and China. The wide distribution is accounted for by its adaptation to a variety of habitats from near river banks to woodlands and rocky hilltops. The tree is hardy to drought and also very tolerant to frost conditions (Immelman et al., 1973). The tree is protected by law in the North West, the Northern Cape and Free State provinces of South Africa.

Vachelia erioloba (Camel thorn)

Bocia albitrunca (Shepherd's tree)

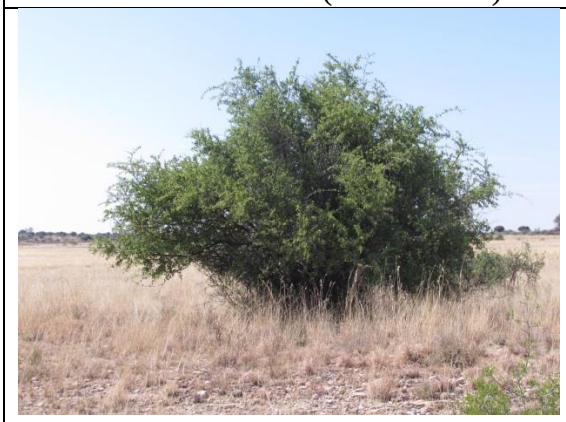

Ziziphus mucronata (Buffalo thorn)

Vachelia karoo (Sweet thorn)

Sersia lancea (Black karee)

Olea Africana (Wild olive)

Figure 1.1: Images of all tree species used in the thesis

Table 1.1: Descriptive characteristics and uses of trees investigated in the study

Descriptive parameter	**Tree name**					
	Camel thorn	Black karee	Buffalo thorn	Sweet thorn	Shepherd's tree	Wild olive
Max. height (m)	18	9	9	10	11	9
Crown	Rounded when young and umbrella shaped on old trees	Rounded	Dense and rounded	Rounded	Compact and flat topped	Dense and spreading
Stem and branches	Single stem and sometimes split at low levels.	Single and branches very low to many thin branches.	Single or multiple with dropping distinctly zigzag branches. Thorns occur in pairs at nodes, one straight and the other hooked.	Single and branch clear off the ground. White or grey thorns, reddened or darkened at apecies and about 40 mm long, occur in pairs at right angles at the nodes.	Single, sturdy and usually crooked and have cavities.	Single and braches very low.
Bark	Grey, grey-brown to blackish with longitudinal fissures.	Dark brown and rough, but young branches are red brown.	Grey with thin fissures in an untidy pattern.	Dark brown to black with rough fissures, but powdery-rusty red when young.	Greyish-white or greenish-yellow	Grey and rough, sometimes peeling off in strips.
Leaves	1 – 7 leaves originate from nodes, petioles are 4 mm long, 1-5 pinna pairs with 16-18 bluish-green leaflet pairs.	Trifoliate, finger-like leaflets on alternate sides of branches. Longest leaflet is about 120 mm. Dark olive-green but paler beneath.	Alternate on sides of branches. Dark-green and glossy but duller beneath. Have 3 veins originating from base.	2-6 pairs of pinna each with 8-20 pairs of pinnules. Dark-green on both sides.	Alternate on sides of branchlets or older wood. Small and narrow, 30-50 mm long, greyish-green with leathery texture.	Grey-green to dark green leaves and silvery or greyish beneath. Narrowly oblong to elliptic and 30-80 mm long.
Flowers	Deep yellow and sweet scented, 45-50 mm long and 10-16 mm wide.	Pale yellow, star-shaped and clustered at ends branchlets and axils of upper leaves.	Yellow-green, tiny, star-like and clustered at axils of leaf stalks.	Bright yellow, sweet scented and grouped at ends of branches. 20 mm wide.	Small, yellowish, star-shaped and heavily scented forming on old wood.	Creamy-white, light scented formed at terminal heads.
Fruits	Pods are sickle	Bunch together like	Yellowish or shiny	Brown pods,	Round, leathery textured,	Spherical, thinly

	shaped, tapered at base with rounded apex. Pods can be 150 mm long, 50 mm wide and 15 mm thick.	grapes, pale green and ripen to yellow brown. Oval shaped and 5 mm in diameter.	red berries, 12 to 20 mm in diameter.	sickle shaped and somehow constricted between seeds. Up to 150 mm long.	green and ripen to yellowish. 10 mm in diameter.	fleshed fruits, purple to black when ripe and 8-10 mm diameter.
Uses	Heartwood provides timber for builing material, fencing and firewood. Leaves, young shoots, flowers and pods are good fooder. Ground pods can make porridge. Seeds can make coffee. Decoction of barks and roots can cure coughs and colds, diarrhea and nose bleeding.	Wood is used for fencing posts, pick and other implements handles, tobacco-pipe bowls and bushman bowls. Bark is used for tanning leather. Leaves can be browsed by animals. Fruits eaten by birds and can maked brew. Tree provides shade in lawns	Leaves and fruits are feed for animals and food for humans. Seeds can make coffee. Used by some African tribes to fetch spirits of people who die away from home. Planted on graves to protect them from animals. Bushmen use sap to make poison for their arrows.	Wood used mainly for firewood and charcoal. Gum used for making glue. Leaves and pods are fodder for animals.	Roots can be used as coffee, boiled to extract sweet syrup, dried and prounded to make porridge and sweet milk or consumed fresh. Roots also have pervasive properties for other foods such as citrus. Leaves are good fodder for animals. Decoction of roots can cure heamorrhoids while fruits can cure epilepsy	Attractive timber for furniture, cabinet work, trinkets and turnery. Wood can also be used for fencing and firewood. Leaves can make tea, eye medican for humans and animals, cure sore throat and provide fodder for animals. Fruits are a favourite for birds, baboons and other animals. Tree used for shade in lawns

References

Barnes, R.D., Fagg, C.W., Milton, S.J., 1997. *Acacia erioloba*, Monograph and Annotated Bibliography, Forestry Papers, 35, Forestry Institute, Oxford.

Canadell, J., Jackson, R.B., Ehleringer, J.R., Mooney, H.A., Sala, O.E., Schulze, E.D., 1996. Maximum rooting depth of vegetation types at the global scale. Oecologia 108, 583-595.

Carr, J.D., 1976. The South African Acacias, Conservation Press (PTY) LTD, Johannesburg, South Africa.

Dawson, T.E., 1996. Determining water use by trees and forests from isotopic, energy balance and transpiration analyses: the roles of tree size and hydraulic lift. Tree Physiol. 16, 263-272.

Dawson, T.E., Ehleringer, J.R., 1991. Streamside trees that do not use stream water. Nature 350(6316), 335-337.

De Vries, J.J., Selaolo, E.T., Beekman, H.E., 2000. Groundwater recharge in the Kalahari, with reference to paleo-hydrologic conditions. J. Hydrol. 38, 110-123.

Evaristo, J., Jasechko, S., McDonnell, J.J., 2015. Global separation of plant transpiration from groundwater and streamflow. Nature 525(7567), 91-101.

FAO, 2002. Irrigation Manual - Planning, Development, Monitoring and Evaluation of Irrigated Agriculture with Farmer Participation, Vol 1, Module 1- 6.

Craig, H., 1961. Isotopic variations in meteoric waters. Science 133(3465), 1702-1703.

Granier A (1987) Evaluation of transpiration in a Douglas-fir stand by means of sap flow measurements. Tree Physiol. 3, 309-320.

Green, S., Clothier, B., Jardine, B., 2003. Theory and practical application of heat pulse to measure sap flow. Agron. J. 95, 1371-1379.

Hillel, D. 1998. Environmental Soil Physics, Academic Press, San Diego, USA.

Immelman, W.F.E., Wicht, C.L., Ackerman, D.P., 1973. Our Green Herritage: The South African Book of Trees, Tarfelberg and Nasionale Boekhandel (Publishers) Ltd., London.

IPCC, 2014. *Climate Change 2014: Synthesis Report. Contribution of Working Groups I, II and III to the Fifth Assessment Report of the Intergovernmental Panel on Climate Change* [Core Writing Team, R.K. Pachauri and L.A. Meyer (eds.)]. IPCC, Geneva, Switzerland.

Libicki, J., 1982. Changes in the groundwater due to mining. Int, J. Mine Water 1, 25-30.

Myers, N., 1993. Population, environment and development. Environ. Conserv. 20, 205-216.

National Forest Act, 1998. Pretoria, South Africa.

Newman, B.D., Wilcox, B.P., Archer, S.R., Breshears, D.D., Dahm, C.N., Duffy C.J., McDowell, N.G., Phillips, F.M., 2006. Ecohydrology of water-limited environments: A scientific vision. Water Resour. Res. 42, 1-15.

Seymour, C., Milton, S., 2003. A collation and overview of research on *Acacia erioloba* (Camel Thorn) and identification of relevant research gaps to inform protection of the species. Department of water affairs and forestry.

Shadwell, E., February, E., 2017. Effects of groundwater abstraction on two keystone tree species in an arid savanna national park. PeerJ *5*, e2923.

Smit, N., 1999. Guide to the Acacias of South Africa, Bizara Publications, Pretoria, South Africa.

Steenkamp, C.J., Vokel, J.C., Fuls, A., van Royen, N., van Rooyen, M.W., 2008. Age determination of *Acacia erioloba* trees in the Kalahari. J. Arid Environ. 72, 302-313.

Swanson, R.H., Whitfield, D.W.A., 1981. A numerical analysis of heat pulse velocity theory and practice. J. Exp. Bot. 32(126), 221-239.

Thornthwaite, C.W., 1948. An approach toward rational classification of climate. Geogr. Rev. 38(1), 55-94.

Zhou, Y., Wenninger, J., Yang, Z., Yin, L., Huang, J., Hou, L., Wang, X., Zhang, D., Uhlenbrook, S., 2013. Groundwater-surface water interactions, vegetation dependencies and implications for water resources management in the semi-arid Hailiutu River catchment, China – synthesis. Hydrol. Earth Syst. Sc. 17, 2435-2447.

2. Global whole tree water use: effects of tree morphology and environmental factors

Abstract

Although tree transpiration (T) studies across multiple spatial scales have been conducted, the global synthesis of the driving factors of tree water use, especially for a variety of species under different climatic conditions has not yet been made. This paper analyses T data from 93 published studies conducted in globally distributed sites between 1970 and 2016, representing 196 data points to seek relations between morphological traits; tree height (H), diameter at breast height (DBH) and environmental factors; mean annual precipitation (MAP), mean annual temperature (MAT) and altitude (Z) on whole tree water use for 130 species of trees. Techniques used in the studies for T measurement were also analysed. Log transformed T (ln T) varied between 0 and 7.1 L day^{-1}. Univariate correlation and regression analysis revealed that ln T was positively and significantly correlated with H ($r_s = 0.55$) and DBH ($r_s = 0.62$) at $P < 0.1$. A weak positive correlation was found between ln T and MAP ($r_s = 0.16$) at $P < 0.1$. The results further showed that during the study period (1970 to 2016), 82% of the studies used thermodynamic methods to measure T, in particular thermal heat dissipation probes were used by 60% of the studies, while 21% reported use of heat pulse velocity. The results contribute to a better understanding of T in forest ecosystems, and the factors of control to inform global scale modelling and ecosystem management. Thermodynamic methods, especially thermal heat dissipation probes and heat pulse velocity are the most prevalent techniques used for whole tree T measurement.

Keywords: tree transpiratio, tree characteristics, environmental influence, transpiration measuring techniques

2.1 Introduction

Trees of forested ecosystems, through transpiration (T), represent a major route by which water in soils and groundwater aquifers re-enter the hydrologic cycle (Dawson, 1996), and thus play an important role in terrestrial hydrology (Bond et al., 2008). The rate and magnitude of water movement along this route is influenced by where trees obtain their water, how they transport and store water, and how leaf stomata regulate water loss by the process of T (Dawson, 1996). In forests, which cover approximately one-third of the earth's land area, accounting for over two-thirds of the leaf area of plants, T generally accounts for most of the evapotranspiration (ET) (Bond et al., 2008). For example, Moreira et al., (1997) found that T was responsible for nearly all the loss in water vapour in the Amazon forest.

Transpiration is by far the largest water flux from earth's continents, representing 80 to 90 per cent of terrestrial ET. In addition, it utilizes almost half of the total solar energy absorbed by the earth's surface (Jasechko et al., 2013). This huge global flux of water vapour passes through stomatal pores on leaf surfaces and represents a fundamental ecosystem service, contributing to the global water cycle and climate regulation by cloud formation (Beerling and Franks, 2010). Whole-tree estimates of water use are becoming increasingly important in forest science (Wullschleger et al., 1998) by providing insights into the physiological regulation of water use at the stand level (Meinzer et al., 2001). The fraction of ET attributed to plant T is an important source of uncertainty in terrestrial water fluxes and land surface modelling, and demands research (Miralles et al., 2011).

The need for generating tree water use data to improve our understanding of the role played by whole tree T in forest ecosystems, and experimental difficulties accompanying large trees, were highlighted several decades ago (Weaver and Mogenson, 1919). Since then, whole tree T has

been quantified using various methods. The methods include porometers (Ansley et al., 1994), lysimeters (Knight et al., 1981), tent enclosures and ventilated chambers (Greenwood and Beresford, 1979), chemical tracers (Sansigolo and Ferraz, 1982), radioisotopes and stable isotopes (Jordan and Kline, 1977). More recent studies determine whole tree T by thermal based methods, which include heat pulse velocity (Swanson and Whitfield, 1981; Green et al., 2003), trunk segment heat balance (Smith and Allen, 1996), stem heat balance (Köcher et al., 2013), heat field deformation (Nadezhdina et al., 2010) and thermal dissipation probes (Granier, 1987). These methods are designed for different conditions and to measure transpiration of different tree sizes and wood characteristics. The merits and drawbacks of these methods are not discussed here, but technological advancement trends in tree T measurements are assessed.

While global sets of precipitation, streamflow (Malone et al., 2014) and groundwater (Jasechko et al., 2013) data are now available for analysis, measurements of plant xylem and thus water moving within plants, remain dispersed throughout primary specialist literature. Some studies have established relationships between whole tree T and tree size (Ryan et al., 2000; Meinzer et al., 2005). Even though a vast body of literature on tree T studies is available, there is no clear consensus on the significance of the key morphological traits and environmental factors of tree T, yet such information can be crucial for calculating water use of forests and managing tree populations and sizes in different environments. The main challenge is that studies of this nature are typically of small sample sizes – that is, one to a few trees in one or a few catchments and usually not replicated (Evaristo and McDonnell, 2017).

In the context of global climatic change (IPCC, 2014), which is expected to affect hydrological processes, it is crucial to account for water use trends in trees with diverse morphological traits under diverse environmental conditions. However, as opposed to the general review of literature

to draw general conclusions in a narrative form, we opted for a more objective and quantitative approach with set criteria of literature search and statistical analysis to integrate and summarize the results of the existing studies reporting tree water use. A meta-analysis was carried out on the reported whole tree water use to assess the effects of morphological traits [height (H) and stem diameter at breast height (DBH)] and environmental controls [mean annual precipitation (MAP), mean annual air temperature (MAT) and elevation above sea level (Z)] on tree T at global scale. Information on the trends of tree T measurement techniques was also compiled for the period 1970 to 2016.

2.2 Materials and Methods

2.2.1 Data collection

2.2.1.1 Literature search

A dataset on whole tree T per day was extracted from scientific articles published in international journals across the world between 1970 and 2016 (Appendix 2.1). The literature search was conducted using electronic databases including EBSCOHost web search engine, which combined the Africa Wide Information, Academic search, Cab Abstracts, eBook Collection and Green File sub-search engines, and sourced articles from bibliographic databases including Science Direct, Springerlink and JSTOR. Using the search keywords “whole tree transpiration” and “tree water use,” a total of 93 articles were identified from which 196 daily T records of 130 tree species in 31 countries were obtained.

2.2.1.2 Data extraction

From each of the studies, tree species, highest daily T (litres), T measurement method, H (m), DBH (mm), MAP (mm), MAT (°C), Z (m) and study location, were extracted. Where tree T was

measured on several trees of the same species, the records of the tree with the highest daily T was used; if the trees were located in different sites, records for all trees were captured. When the GPS coordinates of the site were not stated, Google Earth was used to determine the coordinates using the study site name. If the climatic records of the study area were not stated, they were sourced through websites including Climate-Data.org, World Weather and Climate Information, Climatedata.eu, U.S. Climatedata and ClimaTemps.com. The climatic classification developed by Köppen (1936) was adapted in the present study (Table 2.1). Z was categorised following the procedure of Hijmans (2005). Attepmts to obtain other energy and aerodynamic parameters that are usually employed to model ET and T such as radiation and vapour pressure deficit were not a success due to limitation on the availability of such datasets.

Table 2.2**:** Environmental factors affecting tree water use, and their classification

Environmental factor	**Class**	**Definition**
Mean annual precipitation (MAP)	Dry	0-600 mm
	Moist	>600-850 mm
	Humid	>850-1500 mm
	Wet	>1500 mm
Mean annual temperature (MAT)	Cool	<10 °C
	Warm	>10-20 °C
	Hot	>20 °C
Altitude (Z)	Lowlands	0-100 m
	Uplands	>100-500 m
	Highlands	>500-1000 m
	Mountainous	>1000 m

2.2.2 Data analysis

2.2.2.1 Transformation to normality of dependent variable

The dependent variable (T), was log-transformed (ln T) to achieve normality based on the optimal Box-Cox transformation (Box and Cox, 1964) prior to analysis.

2.2.2.2 Summary and descriptive statistics

Basic statistics including the minimum, maximum, mean, median, standard deviation, skewness, kurtosis, 1st and 3rd quartiles and coefficient of variation were calculated to provide insight in the variability of T with regard to each of the environmental factors (MAP, MAT and Z), tree morphological characteristics (H and DBH), and the different measurement techniques.

2.2.2.3 Univariate analysis: Scatterplots and non-parametric smoother

Scatterplots were used to present the relationship between ln T and the continuous covariates H and DBH. Furthermore, a non-parametric spline smoother was applied to the data, separately for each covariate. The degrees of freedom of the spline smoother were determined using generalized cross-validation (SAS procedure GAM) (SAS, 2013). Sigma Plot 8.0 (Systat Software Inc., Richmond, California, USA) was used to present ln T across the categorical classes of MAP, MAT and Z. **Note:** The data record with Z = 4595 m was removed from further analysis, since this single extreme data point had the potential to create a spurious correlation between ln T and Z (The next highest value of Z in the data base was Z = 2850). Linear regression was used to model the effect of single covariates on ln T. In each case, the linear regression model fitted location as a random effect, in order to account appropriately for the correlation of measurements within a given location (SAS procedure MIXED) (SAS, 2013). Spearman correlation coefficients to determine the sign and strengths of the relationships between the independent variables and ln T were computed.

2.2.2.4 Multiple regression and model selection

Multiple regression was used to assess the ability of a combination of the covariates (DBH, H, MAP, MAT and Z) to predict ln T. Again, all regression models fitted location as a random effect, while measurement method was fitted as a fixed effect (SAS procedure MIXED). Using

the collection of independent variables described above, backward model selection was performed as follows: starting with a fit of the "full model" (all covariates and method are fitted), at each selection step that variable was chosen for exclusion from the model that was least significantly associated with ln T, provided that the P-value was larger than 0.10. The backward model selection was terminated when all effects remaining in the model were significant at the 0.10 level.

The backward model selection process was carried out in two steps: first, using the data as recorded, that is, without imputation of missing values when either DBH or H was missing. Second, as a sensitivity analysis, multiple imputation was used to impute missing values of either DBH or H, when at least one of the two measurements was available. In this way, 100 data sets with imputed missing values were created (multiple imputation), using the fully conditional specification method (SAS procedure MI). Thereafter, the backward model selection process described above was repeated, at each step fitting the model in question to all 100 imputed data sets, and then combining the results from the 100 fits (SAS procedure MIANALYZE) (SAS, 2013).

2.3 Results

2.3.1 Global distribution of sites

Our data included 196 observations. Most sites were located in North America (31%), Australasia (24%) and Europe (21%), followed by Asia (14%), with only a few sites in Africa (5%) and South America (5%) (Figure 2.1).

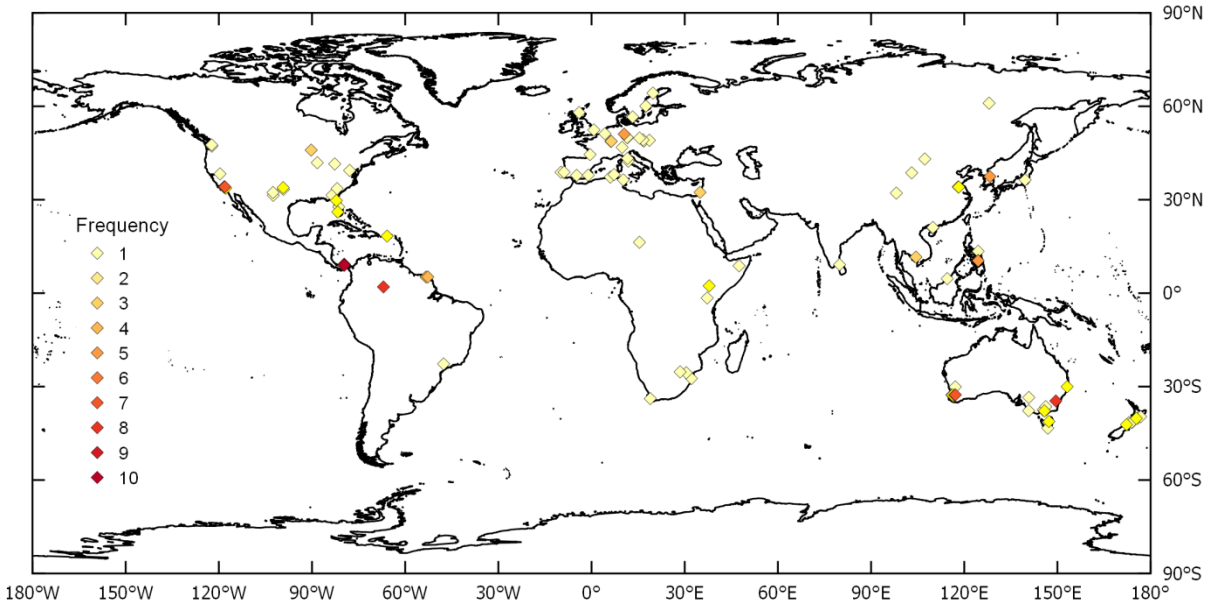

Figure 2.1**:** Location of study sites included in the literature review, and frequency of studies in different locations.

2.3.2 Transpiration and its variables

The sites encompass a wide range of environments (Table 2.2), varying in MAP (280–3500 mm), MAT (1–29 °C), and Z (1–4595 m). Basic descriptive statistics also show that ln T among trees across the world varied between 0 and 7.1 L day^{-1}. Wide ranges were also observed for H (1.5–76 m) and DBH (20–1340 mm).

Table 2.3**:** Descriptive statistics for global log transformed tree transpiration (ln T) and the transpiration variables tree height (H), stem diameter at breast height (DBH), mean annual precipitation (MAP), mean annual air temperature (MAT) and elevation above sea level (Z).

	ln T (L day^{-1})	H (m)	DBH (mm)	MAP (mm)	MAT (°C)	Z (m)
N	196	104	1250	196	196	196
Mean	3.9	20.6	340	1226	16	329
Std	1.1	13.1	230	881	7	505
CV	28	63	680	72	42	154
Min	0	1.5	20	280	1	1
Q1	3.2	12	180	600	10	58
Median	3.8	18	270	860	17	165
Q3	4.6	28	420	1582	20	351
Max	7.1	76	1340	3500	29	4595
Skew	0.01	1.38	15	1.23	0.03	4.41
Kurt	0.53	3.23	28.4	0.51	-0.75	28.83

2.3.3 Morphological and environmental effects on transpiration

The relationship between ln T and DBH was based on data from 125 records (Figure 2.2a). T increases approximately linearly with an increase in stem size, with a possible dampening of the relationship for higher DBH values, which could be modelled either through a quadratic polynomial in DBH, or by regressing ln T against DBH. Figure 2.2b shows the relationship of ln T and H, established from 104 records. Unexpectedly, the predicted ln T decreased with increasing H between 1.5 m and about 12 m. Above 12 m, the daily ln T increased with increasing H.

The mean ln T values were 3.7 L day^{-1} for arid and moist environments, 3.8 L day^{-1} for humid and 4.3 L day^{-1} in wet environments (Figure 2.3). Regarding MAT, the lowest mean ln T of 3.6 L day^{-1} was found in cool areas, followed by 3.8 L day^{-1} in hot areas and the highest (4.0 L day^{-1}) was in warm areas. Regarding Z, the mean ln T ranged from 3.8 L day^{-1} in the uplands to 4.2 L day^{-1} in mountainous areas, and 3.9 L day^{-1} was observed in the both the lowlands and highlands. Spearman rank correlations (r_s) in Table 2.3 susggested significant positive associations between ln T and both morphological traits of interest, $r_s = 0.62$ for DBH and $r_s = 0.55$ for H. There was a

weak positive and significant ($p < 0.1$) correlation between ln T and MAP ($r_s = 0.16$) (Table 2.3). The associations of ln T with MAT ($r_s = 0.04$) and Z ($r_s = 0.01$) were not significant at the 10% significance level.

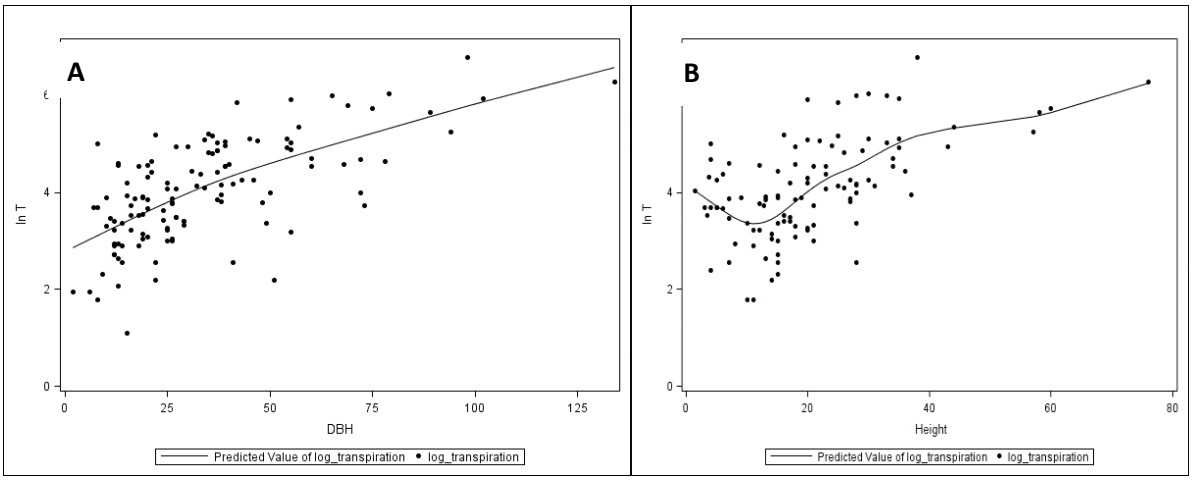

Figure 2.2**:** Relationship between the logarithm of tree transpiration (L day^{-1}) and A) tree stem diameter at breast height (DBH) (cm) and B) tree height (m).

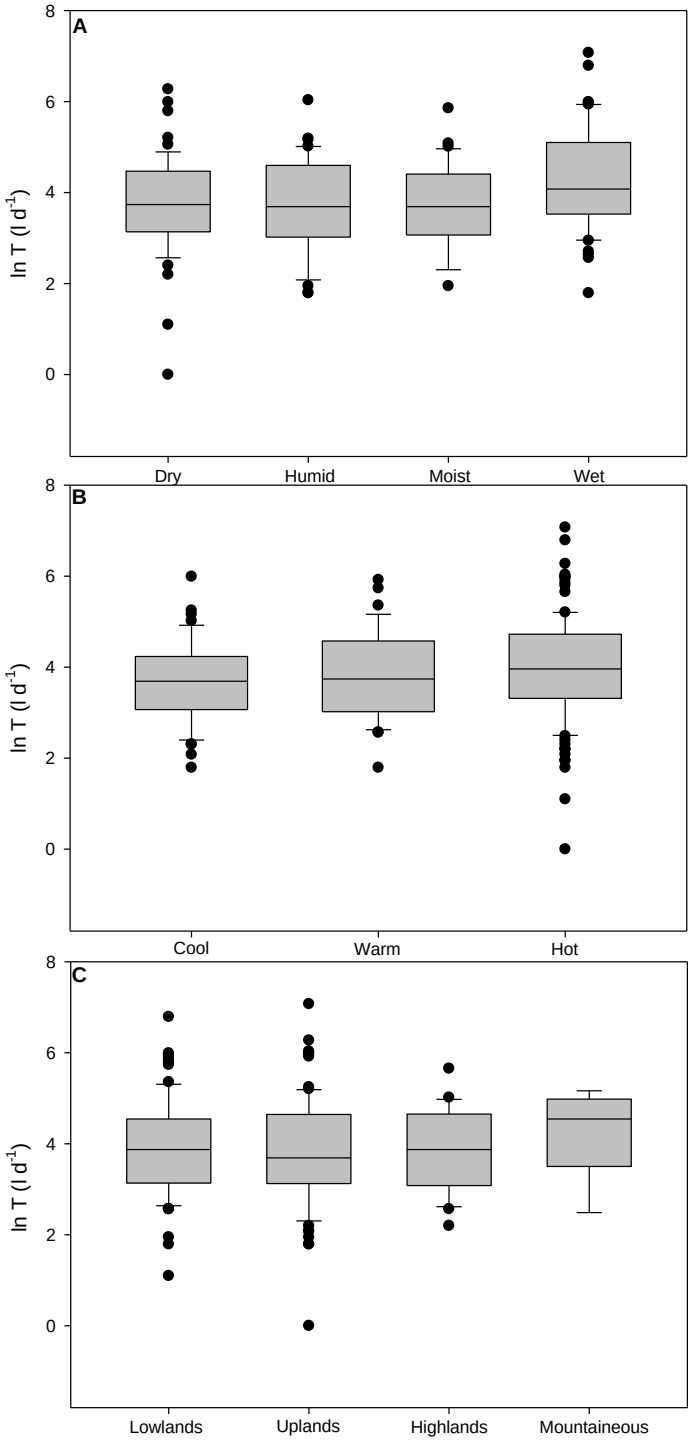

Figure 2.3**:** Comparison of log transformed transpiration (ln T) grouped by (A) mean annual precipitation (MAP), (B) mean annual air temperature (MAT), (C) altitude above sea level (Z). The extents of the boxes show the 25th and 75th percentiles; whiskers show the extent of the outliers. Also shown are the median ranges for each environmental factor.

Table 2.4**:** Spearman correlation coefficients between transformed tree transpiration (ln T) and transpiration variables: tree height (H), diameter at breast height (DBH), mean annual precipitation (MAP), mean annual temperature (MAT) and elevation above the sea level (Z)

	ln T	**H**	**DBH**	**MAP**	**MAT**	**Z**
ln T	1.00					
H	0.55* (<0.001)	1.00				
DBH	0.62* (<0.001)	0.80* (<0.001)	1.00			
MAP	0.16* (0.003)	0.16 (0.19)	-0.10 (0.598)	1.00		
MAT	0.04 (0.579)	-0.23* (0.169)	-0.09 (0.52)	0.28* (<0.001)	1.00	
Z	0.01 (0.437)	-0.04 (0.623)	0.06 (0.382)	-0.26* (0.021)	-0.43* (0.001)	1.00

*Statistically significant at 10% significance level
+ve: factors increase simultaneously, -ve: factor increases with a decrease on the other factor.
Number in parenthesis is the probability

2.3.4 Transpiration measurement methods

T measured by different methods varied considerably (Table 2.4). The number of records using the different techniques also varied. There were under 10 records for heat field deformation, heat ratio, lysimeters and stem heat balance methods, more for radioactive and stable isotopes (n=16), heat pulse velocity (n=20) and ventilated chambers (n=25), and most for thermal dissipation methods (n=117). The ln T mean for lysimeters and thermal dissipation (both 3.9 L day^{-1}) and radioactive and stable isotopes (4.7 L day^{-1}) were the only three methods whose means were equal or greater than the global ln T mean of 3.9 L day^{-1}.

Table 2.5**:** Descriptive statistics of log transformed tree transpiration measurement (L day^{-1}) using different methods (HB = stem heat balance, HFD = heat field deformation, HPV = heat pulse velocity, HRM = heat ratio method, LS = lysimeters, RSI = radioactive and stable isotopes, TD = thermal dissipation and VC = ventilated chambers).

	Global	**Method**							
		HB	HFD	HPV	HRM	LS	RSI	TD	VC
N	196	7	2	20	4	5	16	117	25
Mean	3.9	3.6	3.5	3.7	3.7	3.9	4.7	3.9	3.3
Std	1.1	1.1	0.3	1.0	1.5	0.9	1.2	1.1	0.9
CV	28	30	8	26	39	23	25	27	28
Min	0	2.0	3.3	2.1	1.8	2.6	3.2	1.1	0.0
Q1	3.2	2.9	3.3	3.3	2.6	3.8	3.7	3.1	3.0
Median	3.8	3.2	3.5	3.7	3.9	3.9	4.6	4.0	3.4
Q3	4.6	4.7	3.7	4.3	4.8	4.2	5.6	4.7	3.5
Max	7.1	4.9	3.7	6.0	5.3	5.0	7.1	6.8	5.2
Skew	0.01	-0.22	-	0.36	-0.65	-0.48	0.55	-0.08	-1.34
Kurt	0.53	-1.08	-	0.61	0.54	1.66	-0.59	-0.23	6.96

The methods used to quantify T and their prevalence over the years are shown in Figure 2.4. During the 1970s, radioactive and stable isotopes were the dominant methods. The next decade (1980s) saw the introduction of two thermodynamic methods, the stem heat balance and thermal dissipation. After this period to the present time, thermal dissipation has been the most prevalent quantification method. The latest technology to be reported is the heat ratio method. Lysimeters have been used consistently, and were only not reported between 2000 and 2009, but with few reports in recent years.

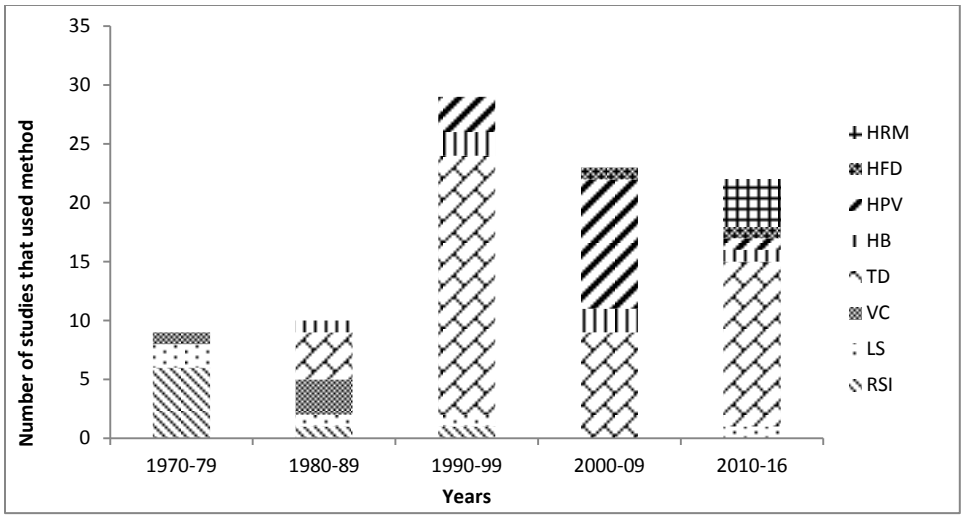

Figure 2.4**:** Tree transpiration methods used (HB = stem heat balance, HFD = heat field deformation, HPV = heat pulse velocity, HRM = heat ratio method, LS = lysimeters, RSI = radioactive and stable isotopes, TD = thermal dissipation and VC = ventilated chambers) and numbers of published studies in different time periods.

2.3.5 Transpiration predictors

The univariate regression analysis (Table 2.5) showed that DBH and H are significant predictors of ln T ($p < 0.001$). Two environmental factors (MAT and Z) were not significantly associated with transpiration ($p > 0.1$), and MAP was significant at 10% significance level.

Table 2.6: Univariate analysis Linear regression coefficients of log-transpiration predictors including measurement methods (HB = stem heat balance, HFD = heat field deformation, HPV = heat pulse velocity, HRM = heat ratio method, LS = lysimeters, RSI = radioactive and stable isotopes, TD = thermal dissipation and VC = ventilated chambers), tree morphology (DBH = diameter at breast height, H = tree height) and environmental factors (MAP = mean annual precipitation, MAT = mean annual temperature, Z = elevation above the sea level) [1](no data imputation).

Independent variable	N		Regression Coefficient	Standard error	Df	t-statistic	P-value
Method	195	Intercept	3.57	0.3573			
		HB	0.08	0.5471	82.9	0.15	0.8812
		HFD	-0.03	0.8388	104	-0.04	0.9679
		HPV	0.15	0.4488	58.6	0.33	0.7415
		HRM	0.13	0.6447	89	0.2	0.8441
		LS	0.03	0.6447	89	0.04	0.9679
		RSI	1.01	0.4994	56.2	2.02	0.0486
		TD	0.48	0.3831	43.1	1.25	0.219
		VC	0	.	.	.	.
DBH	124	Intercept	0.56	0.3665			
		Slope	1.072	0.1098	105	9.76	<.0001
H	103	Intercept	3.25	0.1688			
		Slope	0.04	0.0065	81.5	6.84	<.0001
MAP	195	Intercept	3.66	0.181			
		Slope	0.0002	0.0001	59.6	1.89	0.0633
MAT	195	Intercept	3.8459	0.2638			
		Slope	0.0068	0.0161	75.8	0.42	0.6753
Z	195	Intercept	3.90	0.1295			
		Slope	0.0001	0.0002	118	0.61	0.5453

[1]Linear regression fitting the specified single independent variable, and grouped location as random effect

The results of multiple regressions with backward selection of factors affecting tree water use are shown in Table 2.6. Again the environmental factors (MAT, Z and MAP) were eliminated first as the least significant predictors of tree water use. H was eliminated next, leaving the DBH as the most prominent predictor of tree water use. As expected, method was also a significant indicator of tree water use, more so because the methods are designed for different measuring conditions, including stem characteristics and sizes (Swanson, 1994; Smith and Allen, 1996).

Table 2.7: Multiple linear regression: Backward selection of log-transpiration predictors including measurement method, tree morphology (DBH = diameter at breast height, H = tree height) and environmental factors (MAP = mean annual precipitation, MAT = mean annual temperature, Z = elevation above the sea level) [1](no data imputation).

Step	N	Independent variables in model	Variable to be removed from model	t-statistic (for variable to be removed)	Df	P-value
1	89	Method, DBH, H, MAP, MAT, Z	MAT	0.12	37.1	0.7271
2	89	Method, DBH, H, MAP, Z	Z	0.24	47.1	0.6260
3	89	Method, DBH, H, MAP	MAP	0.28	29.5	0.6014
4	89	Method, DBH, H	H	0.71	66.3	0.2029
5	124	Method, DBH	Not applicable – final model			

[1]Multiple linear regression fitting the specified independent variables, and grouped location as random effect

We note that multiple regression with backward selection using the multiple imputed data (Table 2.7), which was carried out as a sensitivity analysis, yielded very similar results to those presented in Table 2.6. This finding suggests that missing H and DBH data had no appreciable effect on the findings reported here.

Table 2.8: Multiple linear regression: Backward selection of log-transpiration predictors including measurement method, tree morphology (DBH = diameter at breast height, H = tree height) and environmental factors (MAP = mean annual precipitation, MAT = mean annual temperature, Z = elevation above the sea level) 1(Multiple imputation of missing data; N = 138).

Step	Independent variables in model	Variable to be removed from model	t-statistic (for variable to be removed)	Df	P-value
1	Method, DBH, H, MAP, MAT, Z	MAP	0.09	92.6	0.9295
2	Method, DBH, H, MAT, Z	Z	0.20	95.0	0.8402
3	Method, DBH, H, MAT	MAT	-0.36	93.8	0.7174
4	Method, DBH, H	H	1.20	45.2	0.2326
5	Method, DBH	Not applicable – final model			

[1]Multiple linear regression fitting the specified independent variables, and grouped location as random effect.

The predictive power of the model employed is fairly acceptable as shown in Figure 2.5. The scatterplot of the predicted against the observed logarithms of tree transpiration shows a good relationship (RMSE of prediction = 0.692), with a majority of the points close to the 1:1 line.

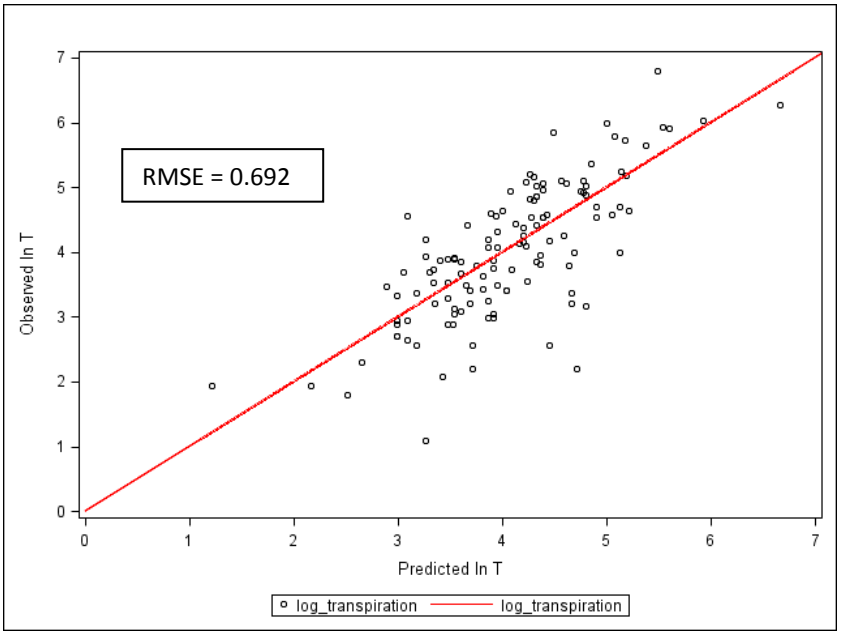

Figure 2.5: Scatterplot of predicted vs. observed logarithms of tree transpiration (L day^{-1}).

2.4 Discussion

2.4.1 Transpiration and stem diameter at breast height

The daily amount of water used by an individual tree was positively correlated with tree size with regard to DBH (r_s = 0.62), suggesting that T increases with increase in DBH. This result is similar to other studies of Vertessy et al. (1995) and Vertessy et al. (1997), who indicated that DBH accounted for 86 to 89% (R^2 values) of the variation in daily tree water use of *Eucalyptus regnans*. A positively correlated association of R^2 = 0.99 was also found by Meinzer et al. (2004) between DBH and tree water use, irrespective of the tree species. Overall, such results imply that the bigger the tree, the higher the water requirements for T despite that wood conductivity, and hence the sap flux density decreases as trees grow older (Meinzer et al., 2001). This is plausible, because the larger the stem, the larger the sapwood area through which water flows to meet canopy T requirements.

2.4.2 Transpiration and tree height

T was positively correlated with H (r_s = 0.55), suggesting that tree water use increases with H. The results of this study concur with findings of Horna et al. (2011) who studied 39 individual trees of seven common tree species in Sulawesi, Indonesia and reported positively correlated association with R^2 values from 0.69 to 0.86 between H and T. Although leaf conductance has been reported to decrease with H (Ambrose et al., 2010), Andrade et al. (1998) reported daily water use ranging from 46 L in an 18 m-tall *Crecropia longipes* tree to 379 L in an *Anacardium excelsum* tree 35 m tall, also confirming an increase of T with H. Pfautsch and Adams (2013) measured daily water use of 70 L in a 30 m-tall *Eucalyptus regnans* tree, while Pfautsch et al. (2010) found daily water use of a 57 m-tall tree of the same species (*Eucalyptus regnans*) to be 190 L. The T of a tree is highly dependent on leaf area (Cunningham et al., 2009), and with increase in H the canopy volume is expected to increase (Marshall and Monserud, 2003), therefore, the direct proportionality of T with H is expected.

2.4.3 Transpiration and mean annual precipitation

There was a slight increase in In T with increasing MAP. In our dataset, the lowest daily water use (1 L) was measured for *Eucalyptus platypus* growing in a dry environment (420 mm, MAP) in Australia (Greenwood and Beresford, 1979). The highest tree water use (1 080 L day^{-1}) was measured for *Eperua purpurea* in a wet environment (3500 mm, MAP) in Venezuela (Jordan and Kline, 1977). This could be attributed to comparatively higher soil water availability in the wet climate of Venezuela than in arid and semi-arid areas. To determine the effect of precipitation on soil water availability and hence T, Limousin et al. (2009) conducted a throughfall exclusion experiment on *Quercus ilex* forest in southern France, they reported a reduction of the input of precipitation to the soil by 29% and a reduction of up to 23% in T. Adaptation of trees to access other sources such as groundwater, especially in dry areas (Lubczynski, 2009) could partly explain the reason behind MAP being a secondary factor, even though it is an important driver for T. On the other hand, forests also influence the climatic conditions of their surroundings. As such, increased aerodynamic roughness of forested areas accompanied by high atmospheric humidity increases the probability of cloud formation and rainfall generation (Bruijnzeel, 2004). High rainfall areas are dominated by high relative humidity compared to arid environments. This limits the amount of water use by trees. Tullus et al. (2012) subjected hybrid aspen trees to increased relative humidity conditions (7% over the ambient level) and observed 30–35% reduction of water use. Overall, our study demonstrated a positively correlated influence of MAP on T.

2.4.4 Transpiration and mean annual air temperature

Globally, MAT was not significantly related to In T. However, some studies, which were conducted under controlled environmental conditions, have reported findings which are contrary to this study. For instance, Pfautsch et al. (2010) conducted an experiment on *Eucalyptus regnans* under adequate soil water conditions and noted a 10% increase on tree water use due to an increase of 1.25°C on maximum air temperature. Barkataky et al. (2013) compared 'Hamlin' sweet orange trees under continuous acclimating temperatures (≤10°C) and growth promoting temperatures. Their findings were that cold temperatures reduced water use by up to 66%. With soil warming of up to 1.6°C within the top 0.2 m more than the control conditions under the canopy areas of *Pinus cembra* L trees at Haggen in Austria, Wieser et al. (2015) reported that tree water use increased by up to 19% with soil warming. Notably in these experiments, all other factors were kept constant, yet under natural conditions single factors do not function in isolation. For instance, the Equatorial Rainforest Region is hot, which is expected to promote water use, but at the same time also humid, which reduces the atmospheric demand for vapour and hence inhibits T. Arid environments are typically hot, but are also dry and as a consequence plants are usually adapted to those conditions through stomata control to avoid water stress. Overall, high air temperature does not necessarily translate to higher T.

2.4.5 Transpiration and elevation

Globally, Z was not significantly associated with tree T. This suggests that so long as there is available soil water and prevailing atmospheric demand for vapour, trees will transpire similarly regardless of altitude. Similarly to our findings, different Z positions ranging from 150-220 m, were found to have no effect on the water use of *Cryptomeria japonica* in Japan (Kumagai et al.,

2007; 2008). On the contrary, Kume et al. (2015) measured approximately 30% lower sap flux density on Japanese cypress trees on the upper slope (300 m absl) than their counterparts on the lower slopes (160 m absl) in Japan. However, despite being the same age, the lower slope trees were taller and had about 23% greater sapwood area than the upper slope trees.

2.4.6 Transpiration measurement methods

The study revealed that thermodynamic methods, especially thermal heat dissipation and heat pulse velocity, were the most prevalent techniques used to measure T. Tree T research has been moving away from lysimeters, ventilated chambers and isotope analysis towards thermodynamic methods. Lysimeters have a high installation cost (Payero and Irmak, 2008) and tree transplants into these facilities is difficult. The requirement of big chambers to cover the whole tree also limits their applicability in studies involving very large trees. Methods employing analysis of isotopes are limited by complicated laboratory procedures (Dawson et al., 2002). Thermodynamic methods, especially thermal dissipation (Granier, 1987) and heat pulse velocity (Green et al., 2003) methods are user friendly, cause minimal damage to the tree, and take simultaneous and continuous measurements with acceptable accuracy on several trees. The recently introduced heat ratio method offers even higher accuracy, especially for very low or even reverse flows (Burgess et al., 2001).

2.5 Conclusions

From the large number of studies and databases analysed, the study demonstrates mainly the positive effect of tree morphological traits; tree height (H), diameter and breast height (DBH) on tree transpiration (T), indicating that T increases with increasing H and DBH. There was a slight tendency for tree T to increase with increasing mean annual precipitation, while mean annual air temperature and elevation above sea level were found not to be significantly correlated with T. The results also showed that during the period 1970 to 2016, thermodynamic methods; in particular thermal heat dissipation probes and heat pulse velocity have become the dominant methods for quantifying T, while the recently introduced heat ratio method holds promise for more accurate water use measurements going forward. This study provides insight for further understanding of T in trees of forested ecosystems, where T generally accounts for most of the evapotranspiration. Overall, assuming a harmonised effect of the aerodynamic parameters which are normally used to model ET and T such as radiation and vapour pressure deficit since T records were source from all over the world, the results demonstrated that tree morphological traits are also key drivers of T rather than environmental factors analysed in this study (MAP, MAT and Z).

References

Ambrose, A.R., Sillett, S.C., Koch, G.W., Van Pelt, R., Antoine, M.E., Dawson, T.E., 2010. Effects of height on tree top transpiration and stomatal conductance in coast redwood (*Sequoia sempervirens*). Tree physiol. 30(10), 1260-1272.

Andrade, J.L., Meinzer, F.C., Goldstein, G., Holbrook, N.M., Cavelier, J., Jackson, P., Silvera, K., 1998. Regulation of water flux through trunks, branches, and leaves in trees of a lowland tropical forest. Oecologia 115(4), 463-471.

Ansley, R.J., Dugas, W.A., Heuer, M.L., Trevini, B.A., 1994. Stem flow and porometer measurements of transpiration from honey mosque (*Prosopis glandulosa*). J. Exp. Bot. 45(275), 847-856.

Barkataky, S., Morgan, K.T., Ebel, R.C., 2013. Plant water requirement of 'Hamlin' sweet orange in cold temperature conditions. Irrigation Sci. 31, 431-443.

Beerling, D.J., Franks, P.J., 2010. Plant science: The hidden cost of transpiration. Nature 464(7288), 495-496.

Bond, B.J., Meinzer, F.C., Brooks, J.R., 2008. How trees influence the hydrological cycle in forest ecosystems. Hydroecology and ecohydrology: Past, present and future, pp.7-28.

Box, G.E.P., Cox, D.R., 1964. An analysis of transformations. J. Roy. Stat. Soc., B 26, 211–234.

Bruijnzeel, L.A., 2004. Hydrological functions of tropical forests: not seeing the soil for the trees? Agr. Ecosyst. Environ. 104, 185-228.

Burgess, S.S.O., Adams, M.A., Turner, N.C., Beverly, C.R., Ong, C.K., Khan, A.A.H., Bleby, T.M., 2001. An improved heat pulse method to measure low and reverse rates of sap flow in woody plants. Tree Physiol. 21, 589-598.

Cunningham, S.A., Pullen, K.R., Colloff, M.J., 2009. Whole-tree sap flow is substantially diminished by leaf herbivory. Oecologia 158, 633-640.

Dawson, T.E., 1996. Determining water use by trees and forests from isotopic, energy balance and transpiration analyses: the roles of tree size and hydraulic lift. Tree Physiol. 16, 263-272.

Dawson, T.E., Mambelli, S., Plamboeck, A.H., Templer, P.H., Tu, K.P., 2002. Stable isotopes in plant ecology. Annu. Rev. Ecol. Syst. 33, 507-59.

Evaristo, J. and McDonnell, J.J., 2017. A role for meta-analysis in hydrology. Hydrol. Process. 1, 1-4.

Granier, A., 1987. Evaluation of transpiration in a Douglas-fir stand by means of sap flow measurements. Tree Physiol. 3, 309-320.

Green, S., Clothier, B., Jardine, B., 2003. Theory and practical application of heat pulse to measure sap flow. Agron. J. 95, 1371-1379.

Greenwood, E.A.N., Beresford, J.D., 1979. Evaporation from vegetation in landscapes developing secondary salinity using the ventilated- chamber technique. I. Comparative transpiration from juvenile Eucalyptus above saline ground-water seeps. J. Hydrol. 42, 369-382.

Hijmans, R.J., Cameron, S.E., Parra, J.L., Jones, P.G., Jarvis, A., 2005. Very high resolution interpolated climate surfaces of global land areas. Int. J. Climatol. 25, 1965-1978.

Horna, V., Schuldt, B., Brix, S., Leuschner, C., 2011. Environment and tree size controlling stem sap flux in a perhumid tropical forest of Central Sulawesi, Indonesia. Ann. For. Sci. 68(5), 1027-1038.

IPCC, 2014. Climate Change 2014: Synthesis Report. Contribution of Working Groups I, II and III to the Fifth Assessment Report of the Intergovernmental Panel on Climate Change (IPCC), Geneva, Switzerland.

Jasechko, S., Sharp, Z.D., Gibson, J.J., Birks, S.J., Yi, Y., Fawcett, P.J., 2013. Terrestrial water fluxes dominated by transpiration. Nature 496(7445), 347-350.

Jordan, C.F., Kline, J.R., 1977. Transpiration of trees in a tropical rainforest. J. Appl. Ecol. 14, 853-860.

Knight, D.H., Fahey, T.J., Running, S.W., Harrison, A.T., Wallace, L.L., 1981. Transpiration from 100-year-old lodgepole pine forests estimated with whole-tree potometers. Ecology 62, 717-726.

Kumagai, T., Aoki, S., Shimizu, T., Otsuki, K., 2007. Sap flow estimates of stand transpiration at two slope positions in a Japanese cedar forest watershed. Tree Physiol. 27, 161-168.

Kumagai, T.O., Tateishi, M., Shimizu, T., Otsuki, K., 2008. Transpiration and canopy conductance at two slope positions in a Japanese cedar forest watershed. Agr. Forest Meteorol. 148(10), 1444-1455.

Kume, T., Tsuruta, K., Komatsu, H., Shinohara, Y., Katayama, A., Ide, J.I., Otsuki, K., 2015. Differences in sap flux-based stand transpiration between upper and lower slope positions in a Japanese cypress plantation watershed. Ecohydrol. doi: 10.1002/eco.1709.

Köcher, P., Horna, V., Leuschner, C., 2013. Stem water storage in five coexisting temperate broad-leaved tree species: significance temporal dynamics and dependence on tree functional traits. Tree Physiol. 33, 817-832.

Köppen, W., 1936. Das geographische system der klimate, in Handbuch der Klimatologie, vol. 1, part C, edited by W. Köppen and R. Geiger, Gebrüder Borntraeger, Berlin, pp. 1–44.

Limousin, J.M., Rambal, S., Ourcival, J.M., Rocheteau, A., Joffre, R., Rodriguez-Cortina, R., 2009. Long-term transpiration change with rainfall decline in a Mediterranean *Quercus ilex* forest. Glob. Change Biol. 15, 2163-2175.

Lubczynski, M.W., 2009. The hydrological role of trees in water-limited environments. Hydrogeol. J. 17, 247-259.

Malone, J., Guleria, R., Craven, C., Horton, P., Järvinen, H., Mayo, J., O'reilly, G., Picano, E., Remedios, D., Le Heron, J., Rehani, M., 2014. Justification of diagnostic medical exposures: some practical issues. Report of an International Atomic Energy Agency Consultation. British J. Radiol.

Marshall, J.D., Monserud, R.A., 2003. Foliage height influences specific leaf area of three conifer species. Can. J. Forest. Res. 33, 164-170.

Meinzer, F.C., Bond, B.J., Warren, J.M., Woodruff, D.R., 2005. Does water transport scale universally with tree size? Funct. Ecol. 19, 558-565.

Meinzer, F.C., Goldstein, G., Andrade, J.L., 2001. Regulation of water flux through tropical forest canopy trees: Do universal rules apply? Tree Physiol. 21, 19-26.

Meinzer, F.C., James, S.A., Goldstein, G., 2004. Dynamics of transpiration, sap flow and use of stored water in tropical forest canopy trees. Tree Physiol. 24, 901-909.

Miralles, D.G., Holmes, T.R.H., De Jeu, R.A.M., Gash, J.H., Meesters, A.G.C.A., Dolman, A.J., 2011. Global land-surface evaporation estimated from satellite-based observations. Hydrol. Earth Syst. Sc. 15, 453–469.

Moreira, M., Sternberg, L., Martinelli, L., Victoria, R., Barbosa, E., Bonates, L., Nepstad, D., 1997. Contribution of transpiration to forest ambient vapour based on isotopic measurements. Glob. Change Biol. 3(5), 439-450.

Nadezhdina, N., David, T.S., David, J.S., Ferreira, M.A., Dohnal, M., Tesar, M., Gartner, K., Leitgeb, E., Nadezhdin, V., Cermak, J., 2010. Trees never rest: the multiple facets of hydraulic redistribution. Ecohydrol. 3, 43-444.

Payero, J.O., Irmak, S., 2008. Construction, installation and performance of two repacked weighing lysimeters. Irrigation Sci. 26, 191-202.

Pfautsch, S., Adams, M.A., 2013. Water flux of Eucalyptus regnans: defying summer drought and a record heat wave in 2009. Oecologia 172(2), 317-326.

Pfautsch, S., Bleby, T.M., Rennenberg, H., Adams, M.A., 2010. Sap flow measurements reveal influence of temperature and stand structure on water use of *Eucalyptus regnans* forests. Forest Ecol. Manag. 259, 1190-1199.

Ryan, M.G., Bond, B.J., Law, B.E., 2000. Transpiration and whole-tree conductance in ponderosa pine trees of different heights. Oecologia 124, 553-560.

Sansigolo, C.A., Ferraz, E.S.B., 1982. Measurement of transpiration and biomass in a tropical *Pinus caribaea* plantation with tritiated water. Agr. Meteorol. 26(1), 25-33.

SAS Institute Inc., 2013. SAS/STAT 13.1 User's Gude. Cary, NC: SAS Institute Inc.

Smith, D.M., Allen, S.J., 1996. Measurement of sap flow in plant stems. J. Exp. Bot. 47, 1833-1844.

Swanson, R.H., 1994. Significant historical developments in thermal methods for measuring sap flow in trees. Agr. Forest Meteorol. 72, 113-132.

Swanson, R.H., Whitfield, D.W.A., 1981. A numerical analysis of heat pulse velocity theory and practice. J. Exp. Bot. 32(126), 221-239.

Tullus, A., Kupper, P., Sellin, A., Parts, L., Sõber, J., Tullus, T., Lõhmus, K., Sõber, A., Tullus, H., 2012. Climate Change at Northern Latitudes: Rising Atmospheric Humidity

Decreases Transpiration, N-Uptake and Growth Rate of Hybrid Aspen. PlosOne 7(8), 1-12.

Vertessy, R.A., Benyon, R.G., O'Sullivan, S.K., Gribben, P.R., 1995. Relationships between stem diameter, sapwood area, leaf area and transpiration in a young mountain ash forest. Tree Physiol. 15, 559-567.

Vertessy, R.A., Hatton, T.J., Reece, P., O'Sullivan, S.K., Benyon, R.G., 1997. Estimating stand water use of large mountain ash trees and validation of the sap flow measurement technique. Tree Physiol. 17, 747-756.

Weaver, J.E., Mogenson, A., 1919. Relative Transpiration of Coniferous and Broad- Leaved Trees in Autumn and Winter. Bot. Gaz. 68(6), 393-424.

Wieser, G., Grams, T.E.E., Matyssek, R., Oberhuber, W., Gruber, A., 2015. Soil warming increased whole-tree water use of *Pinus cembra* at the treeline in the Central Tyrolean Alps. Tree Physiol. 35, 279-288.

Wullschleger, S., Meinzer, F.C., Vertessy, R.A., 1998. A review of whole-plant water use studies in trees. Tree Physiol. 18, 499-512.

3. Drought dynamics and interannual rainfall variability on the Ghaap plateau, South Africa, 1918-2014

Abstract

With drought expected to increase in frequency and severity as a result of climate change, drought and rainfall variability assessments at interannual time scales using long-term rainfall data are necessary to develop drought mitigation strategies and planning measures, especially in semi-arid and arid environments where drought impact is expected to be adverse. The objective of this study was to determine the occurrence and severity of droughts and interannual rainfall variability trends in the Ghaap plateau, Northern Cape Province, South Africa. This study was based on long-term rainfall data for three meteorological stations (Postmasburg, Douglas and Groblershoop) from 1918 to 2014, sourced from the South African Weather Services (SAWS). Calculation of the Standardized Precipitation Index (SPI) showed that more droughts occurred since the 1990s; these droughts were all moderately dry with SPI values ranging between -1.03 to -1.46, except for the 1992 drought at Groblershoop which was severe. The longest drought duration on record in the study area was 2 years. Fitting of the long-term rainfall data to a non-parametric spline smoother revealed that the total annual rainfall, number of rainfall days and extreme rainfall events were essentially stable. The total annual rainfall, however, followed a secular pattern of fluctuations over the years.

Keywords: Drought, Standardized Precipitation Index, Interannual rainfall variability, Spline Smoother, Ghaap plateau.

3.1 Introduction

Drought - a complex natural hazard characterized by below-normal precipitation beyond a given threshold over time, impacts ecosystems and society in several ways (Dai, 2011; Vicente-Serrano et al., 2011; Van Loon, 2015). Drought affects terrestrial ecosystems leading to changes on the spatial and temporal patterns of vegetation (Fernandez-Illescas and Rodriguez-Iturbe, 2004; IPCC, 2014; Gudmundsson et al., 2014; Taufik et al., 2015), aquatic degradation (Lake, 2003) and food web structure (Ledger et al., 2013). In addition, drought results in water shortage, threatening irrigation for crop production, electricity generation and impairing water quality (Tallaksen and Van Lanen, 2004; Wilhite, 2000; Sheffield and Wood, 2007; Van Vliet, 2012). Conventionally, drought is classified into four types: meteorological, hydrological, agricultural and socio-economic. The latter form of drought may be considered a consequence of one or more of the other types of drought. The meteorological drought, which is the focus of the present study, occurs as a result of precipitation shortage for prolonged period of time (Keyantash and Dracup, 2002; Batisani, 2011; Dai, 2011).

Various indices have been developed and applied to quantify and monitor meteorological drought development. These include Discrete and cumulative precipitation anomalies, Rainfall deciles, Palmer Drought Severity Index (PDSI), Drought Area Index (DAI) and Rainfall Anomaly Index (RAI) (Heim, 2000; 2002; Keyantash and Dracup, 2002; Vicente-Serrano et al., 2011; Dai, 2011). The precipitation anomalies and deciles are simple to compute, but they are especially less informative and can easily show end of a drought period even if the precipitation received is not enough to terminate the water shortage. Even though the PDSI, DAI and RAI are robust, they involve complicated computations and are not versatile. DAI for instance was developed specifically for Indian conditions. In addition to these indices is the Standardised

Precipitation Index (SPI) which is based on long-term precipitation data fitted to probability distribution functions (McKee et al., 1993; Guttman, 1998; Komuscu, 1999; Jain et al., 2015; Van Loon, 2015).

The SPI is recommended because of its accuracy and simplicity (Guttman, 1998; Komuscu, 1999; Jain et al., 2015), and versatility allowing it to also detect the occurrence of wet spells at different time scales (Xie et al., 2013; Van Loon, 2015), and is applicable to detect even the hydrological and agricultural droughts. For instance, at time scales of up to 6 months the SPI is useful for agricultural planning, while at longer time scales it is utilised to detect hydrological drought essential for monitoring groundwater levels, stream flows and dam levels (Batisani, 2011). This versatility of the SPI makes it relevant across different sectors such as groundwater management during mining operations, agricultural water management and sustainable management of nature (flora and fauna). The SPI has been applied effectively in dryland regions (Manatsa, 2008; Batisani, 2011; Al Asheikh and Tarawneh, 2013).

In the future, droughts are expected to increase in frequency and severity as a result of climate change which will effect decreases in regional rainfall, but also because of increasing evaporation driven by global warming (Sheffield and Wood, 2008; Dai, 2011). According to the fourth assessment report of the Intergovernmental Panel on Climate Change (IPCC), more intense and longer droughts have been observed globally, particularly in the tropics and subtropics since the 1970s (IPCC, 2012). In Southern Africa, which is largely semi-arid and characterised by high interannual rainfall variability, droughts occur with high frequency and severity, and El Niño Southern Oscillation (ENSO) has been established to be the major driver (Manatsa et al., 2008). In South Africa, Rouault and Richard (2003) analysed drought using the

SPI between 1921 and 2001 and found that droughts have become more prevalent since the 1960s, and more intense within the last 2 decades.

Indeed, the SPI is an attractive tool for detecting the occurrence of drought at specific times within a historical precipitation record. But, it does not account for rainfall trends at inter-annual time scales which may also be linked to the ENSO. Yet, a better understanding of interannual rainfall trends is also important for developing rainfall runoff relationships, which are crucial for agricultural and water resources management (Kampata et al., 2008; Parida and Molafhi, 2008). This is particularly important for a country like South Africa, which is characterised by high prevalence of droughts and erratic rainfall events (Schulze, 2008).

Drought assessments using long-term rainfall data are important at local, regional and continental scales (Masih et al., 2014). Although drought events are increasing in South Africa (Kruger, 2006; Rouault and Richard, 2003), they remain poorly described in the Ghaap plateau despite the field observation that natural vegetation is on the verge of "ecological collapse" due to climate change. As drought occurrence and rainfall variability are some of the main factors driving agricultural activities and nature conservation in these drylands, accurate quantitative information of not only drought, but also interannual rainfall variability are needed to provide a context-specific guide on the development and implementation of better drought mitigation strategies and improved planning measures. The objective of this study was to determine the occurrence and severity of droughts and interannual rainfall variability trends in the Ghaap plateau, Northern Cape Province, South Africa. The plateau falls within arid and semi-arid climatic zones, making it more prone to the adverse impacts of drought and related rainfall variability.

3.2 Materials and methods

3.2.1 Site description

Ghaap Plateau is situated between Kimberley and Upington, north of the Orange River to the Kuruman Hills. Its altitude varies between 900 and 1 600 m above sea level. The topography is comprised of undulating hills, with moderate slopes and flat plains. The mean annual precipitation ranges between 250 and 400 mm, majority of it falling between November and April. July is the driest month with absolutely no rainfall while March receives the highest amount of rainfall. The average maximum temperature is 17°C in June and 31°C in January. The region experiences its coldest temperatures during June and July with a mean cold temperature of 0°C.

The main economic activity on the plateau is open cast mining, which depends primarily on groundwater resources. Second to the mining activity, the population is dependent on rainfall driven activities, including agricultural production and nature conservation. The site is on shallow sandy soils of the Hutton form with red Aeolian sand of the Kalahari group overlying the volcanics and sediments of the Griqualand West Supergroup that outcrops in some places (Mucina and Rutherford, 2006). The predominant vegetation type is the Savanna Biome, which is composed of the Kuruman Mountain Bushveld and Postmasburg Thornveld.

3.2.2 Selection of meteorological stations and source of rainfall data

For this study, three meteorological stations (Postmasburg, Douglas and Groblershoop) were selected for analysis (Figure 3.1). There are few long-term stations in the Northern Cape Province due to the sparse population (Kruger, 2006). The stations were selected based on availability of high quality rainfall data and their proximity to the Kolomela mine, which is the

main experimental site. Daily rainfall data for all the meteorological stations were obtained from the South African Weather Services (SAWS).

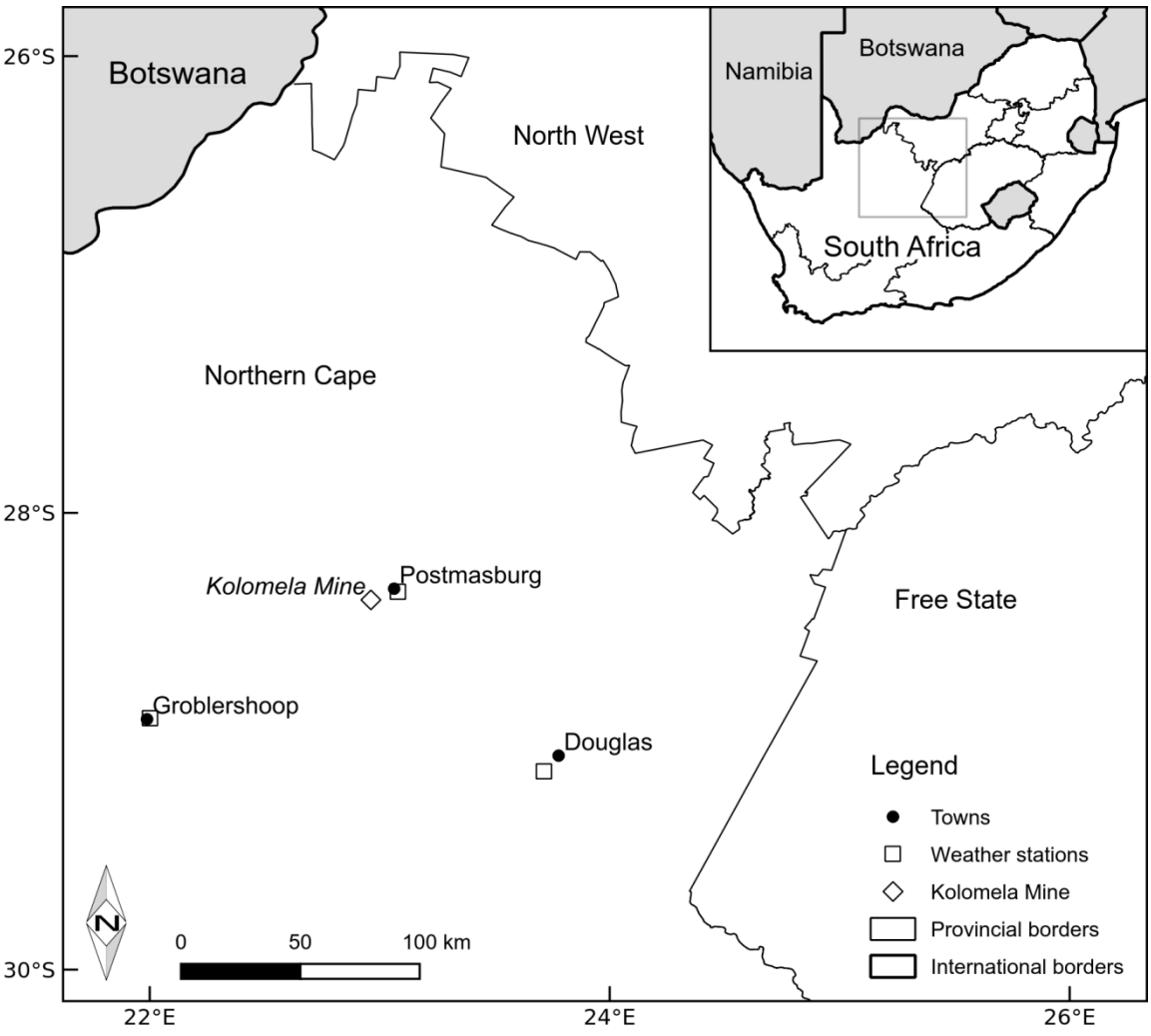

Figure 3.1: Location of selected weather stations in the Northern Cape Province, South Africa used for the characterizing drought and analysis of rainfall trends.

3.2.3 Calculation of aridity index

Aridity Index (AI), a numerical expression of the degree of dryness of the climate was calculated for each meteorological station (Thornthwaite, 1948). The reference evapotranspiration (ETo) data was sourced from the Agricultural Research Council (ARC) of South Africa. AI was calculated following UNSECO (1979):

$$AI = P / ETo \quad (3.1)$$

Where, P is the mean annual rainfall. According to this classification, $AI < 0.03$ is hyper-arid zone, $0.03 < AI < 0.2$ is an arid zone, $0.2 < AI < 0.5$ is semi-arid zone, and $AI > 0.5$ is sub-humid. Table 3.1 shows the geographical position, elevation and record length of rainfall data, average annual rainfall, ETo and AI.

Table 3.1: Geographical positions, elevation, data recording years, average annual rainfall, reference evapotranspiration (ETo) and aridity index (AI) for Postmastburg, Douglas and Groblershoop in the Ghaap plateau.

Weather station	Latitude	Longitude	Elevation (m.a.s.l)	Record length	No. of years	Av. rainfall (mm)	ETo (mm)	AI
Postmasburg	-28.35	23.08	1323	1918 – 2014	97	317	1710	0.1
Douglas	-29.13	23.71	1013	1960 – 2014	55	312	1586	0.2
Groblershoop	-29.90	22.00	871	1939 – 2014	76	201	1641	0.1

3.2.4 Calculation of standardized precipitation index

The SPI was calculated on an annual basis to identify drought years and the severity using long-term rainfall data for the three meteorological stations. The three-parameter Gamma distribution – which includes a threshold parameter – was fitted by maximum likelihood (SAS procedure UNIVARIATE), separately to the annual rainfall data of the three metorological stations. Where the initial estimate of threshold parameter was negative (namely for the Groblershoop and Douglas data), the scale and shape parameters of the Gamma distribution were re-estimated with the threshold parameter fixed at zero. The fitting procedure produces a histogram of the data, overlaid with the fitted Gamma distribution. Furthermore, a non-parametric Kernel density estimate of the distribution of the data is plotted together with the histogram and the fitted Gamma distribution. Given estimates $\hat{\lambda}$, $\hat{\sigma}$ and $\hat{\alpha}$ of the threshold, scale and shape parameters

of the Gamma distribution, respectively, the transformed value of total annual rainfall x, in other words, the Standardized Precipitation Index (SPI), was calculated as follows:

$$SPI(x) = q_{Norm}(F(x;\hat{\lambda},\hat{\sigma},\hat{\alpha})) \quad (3.2)$$

where F is the cumulative distribution function of the Gamma distribution with threshold parameter $\hat{\lambda}$, scale parameter $\hat{\sigma}$, shape parameter $\hat{\alpha}$, and q_{Norm} is the quantile function of the standard Normal distribution. The SPI categories were then used to characterise the intensity of drought as depicted in Table 3.2. According to Guttman (1999), negative SPI value indicates a drought year and vice versa, with the range from >-1 to <1 regarded as normal. The longest duration of drought was taken as the longest period of successive dry years within the record of rainfall data (Al Asheikh and Tarawneh, 2013).

Table 3.2: A list of SPI classes describing the intensity of drought or wetness of a year in relation to the long-term average rainfall (Guttman, 1999).

SPI value	**Classification**
2.0 +	Extremely wet
1.5 to < 2.0	Very wet
1.0 to < 1.5	Moderately wet
>-1.0 to < 1.0	Near normal
-1.0 to > -1.5	Moderately dry
-1.5 to > -2.0	Severely dry
-2.0 and less	Extremely dry

3.2.5 Determining trends of annual rainfall, rainfall days and extreme rainfall events

The trends of total annual rainfall for the three meteorological stations over time were determined by applying a non-parametric smoother to the long-term rainfall data, namely a generalized additive model assuming a Gamma error distribution and using a spline smoother. A generalized cross-validation method (SAS, 2013) was used to determine the degrees of freedom for the spline smoother such that the prediction error of the model was minimized.

Additive models generalize linear models by modelling the dependency between the mean response and a covariate through smooth non-linear functions in addition to the linear function of the covariate. Generalized additive models further accommodate distributions of the response variable other than the Normal. For a response variable y (total annual rainfall) the generalized additive model employed in this study was in the form:

$$\eta = \beta_0 + \beta_1 X + s(X) \qquad (3.3)$$

where $\eta = g(\mu)$ is a monotonic function of the mean, $\mu = E(y)$ of the response y, β_0 and β_1 are intercept and slope parameters, and $s(X)$ is a smooth function (here: non-parametric spline function) of the covariate X (here: time in years).

The Gamma error distribution was chosen because rainfall data is i) generally right-skewed, ii) non-negative and iii) has the variance that increases with the mean (heteroscedasticity). To verify the sensitivity of the Gamma distribution, the generalized additive model was also fitted assuming the Log-normal and Normal distributions (Hastie and Tibshirani, 1990; SAS, 2013).

In the same manner, the non-parametric smoother was also applied to extreme daily rainfall and to the number of rainfall days (1 mm or more). Regarding the number of rainfall days, the generalized additive model was, however, fitted assuming a Poisson Error Distribution, and the logarithm of the number of days (365 or 366 for leap years) was fitted as an offset variable. Observed and fitted (Gamma, Log-Normal and Normal) values of total annual rainfall, extreme daily rainfall and number of rainfall days were plotted using SAS.

3.3 Results

3.3.1 Drought occurrence, severity and duration

Out of the total of 97 years of records at Postmasburg (Figure 3.2A), there were 4 moderately dry years. These were in the years 1993, 1994, 2012 and 2013 with SPI values of -1.26, -1.20, -1.29 and -1.4, respectively. The longest drought duration of 2 consecutive years was recorded from 1993 to 1994 and from 2012 to 2013.

With the record of rainfall data from 1960 to 2014 at Douglas (Figure 3.2B), the first drought occurred in 1992 with SPI value of -1.39 followed by others in 1996 with SPI value of -1.12, 2005 with SPI value of -1.42 and lastly in 2013 with a SPI value of -1.36. All drought years at this location were moderate (SPI -1 to >-1.5). There were no consecutive dry years without an interruption of either a normal or a wet year in this location throughout the years of data record.

At Groblershoop (Figure 3.2C), the drought years and wet years were consistent throughout the 76 year record period. There were 9 drought years spread from 1941 to 2012 with SPI values ranging from -1.46 to -1.03, except for 1992 which was severely dry (SPI of -1.74), the rest of the droughts were moderate. The longest drought of 2 years was recorded from 1965 to 1966.

Worth mentioning is the fact that in all the stations there have been years which were wet to extremely wet. After the year 2000, there were no wet years at Postmasburg and Douglas; At Groblershoop, where the distribution of drought years and wet years was similar throughout the study period, wet years were observed even during the last decade.

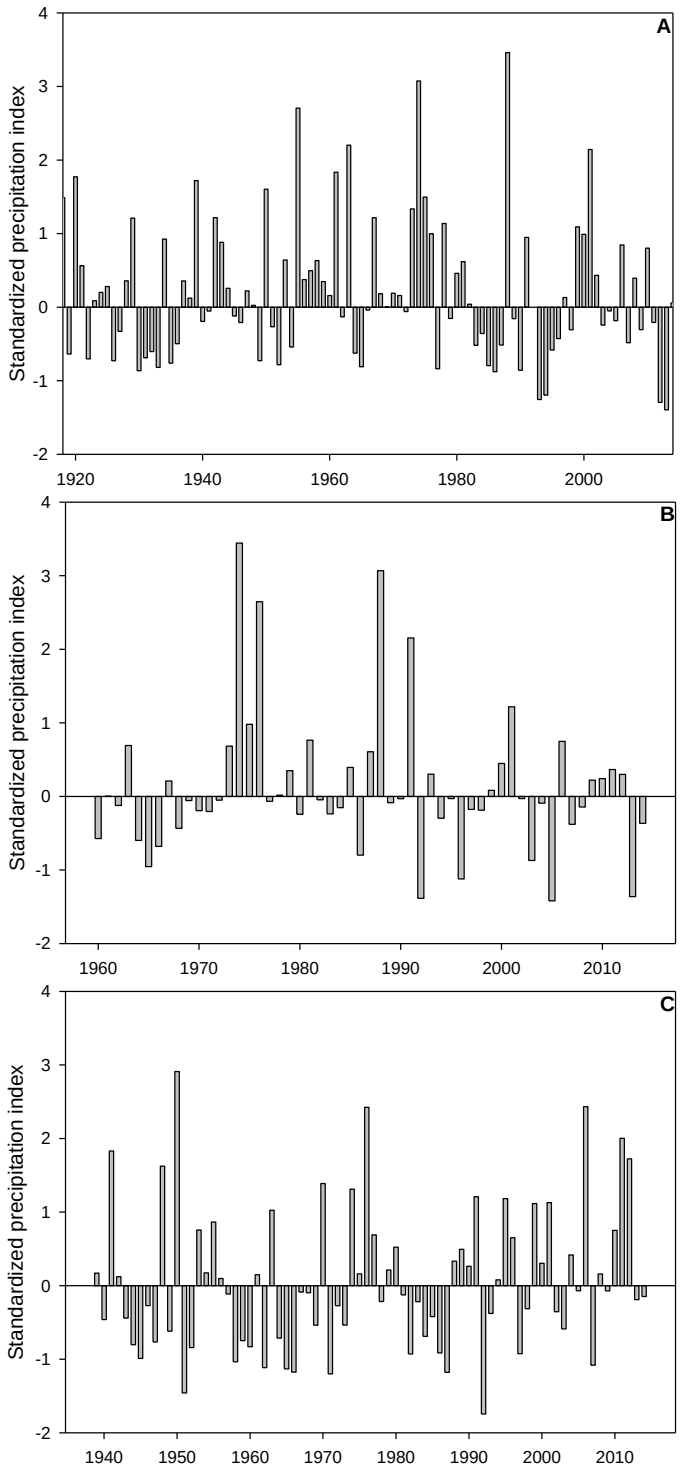

Figure 3.2: Standardized Precipitation Index for (A) Postmasburg (97 years), (B) Douglas (55 years) and (C) Groblershoop (76 years) in the Ghaap plateau, Northern Cape Province, South Africa.

3.3.2 Trends of annual rainfall, rainfall days and extreme rainfall events

At the three meteorological stations studied, there is no evidence of an increase or decline in total annual rainfall over the rainfall data recording periods under analysis (Figures 3.3A-C). However, cyclic trends ranging from 18 – 22 years were observed at Postmasburg. The difference between an adjacent pair of a peak and a trough was up to 90 mm. At Douglas, cycle lengths (peak to peak or trough to trough) ranged between 12 and 16 years. The difference between troughs and peaks adjacent to each was up to 250 mm at this meteorological station. Worth noting was that the differences between adjacent peaks and troughs at the two stations occasionally were small, that is, on average these differences were about 50 mm or less. Likewise, the overall rainfall trend was not showing changes at Groblershoop, where not even cyclic patterns of rainfall were evident.

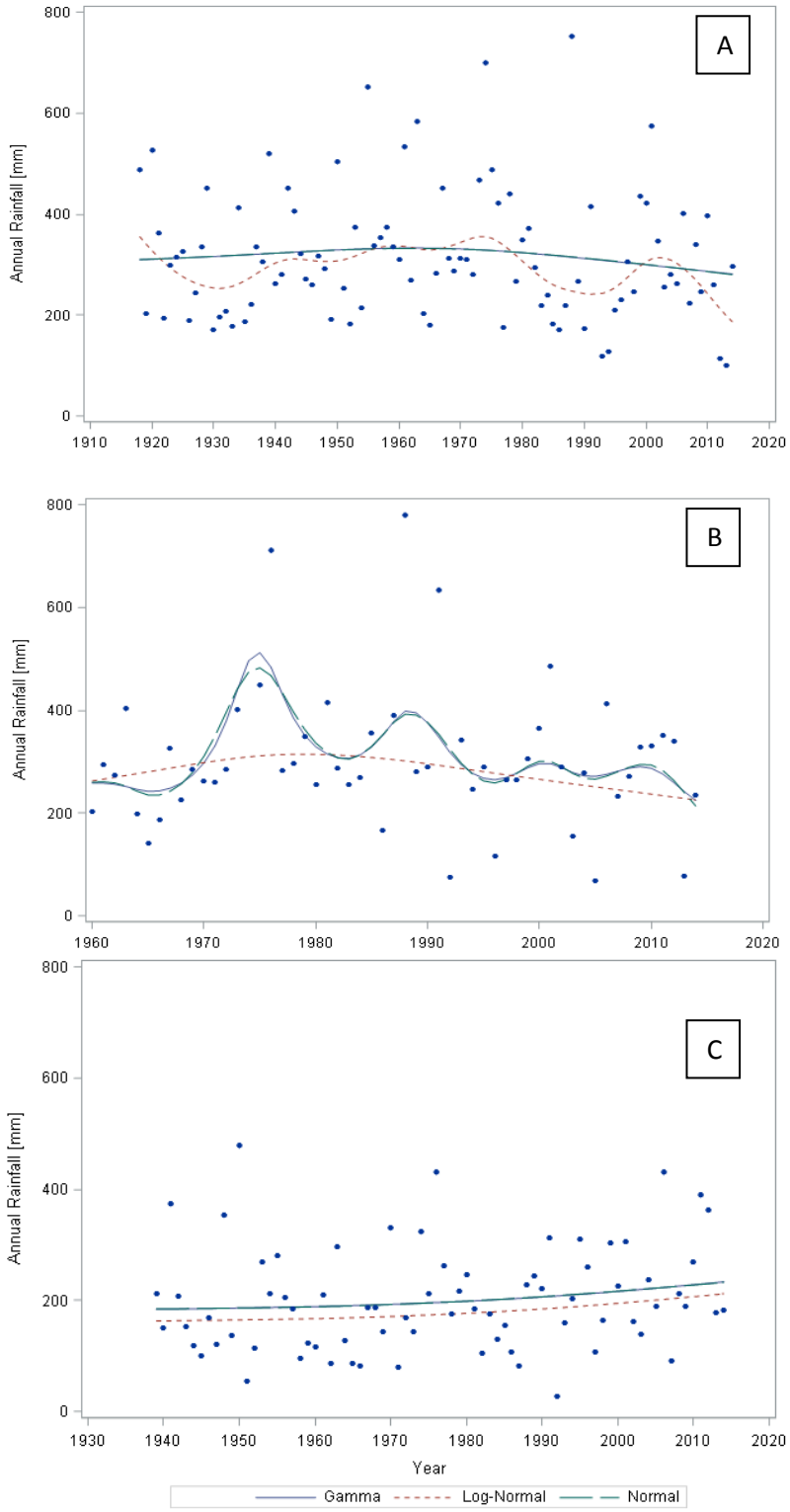

Figure 3.3: Observed (dots) and fitted (lines) values of total annual rainfall for A) Postmasburg (97 years), B) Douglas (55 years) and C) Groblershoop (76 years) for the Ghaap plateau computed using Gamma, Log-normal and normal distribution functions.

The number of rainfall days (Figures 3.4A-C) and the extreme rainfall events (Figures 3.5A-C) seemed stable in all the meteorological stations throughout the recording period. At Douglas though, these parameters (Figure 3.4B and Figure 3.5B) showed some irregular fluctuations which at the end of the day even up to constant trends.

Finally, regarding the results presented in Figures 3.3 and 3.5 we can note that the three alternative distributions used (Gamm, normal and log-normal) yield similar estimates of the long-term trends, which suggests that the results are not sensitive to the assumption of the gamma distribution.

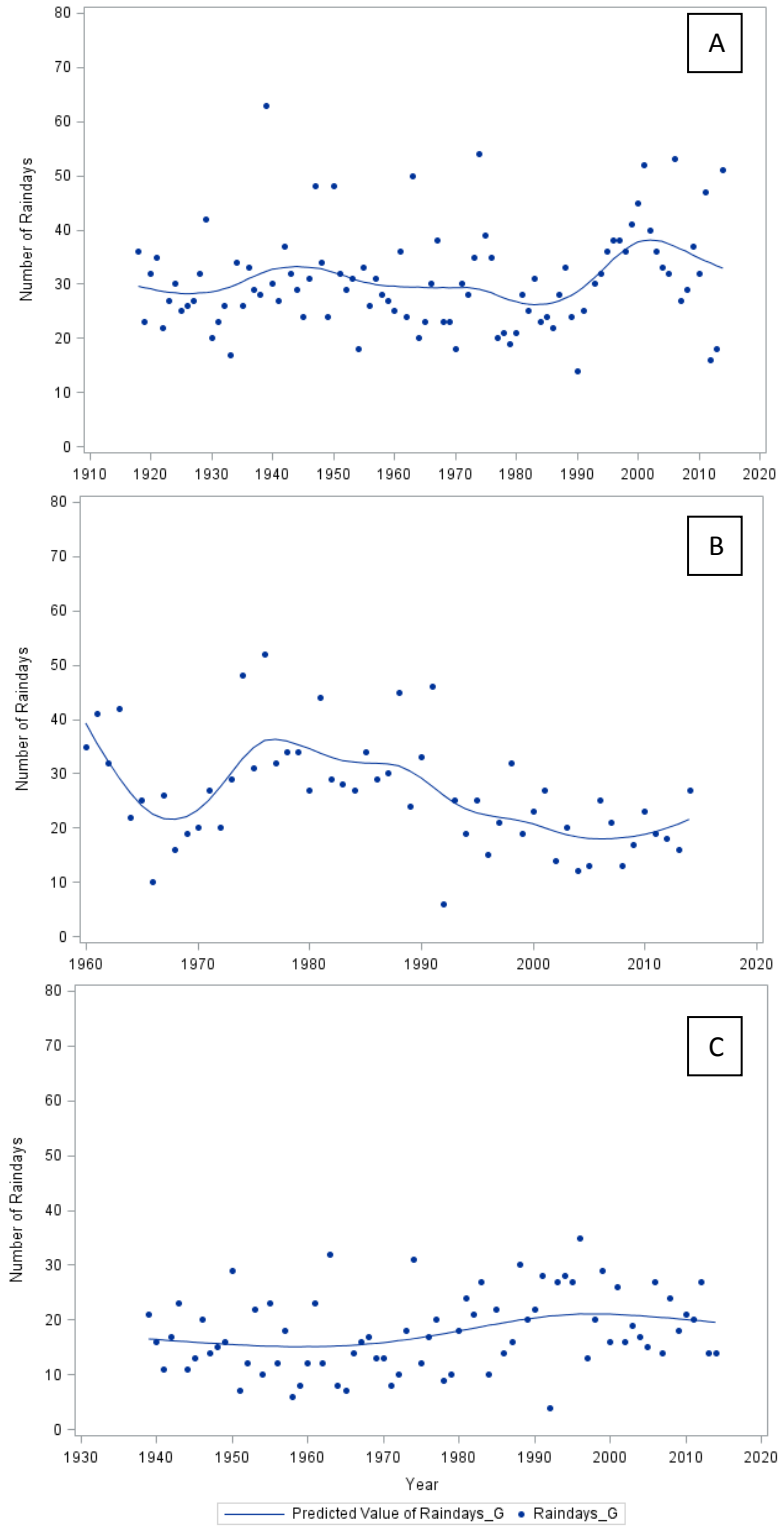

Figure 3.4: Observed number of rainfall days (dots) fitted (lines) using Poisson error distribution for A) Postmasburg (97 years), B) Douglas (55 years) and C) Groblershoop (76 years) in the Ghaap plateau.

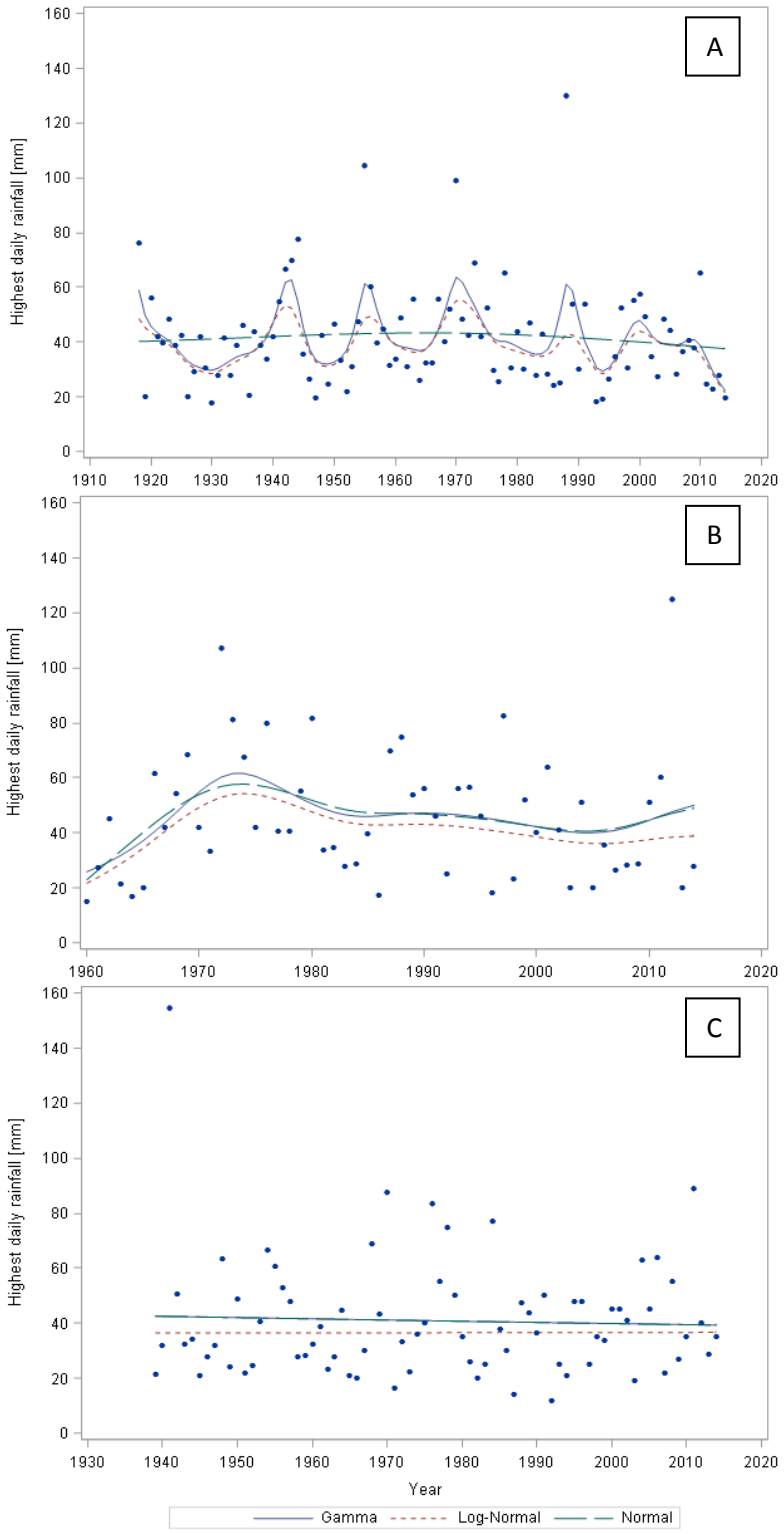

Figure 3.5: Observed extreme daily rainfall events and fitted using Gamma, Log-nomal and nomrmal for A) Postmasburg (97 years), B) Douglas (55 years) and C) Groblershoop (76 years) in the Ghaap plateau.

3.4 Discussion

3.4.1 On drought occurrence, severity and duration of the Ghaap plateau

All the droughts at Postmasburg and Douglas occurred between 1992 and 2013, while at Groblershoop they were evenly distributed throughout the rainfall record period. Wet to extremely wet years were diminishing during this period at the stations where droughts were more prevalent. A study by Ronault and Richard (2003), investigating the intensity and spatial extension of droughts in South Africa, concluded that the most intensive droughts occurred in 1983 and 1992.

In the present study, the SPI values for all the meteorological stations ranged from -1.03 to -1.46 and according to the classification by Guttman (1999), the Ghaap plateau has experienced moderate droughts, except for the one year (1992) which was severely dry at Groblershoop. Similarly Batisani (2011), used the SPI to analyse droughts in Botswana and reported SPI values of -1.16 to 1.29, which fall within the range reported in the present study. In agreement with our findings, Manatsa et al. (2008) using SPI to analyse rainfall data from 1900 to 2000, also identified moderate droughts in Zimbabwe. The occurrence of the anomalous SPI value of -1.74 at Groblershoop in 1992, however, concurs with the findings of Manatsa et al. (2008) who also revealed that the 1991-1992 drought was the most extreme during the 20^{th} century. This was further corroborated by Masih et al. (2014), whose comprehensive review of droughts on the African continent confirmed extremely unique droughts for the years 1991 to 1992.

Notably, the longest duration of drought on the plateau for the record of rainfall data was 2 years for all the meteorological stations. The SPI analyses drought in terms of rainfall, and in future studies it would be ideal to also consider indices like the Standardized Precipitation-Evapotranspiration Index (SPEI) that look into other climatic factors such as temperature.

3.4.2 Trends of annual rainfall, rainfall days and extreme rainfall events

Overall, the total annual rainfall at the Ghaap plateau was essentially stable over the record periods studied. This finding is in contrast to studies done in the neighbouring Vaalharts area in the Northern Cape Province, where Adeyemo et al. (2014) reported declining annual rainfall for the period between 1983 and 2010. Their report was consistent with Parida and Moalafhi (2008), who pointed to a decrease in the annual rainfall from 1981 for similar arid and semi-arid environments in Botswana. However, in line with the findings of the present study are those reported by Tyson et al. (1975) who analysed data from 157 weather stations across South Africa between 1880 and 1972, and reported constant trends of rainfall. Similar to findings of this study, they also reported the secular nature of rainfall patterns in many parts of the country. Tyson et al. (2002) and Nel (2009) also reported the secular fluctuations of rainfall trends over southern Africa and the KwaZulu Natal Drakensberg region, respectively. In both of these studies, no overall changes in the rainfall trends were reported. Tyson et al. (1975) argued that several decades of rainfall data are required to establish rainfall trends, something which might raise questions on the work reported by Ademeyo (2014) where less that 30 years of data was analysed, and that of Parida and Moalafhi (2008) where data from 1961 to 2003 was used. Similarly to the total annuall rainfall, the number of rainfall days and the occurrence of extreme rainfall events did not show any evidence of an increasing or decreasing trend.

Drought, a recurring natural hazard in the Ghaap plateau varies in occurrence and intensity and this has implications for the minining and agricultural activities as well as nature conservation via poor recharge of surface and groundwater resources. The Kolomela mine for instance relies entirely on groundwater resources for water needs of the mining operations and further supply water to surrounding communities. Droughts can also negatively impact the human population

and pastoral livelihoods by exacerbating food insecurity and degradation of pastures. A number of tree species, especially in such dry environments, use substantial amounts of water to meet transpiration requirements (Evaristo and McDonnell, 2017), as such poor recharge of groundwater reserves due to recurring droughts will negatively impact on maintenance of valuable genetic diversity. Farming operations, especially drinking livestock also heavily rely on groundwater sources. The more frequent occurrence of droughts will therefore impact on groundwater recharge and hence the ecosystem components that are supported by groundwater sources. The establishment of the SPI values which is useful for determining drought occurrence and severity, and the determination of the interannual rainfall variability is crucial, especially in the context where drought is expected to increase in frequency and severity in the future as a result of climate change (Sheffield et al., 2012). Accurate quantitative information on drought and interannual rainfall variability is necessary to better prepare for such catastrophes (Vincente-Serrano et al., 2012; Masih et al., 2014). Considering that more droughts have occurred post 1990 in the Ghaap plateau, which is predominantly arid, assessments of drought occurrence and severity and interannual rainfall variability in other dryland regions in the country are key to effectively manage the adverse impact of drought on water resources and food security.

3.5 Conclusions

The objective of this study was to determine the occurrence and severity of droughts, and to assess rainfall trends at the Ghaap plateau, which is located in the Northern Cape Province of South Africa. Two main conclusions can be drawn out from this study; i) droughts have become more prevalent in the plateau post 1990, and a majority of them are moderate, and ii) there is no evidence of change in total annual rainfall, numbers of rainfall days and extreme rainfall events in the plateau. The rainfall trends follow secular fluctuating patterns over the years. Such information can be used in climate models as a predictive tool for early warning against immediate future precipitation shortfalls and forecasting of droughts in the long-term. Drought and rainfall variability assessment could be useful for improved mitigation strategies and better planning measures. However, further studies should consider incorporation of other climatic parameters such as temperature to have a holistic perspective of the anticipated climatic variability at regional and continental levels. Even more so, it is essential to understand the impacts of drought and rainfall variability on water resources under changing climate whereby drought is expected to increase in frequency and severity.

References

Ademeyo, J., Otieno, F., Olumuyiwa, O., 2014. Analysis of temperature and rainfall trends in Vaal-Harts Irrigation Scheme, South Africa. Am. J. Eng. Res. 3(2), 265-269.

Al Asheikh, A.A., Tarawneh, Q.Y., 2013. An analysis of dry spells patterns intensity and duration in Saudi Arabia. Middle-East J. Sci. Res. 13(3), 314-327.

Batisani, N., 2011. The spatio-temporal-severity dynamics of drought in Botswana. J. Environ. Protec. 2 803-816. https://doi.org/10.4236/jep.2011.26092

Dai, A., 2011. Drought under global warming: A review. WIREs Clim. Change 2, 45-65.

Evaristo, J., McDonnell, J.J., 2017. Prevalence and magnitude of groundwater use by vegetation: a global stable isotope meta-analysis. Scientific Reports 7, 1-11.

Fernandez-Illescas, C.P., Rodriguez-Iturbe, I., 2004. The impact of interannual rainfall variability on the spatial and temporal patterns of vegetation in a water limited ecosystem. Adv. Water Resour. 27, 83-95.

Gudmundsson, L., van Loon, A.F., Tallaksen, L.M., Seneviratne, S.I., Stagge, J.H., Stahl, K., van Lanen, H.A.J., 2014. Guidelines for monitoring and early warning of drought in Europe. Technical report no. 21. DROUGHT-R&SPI.

Guttman, N.B., 1998. Comparing the Palmer drought index and the standardized precipitation index. J. Am. Water Resour. As. 34(1), 113-121.

Guttman, N.B., 1999. Accepting the standardized precipitation index: A calculation algorithm. J. Am. Water Resour. As. 35(2), 311-322.

Hastie, T.J., Tibshirani, R.J., 1990. *Generalized Additive Models*. Chapman and Hall, London.

Heim, R.R., 2000. Drought indices: A review. In: Wilhite DA (ed) *A Global Assessment, Hazard Disaster Series.* Routledge, New York.

Heim, R.R., 2002. A riveiw of the twentieth-century drought indices used in the United States. B. Am. Met. Soc. 84, 1149-1165.

IPCC, 2012. *Managing the Risks of Extreme Events and Disasters to Advance Climate Change Adaptation*. A Special Report of Working Groups I and II of the Intergovernmental Panel on Climate Change [Field, C.B., V. Barros, T.F. Stocker, D. Qin, D.J. Dokken, K.L. Ebi, M.D. Mastrandrea, K.J. Mach, G.-K. Plattner, S.K. Allen, M. Tignor, P.M., Midgley (eds.)]. Cambridge University Press, Cambridge, UK, and New York, NY, USA.

IPCC, 2014. *Climate Change 2014: Synthesis Report. Contribution of Working Groups I, II and III to the Fifth Assessment Report of the Intergovernmental Panel on Climate Change* [Core Writing Team, Pachauri, R.K., Meyer, L.A., (eds.)]. IPCC, Geneva, Switzerland.

Jain, V.K., Pandey, R.P., Jain, M.K., Byun, H., 2015. Comparison of drought indices for appraisal of drought characteristics in the Ken River Basin. Weather Clim. Extrem. 8, 1-11.

Kampata, J.M., Parida, P.B., Moalafhi, D.B., 2008. Trend analysis of rainfall of the headstream of the Zambezi River Basin in Zambia. Phys. Chem. Earth 33, 621-625.

Keyantash, J., Dracup, J.A., 2002. The quantification of drought: A review of drought indices. B. Amer. Meteor. Soc. 83, 1167-1180.

Komuscu, A.U., 1999. Using the SPI to analyse spatial and temporal patterns of drought in Turkey. Drought Network News 11(1), 7-13.

Kruger, A.C., 2006. Observed trends in daily precipitation indices in South Africa: 1910-2004. Int. J. Climatol. 26, 2275-2285.

Lake, P.S., 2003. Ecological effects of perturbation by drought in flowing waters. Freshwater Biol. 48, 1161-1172.

Ledger, M.E., Brown, L.E., Edwards, F.K., Hudson, L.N., Milner, A.M., Woodward, G., 2013. Extreme climatic events alter aquatic food webs: A synthesis of evidence from a Mesocosm drought experiment. Adv. Ecol. Res. 48, 343-395.

Manatsa, D., Chingombe, W., Matsikwa, H., Matarira, C.H., 2008. The superior influence of Darwin Sea level pressure anomalies over ENSO as a simple drought predictor for Southern Africa. Theor. Appl. Climatol. 92, 1-14.

Masih, I., Maskey, S., Mussá, F.E.F., Trambauer, P., 2014. A review of droughts on the African continent: a geospatial and long-term perspective. Hydrol. Earth Syst. Sci. 18, 3635–3649.

McKee, T.B., Doesken, N.J., Kleist, J., 1993. The relationship of drought frequency and duration of time scales. *Eighth Conference on Applied Climatology*, 17-22 January, Anaheim, California.

Mucina, L., Rutherford, M.C., 2006. *The Vegetation of South Africa, Lesotho and Swaziland.* South African National Biodiversity Institute, Pretoria, South Africa.

Nel, W., 2009. Rainfall trends in the KwaZulu-Natal Drakensberg region of South Africa during the twentieth century. Int. J. Climatol. 29, 1634-1641.

Parida, B.P., Moalafhi, D.B., 2008. Regional rainfall frequency analysis for Botswana using L-Moments and radial basis function network. Phys. Chem. Earth 33, 614-620.

Rouault, M., Richard, Y., 2003. Intensity and spatial extension of drought in South Africa at different time scales. Water SA 29(4), 489-500.

SAS Institute Inc., 2013: SAS/STAT 13.1 User's Guide. Cary, NC: SAS Institute Inc.

Schulze, R.E., 2008. South African atlas of climatology and agrohydrology. Water Research Commission, Pretoria, RSA. WRC Report 1489/1/08, Section 18.3.

Sheffield, J., Wood, E.F., 2007. Characteristics of global and regional drought, 1950-2000: Analysis of soil moisture data from off-line simulation of the terrestrial hydrologic cycle. J. Geophys. Res. 112, 1-21.

Sheffield, J., Wood, E.F., 2008. Projected changes in drought occurrence under future global warming from multimodel, multi-scenarion, IPCC AR4 simulations. Clim. Dyn. 31, 79-105.

Sheffield, J., Wood, E.F., Roderick, M.L., 2012. Little change in global drought over the past 60 years. Nature 491, 435-438.

Tallaksen, L., Van Lanen, H., 2004. *Hydrological Drought: Processes and Estimation Methods for Streamflow and Groundwater*, Elsevier Science B.V., Oxford.

Taufik, M., Setiawan, B.I., van Lanen, H.A.J., 2015. Modification of a fire drought index for tropical wetland ecosystems by including water table depth. Agr. Forest Meteorol. 203, 1-10.

Thornthwaite, C.W., 1948. An approach toward rational classification of climate. Geogr. Rev. 38(1), 55-94.

Tyson, P.D., Cooper, G.R.J., McCarthy, T.S., 2002. Millennial to multi-decadal variability in the climate of Southern Africa. Int. J. Climatol. 22, 1105-1117.

Tyson, P.D., Dyer, T.G.J., Mametse, M.N., 1975. Secular changes in South African rainfall: 1880 to 1972. Quart. J. R. Met. Soc. 101**,** 817-833.

UNESCO, 1979. Map of the World Distribution of Arid Regions. Accompanied by Explanatory Notes. UNESCO, Paris, France. MAB Technical Note No. 17.

Van Loon, A.F., 2015. Hydrological drought explained. Wiley Periodicals Inc. 2, 359-392.

van Vliet, M.H.T., Yearsely, J.R., Ludwig, F., Vögele, S., Lettenmaier, D.P., Kabat, P., 2012. Vulnerability of US and European electricity supply to climate change. Nature Climate Change 2, 676-681.

Vincente-Serrano, S.M., López-Moreno, J.I., Drumond, A., Gimeno, L., Nieto, R., Morán-Tejeda, E., Lorenzo-Lacruz, J., Beguería, S., Zabalza, J., 2011. Effects of warming process on droughts and water resources in the NW Iberian Peninsula. Clim. Res. 48, 203-212.

Vincente-Serrano, S.M., Beguería, S., Gimeno, L., Eklundh, L., Giuliani, G., Weston, D., El Kenawy, A., López-Moreno, J.I., Nieto, R., Ayenew, T., Konte, D., Ardö, J., and Co-authors 2012. Challenges for drought mitigation in Africa: The potential use of geospatial data and drought information systems. Appl. Geogr. 34, 471-486.

Wilhite, D.A., 2000. Drought as a Natural Hazard: Concepts and Definitions,. In: *Drought: A Global Assessment* (Vol 1 and 2), D.A. Wilhite., Routledge Publishers, London.

Xie, H., Ringler, C., Zhu, T., Waqas, A., 2013. Droughts in Pakistan: a spatiotemporal variability analysis using the Standardized Precipitation Index. Water Int. 38(5), 620-631.

4. Precipitation intensity-duration-frequency curves and their uncertainties for Ghaap plateau

Abstract

Engineering infrastructures such as stormwater drains and bridges are designed using the concept of Intensity-Duration-Frequency (IDF) curves, which assume that the occurrence of precipitation patterns and distributions are spatially similar within the drainage area and remain unchanged throughout the lifespan of the infrastructures (stationary). Based on the premise that climate change will alter the spatial and temporal variability of precipitation patterns, inaccuracy in the estimation of IDF curves may occur. As such, prior to developing IDF curves, it is crucial to analyse trends of annual precipitation maxima. This study aimed to estimate the precipitation intensities and their uncertainties for durations of 0.125, 0.25, 0.5, 1, 2, 4, and 6 hours and return periods of 2, 10, 25, 50 and 100 years in the Ghaap plateau, Northern Cape Province, South Africa using the Generalized Extreme Value (GEV) distribution. Annual precipitation maxima were extracted from long-term (1918 to 2014) data for four meteorological stations (Postmasburg, Douglas, Kuruman and Groblershoop) sourced from the South African Weather Services (SAWS). On average, the estimated extreme precipitation intensities for the plateau ranged from 4.2 mm hr^{-1} for 6 hours storm duration to 55.8 mm hr^{-1} for 0.125 hours at 2 years return period. At 100 year return period, the intensity ranged from 13.3 mm hr^{-1} for 6 hours duration to 175.5 mm hr^{-1} for the duration of 0.125 hours. The lower limit of uncertainty ranged from 11.7% at 2 years return period to 26% at 100 year return period, and from 12.8% to 58.4% for the upper limit for the respective return periods. This methodology can be integrated into policy formulation for the design of stormwater and flood management infrastructures in the Ghaap plateau, where mining is the main economic activity.

Key words: Precipitation Intensity-Duration-Frequency curves, Uncertainty levels, Generalized Extreme Value distribution function, Ghaap plateau.

4.1 Introduction

Municipal stormwater management and the design of engineering infrastructures able to withstand floods and extreme precipitation events are often based on the concept of precipitation Intensity-Duration-Frequency (IDF) curves (Jaleel and Farawn, 2013; Logah et al., 2013; Vivekanandan, 2013; Bhatt et al., 2014; Cheng and Aghakouchak, 2014; Wayal and Menon, 2014). IDF curves are commonly developed using historical annual maximum precipitation data fitted to a probability distribution to estimate the precipitation intensity for a given storm duration and return period (Overeem et al., 2008; Cheng and Aghakouchak, 2014). The IDF curves are based on the assumptions that the occurrence of precipitation patterns and distributions are spatially similar within the drainage area and remain unchanged (stationary) throughout the lifespan of the infrastructures (Cheng and Aghakouchak, 2014). However, the occurrence of significant spatial and temporal variability in frequency and intensity of extreme precipitation events due to climate change (Prodanovic and Simonovic, 2007; Simonovic and Peck, 2009; IPPC, 2014) might invalidate these assumptions and compromise the accurate estimation of IDF curves. This in turn can have serious impacts on the design, operation and maintenance of engineering structures (Cheng et al., 2014; Yilmaz et al., 2014) making them inadequate and vulnerable to floods.

Due to rapid urbanization in many municipalities, previously pervious areas are replaced by impervious surfaces, which invariably alter the characteristics of the surface runoff hydrograph (Lee and Bang, 2000; Goonetilleke et al., 2005; Carter and Jackson, 2007). The process of urbanization involves demographic changes and increased economic activity including traffic patterns, which results in compromised air quality (Zhang et al., 2014; Fang et al., 2015). This is also accompanied by rapid increase in the demand for energy; as such a flexible and secure energy policy is required for sustainable growth to avoid environmental degradation due to

energy generation (Grimm et al., 2008; Fang et al., 2015). Urbanization also comes with replacement of vegetation, which intercepts and stores sizable amounts of precipitation water. Consequently, there is an increase in runoff peaks and volumes in relatively shorter time frames (Kim et al., 2003; Goonetilleke et al., 2005; Chen et al., 2016). The frequency and severity of flooding in these areas is exacerbated by the effects of climate change, which involves occurrence of high intensity precipitation events (Dore, 2005; IPPC, 2014). Yilmaz and Perera (2014) reported a non-stationarity of extreme precipitation events for Melbourne between 1925 and 2010. In this study, 1966 was identified as the change point. For the same region, Jones (2012) reported the extreme precipitation events for the period between 1910 and 1967 to be stationary and for the period between 1968 and 2010 as non-stationary.

To address the challenge of extreme precipitation events on engineering structures, an approach that allows for non-stationarity in IDF curves by incorporating a time parameter, has been proposed (Gregersen et al., 2013; Jacob, 2013; Al Saji et al., 2015; Yilmaz et al., 2014). In a non-stationarity climate, methods for assessing changes in precipitation intensity and duration, and their uncertainty are limited (Cheng and Aghakouchak, 2014). Even though Yilmaz et al. (2014; 2017) found that non-stationary models were not superior to stationary models in Melbourne and Victoria (Australia), it is still important to test non-stationary models in other locations. Owing to its flexibility and robustness in modelling maxima and uncertainty limits, the Generalized Extreme Value (GEV) distribution is used in models that allow for non-stationarity in time series (Overeem et al., 2008; Cheng and Aghakouchak, 2014; Gilleland and Katz, 2014). Furthermore, IDF curves provide a good basis for the design of stormwater and flood management infrastructures by estimating uncertainties damage risk of these structures by flooding is minimized.

In South Africa, Mason et al. (1999) analyzed 60-year (1931-1990) annual precipitation data maxima. They reported increases in intensity of extreme precipitation events between 1961 and 1990 compared to the period between 1931 and 1960. Their study covered a large part (70%) of the country, except for the north-east, north-west and the winter precipitation areas. IDF curves and their uncertainties have not been developed for most parts of the country including the study area. The increase in high intensity precipitation events is expected to continue due to climate change (IPPC, 2014) and demands that our infrastructure is able to withstand the negative impacts of these changes (Cheng and Aghakouchak, 2014). In this study, the objective was to estimate the precipitation intensities and their uncertainties (lower and upper limits) for durations of 0.125, 0.25, 0.5, 1, 2, 4 and 6 hours and return periods of 2, 10, 25, 50 and 100 years in the Ghaap plateau, Northern Cape Province, South Africa using the Generalized Extreme Value (GEV) distribution.

4.2 Materials and Methods

4.2.1 Site description

The Ghaap Plateau is situated between Kimberley and Upington, north of the Orange River to the Kuruman Hills, Northern Cape Province, South Africa. Its altitude varies between 900 and 1 600 m above sea level. The topography comprises undulating hills, with moderate slopes and flat plains. The mean annual precipitation ranges between 250 and 400 mm, with the majority falling between November and April. July is the driest month, often with absolutely no precipitation, while March receives the highest amount of precipitation. The average maximum temperatures are 17°C in June and 31°C in January, with average cold temperatures of 0°C in June and July.

The main economic activity on the plateau is open cast mining, which depends primarily on groundwater resources. Second to mining, the economy depends on precipitation driven activities, including agriculture and nature conservation. The predominant soils in the plateau are of the Hutton form with red Aeolian sand of the Kalahari group overlying the volcanic rock and sediments of the Griqualand West Supergroup, which outcrops in some places. The predominant vegetation type is the Savanna Biome, which is composed of the Kuruman Mountain Bushveld and Postmasburg Thornveld (Mucina and Rutherford, 2006).

4.2.2 Selection of meteorological stations and source of precipitation data

Four meteorological stations (Postmasburg, Douglas, Kuruman and Groblershoop) were selected. There are only few meteorological stations in the Northern Cape Province (Figure 4.1), mainly due to the sparse population and aridity of the region (Kruger, 2006). The stations were selected based on their proximity to the Kolomela mine, which was the main experimental site. Table 4.1 shows the geographical position, elevation and record length of precipitation data and average annual precipitation for the selected meteorological stations. Daily precipitation data for all four meteorological stations were obtained from the South African Weather Services (SAWS).

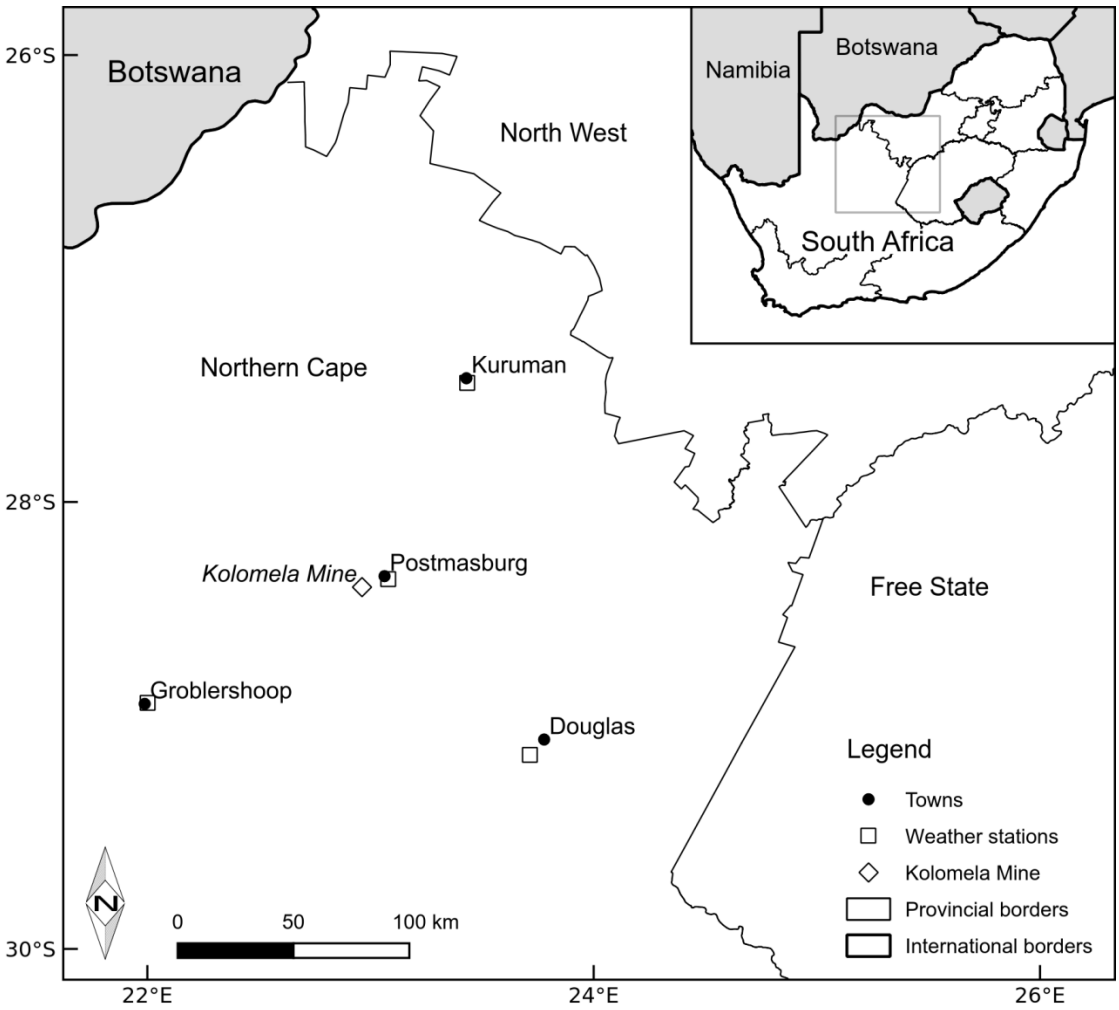

Figure 4.1: Location of selected weather stations used for the development of precipitation Intensity-Duration-Frequency (IDF) curves for the Ghaap plateau in the Northern Cape Province, South Africa.

Table 4.1: Geographical positions, elevation, data recording years and average annual rainfall for Postmasburg, Douglas, Groblershoop and Kuruman in the Ghaap plateau.

Weather station	Latitude	Longitude	Elevation (m.a.s.l)	Period record length	Years	Average rainfall (mm)
Postmasburg	-28.35	23.08	1323	1918 – 2014	97	317
Douglas	-29.13	23.71	1013	1960 – 2014	55	312
Groblershoop	-28.90	22.00	871	1939 – 2014	76	201
Kuruman	-27.47	23.43	1317	1960 – 2014	35	458

4.2.3 Developing precipitation IDF curves

Annual maxima extracted from daily precipitation records were modelled using the GEV distribution for the selected meteorological stations. Firstly, significant trends in the annual maxima were determined. Secondly, point and interval estimates of precipitation intensities were calculated at storm durations of 0.125, 0.25, 0.5, 1, 2, 4, and 6 hours and for return periods of 2, 10, 25, 50 and 100 years. The cumulative distribution function of the GEV(μ, σ, ξ) distribution, for $\xi \neq 0$, is given by:

$$F(x) = \exp\left\{-\left(1 + \xi\left(\frac{x-\mu}{\sigma}\right)\right)^{-\frac{1}{\xi}}\right\} \quad (4.1)$$

Where μ, σ and ξ are the location, scale and shape parameter, respectively (Beirlant et al., 2004; Cheng and AghaKouchak, 2014). Here $F(x)$ is defined for $1+\xi(\frac{x-\mu}{\sigma}) > 0$: elsewhere $F(x)$ is either 0 or 1. For $\xi = 0$, $\xi > 0$ and $\xi < 0$, the GEV leads to the Gumbel, Frechet and Max-Weibull distributions, respectively. To allow for non-stationarity and to determine if there are significant trends in extreme precipitation events, the location parameter of the GEV distribution was allowed to be time dependent following Cheng and AghaKouchak (2014):

$$\mu(t) = \mu_1 t + \mu_0 \quad (4.2)$$

Where t is time, and μ_1 and μ_0 are the respective intercept and slope parameters of the linear model for the GEV location parameter as a function of time. Using SAS procedure MCMC (SAS, 2013), the annual maximum 24-hour precipitation data were fitted to the GEV distribution through a Bayesian method. Specification of the data likelihood and of a prior distribution for the parameters is required (Beirlant et al., 2004) as follows:

$$x_i | \mu, \sigma, \xi \backsim \text{GEV}(\mu, \sigma, \xi), i = 1, \dots, n \quad (4.3)$$

Where x_i is the maximum precipitation for year *i*, and *n* is the number of years of data. With the parameter vector being $\theta = (\mu, \sigma, \xi)$, the prior distribution chosen for the model parameters is the Maximal Data Information (MDI) prior, namely:

$$p(\mu_0, \mu_1, \sigma, \xi) = \exp E\,[\log f(X|\theta)] \propto \frac{1}{\sigma} e^{-\psi(1)(1+\xi)} \quad (4.4)$$

Where $f(X|\theta)$ denotes the probability density function of the distribution, and $\psi(1)$ is Euler's constant (Beirlant et al., 2004). The fit of the Bayesian model yields a joint posterior distribution of the model parameters. Based on this joint posterior distribution, point and interval estimates (the latter are Bayesian Credibility Intervals - BCI) for the model parameters and for suitable functions of model parameters, were calculated. The SAS code for carrying out the analysis is included as supplementary material (Appendix 4.1).

4.3 Results

4.3.1 Point and interval estimates of the GEV parameters

A summary of the point and interval estimates (BCIs) for the location (μ), scale (σ) and shape (ξ) parameters of the GEV distribution fitted to the annual maximum precipitation data for the four meteorological stations is presented in Table 4.2. The estimated μ for the four meteorological stations ranged between 30.9 mm for Douglas to 40.5 mm for Groblershoop. The lower limits for

μ ranged between 27.6 and 34.7 and upper limits ranged between 34.4 and 46.5, also from Douglas and Groblershoop. The scale parameter σ ranged between 12.1 for Kuruman and 17.2 for Postmasburg, with lower limits ranging from 10 to 13.3 and upper limits from 14.5 to 22.1 also from the respective meteorological stations. The ξ ranged from 0 for Groblershoop to 0.2 for Kuruman. Also from the same meteorological stations, the lower limits of the shape parameter ranged from -0.2 to 0 and the upper limits ranged from 0.2 for Groblershoop to 0.4 for both Kuruman and Postmasburg. Thus, the parameters of the fitted GEV distributions for the four stations were quite similar.

Table 4.2: Estimates and Bayesian Credibility Intervals (BCI); (lower and upper limits) for the location (μ), scale (σ) and shape (ξ) parameters of the GEV distribution for annual maximal rainfall data from Postmasburg (97 years), Douglas (55 years), Groblershoop (75 years) and Kuruman (35 years) in the Ghaap plateau.

Station	**Location parameter (μ)**			**Scale parameter (σ)**			**Shape parameter (ξ)**		
	Estimate	BCI		Estimate	BCI		Estimate	BCI	
		Lower limit	Upper limit		Lower limit	Upper limit		Lower limit	Upper limit
Postmasburg	34.6	29.5	40.2	17.2	13.3	22.1	0.1	-0.1	0.4
Douglas	30.9	27.6	34.4	13.5	11.0	16.5	0.2	0.0	0.4
Groblershoop	40.5	34.7	46.5	16.1	12.3	21.3	0.0	-0.2	0.2
Kuruman	32.9	30.2	35.7	12.1	10.0	14.5	0.2	0.0	0.3

4.3.2 Precipitation intensities and uncertainty

The precipitation intensities for Postmasburg shown in Figure 4.2 (solid lines) for short duration (0.125 hours) ranged from 51.9 mm hr^{-1} at return period of 2 years to 161 mm hr^{-1} at longer return period of 100 years. For the longer duration of 6 hours the intensity was 3.9 mm hr^{-1} at 2 year return period and 12.2 mm hr^{-1} at 100 years return period. At Douglas (Figure 4.3) the intensity for short duration (0.125 hours) ranged from 56.9 mm hr^{-1} to 202.3 mm hr^{-1} at the 2 and 100 year return periods respectively. Six hour duration intensity was 4.3 mm hr^{-1} at 2 year return period and 15.3 mm hr^{-1} at the 100 year return period. At Groblershoop (Figure 4.4), the intensity for 0.125 hours duration was 49.9 mm hr^{-1} at 2 year return period and 178.5 mm hr^{-1} at the return period of 100 years. Kuruman (Figure 4.5) had a precipitation intensity of 64.3 mm hr^{-1} and 160.2 mm hr^{-1} at the 2 and 100 year return periods respectively for short duration (0.125hours) storms. For the duration of 6 hours the intensities were 3.9 mm hr^{-1} at 2 years return period and 12.2 mm hr^{-1} at 100 year return period. As expected, in all the meteorological stations, the intermediate storm durations (0.25, 0.5, 1, 2, and 4 hours) and return periods (10, 25, and 50

years) had intensities that fall within the presented extremes at durations 0.125 and 6 hours, as well as return periods of 2 and 100 years.

In Figures 4.2-4.5, broken lines indicate the BCIs for the estimated IDF curves (solid lines), thus providing an indication of the uncertainty associated with the reported estimates. The narrowest range of uncertainty at Postmasburg (Figure 4.2) was from 3.6 mm hr^{-1} to 4.3 mm hr^{-1} at 2 year return period and 6 hours duration. The corresponding lower and upper limits of the estimated intensity (3.9 mm hr^{-1}) deviated by 8.3% and 9.1%, respectively. Higher uncertainty levels at Postmasburg ranged from 123.3 mm hr^{-1} to 234 mm hr^{-1} at 100 year return period and 0.125 hours duration. The corresponding lower and upper limits deviated by 23.4% and 45%, respectively.

At Douglas (Figure 4.3), a narrow uncertainty ranged from 3.7 mm hr^{-1} to 5.0 mm hr^{-1} at a return period of 2 years and 6 hours duration. These corresponded to respective lower and upper limit deviations of 14.4% and 15.8% from the estimated intensity of 4.3 mm hr^{-1}. The widest range of uncertainty from 87.6 mm hr^{-1} to 231.6 mm hr^{-1} at 100 year return period and 2 hours duration had a corresponding lower and upper limit deviation of 31.3% and 81.7%, respectively.

A narrow uncertainty range from 3.4 mm hr^{-1} to 4.2 mm hr^{-1} at Groblershoop (Figure 4.4) was observed at 2 year return period and 6 hour duration. These corresponded to respective lower and upper limit deviations of 10.6% and 11.7%. The highest uncertainty range from 130.4 mm hr^{-1} to 273.7 mm hr^{-1} was observed at 100 year return period and 2 hour duration corresponding to lower and upper limit deviations of 26.9% and 53.4%, respectively.

At Kuruman (Figure 4.5) a narrow range 4.2 mm hr^{-1} to 5.6 mm hr^{-1} was observed at return period of 2 years and duration of 6 hours, corresponding to deviations of 13.4% and 14.6 for the lower and upper limits, respectively. The highest range of uncertainty for this station was from

124.3 mm hr^{-1} to 245.3 mm hr^{-1} at 100 year return period and 6 hour duration, corresponding to deviations of 22.4% and 53.1% for the lower and upper limit, respectively.

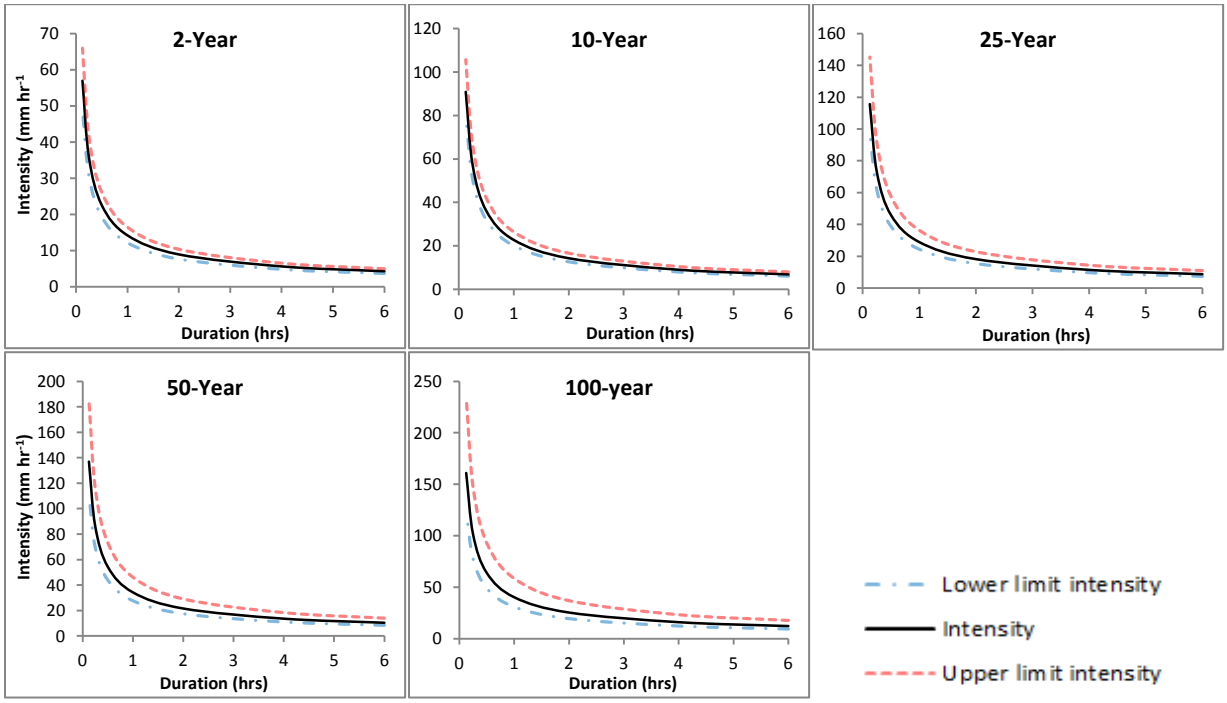

Figure 4.2: Precipitation Intensity-Duration-Frequency (IDF) curves (intensity) and uncertainties (lower and upper limits) for Postmasburg, on the Ghaap plateau, given by Generalized Extreme Value (GEV) distribution for storm durations of 0.125 to 6 hours at 2 to 100 year return periods.

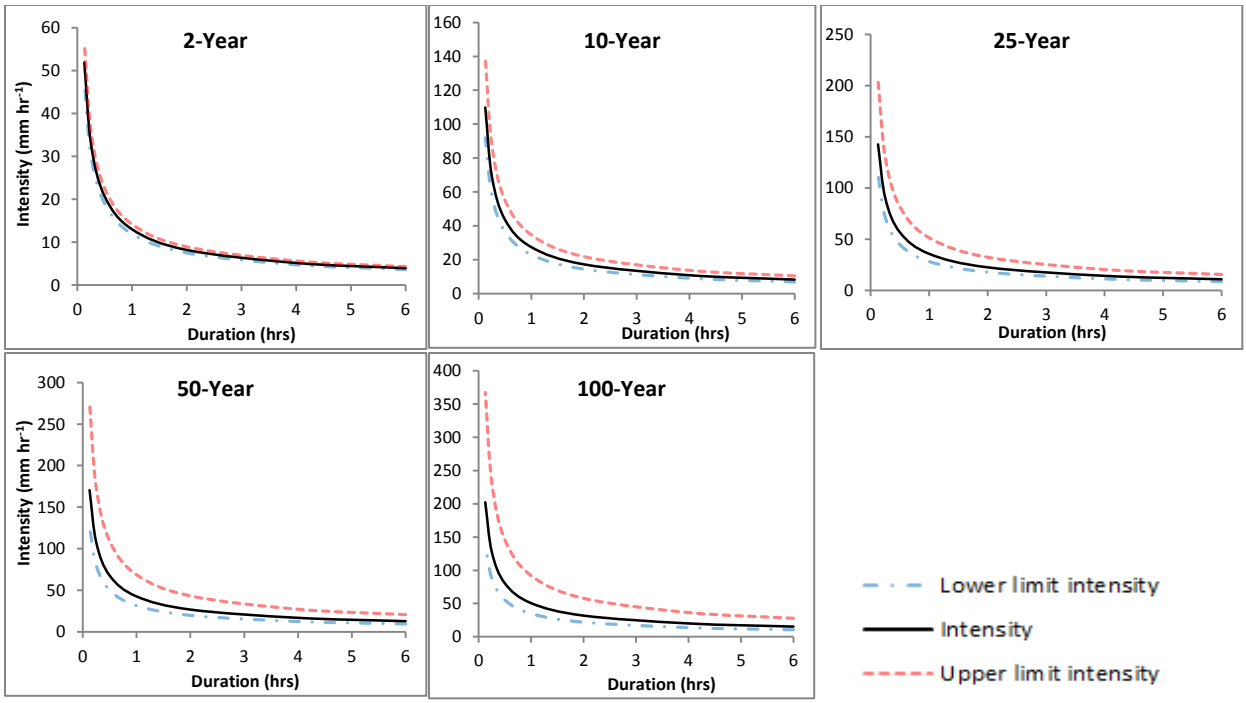

Figure 4.3: Precipitation Intensity-Duration-Frequency (IDF) curves (intensity) and uncertainties (lower and upper limits) for Douglas, on the Ghaap plateau, given by Generalized Extreme Value (GEV) distribution for storm duration of 0.125 to 6 hours at 2 to 100 year return periods.

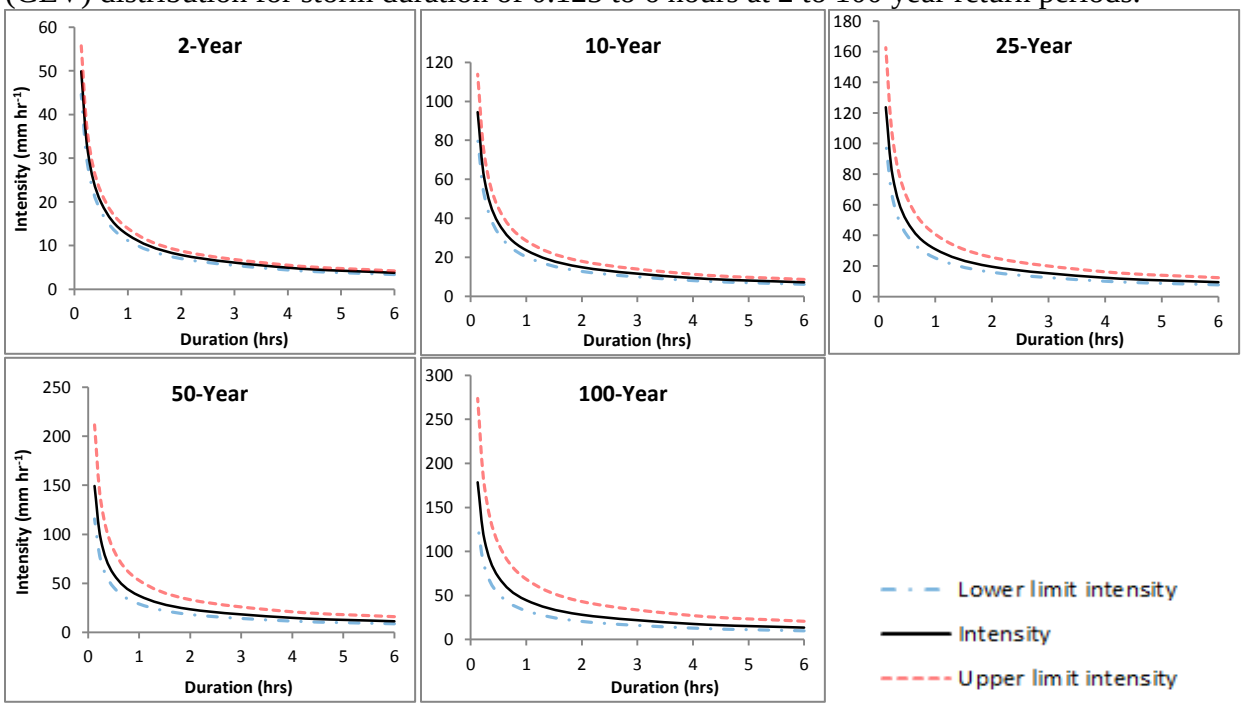

Figure 4.4: Precipitation Intensity-Duration-Frequency (IDF) curves (intensity) and uncertainties (lower and upper limits) for Groblershoop, on the Ghaap plateau, given by Generalized Extreme Value (GEV) distribution for storm duration of 0.125 to 6 hours at 2 to 100 year return periods.

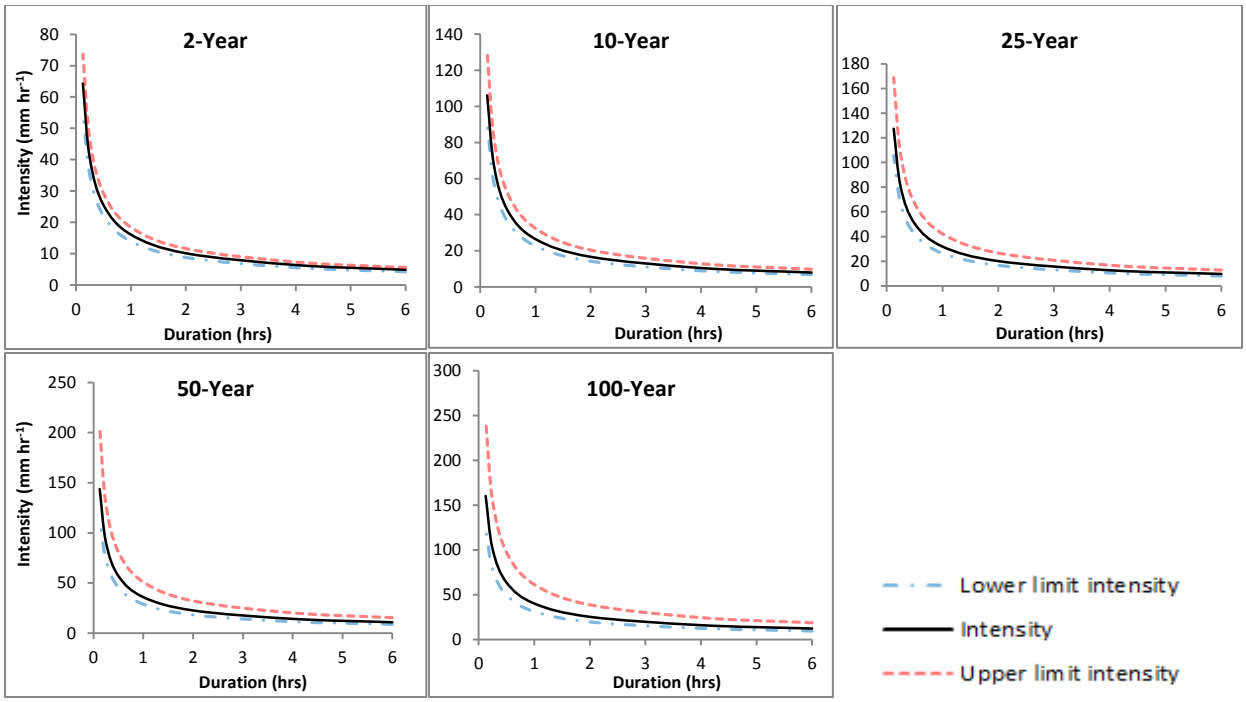

Figure 4.5: Precipitation Intensity-Duration-Frequency (IDF) curves (intensity) and uncertainties (lower and upper limits) for Kuruman, on the Ghaap plateau, given by Generalized Extreme Value (GEV) distribution for storm duration of 0.125 to 6 hours at 2 to 100 year return periods.

4.4 Discussion

4.4.1 Estimated GEV parameters for meteorological stations

For all the meteorological stations used in this study, the initial fit of the GEV distribution with time-dependent location parameter ($\mu(t) = \mu_0 + \mu_1 t$) showed that there was no significant time trend (that is, stationarity can reasonably be assumed) since the estimate of the slope parameter μ_1 (0.1) was close to zero, and its BCI included the value zero. This implies that there is no evidence that the precipitation extremes on the Ghaap plateau have changed significantly over time within the data recording period. According to IPPC (2014), the impacts of climate change are not going to be similar in different regions, with some locations showing large effects, whereas in some no significant changes will be observed, as was the case in the present study area.

4.4.2 On precipitation intensities and uncertainties

On average, the estimated precipitation intensity at 2 year return period ranged from 4.2 mm hr^{-1} for long duration (6 hours) storms to 55.8 mm hr^{-1} for short duration storms (0.125 hours). For the 100 year return period, the precipitation intensity ranged from 13.3 mm hr^{-1} for 6 hours duration to 175.5 mm hr^{-1} for the duration of 0.125 hours. The range of precipitation intensity values is similar to ranges reported elsewhere under similar conditions. For instance, Jaleel and Farawn (2013) used the Gumbel Distribution (GD) to develop IDF curves for Basrah City in Iraq, which has a mean annual precipitation of 161 mm. Using data from 1980 to 2010 they estimated intensities of up to 55 mm hr^{-1} at return periods of 2 years, and up to 170 mm hr^{-1} at 100 year return period. In contrast, higher precipitation intensities were recorded from 1960 to 2005 in higher rainfall areas (up to 5000 mm yr^{-1}). In Bangladesh (Rashid et al., 2012) and India (Bhatt et al., 2014) higher precipitation intensities of up to 985 mm hr^{-1} for 0.167 hours duration and 100 year return period were estimated using the GD. Concurring with other studies (Bazaraa and Ahmed, 1991; AlHassoun, 2011; Ahmed et al., 2012; Elsebaie, 2012), the findings of the present study revealed that the precipitation intensity is inversely proportional to the duration and directly proportional to the return periods, implying that high intensity storms normally last for short durations. This also implies that the high intensity storms with greater potential to damage infrastructures and the environment have a lower frequency of occurrence.

On average, the lower limit of uncertainty, associated with over estimating the risk posed by high intensity precipitation events, and hence over costing infrastructures, ranged from 11.7% at 2 year return period to 26% at 100 year return period. On the other hand, the upper limit, associated with under estimating the risk of infrastructure damage by flooding was 12.8% at 2 year return period and 58.4% at 100 year return period. The uncertainty level increased with an

increase in return period, meaning, the high intensity storms occurring at longer return periods have a higher risk of over or under estimation. The uncertainty in formulation of IDF curves is often disregarded, leading to over or under estimating the risks posed by high intensity precipitation events.

With high intensity precipitation events expected to be more frequent due to climate change (IPPC, 2014), it is important to have IDF curves available for specific locations. In this way municipal stormwater can be better managed and damage to engineering infrastructures by floods, minimized. The present study area is dominated by a growing mining sector, which is associated with rapid urbanization. Urbanization will induce changes such as removal of vegetation and infrastructure development. Vegetation intercepts and stores precipitation, whereas building and pavement infrastructure renders previously pervious areas to be impervious. The subsequent altering of the area's hydrology by reducing the infiltration area and increasing the drainage output will benefit from updated IDF curves, which include uncertainty levels. Engineers may use the IDF curves and uncertainties to properly advise administrators and policy makers on further development of the Ghaap plateau. Insight into the quantification of peak runoff outputs during extreme precipitation events can be given, and hence provide adequate information for infrastructure design.

4.5 Conclusions

The objective of the present study was to estimate the precipitation intensities and their uncertainties for durations of 0.125, 0.25, 0.5, 1, 2, 4, and 6 hours and return periods of 2, 10, 25, 50 and 100 years in the Ghaap plateau, Northern Cape Province, South Africa. The conclusions drawn from this study were that; i) the extreme precipitation on the plateau exhibited consistent trends, ii) the high intensity storms posing higher risk of damage to infrastructure and the environment are less frequent than low intensity storms. However, of critical concern is that their probability of over or under estimation (uncertainty) is higher. In the Ghaap plateau, the development of IDF curves is crucial for stormwater management and design of engineering infrastructures. Administrators and policy makers can use the IDF curves when planning development on the plateau. Further studies should prioritise recording, storage and use of long-term precipitation data to develop IDF curves for other areas of the country, and at regional and continental levels. It is essential to understand and quantify the impacts of increased stormwater and flooding on infrastructure and even on the environment. This is especially so under the context of climate change, where high intensity precipitation events are expected to increase in frequency and magnitude. Future work must also consider assessing the trends of urbanization, particularly removal of vegetation and infrastructure development, which make pervious surfaces to be impervious and changes the surface runoff characteristics of landscapes.

References

Ahmed, Z., Rao, D.R., Reddy, K.R.M., Raj, E., 2012. Rainfall intensity variation for observed and derived data – a case study of Imphal. APRN J. Eng. App. Sci. 7(11), 1506-1513.

Al Saji, M., O'Sullivan, J.J., O'Connor, A., 2015. Design impact and significance of non-stationarity of variance in extreme rainfall. Proc. IAHS. 371, 117-123.

AlHassoun, S.A., 2011. Developing empirical formulae to estimate rainfall intensity in Riyadh region. J. King Saud Univ. 23, 81-88.

Bazaraa, A.S., Ahmed, S. 1991. Rainfall characterization in an arid area. Engi. J. Qatar Univ. 4, 35-50.

Beirlant, J., Goegebeur, Y., Teugels, J., Segers, J., 2004. Statistics of Extremes. Theory and Applications. Chichester: Wiley.

Bhatt, J.P., Gandhi, H.M., Gohil, K.B., 2014. Generation of intensity duration frequency curves using daily rainfall data for different return periods. J. Inter. Aca. Res. Multidisc. 2(2), 717-722.

Carter, T., Jackson, C.R., 2007. Vegetated roofs for stormwater management at multiple spatial scales. Landsc. Urban Plan. 80, 84-94.

Chen, Y., Samuelson, H. W., Tong, Z., 2016. Integrated design workflow and a new tool for urban rainwater management. J. Environ. Manage. 180, 45-51.

Cheng, L., AghaKouchak, A., 2014. Nonstationary precipitation Intensity-duration-frequency curves for infrastructure design in a changing climate. Scientific Reports 4, 1-6.

Cheng, L., AghaKouchak, A., Gilleland, E., Katz, R.W., 2014. Non-stationary extreme value analysis in a changing climate. Climatic Change 127, 353-369.

Dore, M.H., 2005. Climate change and changes in global precipitation patterns: what do we know? Environ. Int. 31, 1167-1181.

Elsebaie, I.H., 2012. Developing rainfall intensity-duration-frequency relationship for two regions in Saudi Arabia. J. King Saud Univ. Eng. Sc. 24, 131-140.

Fang, G.E., Liu, H., Li, G., Sun, D., Miao, Z., 2015. Estimating the impact of urbanization on air quality in China using spatial regression models. Sustainability 7, 15570-15592.

Gilleland, E., Katz, R.W., 2014. New software to analyze how extremes change over time. Eos 92(2), 13-14.

Gregersen, I.B., Madsen, H., Rosbjerg, D., Arnbjerg-Nielsen, K., 2013. A spatial and nonstationary model for the frequency of extreme rainfall events. Water Resour. Res. 49, 127-136.

Goonetilleke, A., Thomas, E., Ginn, S., Gilbert, D., 2005. Understanding the role of land use in urban stormwater quality management. J. Environ. Manage. 74, 31-42.

Grimm, N.B., Faeth, S.H., Golubiewski, N.E., Redman, C.L., Wu, J.G., Bai, X.M., Briggs, J.M., 2008. Global change and the ecology of cities. Science 319, 756-760.

IPCC, 2014. Climate Change 2014: Synthesis Report. Contribution of Working Groups I, II and III to the Fifth Assessment Report of the Intergovernmental Panel on Climate Change (IPCC), Geneva, Switzerland.

Jacob, D., 2013. Nonstationarity in extremes and engineering design. In: AghaKouchak, A., Easterling, D., Hsu, K., Schubert, S., Sorooshian, S. (eds.), Extremes in a Changing Climate. Springer, Dordrecht, pp 363–417.

Jaleel, L.A., Farawn, M.A., 2013. Developing rainfall intensity-duration-frequency relationship for Basrah city. Kufa J. Eng. 5(1), 105-112.

Jones, R.N., 2012. Detecting and attributing nonlinear anthropogenic regional warming in south-eastern Australia. J. Geophys. Res. 117, D04105, doi:10.1029/2011JD016328

Kim, H., Seagren, E.A., Davis, A.P., 2003. Engineered bioretention for removal of nitrate from stormwater runoff. Water Environ. Res. 355-367.

Kruger, A.C., 2006. Observed trends in daily precipitation indices in South Africa: 1910-2004. Int. J. Climatol. 26, 2275-2285.

Lee, J.H., Bang, K.W., 2000. Characterization of urban stormwater runoff. Water Res. 34, 1773-1780.

Logah, F.Y., Kankam-Yeboah, K., Bekoe, E.O., 2013. Developing short duration rainfall intensity frequency curves for Accra in Ghana. Inter. J. Lat. Res. Eng. Comp. 1(1), 67-73.

Mason, S.J., Waylen P.R., Mimmack, G.M., Rajaratnam, B., Harrison, J.M., 1999. Changes in extreme rainfall in South Africa. Climatic Change 41, 249-257.

Mucina, L., Rutherford, M.C., 2006. The vegetation of South Africa, Lesotho and Swaziland, South African National Biodiversity Institute, Pretoria, South Africa.

Overeem, A., Buishand, A., Holleman, I., 2008. Rainfall depth-duration-frequency curves and their uncertainties. J. Hydrol. 348, 124-134.

Prodanovic, P., Simonovic, S.P., 2007. Development of rainfall intensity duration frequency curves for the city of London under changing climate. Water Resources Research Report no: 058, UK.

Rashid, M.M., Faruque, S.B., Alam, J.B., 2012. Modeling of short duration rainfall intensity duration frequency (SDR-IDF) equation for Sylhet City in Bangladesh. APRN J. Sci. Tech. 2(2), 92-95.

SAS Institute Inc, 2013. SAS/STAT 13.1 User's Guide. Cary, NC: SAS Institute Inc.

Simonovic, S.P., Peck, A., 2009. Updated rainfall intensity duration frequency curves for the city of London under changing climate. Water Resources Research Report no: 065, UK.

Vivekanandan, N., 2013. Development of intensity-duration-frequency relationships using OSA estimators of probability distributions. J. Res. Archit. Civil Eng. 1(2), 1-7.

Wayal, A.S., Menon, K., 2014. Intensity-duration-frequency curves and regionalization. Inter. J. Innov. Res. Adv. Eng. 1(6), 28-32.

Yilmaz, A., Hossain, I., Perera, B., 2014. Effect of climate change and variability on extreme rainfall intensity-frequency-duration relationships: a case study of Melbourne. Hydrol. Earth Syst. Sci. 18, 4065-4076.

Yilmaz, A., Perera, B., 2014. Extreme rainfall nonstationarity investigation and intensity-frequency-duration relationship, J. Hydrol. Eng. 19, 1160-1172.

Yilmaz, A.G., Imteaz, M.A., Perera, B.J.C., 2017. Investigation of non-stationarity of extreme rainfalls and spatial variability of rainfall intensity-frequency-duration relationships: a case study of Victoria, Australia. Int. J. Climatol. 37(1), 430-442.

Zhang, D., Liu, J., Li, B., 2014. Tackling air pollution in China - what do we learn from the great smog of 1950s in London. Sustainability 6, 5322-5338.

5. A new *in situ* procedure for sampling indigenous tree – soil monoliths to study water use in lysimeters

Abstract

Transplanting of grown trees into lysimeters to study their water use has been a challenge because of their massive sizes and low probability to stand transplant shock. The aim of this study was to develop a procedure for sampling already grown trees for water use analysis in lysimeters. Four indigenous trees, *Vachelia karroo, Olea Africana, Sersia lancea* and *Ziziphus mucronata*, were sampled together with 1.2 m^3 soil monolith using a locally designed sampler. A step by step procedure for sampling is presented and illustrated. The water use of the trees, measured two years after transplanting, ranged between 7 and 14 L day^{-1}. These are within the range of water use for the trees of these sizes under investigation. It was concluded that the procedure is appropriate for tree – soil monolith sampling. With these lysimeter units, tree water use related studies can be carried out producing high quality data for decision making and support.

Keywords: Indigenous trees, soil monolith sampling procedure, lysimeter studies, tree water use

5.1 Introduction

Lysimeters have been used for a long time (Kohnke et al., 1940) and still remain one of the standard procedures which other methods are calibrated against to establish water use by plants (McLay, 1992; Johnson et al., 2005; Yoder et al., 2005; Allen et al., 2011; Phogat et al., 2013). Lysimeter is a means of direct measurement and provides accurate quantity of water consumed by the crop (Payero and Irmak, 2008). The device can be in the form of repacked soils or soil monolith. Irrespective of the crops, the soil water dynamics, root development and plant growth in repacked soil lysimeters are severely altered from the natural field conditions (Meyer et al., 1990; Tan et al., 1990; Cameron et al., 1992; McLay et al., 1992) making undisturbed soils to be the better option. However, it is not easy to sample soil monolith together with living trees for lysimeter studies. In previous research where lysimeters were used to study tree water use, trees were planted in already established lysimeter facilities instead of transplanting grown trees (Renquist et al., 1994; Müller, 2009; Müller and Bolte, 2009; Phogat et al., 2013; Puppo et al., 2014). The limitation here is the time the trees require to grow to a stage where meaningful data for grown trees will be produced. Thus, the need for tree-soil monolith sampling methodology for quicker tree water use studies in lysimeters.

However, there are constraints when setting up a tree-soil monolith in a lysimeter. The set-up, labour, cost, technical know-how, sampling procedures and transportation are among these challenges (Allaire and van Bochove, 2006). Majorly, there is lack of information on the techniques used for sampling and setting up soil monoliths especially for trees (Thomson et al., 1997; Meshkat et al., 1999; Allaire and van Bochove, 2006). A sampling procedure was employed by Hensley (1984) where a soil block was wrapped in metal sheets before hammering a base plate underneath. This practice (hammering) is more likely to shake the soil and affect its

structure or affect the root-soil contact if there is a plant growing on the soil block. Keeping the soil structure intact during the sampling is part of the challenges faced during the sampling procedures (Allaire and van Bochove, 2006; Meissner et al., 2009). This is of critical importance for establishing flow and transport conditions that corresponds approximately to natural field conditions (Allaire and van Bochove, 2006; Meissner et al., 2009). Green et al. (2003) isolated the soil monolith with the tree from the surroundings by digging a trench around the canopy area and aligned it with plywood wall before back filling the trench with soil. This was done to eliminate lateral flow of water but, without completely detaching the soil block from its natural position at the bottom. Another procedure was reported by Cameron et al. (1992) where a monolith was dug out and a lysimeter wall constructed around it before being transported to the laboratory. The reported sampled monolith was small and had no plant on it. In respect to current situation, any sampling procedure for soil monolith should be able to avoid structural damages, premature death of the trees and substantially reduce the cost incurred during monolith extraction.

Sampling of monoliths with trees for lysimeter studies has not been well documented prior to the present study. Therefore, a procedure enabling sampling already grown trees in a monolith form without affecting their physiological functioning such as transpiration, and hence buying time spent waiting for them to grow in the lysimeter facility is required. The aim of this paper is to present a sampling procedure for moderately grown indigenous trees with soil monoliths for water use studies in lysimeters.

5.2 Sampling equipment and procedure

5.2.1 Study site description

The procedure was developed at the Kenilworth Experimental Farm, Department of Soil, Crop and Climate Sciences, University of the Free State, Bloemfontein, South Africa. The farm is located at latitude -29.02°, longitude 26.15° and altitude 1354 m. The area is categorized as semi-arid, with mean annual rainfall of 528 mm mostly falling between October and April. The annual mean minimum and maximum temperatures are 11.0 °C and 25.5 °C, respectively. Three trees used in this study were sampled within a radius of 3 km from the farm while the fourth tree was sampled within the premises of the Bloemfontein campus of the university (15 km south west of the farm). The soil form where the first three trees were sampled was Plinthustulf (Soil Survey Staff, 2014) or Bainsvlei (Soil Classification Working Group, 1991). The soil form where the fourth tree was sampled at the campus was Fibrists (Soil Survey Staff, 2014) or Bloemdal (Soil Classification Working Group, 1991).

Laboratory analysis of the soil samples presented in Table 5.1 showed that the soils were sandy loam (68-79% sand, 6-16% silt and 8-21% clay), loamy fine sand (79-88% sand, 5-12% silt and 5-10% clay), sandy clay loam (49-67% sand, 1-17% silt and 21-33% clay) and sandy clay (49% sand, 16% silt and 35% clay). The bulk density ranged from 1.15 g cm^{-3} to 1.29 g cm^{-3} for sandy loam, 1.35 g cm^{-3} to 1.42 g cm^{-3} for loamy fine sand, 1.17 g cm^{-3} to 1.27 g cm^{-3} for sandy clay loam and 1.15 g cm^{-3} for the sandy clay. The pH ranged between 5.81 and 7.31 amongst the three textural classes.

Table 5.1: Soil textural characteristics at different depths for the 4 sampling stations where the trees were sampled together with soil monoliths.

Station	Soil class	Depth (m)	% sand	% silt	% clay	B. density (g/cm^3)	pH
1	Sandy loam	0-0.15	77	10	11	1.16	7.31
1	loamy fine sand	0.15-0.3	83	8	9	1.35	7.24
1	loamy fine sand	0.3-0.5	88	7	5	1.39	7.11
1	loamy fine sand	0.5-0.7	88	5	6	1.42	6.93
1	loamy fine sand	0.7-0.9	86	6	7	1.39	6.59
1	Loamy fine sand	0.9-1.2	83	7	10	1.38	6.4
2	sandy loam	0-0.15	74	16	8	1.17	7.1
2	loamy fine sand	0.15-0.3	79	12	8	1.39	7.12
2	sandy loam	0.3-0.5	79	10	10	1.20	6.86
2	Sandy clay loam	0.5-0.7	67	9	21	1.27	6.56
2	Sandy clay loam	0.7-0.9	67	7	25	1.19	6.27
2	Sandy clay loam	0.9-1.2	65	9	26	1.18	6.3
3	loamy fine sand	0-0.15	82	7	10	1.39	6.5
3	sandy loam	0.15-0.3	78	7	14	1.27	6.34
3	sandy loam	0.3-0.5	73	6	19	1.30	6.1
3	sandy loam	0.5-0.7	74	6	18	1.15	6.07
3	sandy loam	0.7-0.9	75	7	18	1.19	6
3	Sandy loam	0.9-1.2	72	7	21	1.18	6.2
4	sandy loam	0-0.15	76	13	10	1.29	5.81
4	sandy loam	0.15-0.3	70	16	15	1.13	5.95
4	sandy loam	0.3-0.5	68	15	15	1.29	6.1
4	sandy loam	0.5-0.7	68	12	19	1.23	6.09
4	Sandy clay loam	0.7-0.9	49	17	33	1.17	6.82
4	Sandy clay	0.9-1.2	49	16	35	1.15	6.6

5.2.2 Equipment

The sampling equipment and the lysimeter containers were designed at the Department of Soil, Crop and Climate Sciences of the University of the Free State and constructed locally by a reputable Engineering Company in Bloemfontein. The sampler (Figure 5.1), made of 5 mm thick metal sheets, was designed to have two segments; the lower segment (LS), 0.4 m in height, can be dismantled from the upper segment (US) which is 0.8 m. Both the LS and US have three fixed sides and the fourth side is a door, referred to here as LD for the lower door and UD for the upper door. These doors can be removed when necessary. All the surfaces including the doors

have V-shaped steel beams for support against the side pressure exerted by the mass of the soil monolith during sampling. The LS has two tracks at the base of the two opposite sides of the fixed frame. The base plates (BPs) are pushed through these tracks on completion of the excavation. The sampler is 1 m x 1 m x 1.2 m depth making a volume of 1.2 m^3. Lysimeter containers with equal dimensions as the sampler were also constructed. These had three sides and a base, and were made of galvanized metal sheets (5 mm thick). The fourth side was closed with a Perspex material (10 mm thick) to allow monitoring the root development.

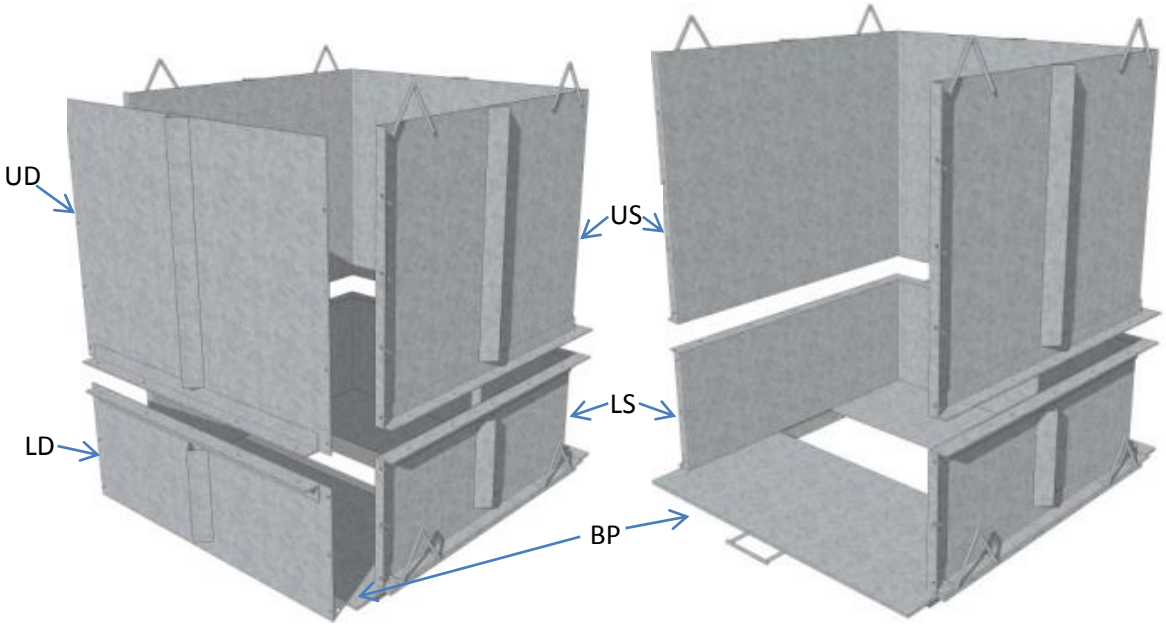

Figure 5.1: Design of sampler that illustrates the two segments of the sampler, i.e. the upper segment (US) and the lower segment (LS) with the base plate (BP) that slides on the LS. Both segments are equipped with doors, i.e. the upper door (UD) and lower door (LD).

5.2.3 Tree selection

With permission granted by the Department for Environmental Affairs, Government of South Africa, four indigenous trees, sweet thorn (*Vachelia karroo*), wild olive (*Olea africana*), black karee (*Sersia lancea*) and buffalo thorn (*Ziziphus mucronata*), were selected for sampling. The trees selected were approximately 2-3 m height and stem diameter between 80 and 120 mm. Part

of the criteria was to look for healthy trees to increase survival probability during sampling and transplanting. Trees with single and comparatively straight stems were selected for ease of installing them with sap flow meters to monitor their water use.

5.2.4 Monolith sampling procedure

Soil preparation before sampling

Two to three days before sampling of the trees, an area of 2 m x 2 m was thoroughly wetted (2.5 m^3 of water) around the target tree. The wetting helped to lower the soil strength (Al Aqtash and Bandini, 2015; Wang et al., 2016) in preparation for digging the trench around the tree, and provided sufficient water within the monolith to meet atmospheric demand during the process of sampling.

Soil excavation and sliding sampler over monolith

During sampling, the LS of the sampler was placed around the stem (Figure 5.2a) before closing with LD (Figure 5.2b) ensuring the stem is at the centre. The soil along the outside of the sampler was then carefully trimmed using a spade and protruding roots were trimmed using secateurs. The sampler was slid downward over the monolith gradually, simultaneously with the excavation exercise (Figure 5.2c-f).

Installing base plate:

On completion of the excavation and sliding of the sampler, two metallic BPs sharpened at the front were driven through the designed tracks from opposite ends at the base of the sampler using a hydraulic jack (Figure 5.2g). In other studies (Hensley, 1984; Cameron et al., 1992) the BPs were driven in by hammering, which shook the monolith and possibly altered the soil structure and hence affected the root – soil contact. The use of a hydraulic jack in this procedure presents a

smooth insertion of the BPs, something which was lacking in methodologies presented by other researchers previously. The BPs are the ones which cut the taproot if it existed at that depth. However, if the taproot could not be cut using BP, a hole was dug beneath the BP and the tap root was cut using a hand saw.

Lifting and transport of monolith

The enclosed soil monolith was tied with webbing straps at the design hooks of the sampler (Figure 5.2h). The webbing straps were then hooked to a chain block supported by a two legged stand made of steel. The tree with its soil was lifted up and a lowbed trailer was driven under it. Four tyres were placed on the lowbed trailer to act as shock absorbers to the monolith during transportation to Kenilworth Experimental Farm. The actual sampling process and transplanting of the trees is further illustrated by Appendices 5.1, 5.2 and 5.3.

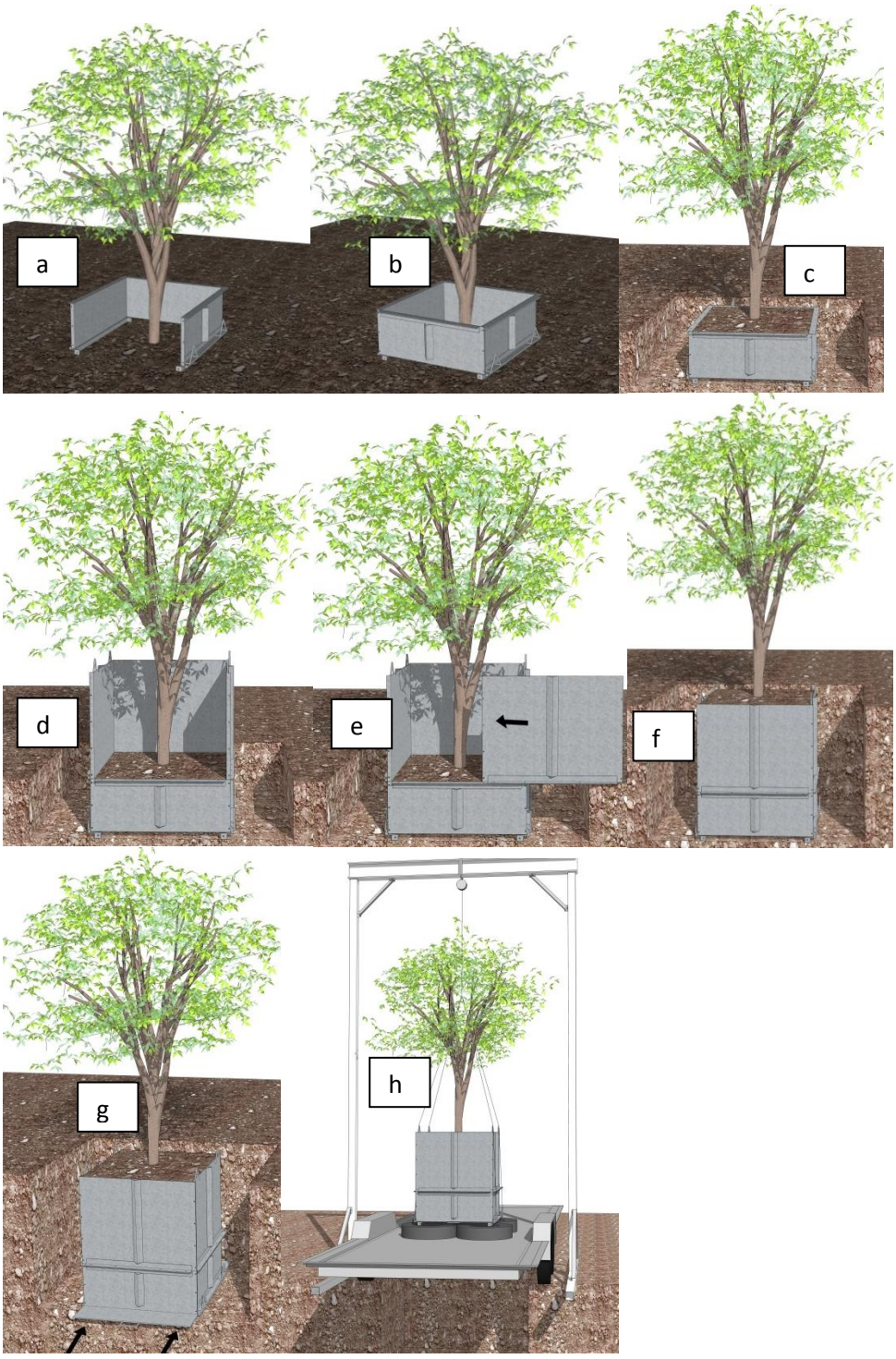

Figure 5.2: Step by step proceedure for tree-soil monolith sampling, from excavation and sliding sampler (a-f), installing base plate (g) and lifting and monolith transportation (h).

5.2.5 Transfer of monoliths to lysimeter containers

At Kenilworth farm, the trees were transplanted into the lysimeter containers as follows:

i) A metal sheet cut to a square of 0.9 m x 0.9 m with at least 6 bolts welded on the lower side was placed underneath the sampler before pulling out the two BPs (Figure 5.3a).

ii) After the base plates were removed, some straps were pushed down through the inside of the sampler, passed below the new metal sheet and upward inside the sampler from opposite surfaces. The soil monolith with the tree was rested on the newly placed metal sheet and hung from the straps with the sampler supporting the soil on the sides (Figure 5.3b).

iii) With the soil monolith and the tree lifted high, the lysimeter container was positioned directly underneath. The soil monolith and the tree were released slowly into the lysimeter. The sampler was removed by dismantling it step by step starting with the top segment as its contents were lowered into the lysimeter container.

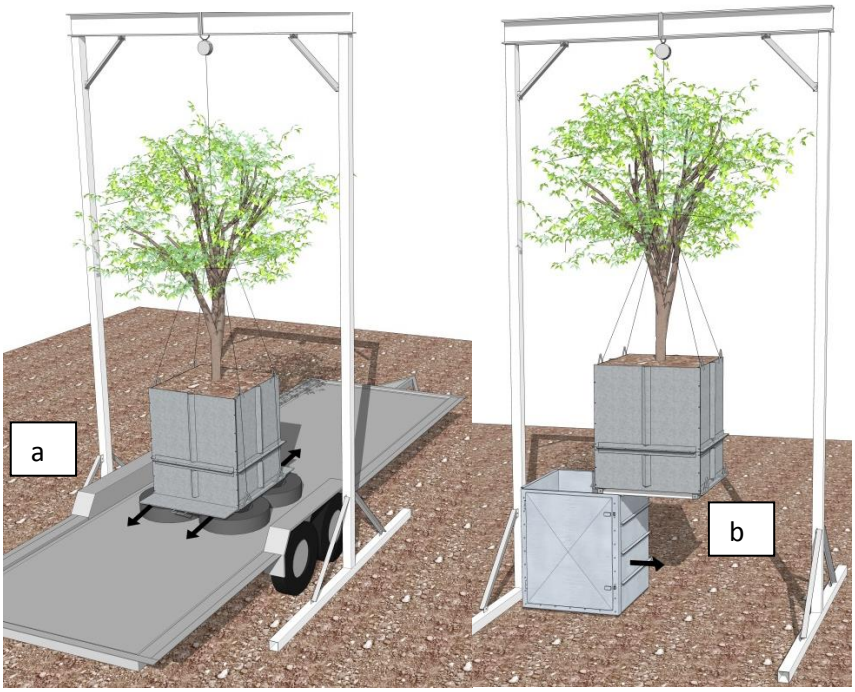

Figure 5.3: Transfer of tree-soil monolith from field sampling equipment into lysimeter container at the experimental site.

5.3 Lysimeter calibration and performance

The wiring and calibration of the load cells were carried out to complete the construction and installation of the lysimeter units for the studies on water uptake of the trees. After confirming that the trees were still alive, each monolith was mounted on a platform load cell. The platform load cell type is a Loadtech LT 1300 model with 1 m x 1 m dimension. The load cell specifications are illustrated in Table 5.2. All the load cells were connected to a datalogger (CR3000, Campell Scientific, Inc, Logan, UT, USA). The datalogger was programmed to sample the output of the load cells every 30 seconds, average made over 5 minutes interval and stored during the calibration. Despite the fact that the load cells were calibrated before installations, calibration was also carried out after installation to test for linearity and hysteresis. Calibration was carried out individually for each lysimeter unit following a procedure suggested by Wheeler and Ganji (1996). The calibration procedure involved loading and unloading standard masses of 1 ±0.05 kg, 2 ±0.05 kg, 3 ±0.05 kg, 5 ±0.05 kg and 10 ±0.05kg and noting the recorded mass changes. It was repeated three times for each lysimeter unit before mass measurement was satisfactory and precision was above R^2 of 0.9. Prior to the beginning of the calibration procedure, each lysimeter surface was covered with Styrofoam (100 mm thick layer), overlain by a layer (20 mm) of gravel to eliminate evaporation during calibration (Allen and Fischer, 1990). The procedure was carried out very early in the morning when the wind was close to zero to prevent noise in the logged data. To evaluate the accuracy level of each lysimeter unit, the recorded data were compared with the known masses by the absolute errors (AE) (Walther and Moore, 2005; Mjanyelwa et al., 2016). Repeatability and sensitivity were evaluated using standard deviation (SD) and standard error (SE), respectively (Martin et al., 2001; Scheneider et al., 1998).

Table 5.2: Selected load cell specifications (Loadtech LT 1300 model).

Specifications	**Value**
Load capacity	5 000 kg
Excitation voltage (Sense included)	+5Vdc Fixed
Excitation current	Max. 90 mA
Current output compliance (max load)	500 Ω (Current is source, not sink)
Voltage output compliance (min load)	1kΩ
Linearity	< 0.01% of full scale
Accuracy	0.05% of full scale
Operating temperature range	-10 to +50 ºC
Storage temperature range	-40 to +80 ºC
Operating and storage humidity	< 85% RH non-condensing

The results of the calibration of the load cells are shown in Figure 5.4. From the results, there was a strong linear relationship between the lysimeter mass and the masses loaded and unloaded for all the lysimeter units. There was no shift in the calibration line during the loading and offloading of known masses. This shows that the lysimeters have high linearity and no hysteresis (Payero and Irmak, 2008). The accuracy of measuring known masses was between 0.027 to 0.056 kg for all the lysimeter units (Table 5.3). It can be seen that the error of measurement was 0.041 kg on the average for all the lysimeter which translates to 0.041 mm of water considering the surface area of the lysimeters (1 m^2). Moreover, the repeatability of measurements and sensitivity of the lysimeters ranged between 0.052 – 0.090 kg and 0.030 – 0.044 kg, respectively. The consistency of measuring the same mass under the same conditions for these lysimeter units is very high. The measurement of SE of the readings shows how sensitive the lysimeter units are. The lysimeter units will be able to detect as little as 0.045 kg (0.045 mm) of evaporation or transpiration. The observed high sensitivity of the lysimeter units falls within the range of sensitivity reported for different types and sizes of lysimeters. Marek et al. (2006) reported high

sensitivity of 0.004 mm for a monolithic weighing lysimeter constructed to measure crop evapotranspiration. Howell et al. (1995) also reported sensitivity of 0.05 mm for a large weighing lysimeter during a calibration procedure. On the contrary, McFarland et al. (1983) observed sensitivity as low as 1.0 mm for a twin weighing lysimeter for fruit trees.

Table 5.3: Statistical values for absolute error (AE), standard deviation (SD) and standard error (SE) as the measurement of accuracy, repeatability and sensitivity of the 4 lysimeter units.

Stations	AE (kg)	SD (kg)	SE (kg)
1	0.056	0.076	0.044
2	0.032	0.090	0.052
3	0.050	0.096	0.055
4	0.027	0.052	0.030
Average	**0.041**	**0.078**	**0.045**

5.4 End note

Approximately two years after the trees were transplanted; the water use of the trees was monitored over three days from load cell measurements (Figure 5.5). This short period of continuous measurements was done just to verify if the water use patterns of the trees ressembled those of trees in the natural conditions. It was a preparatory exercise to more intensive experiments (Chapters 7 and 8). The peak water use rates for the trees on well watered conditions of a clear day were approximately 2 kg h^{-1} for *Z. mucronata*, 1 kg h^{-1} for *O. Africana*, 0.75 kg h^{-1} for *S. lancea* and 0.5 kg h^{-1} for *V. karoo*. The sum of the water use over 24 hours (daily) was 14 kg for *Z. mucronata*, 7 kg for *O. Africana*, 12 kg for *S. lancea* and 8 kg for *V. karoo*. These can also be expressed in L since the density of water is 1. The water use rates recorded here concur with other findings of tree water use reported by other researchers under natural conditions. For instance, Hunt and Beadle (1998) reported water use of 8 kg day^{-1} on acacia species of almost similar size as ours. On a bigger tree of wild olive in Tunisia,

Vandegehuchte and Steppe (2012) reported water use of up to 34 kg day^{-1}. The water use patterns of all the trees also followed the normal diurnal sequence of being very minimal at night, gradually increasing from dawn to peak just after midday before gradually decreasing again towards end of the day (Figure 5.5). This is enough evidence that the procedure employed here successfully maintained the vitality of the trees for water use studies in lysimeters.

For the first time, a sampling procedure for moderately grown trees with soil monolith for immediate lysimeter studies has been successfully developed and implemented. The applications of this exercise can also include nutrient uptake analysis, tree and root development studies and hence improve management and conservation of indigenous trees on a sustainable basis. With these units in place, numerous studies relating to water use of trees can be easily carried out producing high quality data for decision support and decision making.

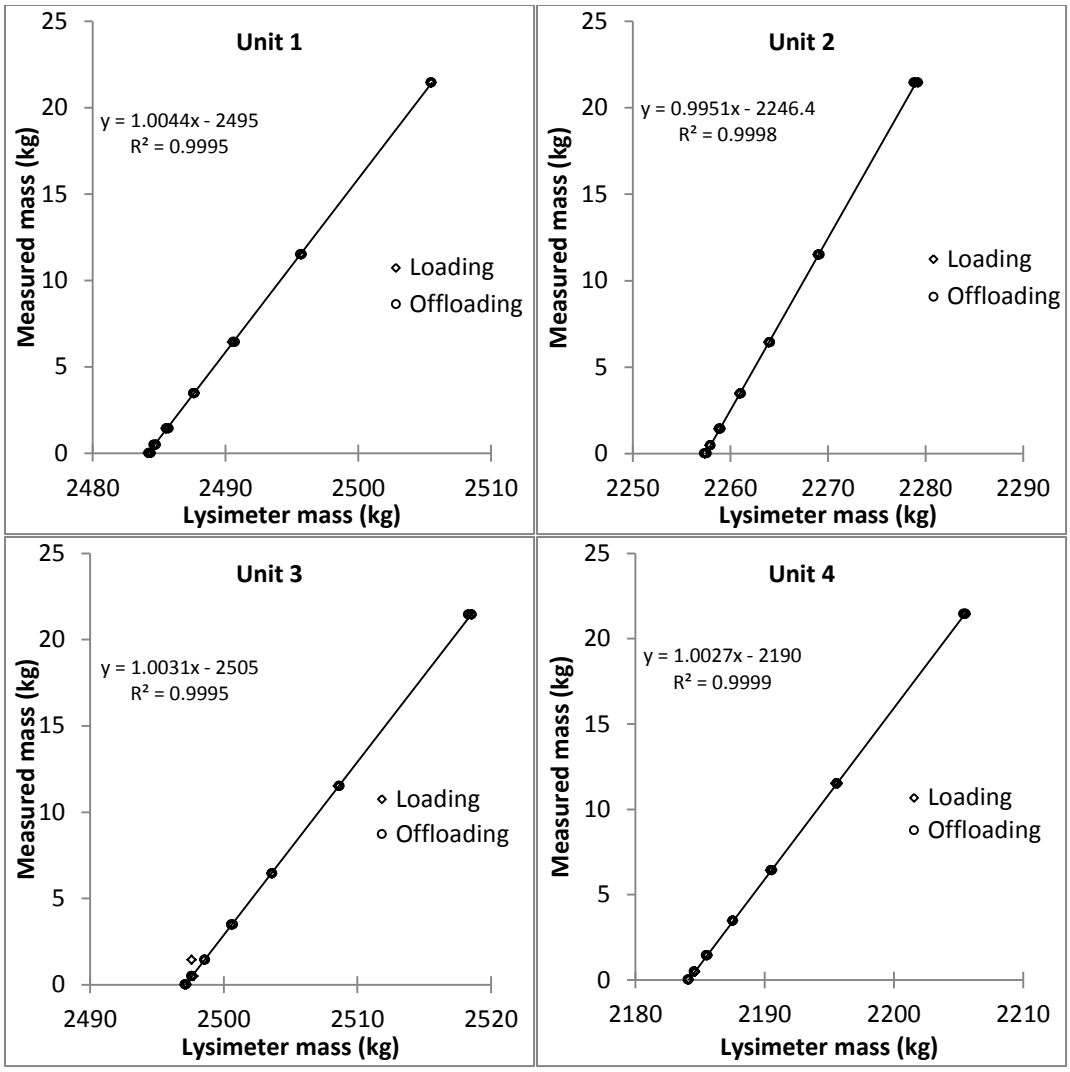

Figure 5.4: Calibration of lysimeter units for linearity and hysteresis by loading and unloading known standard masses.

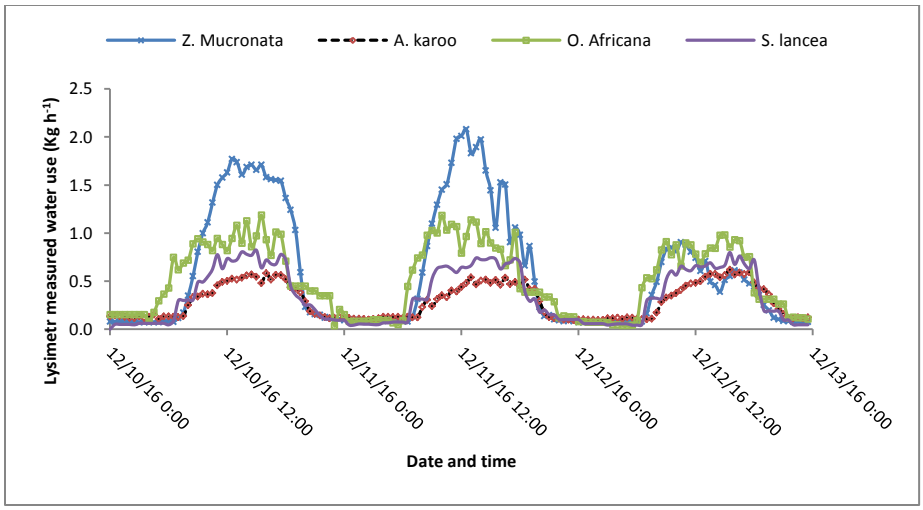

Figure 5.5: Lysimeter measured water use for *Vachelia karroo*, *Olea Africana*, *Sersia lancea* and *Ziziphus muncronata* measured over a period of 3 days in summer (10-12 December 2016).

References

Al Aqtash, U., Bandini, P., 2015. Prediction of unsaturated shear strength of an adobe soil from the soil–water characteristic curve. Constr. Build. Mater. 98, 892-899.

Allaire, S. A., van Bochove, E., 2006. **C**ollecting large soil monoliths. Can. J. Soil Sci. 86, 885-896.

Allen, R.G., Fisher, D.K., 1990. Low-cost electronic weighing lysimeters. T. ASAE 33(6), 1823-1833.

Allen, R.G., Pereira, L.S., Howell, T.A., Jensen, M.E., 2011. Evapotranspiration information reporting: I. Factors governing measurement accuracy. Agr. Water Manage. 98, 899-920.

Cameron, K.C., Smith, N.P., McLay, C.D.A., Fraser, P.M., McPherson, R.J., Harrison, D.F., Harbottle, P., 1992. Lysimeters without edge flow: An improved design and sampling procedure. Soil Sci. Soc.Am. J. 56, 1625-1628.

Green, S.R., Vogeler, I., Clothier, B.E., Mills, T.M., van den Dijssel, C., 2003. Modeling water uptake by mature apple tree. Aust. J. Soil Res. 41, 365-380.

Hensley M., 1984. The Determination of Profile Available Water Capacities of Soils. PhD Thesis, University of the Orange Free State, Bloemfontein, South Africa.

Howell, T.A., Schneider, A.D., Dusek, D.A., Marek, T.H., Steiner, J.L., 1995. Calibration and scale performance of Bushland weighing lysimeters. T. ASABE 38, 1019-1024.

Hunt, M.A., Beadle, C.L., 1998. Whole-tree transpiration and water-use partitioning between *Eucalyptus nitens* and *Acacia dealbata* weeds in a short-rotation plantation in northeastern Tasmania. Tree Physiol. 18(8), 557-563.

Johnson, R.S., Williams, L.E., Ayars, J.E., Trout, T.J., 2005. Weighing lysimeters aid study of water relations in tree and vine crops. Calif. Agric. 59(2), 133-136.

Kohnke, H., Dreirelbis, F.R., Davidson, J.M., 1940. A survey and discussion of lysimeters and a bibliography of their construction and performance. United States Department of Agriculture, Miscellaneous Publication No 372.

Marek, T., Piccinni, G., Schneider, A., Howell, T., Jett, M., Dusek, D., 2006. Weighing lysimeters for the determination of crop water requirements and crop coefficients. Appl. Eng. Agric. 22, 851-856.

Martin, E.C., de Oliveira, A.S., Folta, A.D., Pegelow, E.J., Slack, D.C., 2001. Development and testing of a small weighable lysimeter system to assess water use by shallow-rooted crops. T. ASABE 41, 71-78.

McFarland, M.J., Worthington, J.W., Newman, J.S., 1983. Design, installation and operation of a twin weighing lysimeter for fruit trees. T. ASAE 26, 1717-1721.

McLay, C.D.A., Cameron, K.C., McLaren, R.G., 1992. Influence of soil structure on sulphate leaching from a silt loam. Aust. J. Soil Res. 30, 443-455.

Meissner, R., Rupp, H., Weller, U., Vogel, H.J., 2009. Comparison of soil-monolith extraction techniques. In: European Geosciences Union General Assembly Conference Abstracts Vol. 11. pp 2674.

Meshkat, M., Warner, R. C., Walton, L. R., 1999. Lysimeter design, construction, and instrumentation for assessing evaporation from large undisturbed soil monolith. Appl. Eng. Agric. 15, 303-308.

Meyer, W.S., Tan, C.S., Barrs, H.D., Smith, R.C.G., 1990. Root growth and water uptake by wheat during drying of undisturbed and repacked soil in drainage lysimeters. Aust. J. Agr. Res. 41, 253-265.

Mjanyelwa, N., Bello, Z.A., Greaves, W., van Rensburg, L.D., 2016. Precision and accuracy of DFM soil water capacitance probes to measure temperature. Comput. Electron. Agr. 125, 125-128.

Müller, J., 2009. Forestry and water budget of the lowlands in northeast Germany – consequences for the choice of tree species and for forest management. J. Water Land Dev. 13(a), 133-148.

Müller, J., Bolte, A., 2009. The use of lysimeters in forest hydrology research in north-east Germany. Agr. Forest. Res. 1(59), 1-10.

Payero, J.O., Irmak, S., 2008. Construction, installation and performance of two repacked weighing lysimeters. Irrigation Sci. 26, 191-202.

Phogat, V., Skewes, M.A., Cox, J.W., Alam, J., Grigson, G., Šimůnek, J., 2013. Evaluation of water movement and nitrate dynamics in a lysimeter planted with an orange tree. Agri. Water Manage. 127, 74-84.

Puppo, L., García, C., Girona, J., García-Petillo, M., 2014. Determination of Young Olive-Tree Water Consumption with Drainage Lysimeters. J. Water Resource Prot. 6, 841-851.

Renquist, A.R., Caspari, H.W., Behboudian, M.H., Chalmers, D.J., 1994. Stomatal conductance of lysimeter-grown Asian pear trees before and during soil moisture deficits. J. Am. Soc. Hort. Sci. 119(6): 1261-1264.

Schneider, A.D., Howell, T.A., Moustafa, A.T.A., Evett, S.R., Abou-Zeid, W., 1998. A simplified weighing lysimeter for monolithic or reconstructed soils. Appl. Eng. Agric. 14, 267-273.

Soil Classification Working Group, 1991. Soil classification: a taxonomic system for South Africa. Department of Agricultural Development, Pretoria.

Soil Survey Staff, 2014. *Keys to Soil Taxonomy*. United States Department of Agriculture, Natural Resource Conservation Service.

Tan, C.S., Meyer, W.S., Smith, R.C.G., Barrs, H.D., 1990. Alternative methods of estimating water deficit stress of wheat grown on undisturbed and repacked soil in drainage lysimeters. Aust. J. Agr. Res. 41, 267-76.

Thomson, P.E., Parker, J.P., Arah, J.R. M., Clayton, H., Smith, K.A., 1997. Automated soil monolith-flux chamber system for the study of trace gas fluxes. Soil Sci. Soc. Am. J. 61, 1323-1330.

Vandegehuchte, M.W., Steppe, K., 2012. Use of the correct heat conduction–convection equation as basis for heat-pulse sap flow methods in anisotropic wood. J. Exp. Bot. 63(8), 2833-2839.

Walther, B.A., Moore, J.L., 2005. The concepts of bias, precision and accuracy, and their use in testing the performance of species richness estimators, with a literature review of estimator performance. Ecography 28, 815-829.

Wang, D., Tang, C., Cui, Y., Shi, B., Li, J., 2016. Effects of wetting – drying cycles on soil strength profile of a silty clay in micro – penetrometer tests. Eng. Geol. 206, 60-70.

Wheeler, A.J., Ganji, A.R., 1996. Introduction to engineering experimentation. Prentice Hall: New Jersey.

Yoder, R.E., Odhiambo, L.O., Wright, W.C., 2005. Evaluation of the methods for estimating daily reference crop evapotranspiration at a site in the humid southeast United States. Appl. Eng. Agric. 21(2), 197-202.

6. Laboratory versus field calibration of HydraSCOUT probes for soil water measurement

Abstract

Accurate volumetric soil water content (θv) measurement is essential for efficient soil water management. HydraSCOUT (HS), a capacitance probe for θv measurement offers to achieve good accuracy of measurement, but requires calibration for different soils types. The objectives of this study were to develop calibration equations in the field and laboratory, and then compare their accuracy to estimate θv for selected soil types. HydraSCOUT capacitance probes were installed at four sites. The sites had the Plinthosol (Bainsvlei) and Ferralsol (Bloemdal) soil types, containing loamy fine sand, sandy loam and sandy clay loam soils at different soil profile depths. The probes were calibrated through establishing relationships between the probe readings and gravimetrically measured θv in the field and laboratory. These relationships from the two scenarios (field and laboratory) were validated by testing their abilities to estimate measured θv from a given corresponding set of probe readings. For field calibration, the relationships between the probe readings and measured gravimetric soil water content were described by both linear and polynomial functions (R^2 from 0.33 to 0.65), while that of the laboratory calibration was only described by polynomial functions (R^2 from 0.96 to 0.99) for all soil types. Laboratory equations estimated θv better (RMSE=0.001 m^3 m^{-3} - 0.015 m^3 m^{-3}) than field calibration equations (RMSE=0.004 m^3 m^{-3} - 0.026 m^3 m^{-3}). Laboratory calibration of HS probes was recommended for better estimate of θv.

Keywords: Volumetric soil water content, Field and laboratory calibration, HydraSCOUT probes

6.1 Introduction

Accurate volumetric soil water content (θv) measurement is essential in agricultural and environmental studies for water balance calculations in response to ecohydrological changes at the continental to the watershed scales (Robinson et al., 2008). The gravimetric method of θv measurement remains the most accurate than any other indirect method (Zerizghy et al., 2013; Zanetti et al., 2015). However, this method is time consuming, employs destructive sampling and does not allow repeated measurements on the same spot (Kaleita et al., 2005). To solve these problems, non-destructive techniques of monitoring soil water such as neutron probes (Gardner et al., 1991; Evett et al., 2006), time domain reflectometry (TDR) (Topp et al., 1980), frequency domain reflectometry (FDR) and capacitance methods (Starr and Paltineanu, 1998; Girona et al., 2002; Fares and Polyakov, 2006) have been developed. These techniques are highly accurate, inexpensive per location, fast, ease of measurement and large soil sensing volume measurements can be at different depths at the same location. Apart from neutron probe technique which is considered health risk due to the radioactive source required for neutron scattering (Chanasyk and Naeth, 1996; Robock et al., 2000), other mentioned devices are capable of automatic data acquisition. This is continuous, multiple parameters monitoring and data can be either stored on site or transmitted via internet as short as on a minute basis (Bandaranayake et al., 2007; Cobos and Chambers, 2010 Scudiero et al., 2012; Zerizghy et al., 2013; Mjanyelwa et al., 2016). Recently, capacitance probes have been the choice of measuring volumetric soil water content since they are cheap, easy to maintain and user friendly.

The HydraSCOUT (HS) probe, manufactured by Hydra Sensor Technologies International Ltd is among the latest developed (2014) capacitance type probes in South Africa. The advantages of this probe includes all the stated importance of capacitance probes, even data from the HS probes

can be monitored through the internet and downloaded wherever an internet connection is available.

Simple and practical irrigation guidelines are essential to achieve optimal yield and quality. Therefore, procedures and or actions to ensure accurate measurement of soil water are important. Contrarily, irrigation is still being managed poorly by the farmers because capacitance probes, soil water measuring devices, are commonly used without calibration. Once change in θv is noted via graphical trends in soil profile water dynamics due to various components of water balance in the irrigated field, then irrigation amount and timing will be determined accordingly (Starr et al., 2009). Better accuracy of soil water measurement can be achieved through calibration of capacitance probes. These have been proved over time with different studies and different capacitance probes (Gabriel et al., 2010; Paraskevas et al., 2012; van Westhuizen and van Rensburg, 2013). Irrespective of stipulated accuracy level by the manufacturers, capacitance probes have been reported to require calibration for different soil types (Morgan et al., 2001; Lane and Mackenzie, 2001; Seyfried and Murdock, 2001; Seyfried and Murdock, 2004; Geesing et al., 2004; Kelleners et al., 2004; Gabriel et al., 2010) which made them site specific. The use of default calibration equations from the manufacturers can also lead to poor estimates of θv, meanwhile, site specific calibrations are recommended (Kelleners et al., 2004; Abbas et al., 2011). Some of the reasons for this observation are due to differences in electrical conductivity and soil dielectric properties.

Capacitance probes can be calibrated under laboratory or field conditions. Laboratory calibration is non-destructive, enables continuous θv measurements to be taken within a relatively short time, easy to reproduce, and require less labour compared to field calibration (Starr and Paltineau, 2002; Gabriel et al., 2010). Laboratory calibration can make provision for the soils to

be repacked or undisturbed. In comparison to repacked soil sampling, undisturbed soil samples minimize the occurrence of undesired effects of soil sampling and present a more realistic scenario with regards to the field conditions. However, laboratory facilities are costly and more so, the sampling of soils for laboratory studies may alter the soil from those of the field. Field calibration, on the other hand, is done under natural conditions which relates better to site measurements. The limitation of this operation is in terms of the limited number of real time readings for comparison, time consumption, labor intensive and continuous sampling and measurements on the same spot are not possible. In terms of the capacitance probe in question, HS, there is no information on its performance to measure soil water contents and that of its calibration procedures. The question is, will there be no need for calibration of the probe for different soil types? The ease of calibration is also important. Can the calibration equations developed under laboratory condition be used for field soil water measurements? Therefore, the objectives of this study were to: (1) develop calibration equations for the HS probe for selected soils under laboratory and field conditions; (2) evaluate the performance of both sets of calibration equations for estimating θv for the selected soil types.

6.2 Materials and Methods

6.2.1 Capacitance probe description

Theory

The sensors of the HS probe use the principle of measuring two components (real and imaginary) of the composite permittivity (ε) of the mineral soil particles, water and other constituents contained in the soil around the probe (Dean et al., 1987; Kelleners et al., 2005; Regaldo et al., 2007). The complex (ε) number is expressed as

$$\varepsilon = \varepsilon' - j\varepsilon'' \tag{6.1}$$

Where ε' is the real component and ε'' is the imaginary component, of energy losses to an applied electric field. The real part of ε is the dielectric constant and provides a surrogate measure of the θv. The imaginary part of ε depends on the frequency of measurement of the applied electric field, F (Hz) and the soil bulk electrical conductivity, σ (S m^{-1}), such that

$$\varepsilon'' = \sigma / 2\pi F\varepsilon_0 + \varepsilon''_{rel} \tag{6.2}$$

Where ε''_{rel} is the permittivity due to molecular relaxation and is the permittivity in vacuum (ε_0 =8.854 x 10^{-12} F m^{-1}). The frequency of operation for the HS probe is 50 MHz. Kelleners et al. (2005) reported a strong dependency of the real part of the permittivity on frequencies below 500 MHz, especially on soils containing clay minerals. Permittivity measurements may also be biased by salinity of soils ($\sigma \geq 10$ dS m^{-1}) (Campbell, 2002).

Polar molecules orient themselves with the applied electric field and absorb energy from it. Naturally, water is the most common polar liquid with a relative permittivity of ~80 compared to ~4 for dry soil and 1 for air (Hillel, 2003). The availability of water within any porous media such as soil therefore, is strongly influential to the apparent permittivity (ε_a) of the mixture (Dean et al., 1987; Robinson et al., 1999; Evett et al., 2006).

$$\varepsilon_a = (\varepsilon'/2)[1+(1+\tan^2\delta)^{0.5}] \quad (6.3)$$

Where $\tan\delta$ is the loss tangent defined as the ratio of the imaginary to the real permittivity, $\varepsilon''/\varepsilon'$. The HS probe considers the soil-probe media as a capacitor whose capacitance (C) is

$$C = g\varepsilon'\varepsilon_0 \quad (6.4)$$

Where g (m) is a geometric factor associated with the electrode configuration and the shape of the electromagnetic filed penetrating the medium. The final water content (θ) output reading of the HS probe expressed in percentages (%) is derived from the empirical equation of Topp et al. (1980),

$$\theta = -5.3\times10^{-2} + 2.92\times10^{-2}\varepsilon_a - 5.5\times10^{-4}\varepsilon_a^2 + 4.3\times10^{-6}\varepsilon_a^3 \quad (6.5)$$

This equation is only applicable for θv water content within the range of 0 and 0.55 m^3 m^{-3} (Topp et al., 1980). The value of (θ) is calibrated for different soil types using a reliable standard of measuring the θv to establish an empirical function of converting θ to θv. For θv greater than 0.55, the semitheoretical linear relationship below may be used (Heimovaara, 1993),

$$\theta = a\sqrt{\varepsilon_a} + b \quad (6.6)$$

Where a = 0.145 and b = -0.305.

Physical description

The probes are available in different lengths ranging from 0.2 to 2 m. A drawing of a 0.8 m length HS probe with 5 sensors is shown in Figure 6.1. Specific lengths with specific measurement depth intervals can be supplied according to the user's requirements. The HydraSCOUT probe requires 5-24 volts of power, and operates between ambient temperatures of 0 ºC and 60 ºC. Two different length types were used in this study. For field calibration, probes of 0.8 m length with 5 sensors placed at depths of 0.1, 0.2, 0.4, 0.6 and 0.8 m were used, while

probes of 0.2 m length with only 2 sensors placed 0.1 m apart were used for laboratory calibration. The 2 sensors of the 0.2 m probes were referred to as lower and upper sensors based on the direction from the top. The top of each probe has a 40 mm (long) x 70 mm (diameter) PVC cap. The rest of the tube is 38 mm in diameter, tapering at the last 30 mm length for ease of penetration during installation.

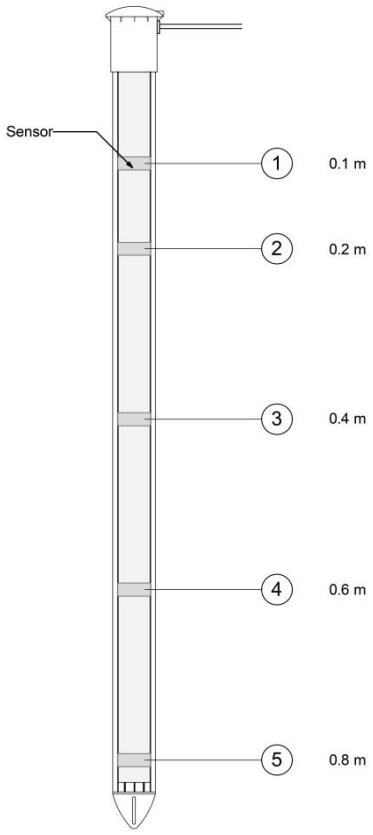

Figure 6.1: HydraSCOUT probe 0.2 m in length with 2 sensors spaced 0.1 m apart.

6.2.2 Preliminary studies

A preliminary study was carried out for all the probes that were used in the study prior to laboratory and field calibration procedures. One of the objectives of the preliminary tests was to confirm identical output of all the sensors under identical circumstances. The other objective was to evaluate the effect of temperature on the sensor readings. The probes were hung in the air

for 24 hours to check for the least (open end) readings of all the sensors and thereafter, all the probes were immersed in distilled water for 24 hours as well to test for the reading at saturation. Distilled water was used to avoid impurities, salinity effect and to create an identical situation. For all the sensor readings over the observation periods, it was observed that the initial or least reading of the sensors was 0% for all the sensors. The mean for all the sensors readings at saturation was 99% and the standard deviation was 2.66% (data not shown). The probes were inserted into soil cores and, thereafter left to drain for 1 day. The whole soil column was wrapped with transparent plastic to prevent evaporation in order to maintain constant mass. The probes were tested for the effect of temperature on sensor readings by varying the temperature of the chamber within the range of 2ºC to 48ºC at the constant mass which represented constant water content. There was no temperature effect on sensor readings for all the sensors between 15ºC and 40ºC , which was within the range of temperature that the study was carried out both in the laboratory and the field. The laboratory calibration study was carried out at the temperature of 26ºC while the soil temperature was between 20ºC and 35ºC during the field study.

6.2.3 Field calibration

Study sites

Field calibration was done at 4 sites around Bloemfontein. The first 3 sites were located around Kenilworth Experiment Farm of the Department of Soil, Crop and Climate Sciences, University of the Free State (lat. -29.02°, long. 26.15° and alt. 1354 m) while the 4th site was located on the main campus of the University of the Free State (lat. -21.1°, long. 26.2° and alt. 1421 m). The soil forms were classified as Plintosols (FAO, 2015) or Bainsvlei (Soil Classification Working Group, 1991) for the first 3 sites and Ferralsol (Soil Survey Staff, 2014) or Bloemdal (Soil

Classification Working Group, 1991) for the 4th site. Particle size distribution was determined using the pipette method described by Day (1965).

Calibration procedure

On each of the 4 sites, a basin of 2 m x 2 m was made by forming a soil ridge of approximately 0.3 m. Within each basin, 2 HS probes, with sensors at depths of 0.1, 0.2, 0.4, 0.6 and 0.8 m were installed for taking continuous θv measurements. The field experiment setup is shown in Figure 6.2. In the installation process, the soil was drilled using a drill bit which was slightly thinner in diameter (37 mm) than the probe (38 mm) to ensure full contact of the probe with the soil. The probe was then manually pushed into the soil.

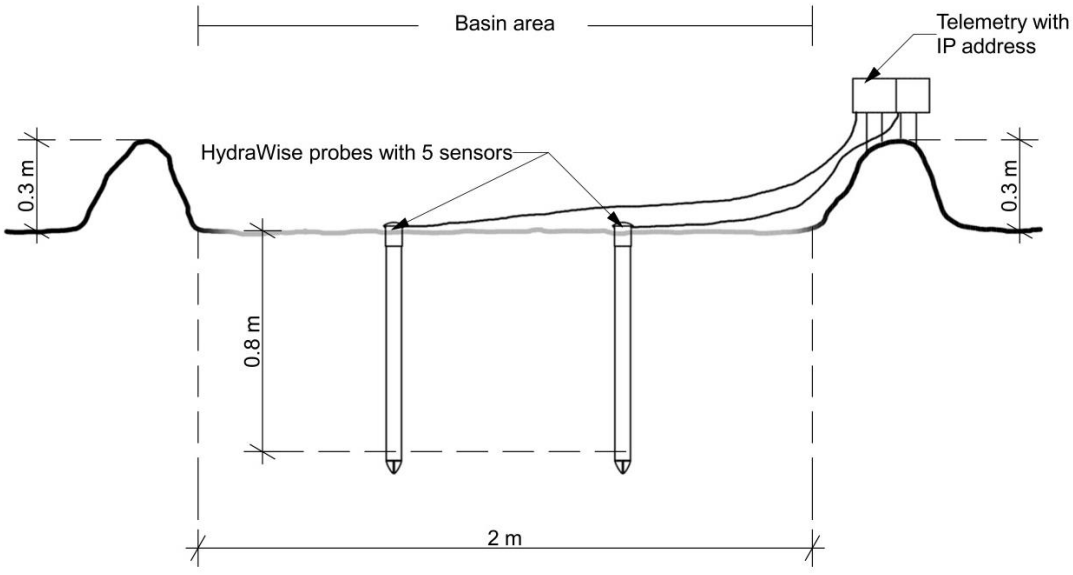

Figure 6.2: Cross sectional diagram illustrating the setup of the field experiment showing the basin area where HydraSCOUT volumetric soil water measuring probes were installed.

A water tank was used to fill the basin with water until the θv was near saturation at all sensor depths. From a day after wetting, 2 soil samples were taken from the basin area to determine gravimetric soil water content at the same depth of sensor installation as the soil profiles dried

over a period of at least 8 days per drying cycle. The θv of the 2 samples taken per sensor depth at the same time was averaged to counter the effects of spatial variation within the basin, even though the heterogeneity was not anticipated within the approximately 1 m radius around the installed HS probes. The sampling process was done for 5 drying cycles which were taken as replicates over a period of 53 days. A minimum radius of 0.5 m away from the probes was maintained to avoid their damage during the sampling process. Samples were collected with an auger and immediately sealed in plastic containers and taken to the laboratory for weighing, and then put into the oven for drying at 105°C for 24 hours. The sampling process for gravimetric soil water content measurements was done over a few days as the soil was drying, before wetting the basin to mark the onset of the next drying cycle.

The samples were re-weighed after drying to determine the gravimetric water content, and subsequently converted to volumetric water content using the *in situ* measured bulk densities. The time of taking a sample was noted so as to match the gravimetric and sensor measurements. After installing the probes on the 2nd September 2015, gravimetric soil water content samples were collected between 9 September 2015 and 31 October 2015. This was before the onset of the rainy season, which enabled the soil to dry quicker. Data sets for the same soil class were grouped together regardless of the measurement depth and then divided into 2 sets, one used for the calibration and the other for validation of both the field and laboratory calibration equations. The θv measurements were plotted against the probe readings to develop calibration equations for different soil texture classes.

6.2.4 Laboratory calibration

Study site

Laboratory calibration was carried out at the climate cabinet facility of the Department of Soil, Crop and Climate Sciences located at the main campus of the University of the Free State, Bloemfontein, South Africa. The facility consisted of five units of cabinets (2 m x 3 m x 5 m per cabinet). Each cabinet unit was equipped with a digitally controlled air conditioner, which enabled air temperature regulation inside the cabinet. Inside each cabinet there were three welded steel frames for hanging S- type load cells.

Other equipment needed for the calibration procedure included vacuum chamber units shown in Figure 6.3, and a Campbell Scientific CR 3000 data logger. A vacuum chamber unit consisted of two cylinders, one for de-airing and the other containing distilled water for saturation. Each cylinder was made of PVC with a 0.4 m diameter and 0.55 m length. A pipe fitted with valves to control air flow was connected from the vacuum tight lids of both cylinders to a pressure pump.

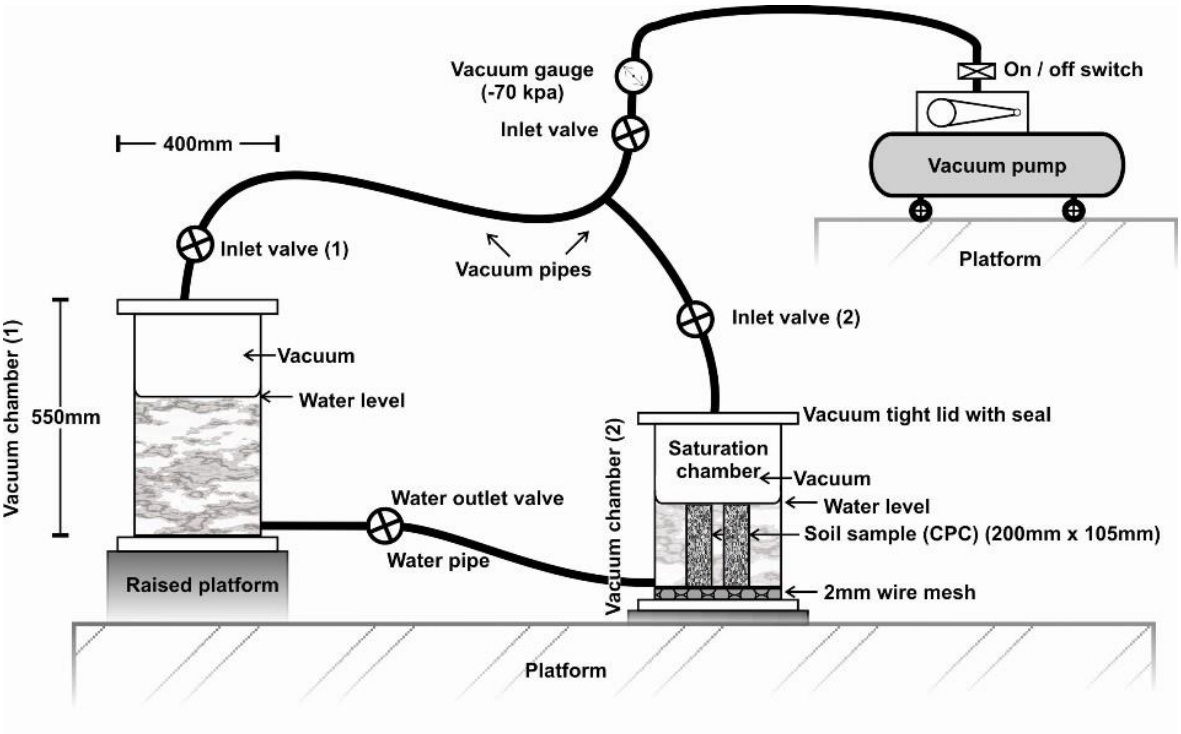

Figure 6.3: Diagram illustrating the setup of the vacuum and saturation chamber apparatus used for removing air from the water and pore spaces of the undisturbed core soil samples (Nhlabatsi, 2010).

Calibration procedure

Five undisturbed core soil samples (to maintain the natural state as in the field) of each of the soil types used for the field calibration were collected with perforated PVC cylindrical pipes (115 mm diameter and 300 mm length). Each end of the pipes was protected with cylindrical plastic cover for ease of transport from the field. The core soil sampling procedure used during the present study is fully explained in Nhlabatsi (2010). In this procedure, a profile pit was dug to enable sampling to be done horizontally across the soil profile. The soil samples were taken at depths of 0.1 to 0.8 m. Different soil types were found at different depths and similar soils were pooled together in the calibration process. For instance the general trend was an increase in the clay content dwon the profile. A metallic core head housing the perforated PVC pipes was

pushed into the wall of the pit using a hydraulic jack which was supported by a metal plate at the back against the opposite wall to ensure that the wall supporting the jack does not break. After the head core was fully into the soil profile, it was removed and the PVC pipe containing the undisturbed soil sample was removed. The ends of this pipe were then sealed with plastic stoppers. The soil samples were weighed, oven dried at 105°C for 24 hours and weighed again to determine water content and bulk density.

The calibration procedure was divided into de-airing, saturation and evaporation. De-airing was carried out at a pressure of -70 kPa for 48 hours. This was to ensure total removal of air from the water and pore spaces in the soil cores. The de-airing apparatus consisted of cylinders (chambers) that could be subjected to suction. Each chamber could accommodate 5 core soil samples at once. These were placed vertically in the chamber for ease of exchange of air through the perforated pore spaces. However, the chamber with distilled water was placed on an elevated platform to ensure free gravitational flow of water from the first to the second chamber.

At the end of de-airing, the valve that connects the two cylinders (chambers 1 and 2 in Figure 6.3) near their bottoms was opened such that the distilled water was slowly flowing from chamber 1 which was elevated, to the saturation chamber (Chamber 2). This enabled core soil sample saturation in the saturation chamber by gradually wetting the sample from the bottom upwards. Saturation time of core soil samples differed depending on soil type. After saturation, a hole was carefully drilled into the soil core using a 37 mm diameter drill bit which was slightly smaller (by 1 mm) than the probes to ensure full contact of the probe and soil. The probes were inserted into the soil cores through the drilled holes. The sphere of measurement by the HS probes of 35 mm (according to the manufacturer) was completely within the radius of the core soil samples; hence no electromagnetic fields were created outside the cores with a possibility of

causing noise on sensor readings. The soil removed from each of the core samples during the drilling was labeled accordingly, oven dried and weighed. The core soil samples with the inserted probes were left to drain and hung on the load cells immediately after drainage stopped. This point was taken as the field capacity for each soil sample.

Prior to hanging core soil samples (Figure 6.4), the load cells were calibrated by adding and removing known weights before finding a relationship between weights and millivolts. The load cells output of millivolt was converted to kg with calibration equations derived from the relationships. The continuous weight loss measurements of core soil samples hung on load cells were monitored and recorded until a constant weight was achieved. This was taken as the permanent wilting point where no further water loss occurred. The ambient temperature of the chamber was maintained at 26°C. Hourly mass and probe readings were recorded with CR 3000 data logger for the period of the study.

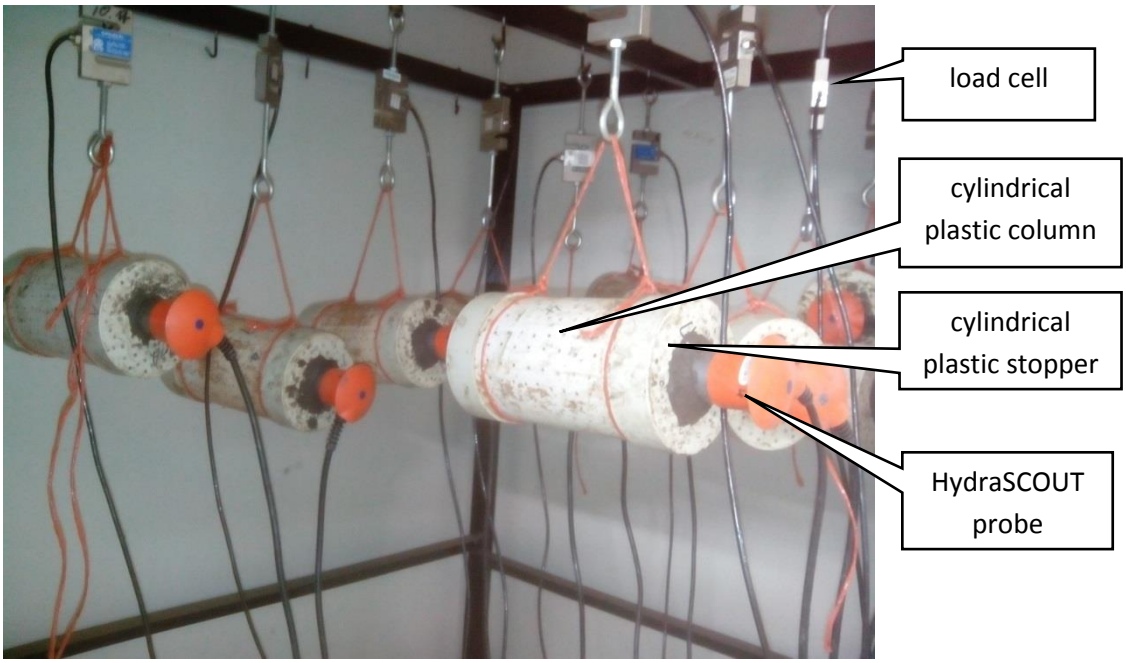

Figure 6.4: Perforated cylindrical plastic columns (105 mm diameter and 200 mm length) containing undisturbed soil samples with HydraSCOUT probes installed in each and hanged from load cells for continuous measurement of volumetric soil water content in a constant air temperature climate cabinet.

The gravimetric water contents of the core soil samples were converted to volumetric water content using bulk density obtained from different core soil samples. Five HydraSCOUT 0.2 m length probes, each with two sensors 0.1 m apart were used in this experiment. The upper five 0.1 m sensor readings were used for calibration while the lower five 0.2 m sensor readings were used for evaluating the accuracy of the calibration equations. The number of sensors (5) in each of the soil columns of the various soil types was taken as replicates. Volumetric water contents were plotted against the probe readings for different soil samples to develop calibration equations for each soil textural class.

6.2.5 Validation of the field and laboratory calibrations

The calibration equations developed for each soil textural classes in both the field and laboratory calibrations were applied on the second set of field probe data for each of the corresponding soil textural classes. This means that two equations (field and laboratory) were applied on the same probe data set to estimate θv in each of the three soil types used in the study. The accuracy with which the calibration equations from the field and laboratory estimated the field θv measured gravimetrically was established through applying these equations on the probe readings.

6.2.6 Statistical analysis

It was ensured that the best fit of the regression function for each soil type was used on the basis of highest coefficient of determination (R^2) determined from a linear or a polynomial function.

Regression analysis (P-value at 95% confidence level) was done to test the significance of the relationships between the sensor readings and θv during calibration. During the validation exercise, evaluation of the accuracy of the developed calibration equations to estimate the measured θv was done with the aid of root mean square of error (RMSE). The mean bias error (MBE) was computed to quantify the deviation of the estimated θv means from the observed θv (Walther and Moore, 2005; Evett et al., 2006; Abbas et al., 2011).

$$RMSE = [n^{-1} \sum_{i=1}^{n} (S_i - O_i)^2]^{0.5} \quad (6.7)$$

$$MBE = [\sum_{i=1}^{n} (S_i - O_i)]/n \quad (6.8)$$

where n is the number of observations, S_i and O_i are the estimated and observed values, respectively. The calibration equation shows a good performance with value of RMSE closer to 0. A negative MBE indicates that the sensor is underestimating the actual θv and vice versa. The closer the MBE value is to 0, the better.

6.3 Results

6.3.1 Soil characteristics

The soil characteristics per profile depth showed that the soils were sandy loam (68-79% sand, 6-16% silt and 8-19% clay), loamy fine sand (79-88% sand, 5-12% silt and 5-10% clay) and sandy clay loam (49-67% sand, 1-17% silt and 21-33% clay) (Table 6.1). The bulk density, determined using the core method ranged from 1.45 g cm^{-3} to 1.59 g cm^{-3} for sandy loam, from 1.65 g cm^{-3} to 1.72 g cm^{-3} for loamy fine sand and from 1.47 g cm^{-3} to 1.57 g cm^{-3} for sandy clay loam. The pH ranged between 5.81 and 7.31 amongst the 3 textural classes.

Table 6.1: Soil characteristics at the sampling stations and depths for the soils used for field and laboratory calibration of the HydraSCOUT probes.

Station	Soil class	Depth (m)	% sand	% silt	% clay	Bulk density (g/cm^3)	pH
1	Sandy loam	0-0.1	77	10	11	1.46	7.31
1	Loamy fine sand	0.1-0.2	83	8	9	1.65	7.24
1	Loamy fine sand	0.2-0.4	88	7	5	1.69	7.11
1	Loamy fine sand	0.4-0.6	88	5	6	1.72	6.93
1	Loamy fine sand	0.6-0.8	86	6	7	1.69	6.59
2	Sandy loam	0-0.1	74	16	8	1.47	7.1
2	Loamy fine sand	0.1-0.2	79	12	8	1.69	7.12
2	Sandy loam	0.2-0.4	79	10	10	1.50	6.86
2	Sandy clay loam	0.4-0.6	67	9	21	1.57	6.56
2	Sandy clay loam	0.6-0.8	67	7	25	1.49	6.27
3	Loamy fine sand	0-0.1	82	7	10	1.69	6.5
3	Sandy loam	0.1-0.2	78	7	14	1.57	6.34
3	Sandy loam	0.2-0.4	73	6	19	1.60	6.1
3	Sandy loam	0.4-0.6	74	6	18	1.45	6.07
3	Sandy loam	0.6-0.8	75	7	18	1.49	6
4	Sandy loam	0-0.1	76	13	10	1.59	5.81
4	Sandy loam	0.1-0.2	70	16	15	1.43	5.95
4	Sandy loam	0.2-0.4	68	15	15	1.59	6.1
4	Sandy loam	0.4-0.6	68	12	19	1.53	6.09
4	Sandy clay loam	0.6-0.8	49	17	33	1.47	6.82

6.3.2 Calibration equations

The relationships between the volumetric water content and probe measurements for the field and laboratory calibrations of the capacitance probe for the 3 soil classes are presented in Figure 6.5 (a-f). The field calibrations for the loamy fine sand and sandy loam soils were best described by linear relationships, while the rest of the equations were polynomial. These best fitting relationships were based on the highest R^2 values produced by either the polynomials or straight lines. The R^2 values for the loamy fine sand soil were 0.65 for field calibration and 0.96 for laboratory calibration. During the calibration, R^2 values of 0.33 and 0.99 were obtained for sandy

loam, while 0.53 and 0.96 were obtained for the sandy clay loam for the field and laboratory calibration, respectively.

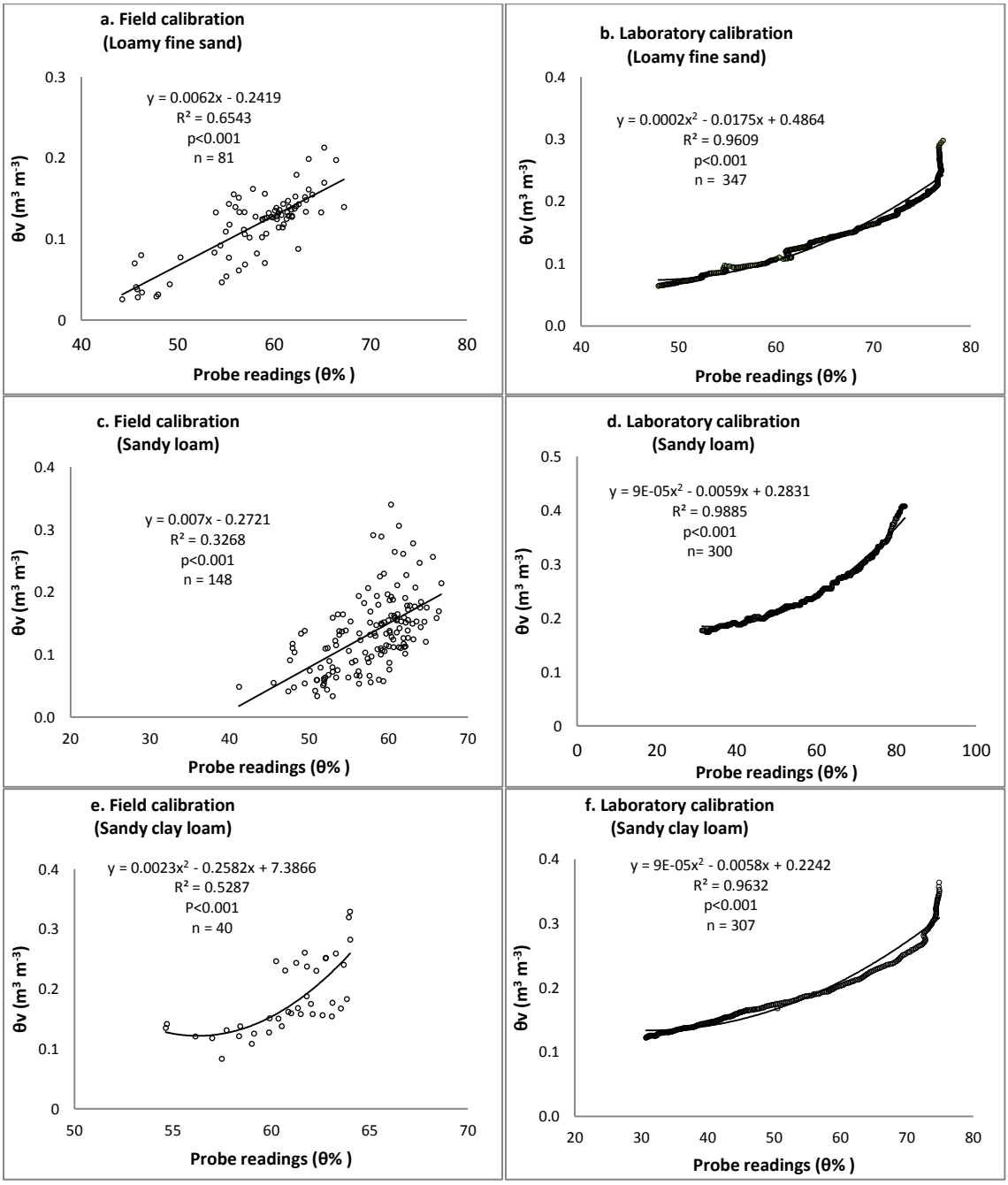

Figure 6.5: Relationship between probe readings of volumetric soil water content (%) and observed volumetric water content (m^3 m^{-3}) for field and laboratory calibrations for loamy fine sand (a,b), sandy loam (c,d) and sandy clay loam (e,f) soils.

All the calibrations revealed a highly significant ($P<0.001$) relationship between the sensor readings and the observed θv for all three soil textural classes, both in the field and laboratory calibrations as shown on Figure 6.5.

6.3.3 Field validation of the calibration equations

The applications of both the field and laboratory equations in the field (validation) for the 3 textural classes are presented in Figure 6.6 (a-f). The estimated θv using field calibration equations were more scattered than the estimated θv using laboratory equations for all the soil textural classes used in this study.

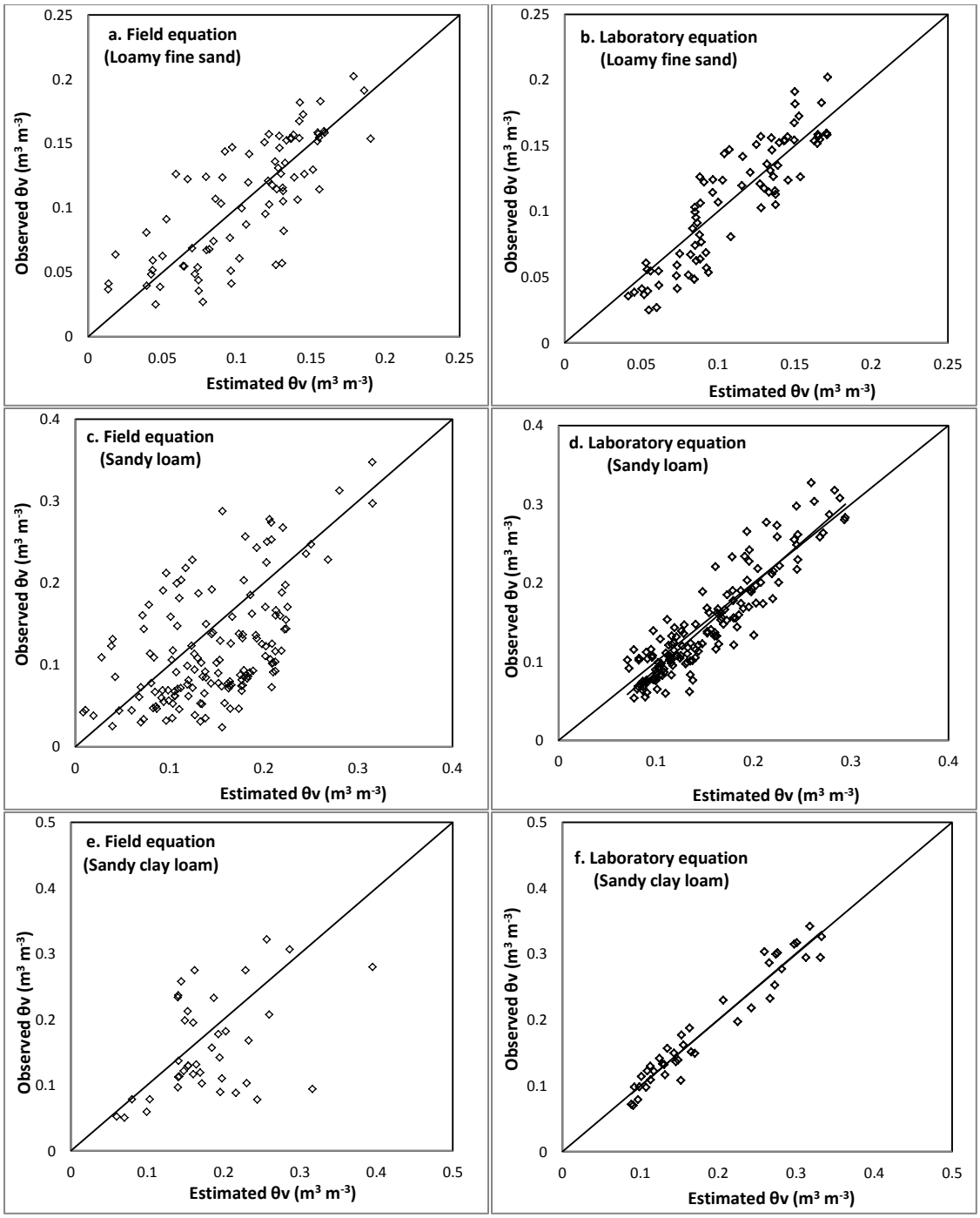

Figure 6.6: The relationship between the observed volumetric soil water content (θv) and θv estimated using field and laboratory calibration equations for loamy fine sand (a, b), sandy loam (c, d) and sandy clay loam (e, f) soils.

The RMSE for validation of the field equations ranged from 0.004 m^3 m^{-3} to 0.026 m^3 m^{-3}, and from 0.001 m^3 m^{-3} to 0.015 m^3 m^{-3} for laboratory equations (Table 6.2). For both the field and laboratory equations, the RMSE values were smallest for loamy fine sand soil (0.004 m^3 m^{-3} and 0.001 m^3 m^{-3}) and largest for sandy clay loam (0.026 m^3 m^{-3} and 0.015 m^3 m^{-3}), with sandy loam in between the 2 textural classes (0.007 m^3 m^{-3} and 0.004 m^3 m^{-3}). The MBE values were <0.001 in all the estimations of θv when using both the laboratory and field calibration equations.

Table 6.2: Comparison of statistical parameters of the field validation for the field and laboratory calibration equations for volumetric water content for loamy fine sand, sandy loam and sandy clay loam soils measured with a HydraSCOUT capacitance probe.

Calibration	Soil class	RMSE (m^3 m^{-3})	MBE	R^2	P value	N
Field	Loamy fine sand	0.004	<0.001	0.61	<0.001	81
	Sandy loam	0.007	<0.001	0.29	<0.001	149
	Sandy clay loam	0.026	<0.001	0.27	0.001	41
Laboratory	Loamy fine sand	0.001	<0.001	0.80	<0.001	81
	Sandy loam	0.004	<0.001	0.83	<0.001	149
	Sandy clay loam	0.015	<0.001	0.94	<0.001	41

The coefficient of determination (R^2) for loamy fine sand was 0.61 for validation of the field calibration equation and 0.80 for the laboratory equation on the same soil class. For sandy loam, the R^2 values were 0.29 for the validation of the field equation and 0.83 for the laboratory equation (Table 6.2). Finally, the sandy clay loam showed R^2 values of 0.27 for the validation of the field equation and 0.94 for the laboratory equation.

6.4 Discussion

Extensive research has been done on calibration of different θv measuring devices. Concurring with previous research, our findings showed better agreement between the estimated and measured θv when the calibration for a specific soil type is performed in the laboratory compared to field calibration as indicated by the higher R^2. Kinzli et al. (2012) calibrated 6 textural soil classes and reported adjusted R^2 values varying between 0.26 and 0.95 for field calibration, and adjusted R^2 values varying between 0.88 and 0.99 for laboratory calibration. Gabriel et al. (2010) reported R^2 values of up to 0.92 with field calibration and up to 0.96 on laboratory calibration.

On the field validation of the calibration equations, the RMSE values were smaller when using the laboratory equations (0.001 m^3 m^{-3} to 0.015 m^3 m^{-3}) than when using the field equations (0.004 m^3 m^{-3} to 0.026 m^3 m^{-3}) in all textural classes. This meant that the laboratory equations estimated the θv with higher accuracy compared to the field equations. Comparing laboratory and field calibration equations, Gabriel et al. (2010) also observed that application of the laboratory equation to sensor reading estimated θv closest to the measured value (RMSE=0.019) when compared to application of the field calibration equation (RMSE=0.023). In the study reported by Kinzli et al. (2012), a smaller average absolute error of 0.012 was observed when applying the laboratory calibration equation to sensor readings in order to estimate measured θv compared to 0.432 when the field calibration was applied. Similar to the calibration data, the field validation agreement (R^2) between the estimated and measured θv was higher when using the laboratory equation than when using the field equation irrespective of soil type.

Better estimation of volumetric water content by the laboratory equations than the field equations could be due to many factors. These factors could be possibilities of having broad range of soil water content per different soil type during the laboratory calibration procedure which makes it

easy to minimize the presence of large air gaps and spatial variability were able to be put under control. The large range of soil water content measurement will help to reduce errors observed during the relationship between the probe output and the soil water content of the soil cores. These are difficult to control under field condition. The possibility of taking more laboratory calibration measurements than in the field, also observed by Geesing et al. (2004) and Kinzli et al. (2012), and the fact that the sensor readings are recorded on the same soil volume that is weighed for gravimetric water content (colocation) in the laboratory, both work in favor of the laboratory calibration to produce more accurate estimations. In the field calibration, the sensor measures a certain soil volume continuously, but the gravimetric soil water content is determined using a soil sample taken away from the sensor, which increases the chance of variability among the collected soil samples, and variability between those samples and the soil at the spot where the sensor is located. Evett et al. (2006) and Geesing et al. (2004) argued that the sphere of influence from which capacitance probes determine the θv is small, and hence compromises the success of field calibrations in many soils since soil sampling within that volume is difficult with existing soil sampling equipment.

The RMSE indicated compromised accuracy with the sandy clay loam soil, implying that higher clay content in soils influence the accuracy of probe calibration. This was especially so in sandy clay loam (RMSE=0.026 m^3 m^{-3}). This may be due to the fact that in clayey soils, water bound within clay particles is sometimes not detected by the electromagnetic field of capacitance sensors, yet this is accurately measured by the gravimetric method which involves oven drying of soil samples where even the bound water is released. Kinzli et al. (2012) also reported greater success of field calibration in sandy soils compared to soil textural classes with higher clay

content. Zettl et al. (2015) highlighted that the sensor accuracy can indeed be affected by the soil properties.

No under or overestimating the θv by the HS probe was observed (MBE<0.001) with the use of either field or laboratory calibration equations. Overall, the higher accuracy of the laboratory calibration equations to estimate θv compared to field calibration equations rendered them more suitable for θv monitoring using the HS probe, and hence laboratory calibration is recommended.

6.5 Conclusion

The study intended to develop field and laboratory calibration equations for HS probes, and compared their accuracy in estimating θv in the field. Calibration equations of both linear and polynomial functions were produced during the field study while only calibration equations of polynomial functions were produced during the laboratory calibration procedure. It was observed that the calibration of HS probes in the laboratory produced equations that estimated θv with higher accuracy than field calibration equations. The accuracy of estimation could also be soil texture dependent, which is also inclined to the depth within the soil profile. In particular, the lowest accuracy of estimate for θv was found in soils with higher clay content for both the field and laboratory calibration equations. The use of laboratory calibration equations presents an opportunity to increase water productivity. Thus sustainable management in agriculture and the environmental sector with more accurate θv estimation is possible. Therefore, laboratory calibration of the HS capacitance probes should be given preference over field calibration for monitoring of θv.

References

Abbas, F., Fares, A., Fares, S., 2011. Filed calibration of soil moisture sensors in a forested watershed. Sensors 11, 6354-6369.

Bandaranayake, W.M., Parsons, L.R., Borhan, M.S., Holeton, J.D., 2007. Performance of a capacitance-type soil water probe in a well-drained sandy soil. Soil Sci. Soc. Am. J. 71, 993-1002.

Campbell, J.E., 2002. Salinity effects in capacitive soil moisture measurement. Pap. no. 1.2. *In* I.C. Paltineau (ed.) Trans. Int. Symp. on Soil Water Measurement Using Capacitance and Impedance, 1st, Beltsville, MD. 5-7 Nov. 2002. PALTIN Int., Laurel, MD.

Chanasyk, D.S., Naeth, M.A., 1996. Filed measurement of soil moisture using neutron probes. Can. J. Soil Sci. 76, 317-323.

Cobos, D.R., Chambers, C., 2010. Calibrating ECH2 O soil moisture sensors. Application note. <http://www.decagon.com/assets/Uploads/13393-04-CalibratingECH2OSoilMoistureProbes.pdf> (Accessed: March, 2015).

Day, P.R., 1965. Particle fractionation and particle-size analysis. In: Black CA (ed) Methods of soil analysis, part I. Agronomy Monographs 9. ASA, Madison, WI.

Dean, T.J., Bell, J.P., Baty, A.J.B., 1987. Soil moisture measurement by an improved capacitance technique, Part 1. Senor Design and performance. J. Hydrol. 930, 67-78.

Evett, S.R., Tolk, J.A., Howell, T.A., 2006. Soil profile water content determination: sensor accuracy, axial response, calibration, temperature dependence, and precision. Vadose Zone J. 5, 894-907.

FAO (Food and Agriculture Organization), 2015. World Base Reference Base for soil resources (2014) update of 2015.

Fares, A., Polyakov, V., 2006. Advances in crop water management using capacitive water sensors. Adv. Agron. 90, 43-77.

Gabriel, J.L., Lizaso, J.I., Quemada, M., 2010. Laboratory versus field calibration of capacitance probes. Soil Sci. Soc. Am. J. 74, 593-601.

Gardner, C.M.K., Bell, J.P., Cooper, J.D., Dean, T.J., Garden, N., Hodnett, M.G., 1991**.** Soil water content. In: Soil Analysis: Physical Methods. Dekker Press, New York.

Geesing, D., Bachmaier, M., Schmidhalter, U., 2004. Field calibration of capacitance soil water probe in heterogeneous fields. Aust. J. Soil Res. 42, 289-299.

Girona, M., Mata, M., Fereres, E., Goldhamer, D.A., Cohen, M., 2002. Evapotranspiration and soil water dynamics of peach trees under water deficits. Agric. Water Manage. 54**,** 107-122.

Heimovaara, T.J., 1993. Design of triple-wire time domain reflectometry probes in practice and theory. Soil Sci. Soc. Am. J. 57(6), 1410-1417.

Hillel, D., 2003. *Introduction to environmental soil physics*. Academic press.

Kaleita, A.L., Heitman, J.L., Logsdon, S.D., 2005. Field calibration of the Theta probe for Des Moines Lobe soils. Appl. Eng. Agric. 21(5), 865-870.

Kelleners, T.J., Soppe, R.W.O., Ayars, J.E., Skaggs, T.H., 2004. Calibration of capacitance probe sensors in a saline silty clay soil. Soil Sci. Soc. Am. J. 68, 770-778.

Kinzli, K., Manana, N., Oad, R., 2012. Comparison of laboratory and field calibration of a soil-moisture capacitance probe for various soils. J. Irrig. Drain. E-ASCE 138(4), 310-321.

Lane, P.N.J., Mackenzie, D.H., 2001. Field and laboratory calibration and test of TDR and capacitance techniques for indirect measurement of soil water content. Aust. J. Soil Res. 39, 1371-1386·

Mjanyelwa, N., Bello, Z.A., Greaves, W., van Rensburg, L.D., 2016. Precision and accuracy of DFM soil water capacitance probes to measure temperature. Comput. Electron. Agr. 125, 125-128.

Morgan, K.T., Parsons, L.R., Wheaton, T.A., Pitts, D.J., Obreza, T.A., 2001. Field calibration of a capacitance water content probe in fine sand soils. Soil Sci. Soc. Am. J. 63, 987–989.

Nhlabatsi, N.N., 2010. Soil surface evaporation studies on the Glen/Bonheim ecotope. PhD thesis, University of the Free State, Bloemfontein, South Africa.

Oates, M.J., Fernández-López, A., Ferrández-Villena, M., Ruiz-Canales, A., 2016. Temperature compensation in a low cost frequency domain (capacitance based) soil moisture sensor. Agr. Water Manage. 183, 86-93.

Paraskevas, C., Georgiou, P., Ilias, A., Panoras, A., Babajimopoulos, C., 2012. Calibration equations for two capacitance water content probes. Int. Agrophys. 26, 285-293.

Regalado, C.M., Ritter, A. and Rodríguez-González, R.M., 2007. Performance of the commercial WET capacitance sensor as compared with time domain reflectometry in volcanic soils. Vadose Zone J. 6(2), 244-254.

Robinson, D.A., Campbell, C.S., Hopmans, J.W., Hornbuckle, B.K., Jones, S.B., Knight, R., Ogden, F., Selker, J., Wendroth, O., 2008. Soil moisture measurement for ecological and hydrological watershed-scale observatories: A review. Vadose Zone J. 7(1), 358-389.

Robinson, D.A., Gardner, C.M.K., Cooper, J.D., 1999. Measurement of relative permittivity in sandy soils using TDR, capacitance and theta probes: comparison, including the effects of bulk soil electrical conductivity. J. Hydrol. 223(3), 198-211.

Robock, A., Vinnikov, K.Y., Srinivasan, G., Entin, J.K., Hollinger, S.E., Speranskaya, N.A., Liu, S., Namkhai, A., 2000. The global soil moisture data bank. B. Am. Meteorol. Soc. 81(6), 1281-1299.

Scudiero, E., Berti, A., Teatini, P., Morari, F., 2012. Simultaneous monitoring of soil water content and salinity with a low-cost capacitance-resistance probe. Sensors 12, 17588-17607.

Seyfried, M.S., Murdock, M.D., 2001. Response of a new soil water sensor to variable soil, water content, and temperature. Soil Sci. Soc. Am. J. 65, 28-34.

Seyfried, M.S., Murdock, M.D., 2004. Measurement of soil water content with a 50-MHz soil dielectric sensor. Soil Sci. Soc. Am. J. 68, 394-403.

Soil Classification Working Group, 1991. *Soil classification: a taxonomic system for South Africa*. Department of Agricultural Development, Pretoria.

Soil Survey Staff, 2014. *Keys to Soil Taxonomy*. United States Department of Agriculture, Natural Resource Conservation Service.

Starr, J.L., Paltineanu, I.C., 1998. Soil water dynamics using multisensor capacitance probes in non-traffic interrows of corn. Soil Sci. Soc. Am. J., 62, 114-122.

Topp, G.C., Davies, J.L., Annan, A.P., 1980. Electromagnetic determination of soil water content: measurements in coaxial transmission lines. Water Resour. Res. 16, 574-582.

Walther, B.A., Moore, J.L., 2005. The concepts of bias, precision and accuracy, and their use in testing the performance of species richness estimators, with literature review of estimator performance. Ecography 28, 815-829.

Zanetti, S.S., Cecílio, R.A., Silva, V.H., Alves, E.G., 2015. General calibration of TDR to assess the moisture of tropical soils using artificial neural networks. J. Hydrol. 530, 657-666.

Zerizghy, M.G., van Rensburg, L.D., Anderson, J.J., 2013. Comparison of neutron scattering and DFM capacitance instruments in measuring soil evaporation. Water SA 39(2), 183-190.

Zettl, J.D., Huang, M., Barbour, S.L., Si, B.C., 2015. Density-dependent calibration of multisensor capacitance probes in coarse soil. Can. J. Soil Sci. 95, 331-336.

7. Calibration of compensation heat pulse velocity technique for measuring transpiration of selected indigenous trees using weighing lysimeters

Abstract

The compensation heat pulse velocity (CHPV) is one of the most widely used methods to measure sap flow in woody plants. However, the accuracy of this method has not been fully explored especially for indigenous tree species of South Africa. The aim of this study was to evaluate the accuracy of the CHPV method in quantifying tree transpiration for selected tree species. Three indigenous trees sampled in a monolith form; black karee (*Sersia lancea*), buffalo thorn (*Ziziphus mucronata*) and wild olive (*Olea africana*) grown on weighing lysimeters (1 m × 1m × 1.3 m) were installed with CHPV probes to measure sap flow on the stem half hourly, simultaneously with lysimeter measurements of transpiration. The surfaces of the lysimeters were covered with a 100 mm layer of Styrofoam, overlain by a 20 mm layer of gravel to minimize evaporation to a negligible level. Both the lysimeter and CHPV measurements were divided into two sets. The first set was used to develop tree specific calibration equations as well as an equation combining the three species used, here called a combination equation. The second set of data was used for validating the equations. Transpiration rates ranged from negligible at night to daily peaks of 3.5, 1.7 and 1.4 L hr^{-1} for buffalo thorn, black karee and wild olive, respectively. Good agreement indices between CHPV and lysimeters were obtained when using both the tree specific equations and combination equation across species (D = 0.778-1.000, RMSE = 0.001-0.017 L hr^{-1}, MAE < 0.001 L hr^{-1} and MBE = -0.0007-0.0008 L hr^{-1}). It was concluded that the CHPV method can accurately measure tree water use, and therefore can be useful for water resources management in forested areas.

Keywords: Sap flow calibration; tree water use; indigenous South African trees.

7.1 Introduction

There are various ways of quantifying transpiration of field crops, but, for trees, sap flow measurement remains the most prominent. An array of automated thermodynamic techniques which use heat as a tracer of sap flow, have for several decades been employed to quantify water fluxes in the soil – plant – atmosphere continuum at the tree scale. Amongst the thermal based methods of sap flow measurement, the most common are the compensation heat pulse velocity (CHPV) (Huber 1932; Marshall, 1958; Swanson, 1962; Swanson and Whitfield, 1981; Fernández et al., 2001; Green et al., 2003) and thermal heat dissipation (THD) (Granier 1987; Lu et al., 2004) methods. These methods are user friendly and cause minimal damage to the tree stems (Granier, 1987; Green et al., 2003).

The CHPV method also has an advantage of using less energy as it works on pulses of heat as opposed to the continuous heating principle of the THD (Fernández et al., 2006; Nourtier et al., 2011). The CHPV method has also been employed to measure transpiration of local and exotic commercial forest species of South Africa such as *Eucalyptus species* (Morris et al., 2004; Wildy et al., 2004) and *Jatropha curcas* (Gush, 2008). The accuracy of the CHPV method in measuring sap flow in indigenous trees of South Africa has unfortunately not been explored. A majority of the water use studies of indigenous trees in South Africa have employed the HR method (Everson et al., 2011; Clulow et al., 2013; Scott-Shaw et al., 2017) and aerodynamic based methods such as the Eddy covariance (Everson et al., 2011; Everson et al., 2013; Clulow et al., 2015).

Lysimetry is considered as one of the standard methods to quantify plant water use (Johnson et al., 2005; Clawson et al., 2009), especially if their load cells are correctly calibrated (Misra et al., 2011) and can account for various components of the soil water balance while keeping other

components under control (Dlamini et al., 2016). Even though lysimeters can accurately measure plant water use and can be applied in a number of studies such as soil nutrients, evaporation and drainage analysis, it has its own drawbacks such as high cost and limited replication. The indigenous trees in South Africa contribute significantly to the economy of the country in the form of goods and services (Gush et al., 2015). However, knowledge on the transpiration of most of these indigenous trees is limited (Dye et al., 2008). The objective of the present study was to evaluate the accuracy of CHPV method in measuring transpiration of selected indigenous tree species of South Africa.

7.2 Materials and Methods

7.2.1 Study site description

The study was conducted at Kenilworth Experiment Farm (latitude: -29.02°, longitude: 26.15° and altitude: 1354 m) in the Department of Soil, Crop and Climate Sciences at the University of the Free State, in Bloemfontein, South Africa. This experiment was implemented over a period of 107 days during the summer season, from 9th December 2016 to 25th March 2017. The study area, with a mean annual precipitation of 528 mm mostly falling between October and April and average reference evapotranspiration (ETo) of 1 604 mm is classified as warm semi-arid (Thornthwaite, 1948; UNESCO 1979; Peel et al., 2007). The mean annual minimum and maximum air temperatures are 11.0 °C and 25.5 °C, respectively.

7.2.2 Trees and lysimeter facility

An illustration of the equipment setup during the experiment is shown in Figure 7.1. Three indigenous trees of dominant species within the study area; black karee (*Sersia lancea*), buffalo

thorn (*Ziziphus mucronata*) and wild olive (*Olea africana*) were transplanted from within a radius of 3 km away from the study area into lysimeters (January, 2015) with their natural soil monoliths. The fourth sampled tree, sweet thorn (Vachelia karoo) as stated in Chapter 5 was not included in this study due to some technical fault in the load cells on which it was placed. On average, the trees were 3 m (2 m to 4 m) in height and stem diameter between 90 and 120 mm. The ages of the trees were estimated to be within the range of 7 to 10 years. The dimensions of lysimeters were 1 m × 1 m and 1.3 m in depth. The lysimeter containers with their contents (soil and trees) were placed on top of Loadtech LT 1300 type of load cells supplied by Loadtech Load Cells (Pty) Ltd, South Africa. The load cells were placed on top of flat concrete slabs to ensure they remain level during the experiment. The soil surface on top of the monoliths was covered by a 100 mm layer of Styrofoam and then overlain by a 20 mm layer of gravel to minimize evaporation to negligible levels.

7.2.3 Compensation Heat Pulse Velocity Theory

In the CHPV method, two temperature sensors are inserted at unequal distances, downstream and upstream of a radially inserted heater in the stem. The upstream probe is placed closer to the heater (5 mm) and increase temperature faster (through conduction) than the downstream probe (placed 10 mm away) whose temperature change is influenced by transfer of energy by conduction through the wood and convection through the flowing sap whenever a heat pulse is released by the heater. The time taken by the two sensors to record equal temperature rise is related to the movement of sap flow and hence the plant water uptake (Swanson and Whitfield, 1981; Green et al., 2003). The heat pulse velocity (V_h) in cm hr^{-1}, is calculated from the time (t)

taken to record equal temperatures by the sensors at distances (X_u), upstream and (X_d) downstream as:

$$V_h = \frac{X_u + X_d}{2t} \quad (7.1)$$

V_h is basically indirectly proportional to t. This implies that if the sap movement is high, the convection of the heat pulse through the moving sap will be enhanced and then the recorded t will be minimal. Early studies revealed that the movement of the sap is a few folds more than the movement of heat in terms of sap flow density through the sapwood because the heat is also dependent on conduction through the stationary, interstitial tissue between the xylem vessels or tracheids. Marshall (1958) established a relationship between V_h and the sap flux (Q) and expressed it as:

$$Q = a\,u = (\frac{\rho_{sm}\, c_{sm}}{\rho_s\, c_s})V_h \quad (7.2)$$

where a is the fraction of the cross sectional area of the conducting sapwood occupied by moving sap, u is the velocity of sap, ρ and c are density and specific heat capacity with subscripts s and sm referring to the sap and sap plus woody matrix respectively. V_h can be expressed in terms of the basic density (ρ_b) and the water content (w_c) of the sapwood as estimated as:

$$\rho_b = \frac{\text{oven dried mass of wood}}{\text{fresh volume of wood}} \quad (7.3)$$

$$\mathrm{w}_c = \frac{\text{fresh mass of wood} - \text{oven dried mass of wood}}{\text{oven dried mass of wood}} \quad (7.4)$$

The density (ρ) of the fresh wood can also be expressed:

$$\rho = \rho_b(1 + \mathrm{w}_c) \quad (7.5)$$

The specific heat (c) can be expressed as:

$$\mathrm{c} = \frac{c_w + \mathrm{w}_c\, c_s}{1 + \mathrm{w}_c} \quad (7.6)$$

where c_w = specific heat of oven dry wood = 0.33

c_s = specific heat of sap (water) = 1.0

s = density of sap = 1.0

Equation 7.2, on substitution then becomes:

$$Q = \rho_b(\mathrm{w}_c + 0.33)V_h \quad (7.7)$$

Sap flux estimated using Equation 7.7 can be referred to as raw values of sap velocity as the procedure that was used to obtain this equation assumed the sapwood material to be isotropic (Marshall, 1958), something which is not a true reflection of reality. The velocity of sap varies with radial depth into the stem. Before the application of Equation 7.7 to establish the flux density of sap, the measured values of V_h must be corrected to account for i) the influence on heat transfer of the material used to construct the heater and sensor probes and ii) the effects of the wounding due to drills into the wood. Empirical functions to make these corrections for a variety of materials used to construct heaters and sensors and for a range of drill spacing were derived by Swanson and Whitfield (1981), Green and Clothier (1988) and Green et al. (2003).

To establish the volumetric flow rates (Q_v), the sap flux is measured at different depths below the cambium of a stem in order to determine a radial profile of sap flux across the sapwood. A second-order least squares regression equation fitted to the sap velocity profile is used to calculate Q_v (L hr^{-1}) (Edwards and Warwick, 1984; Green and Clothier, 1988; Green et al., 2003) as:

$$Q_v = 2\pi \int_H^R rQ(r)dr \quad (7.8)$$

where R (m) is the cambium radius of the stem and H is the heartwood radius.

7.2.4 Tree water use measurements

Water use by the trees was monitored using the prior calibrated load cells and the CHPV technique. Changes in mass, indicating water gain or loss in each of the lysimeters was obtained from the outputs of the load cells which were all connected to a data logger (CR 3000, Campell Scientific, Inc, Logan, UT, USA). The signals from the load cells were sampled every minute and the average stored half hourly. The change in mass recorded by the load cell was converted into transpiration (T) in (L hr^{-1}) as follows:

$$T = 2(X_1 - X_2) \quad (7.9)$$

where X_1 is the initial mass at the beginning of half an hour and X_2 is the final mass at the end every half an hour. Alongside the load cell measurements, tree water uptake was monitored using the CHPV technique installed on the stems at approximately 0.5 m above the soil surface. To make provision for the bias due to the variation in azimuthal variability of the sap flow density during the day or season (Wullschleger and King, 2000; Saveyn et al., 2008), two sets of the CHPV technique were installed on an individual tree in a spiral pattern around the tree stem. For each set, the two temperature sensor probes, installed upstream and downstream of the heater had thermistors at depths of 5, 15, 25 and 40 mm below the cambium. In this way, assessment of radial profile and its temporal variability for individual tree were made possible. Sap flow data were recorded and stored in a datalogger (CR1000, Campell Scientific, Inc, Logan, UT, USA). The sap flow gadgets were covered by aluminium foil to minimize external environmental effects on the sensors. These measurements were taken across a range of soil water content from near saturation to at least 30% of available water (AW) in the top 0.8 m. AW is the difference between the predetermined drained upper limit and drained lower limit of the soil as explained by (Hensley et al. (2011). The soil water content was always brought back to field capacity

whenever AW approached 30%. Part of the irrigation aim for the study was to ensure that the trees did not go into stress throughout the year. HydraSCOUT (HS) capacitance probes, manufactured by Hydra Sensor Technologies International Ltd in South Africa, was used to monitor the soil water content throughout the experiment. Prior to the beginning of the study, HS probes were calibrated in the laboratory and in the field against the standard gravimetric method for soil water measurements across the depth of each soil profile in all the points where trees were sampled. The accuracy of the CHPV method to estimate water use by the selected indigenous trees was tested against the lysimeter measurements.

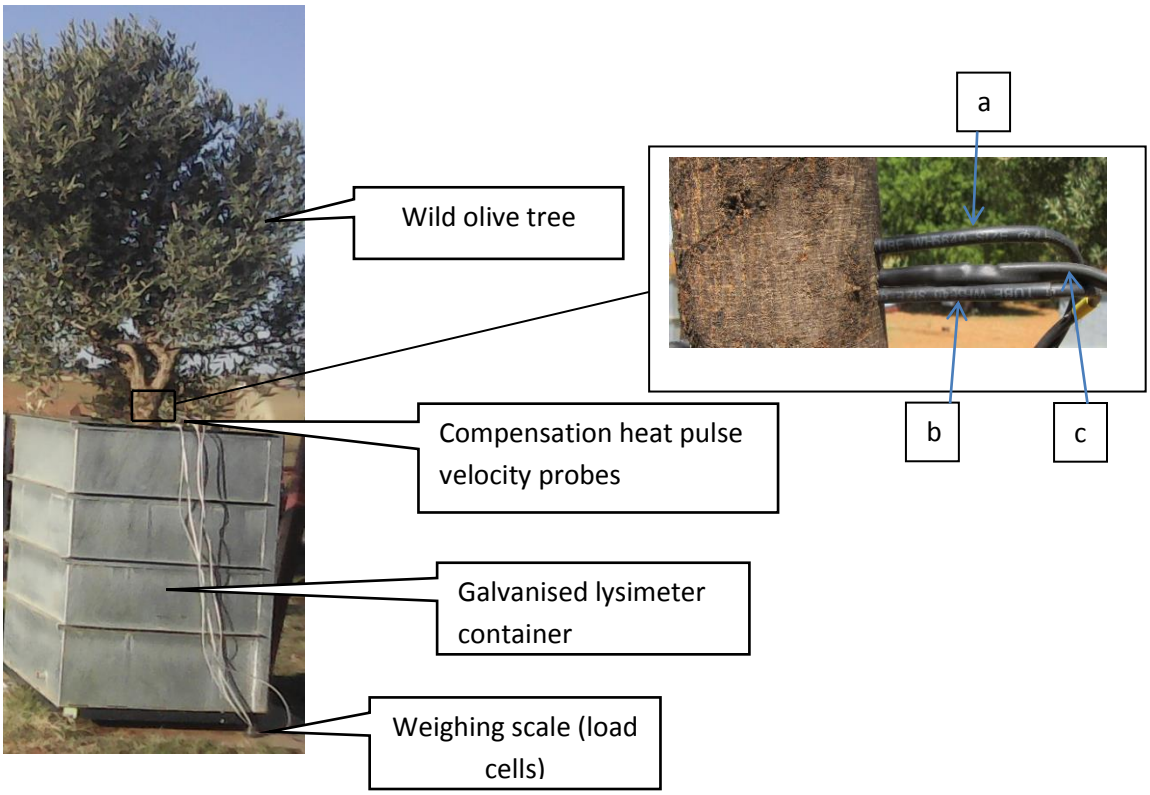

Figure 7.1: An illustration of the experimental setup showing a wild olive tree installed with compensation heat pulse velocity sap flow probes, growing in a galvanized lysimeter container. Insert: a = downstream probe, b = upstream probe and c = heater probe.

7.2.5 Statistical analysis

Tree water use data measured by both the lysimeter and CHPV techniques were divided into two sets. The first set of data was used to generate the calibration equations by regressing the lysimeter transpiration data against the CHPV data for the three trees. The calibration data from the three lysimeter units were also pooled together to form a relationship referred to as the combination equation, an equation combining data of the three tree species. The four equations (three tree specific and combination) were evaluated by applying them on the CHPV data from the second data set to estimate the corresponding lysimeter data for a particular time. To test the versatility of the equations across tree species, each of the four equations was applied in all the three tree species. The goodness of fit for the predicted transpiration values against the lysimeter measurements was determined by the coefficient of determination (R^2) and D-index of agreement (D) (Equation 7.10). The accuracy of estimation was determined by the root mean square error (RMSE) (Equation 7.11) and mean absolute error (MAE) (Equation 7.12). The mean bias error (MBE) (Equation 7.13) was computed to determine the deviation of the predicted tree transpiration from the lysimeter measured transpiration (Willmott, 1982; Walther and Moore, 2005).

$$D = 1 - \frac{\sum_{i=1}^{n}(E_i - O_i)^2}{\sum_{i=1}^{n}(|E_i - \bar{O}| + |E_i - \bar{O}|)^2} \quad (7.10)$$

$$RMSE = [n^{-1}\sum_{i=1}^{n}(E_i - O_i)^2]^{0.5} \quad (7.11)$$

$$MAE = \frac{1}{n}\sum_{i=1}^{n}(E_i - O_i) \quad (7.12)$$

$$MBE = \sum_{i=1}^{n}(E_i - O_i)/n \quad (7.13)$$

where n is the number of observations, E_i, O_i and $\bar{O}$ are the estimated (sap flow transpiration), observed or measured (lysimeter transpiration) and mean values for the lysimeter measurements, respectively. Any model with R^2 approaching 1 has a good performance, a D-index close to 1, as

well as RMSE and MAE close to 0 indicates good agreement between measured and estimated values (Willmott, 1982). A negative MBE indicates that the sap flow measurement is underestimating the lysimeter measured transpiration and vice versa. The closer the MBE value is to 0, the better (Abbas et al., 2011).

7.3 Results

7.3.1 Calibration equations

After the tree transpiration measured by lysimeter and sap flow meter has been converted to the same unit (L hr^{-1}), it can be observed that different ranges of transpiration were observed for different tree species (Figure 7.2). Out of the 3 tree species, the maximum transpiration was observed in buffalo thorn which was above 3.5 L hr^{-1} from lysimeter measurement. Transpiration rates of up to 1.7 L hr^{-1} and 1.4 L hr^{-1} were observed for black karee and wild olive, respectively. The relationships between the lysimeter transpiration and sap flow measurements on the different trees individually, and across tree species is presented in Figure 7.2. Based on the highest R^2, these relationships were described by linear equations. The R^2 values were 0.65 for black karee, 0.75 for buffalo thorn, 0.62 for wild olive and 0.69 for the combination calibration.

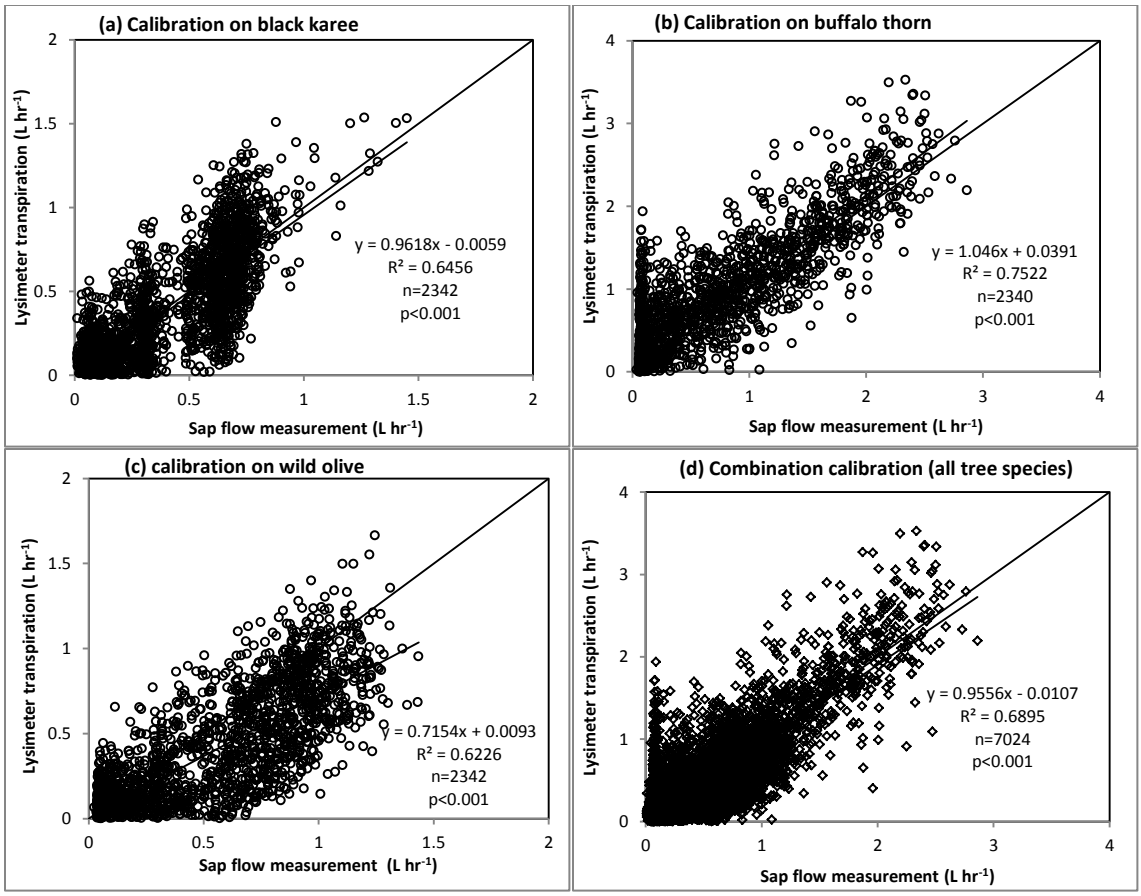

Figure 7.2: Relationship between sap flow and lysimeter measured transpiration (L h^{-1}) on (a) black karee (b) buffalo thorn (c) wild olive and (d) across the tree species.

7.3.2 Validation of the calibration equations

The application of all the tree specific and combination calibration equations on the second set of data for each of the three tree species to estimate transpiration using the sap flow data is presented in Figure 7.3(a-l). The summary of statistical performance of the developed equations is presented in Table 7.1. The observed RMSE values were all small (0.001-0.017 L hr^{-1}), for the tree specific calibration equations and the combination equation across the trees.

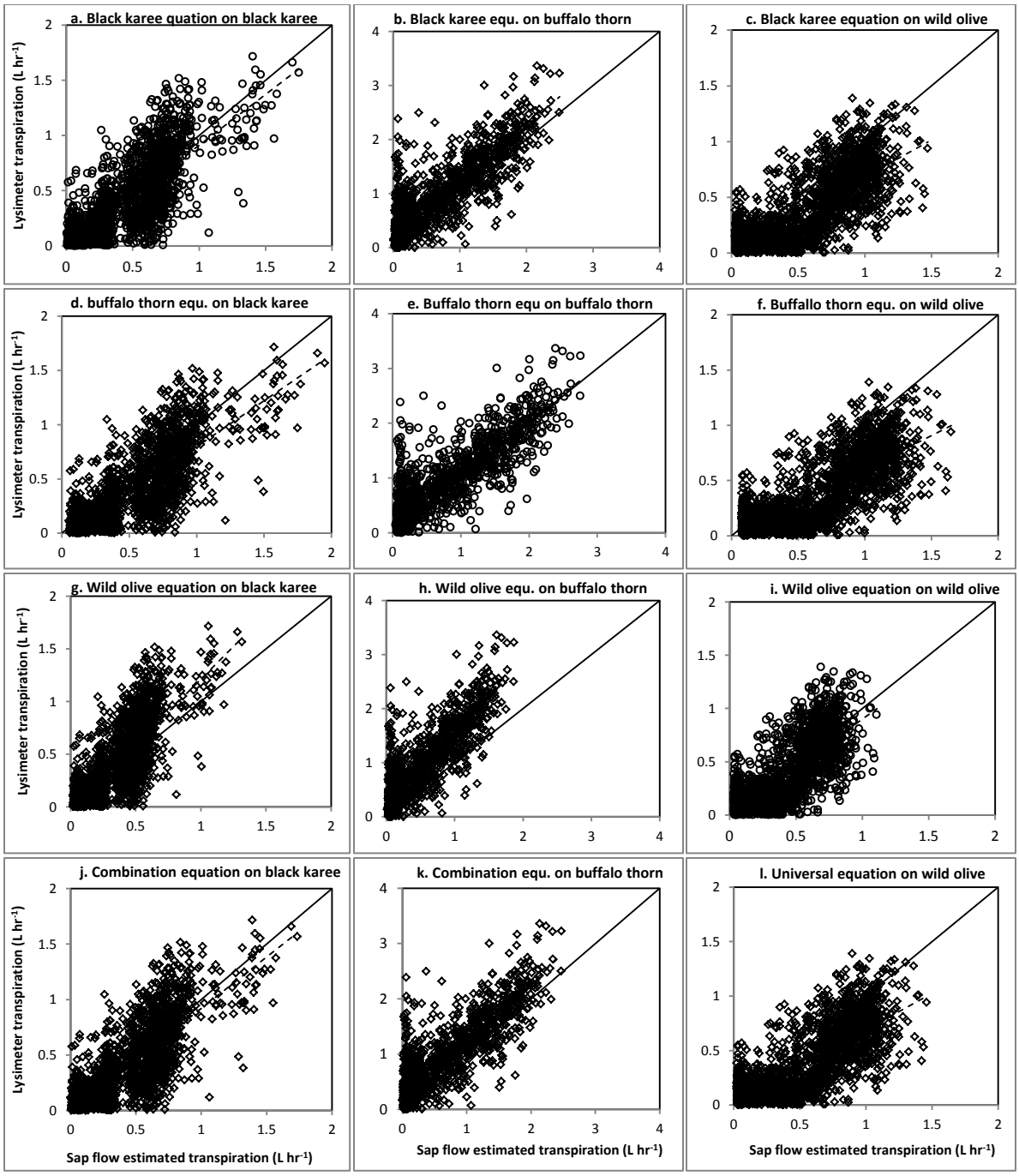

Figure 7.3: The relationship between the observed lysimeter and the sap flow estimated transpiration of the different trees (L hr^{-1}) using all the four calibration equations (rows) on each of the three tree species (columns).

Table 7.1: Comparison of statistical parameters (root mean squared error (RMSE), mean absolute error (MAE), mean bias error (MBE), coefficient of determination (R^2), slope and y-intercept (Y-I)) of the validation for the tree specific and combination sap flow calibration equations to estimate transpiration (L hr^{-1}) in black karee, buffalo thorn and wild olive trees.

Calibration equation	Tree species	RMSE (L hr^{-1})	MAE (L hr^{-1})	MBE (L hr^{-1})	R^2	Slope	Y-I	D-index	N
Black karee	Black karee	0.002	<0.001	0.0005	0.641	0.696	0.145	0.887	2323
Buffalo thorn	Black karee	0.004	<0.001	0.0008	0.641	0.757	0.204	0.871	2323
Wild olive	Black karee	0.001	<0.001	-0.0006	0.641	0.518	0.122	0.843	2323
Combination	Black karee	0.002	<0.001	0.0004	0.641	0.691	0.139	0.888	2323
Buffalo thorn	Buffalo thorn	0.016	<0.001	0.0000	0.763	0.764	0.086	0.988	2341
Black karee	Buffalo thorn	0.017	<0.001	-0.0003	0.763	0.702	0.044	1.000	2341
Wild olive	Buffalo thorn	0.017	<0.001	-0.0007	0.763	0.522	0.042	0.996	2341
Combination	Buffalo thorn	0.017	<0.001	-0.0002	0.763	0.697	0.033	0.999	2341
Wild olive	Wild olive	0.003	<0.001	0.0001	0.600	0.671	0.148	0.869	2341
Black karee	Wild olive	0.008	<0.001	0.0008	0.600	0.901	0.182	0.831	2341
Buffalo thorn	Wild olive	0.011	<0.001	0.0008	0.600	0.980	0.243	0.778	2341
Combination	Wild olive	0.008	<0.001	0.0006	0.600	0.895	0.176	0.835	2341

The R^2 values that ranged between 0.60 and 0.76 with D-index values that are very close to 1 (0.778-1.000) showed good agreement between the estimated and observed values of tree transpiration. These were notably similar in each of the tree species regardless of the equation employed to estimate transpiration. It is worth noting that the D-index when using the combination equation of three tree species was always the closest to that obtained when using a tree specific equation to estimate water use for a particular tree. For instance, when estimating the water use for black karee using the black karee equation (Table 7.1), the D-index was 0.887.

The D-index of 0.888 obtained when the combination equation was used is closer (almost equal to 0.887) than the D-indices of 0.871 and 0.843 obtained when using the buffalo thorn and wild olive calibration equations, respectively. This good agreement was further confirmed by MAE (<0.001 L hr^{-1}) values which were optimal in all cases. From the MBE values which ranged between -0.0007 and 0.0008 L h^{-1}, it shows that tree transpiration was estimated with high accuracy for all the trees by all the equations (Table 7.1). The slopes of the relationship between the estimated and observed tree water use ranged from 0.691 to 0.980 across all the trees when using the black karee, buffalo thorn and combination calibration equations. The slopes when using the wild olive calibration equation were between 0.518 and 0.671, which were outside the range obtained from the other equations. These were however all good as they were close to 1. The y-intercepts were all closer to 0, also indicating good accuracy of the CHPV method even at small tree water use levels.

7.4 Discussion

Limited research has been done on the calibration of the CHPV method, especially on indigenous trees. The findings of this study revealed a relatively good agreement between the sap flow estimated tree transpiration and the transpiration measured using lysimeters in both the calibration and validation exercises. This was indicated by the high R^2 values, very low RMSE and MAE values, slopes of the relationships between estimated and observed water use closer to 1 and y-intercepts closer to 0. This implied that the estimate given by the sap flow measurement was as good as the transpiration measurement given by the pre-calibrated weighing load cells of the lysimeters. Dye et al. (1996) conducted an experiment and compared sap flow measured with CHPV method on an excised tree with its water uptake from a big bucket in which the cut stem

was submerged. In their experiment they also got high R^2 values (mean = 0.79) between the sap flow estimated transpiration and observed water uptake from the bucket. Dragoni et al. (2005) also found good agreement (R^2 values between 0.87 and 0.94) between the CHPV method and whole tree canopy chambers on apple trees. Using the THD method, McCulloh et al. (2007) compared sap flow measurements to gravimetrically measured water loss for potted *Pseudobombax Septanatum* and *Calophyllum longfollium* tree and found them to be statistically similar ($P < 0.05$), indicating a good agreement between the measurement techniques.

Estimations of the tree transpiration were of high accuracy in terms of MBE values that were close to 0. This was truly so when using the tree specific equations as well as the combination equation of the three tree species used. With the CHPV method, over or under estimations of tree water used has previously been attributed to inappropriate wound correction factors (Poblete-Echeverría et al., 2012). In the present study the appropriate correction factor of 2.8 for the 2 mm drill bit was used as recommended by Green et al. (2003).

The CHPV sap flow method is a good candidate for measuring transpiration of South African indigenous trees as it produces accurate estimates. However, appropriate methods for scaling up from plant to stand, and to the whole landscape should be used for water balance calculations. All the tree specific calibration equations could be applied on other trees with good accuracy of estimating water use. This basically implied that a once off calibration for a certain type of trees (e.g. woody, herbaceous, etc.) can be sufficient for using the CHPV method to estimate water use. The higher agreement between the combination calibration equation ($y = 0.9556x - 0.0107$) (Figure 7.2d) and the tree specific equations warrants its recommendation for water use estimates of indigenous woody tree species of South Africa. This can eliminate the costs and save time on calibration exercises. However caution should be taken on the wood characteristics

of trees growing in different climatic zones as the equation may lead to inaccurate tree water use estimations. Desert trees may exhibit different flow channels within their vascular bundles. With the present results it can be ascertained that the combination equation can be applicable on the investigated tree species as well as other woody trees within semi-arid and arid regions.

Future work should consider development of calibration equations for other types of plants such as herbaceous trees and test them across different climatic zones. Since there was no default calibration equations from the manufacturer, the combination equation derived during this study can be recommended as the default (manufacturer`s) equation for these specific types of trees. Default calibration equations from the manufacturer were also found to estimate with high accuracy stem water content of *Prosopis juliflora* (Sw.), *Tamarix ramosissima* Ledeb. and *Prosopis pubescens* Benth, invasive tree species in Sudan and United States (Saito et al., 2016). Future work can employ the CHPV technique to take continuous measurements of tree transpiration to inform scientists, and hence policy makers and administrators on sustainable management of water resources.

7.5 Conclusions

Relationships were developed between the CHPV estimated tree transpiration and lysimeter measured tree transpiration resulting in tree specific and a combination equation for the three species. The resulted equations were evaluated for accuracy. From the results, it was observed that irrespective of the tree species, the CHPV estimated tree transpiration with high accuracy shown by high D-indices and low RMSE and MAE. Though, the developed tree specific calibration equations estimated tree transpiration with high accuracy but were relatively as good as the developed combination calibration equation. Therefore, the developed combination calibration equation can be used across the three tree species used in this investigation and other species with similar wood characteristics. Since the performance of the calibration equations were similar, a once off calibration equation from one tree species can be used to estimate transpiration for the other two species under investigation in this study.

References

Abbas, F., Fares, A., Fares, S., 2011. Filed calibration of soil moisture sensors in a forested watershed. Sensors 11, 6354-6369.

Clawson, E.L., Hribal, S.A., Piccini, G., Hutchinson, R.L., Rohli, R.V., Thomas, D.L., 2009. Weighing lysimeters for evapotranspiration research on clay soil. Agron. J. 101(2), 836-840.

Clulow, A. D., C. S. Everson, M. G. Mengistu, J. S. Price, A. Nickless, and G. P. W. Jewitt. "Extending periodic eddy covariance latent heat fluxes through tree sapflow measurements to estimate long-term total evaporation in a peat swamp forest." *Hydrology and Earth System Sciences Discussions* 11, no. 12 (2014): 13607-13661.

Clulow, A.D., Everson, C.S., Price, J.S., Jewitt, G.P.W., Scott-Shaw, B.C., 2013. Water-use dynamics of a peat swamp forest and a dune forest in Maputaland, South Africa. Hydrol. Earth Syst. Sci. 17(5), 2053-2067.

Dlamini, P., Ukoh, IB., van Rensburg, L.D., du Preez, C.C., 2016. Reduction of evaporation from bare soil using plastic and gravel mulches and assessment of gravel mulch for partitioning evapotranspiration under irrigated canola. Soil Res. 55(3), 222-233.

Dragoni, D., Lakso, A.N., Piccioni, R.M., 2005. Transpiration of apple trees in a humid climate using heat pulse sap flow gauges calibrated with whole-canopy gas exchange chambers. Agr. Forest Meteorol. 130(1), 85-94.

Dye, P.J., Gush, M.B., Everson, C.S., Jarmain, C., Clulow, A., Mengistu, M., Geldenhuys, C.J., Wise, R., Scholes, R.J., Archibald, S., Savage, M.J., 2008. Water-use in relation to biomass of indigenous tree species in woodland, forest and/or plantation conditions. WRC Report TT 361/08, Water Research Commission, Pretoria, South Africa.

Edwards, W.R.N., Warwick, N.W.M., 1984. Transpiration from a kiwifruit vine as estimated by the heat-pulse technique and the Penman-Monteith equation. N.Z. J. Agric. Res. 27, 537–543.

Everson, C.S., Dye, P.J., Gush, M.B., Everson, T.M., 2011. Water use of grasslands, agroforestry systems and indigenous forests. Water Sa, 37(5), 781-788.

Everson, C.S., Mengistu, M.G., Gush, M.B., 2013. A field assessment of the agronomic performance and water use of Jatropha curcas in South Africa. Biomass Bioenerg. 59, 59-69.

Fernández, J.E., Durán, P.J., Palomo, M.J., Diaz-Espejo, A., Chamorro, V., Girón, I.F., 2006. Calibration of sap flow estimated by the compensation heat pulse method in olive, plum and orange trees: relationships with xylem anatomy. Tree Physiol. 26(6), 719-728.

Fernández, J.E., Palomo, M.J., Díaz-Espejo, A., Clothier, B.E., Green, S.R., Girón, I.F., Moreno, F., 2001. Heat-pulse measurements of sap flow in olives for automating irrigation: tests, root flow and diagnostics of water stress. Agric. Water Manage. 51, 99–123.

Granier, A., 1987. Evaluation of transpiration in a Douglas-fir stand by means of sap flow measurements. Tree Physiol. 3, 309-320.

Green, S.R., Clothier, B.E., 1988. Water use of kwiwifruit vines and apple trees by the heat pulse technique. J. Exp. Bot. 39 (198), 115-123.

Green, S., Clothier, B., Jardine, B., 2003. Theory and practical application of heat pulse to measure sap flow. Agron. J. 95, 1371-1379.

Gush, M.B., 2008. Measurement of water-use by Jatropha curcus L. using ther heat pulse velocity technique. Water SA 34(5), 1-5.

Gush, M.B., de Lange, W.J., Dye, P.J., Geldenhuys, C.J., 2015. Water Use and Socio-Economic Benefit of the Biomass of Indigenous Trees. WRC Report 1876/1/15, Water Research Commission, Pretoria, South Africa.

Hensley, M., Bennie, A.T.P., Van Rensburg, L.D., Botha, J.J., 2011. Review of 'plant available water' aspects of water use efficiency under irrigated and dryland conditions. Water SA, 37(5), 771-779.

Huber, B., Schmidt, E., 1937. Eine Kompensationsmethode zur thermoelektrischen Messung langsamer Saftströme. Ber. Deutch. Bot. Ges. 55, 514-529.

Johnson, R.S., Williams, L.E., Ayars, J.E., Trout, T.J., 2005. Weighing lysimeters aid study of water relations in tree and vine crops. Calif. Agric. 59(2), 133-136.

Lu, P., Urban, L., Ping, Z., 2004. Granier's thermal dissipation probe (TDP) method for measuring sap flow in trees: theory and practice. Acta. Botanica. Sinica 46(6), 631-646.

Marshall, D.C., 1958. Measurement of sap flow in conifers by heat transport. Plant Physiol. 33, 385-396.

McCulloh, K., Winter, K., Meinzer, F.C., Carcia, M., Aranda, J., Lachenbruch, B., 2007. A comparison of daily water used estimates derived from constant-heat-sap-flow probe values and gravimetric measurements in pot grown sapplings. Tree Physiol. 27, 1355-1360.

Misra, R.K., Padhi, J., Payero, J.O., 2011. A calibration procedure for load cells to improve accuracy of mini-lysimeters in monitoring evapotranspiration. J. Hydrol. 406(1), 113-118.

Morris, J., Ningnan, Z., Zengjiang, Y., Collopy, J., Daping, X., 2004. Water use by fast-growing Eucalyptus urophylla plantations in southern China. Tree Physiol. 24(9), 1035-1044.

Nicolas, E., Torrecillas, A., Ortuno, M.F., Domingo, R., Alarcón, J.J., 2005. Evaluation of transpiration in adult apricot trees from sap flow measurements. Agr. Water Manage. 72(2), 131-145.

Nourtier, M., Chanzy, A., Granier, A., Huc, R., 2011. Sap flow measurements by thermal dissipation method using cyclic heating: a processing method accounting for the non-stationary regime. Ann. For. Sci. 68(7), 1255-1264.

Ortuño, M.F., Alarcón, J.J., Nicolás, E., Torrecillas, A., 2004. Interpreting trunk diameter changes in young lemon trees under deficit irrigation. Plant Sci. 167, 275-280.

Peel, M.C., Finlayson, B.L. and McMahon, T.A., 2007. Updated world map of the Köppen-Geiger climate classification. Hydrol. Earth Syst. Sci. 4(2), 439-473.

Poblete-Echeverría, C., Ortega-Farias, S., Zuñiga, M., Fuentes, S., 2012. Evaluation of compensated heat-pulse velocity method to determine vine transpiration using combined measurements of eddy covariance system and microlysimeters. Agr. Water Manage. 109, 11-19.

Saito, T., Yasuda, H., Sakurai, M., Acharya, K., Sueki, S., Inosako, K., Yoda, K., Fujimaki, H., Abd Elbasit, M.A., Eldoma, A.M., Nawata, H., 2016. Monitoring of Stem Water Content of Native and Invasive Trees in Arid Environments Using GS3 Soil Moisture Sensors. Vadose Zone J. 15(3), 1-9.

Saveyn, A., Steppe, K., Lemeur, R., 2008. Spatial variability of xylem sap flow in mature beech (Fagus sylvatica) and its diurnal dynamics in relation to microclimate. Botany 86, 1440-1448.

Scott-Shaw, B.C., Everson, C.S., Clulow, A.D., 2017. Water-use dynamics of an alien-invaded riparian forest within the Mediterranean climate zone of the Western Cape, South Africa. Hydrol. Earth Syst. Sci. 21(9), p4551

Swanson, R.H., 1962. An instrument for detecting sap movement in woody plants. USDA Forest Service, Rocky Mountain Forest and Range Experiment Station, Fort Collins, Colorado. Station Paper 68:16.

Swanson, R.H., Whitfield, D.W.A., 1981. A numerical analysis of heat pulse velocity theory and practice. J. Exp. Bot. 32(126), 221-239.

Thornthwaite, C.W., 1948. An approach toward rational classification of climate. Geogr. Rev. 38(1) 55-94.

UNESCO, 1979. Map of the World Distribution of Arid Regions. Accompanied by Explanatory Notes. UNESCO, Paris, France. MAB Technical Note No. 17.

Walther, B.A., Moore, J.L., 2005. The concepts of bias, precision and accuracy, and their use in testing the performance of species richness estimators, with literature review of estimator performance. Ecography 28, 815-829.

Wildy, D.T., Pate, J.S., Bartle, J.R., 2004. Budgets of water use by *Eucalyptus kochii* tree belts in the semi-arid wheatbelt of Western Australia. Plant Soil 262(1), 129-149.

Willmott, C.J., 1982. On the validation of models. Phys. Geogr. 2, 184-194.

Wullschleger, S.D., King, A.W., 2000. Radial variation in sap velocity as a function of stem diameter and sapwood thickness in yellow-poplar trees. Tree Physiol. 20, 511-518.

8. A water balance approach to partition tree transpiration into soil water and groundwater

Abstract

Measurements of tree transpiration (*T)* and water sourcing are crucial for water resources management, especially in arid environments. Usually, analysis of stable isotopes which requires expensive and complicated laboratory procedures is used to determine the water sources. The objective of this study was to partition tree T under shallow water table conditions into groundwater (T_{gw}) and soil water (T_{sw}) using a water balance approach. Three indigenous trees; buffalo thorn (*Ziziphus mucronata*), sweet thorn (*Vachelia karoo*) and black karee (*Sersia lancea*) growing in lysimeters were installed with the compensation heat pulse velocity (CHPV) method to measure stem sap flow (transpiration) at half hourly intervals. Soil water content was continuously monitored using HydraSCOUT (HS) capacitance probes. A constant water table of 0.2 m depth was maintained, and the daily water replenishment to maintain the constant water table was acquired from readings on a graduated automatic water supply bucket system. The contribution of T_{gw} towards total T for the investigated trees ranged between 31% and 97% when the top soil was wet and dry, respectively. The contribution of T_{sw} ranged from 3% when the top soil was dry to 69% after an irrigation event. It was concluded that the selected trees switch to source water from the superficial soil layers when the top soil is wet and from the groundwater during dry conditions. The water balance approach was revealed as a good candidate for estimating tree T water sources, and as such it was also recommended as valuable tool to generate information to support modelling hydrological processes of forested areas.

Keywords: Indigenous trees, transpiration, soil water contribution, groundwater contribution, water balance approach

8.1 Introduction

Tree transpiration (T) measurement has in the recent years become valuable in many fields including; understanding the role played by vegetation in the hydrologic cycle in the field of ecohydrology (Roberts, 2009), water resources management especially in water limited environments (Lubczynski, 2009), and for establishing crop water requirements in agriculture (Liu et al., 2012; Roets et al., 2013). Accurate plant T measurements can therefore play a pivotal role in planning the general ecosystem water management practices (Reyes-Acosta and Lubczynski, 2013; Ungar et al., 2013).

The concept of sap flow measurement, initiated in the early years of the previous century by Huber (1932), is the most prominent means of quantifying tree water use (Wullchleger et al., 1998). The compensation heat pulse velocity method (CHPV) has over the years gained wide international acceptance and recognition as a technique for the measurement of sap flow of woody plants (Marshall, 1958; Swanson and Whitfield, 1981; Green et al., 2003; Fernández et al., 2006). This method (CHPV) has also been extensively applied in South Africa (Dye et al., 1996; Gush, 2008; Tfwala et al., 2018).

Soil water availability is one of the major limiting factors to plant growth and productivity (Pinto et al., 2014), a situation which is on the extreme end in water limited environments (Newman et al., 2006; Lubczynski, 2009). It is necessary to have accurate means to measure volumetric soil water content (θv) in order to quantify plant water uptake and hence determine optimal requirements for both agricultural production and environmental sustainability. Lysimetry has over the years been used to quantify plant water use (Johnson et al., 2005; Bello and Van Rensburg, 2017). The advantages of lysimeters include the possibility to account or to keep various components of the water balance such as drainage and evaporation under control.

However, the spatial distribution of water across the soil profile is not possible to detect through lysimetry. Various techniques including gravimetric soil sampling, neutron probe, time domain reflectometry and many others have been developed to determine soil water content at different soil profile depths. Recent studies have used automated capacitance probes to take continuous θv measurements (Robinson et al., 2008; Evett et al., 2012).

It has already been established that most tree species use both the groundwater (T_{gw}) and soil water (T_{sw}) to meet T requirements (Canadell et al., 1996; Reyes-Acosta and Lubczynski, 2011; Barbeta and Peñuelas, 2017). The means of identifying the water sources in the mentioned and other studies has all along been predominantly the use of isotope tracers (Dawson and Ehleringer, 1991; Dawson, 1996). The lack of laboratory facilities and complicated laboratory procedures necessitate the development of an alternative procedure to partition tree T into T_{sw} and T_{gw}. A combination of different techniques can provide a comprehensive understanding of the hydrological processes. This can provide information on the amount and sources of water use of the trees. The CHPV sap flow technique, continuous θv measurements and monitoring water table fluctuations were employed to determine T and the source of water for three native tree species of South Africa, growing in lysimeters. The aim of the study was to partition T of indigenous trees under shallow water table conditions into T_{gw} and T_{sw} using the water balance approach.

8.2 Materials and methods

8.2.1 Study area

The study was conducted at Kenilworth Experiment Farm (latitude: -29.02°, longitude: 26.15° and altitude: 1354 m) in the Department of Soil, Crop and Climate Sciences at the University of the Free State, in Bloemfontein, South Africa. The farm is about 15 km north west of the Bloemfontein campus of the university. This experiment was carried out over a period of 33 days when the trees were presumably at the peak of seasonal water use during the summer season, from December 2017 to January 2018. The study area has a mean annual precipitation of 528 mm, a majority of which falls between October and April. The average annual reference evapotranspiration (ETo) is 1 604 mm. The mean annual minimum and maximum air temperatures are 11.0°C and 25.5°C, respectively.

8.2.2 Trees and lysimeter facilities

Three indigenous trees, sweet thorn (*Vachelia karoo*), black karee (*Sersia lancea*) and buffalo thorn (*Ziziphus mucronata*) were together with their natural monolith soil volume of 1 m x 1 m with a depth of 1.2 m each, grown in lysimeter containers of the same monolith area but depth of 1.3 m. The trees were approximately 2 – 4 m height and stem diameter between 90 and 120 mm. The fourth sampled tree in Chapter 5 (wild olive), was not included in this study due to some technical failure of the HS capacitance probes used for irrigation scheduling and quantifying soil water uptake. At the base, each of the four lysimeter containers had a control valve which enabled the regulation of the water table to a desired depth. There was no other outlet or inlet of water other than the inlet to maintain a constant water table depth. One of the sides of lysimeter containers was made of Perspex glass which enabled visualization of the water table depth and

root development through the soil profile. The soil surface at the top of the monoliths was covered by a 100 mm layer of Styrofoam and then overlain by a 20 mm layer of gravel and thereafter covered by plastic to eliminate precipitation input and prevent direct surface evaporation.

8.2.3 Sap flow instrumentation and transpiration measurement

The CHPV method (Swanson and Whitfield, 1981; Green 2003) was employed for tree T measurement in this study. Each set of the instrumentation consisted of two temperature sensors and a heater. The CHPV sensor units had an electronic circuitry connected to a CR 1000 data logger and an AM32B multiplexer (Campell Scientific, Inc, Logan, UT, USA) powered by a 12 V battery. Each of the three trees had two sets of heaters and sensors monitoring sap flow at radial depths of 5, 15, 25 and 40 mm below the cambium. These were installed by drilling holes into the stem using a high speed hand drill with 2 mm diameter drill bits. A stainless guide taped firmly on the stem was used to ensure that the drills were correctly spaced and aligned vertically on straight surfaces of the stems at about 0.5 m above the ground surface. The heater probe was inserted in the middle of the two temperature sensor probes; one of the sensors was positioned 5 mm upstream and the other at 10 mm downstream. The temperature sensors were inserted first by pushing them alternatively at magnitudes of 5-10 mm before inserting the heater probes. The sap flow apparatus was then covered by aluminium foil to eliminate external environmental effects. The T of the trees was monitored continuously, with measurements collected every 30 minutes and converted into sap flux rates (L hr^{-1}) following Edwards and Warwick (1984), Green and Clothier (1988) and Green et al. (2003).

8.2.4 Water management

Monitoring of θv and irrigation scheduling of the top 0.8 m of the soil was done with the aid of pre-calibrated HS capacitance probes, manufactured by Hydra Sensor Technologies International Ltd, South Africa, which had telemetries with IP address such that data could be accessed through internet connection. The HS probes were calibrated against the standard gravimetric method of measuring θv prior to the execution of this study on all the soil monolith profiles. Water was supplied through irrigation on top as well as from the bottom of the lysimeters. The allowable depletion of the available water within the top 0.8 m of the soil profile was 70%. Whenever the available water of this profile approached 30%, irrigation was done from the surface to bring the θv back to near the drained upper limit (DUL). The available water is defined as the difference between DUL and the drained lower limit (DLL) (Ratliff et al., 1983; Hensley et al., 2011). Data from 3 drying cycles of approximately 10 days each, after irrigation at the top on days 0, 11 and 22 were used for measurements of T, soil water depletion and groundwater uptake. The change in θv estimated using the HS over 24 hours was expressed in litres (L) to align it with the sap flow measurement units, based on the soil volume in which the probes were taking measurements within the lysimeter containers.

Regarding groundwater supply, a constant water table level of approximately 0.2 m was maintained at the bottom of each of the lysimeters. The source of this water was a graduated water supply bucket which was connected to the bottom of the lysimeter via a box which was equipped with an automatic valve (Figure 8.1). Each time water was depleted from the saturated zone (water table depth + capillary fringe) in the lysimeter, the valve opened such that the depleted water was replaced instantly. The replacement quantity of water, which was equal to the depletion from the saturated zone, was read from the supply bucket. The supply bucket was

covered by its lid to prevent direct evaporation, with only a 2 mm diameter hole to allow flow of water through the system by allowing air to replace the displaced water, while avoiding any significant evaporation from the bucket. The box which had the automatic valve was also wrapped in foil paper to eliminate the effects of external environmental factors such as direct radiation.

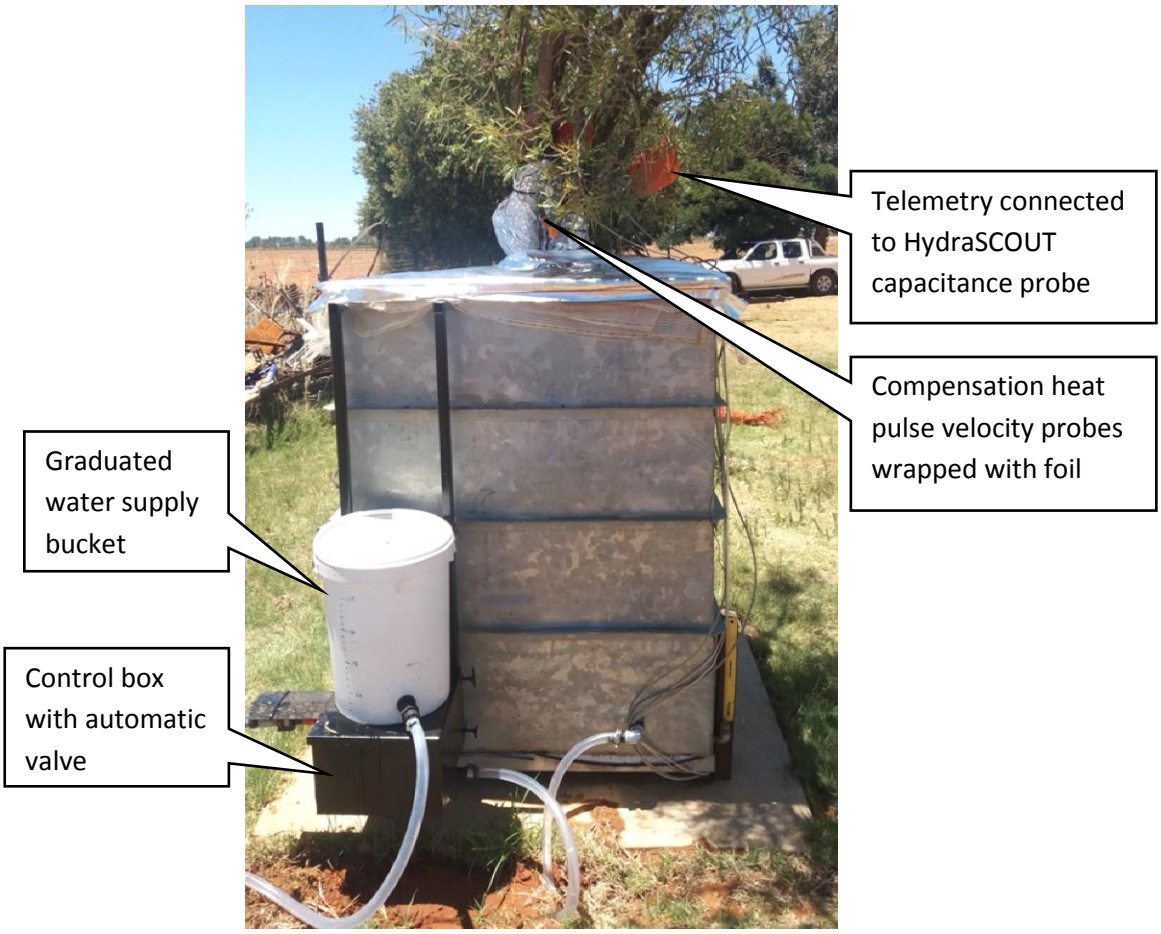

Figure 8.1: An illustration of the experimental setup showing a black karee tree installed with compensation heat pulse velocity sap flow probes, growing in a galvanized lysimeter container with soil water measuring probes and a constant water table control system.

8.2.5 Water balance calculations

The soil water balance theory and the water balance calculations done in this study are detailed below.

Soil water balance theory

The soil water balance principle states that any change in the soil water content (ΔW) during a given time period must equal the difference of the amount of water added and the amount of water lost, during the same period (Hillel, 1998; Dlamini et al., 2016). The water balance can be computed for a sample of soil or a whole catchment. However, from an ecological or agricultural perspective, the water balance of the root zone is considered. This can integrally be expressed as (Marshall et al., 1996; Hillel, 1998):

$$\Delta W = (P + I + U) - (R + D + E + T) \quad (8.1)$$

where the first bracket represents soil water gains through precipitation (P), irrigation (I) and upward capillary flow (U), while the second bracket has water losses through runoff (R), downward drainage (D), direct evaporation from the soil surface (E), and transpiration by plants (T).

Water balance calculation in this experiment

From Equation 8.1, we remain with only U from the left hand side bracket, since P is eliminated from the lysimeter facility and I is only applied to refill θv to near DUL. Continuous measurements of θv were taken across a drying cycle (period) which began a day after the irrigation event. Losses due to R, D and E are also not contributing in this system, hence the only water loss is via T. In this study therefore the water balance is represented by:

$$\Delta W = U - T \quad (8.2)$$

where ΔW is representing the top soil water depletion (T_{sw}) and U represents sub-surface irrigation or ground water supply (T_{gw}). Since the water table in this system is constant, the saturated zone and the capillary fringe are in principle expected, and here also assumed to remain constant within the lysimeter system. Any changes in the soil water content (ΔW) measured using the HS capacitance probes within the top soil therefore represents a zone above the capillary fringe and hence, T_{sw}. This depletion of water is a negative change in θv ($-\Delta W$). Making T the subject from Equation 8.2 gives:

$$T = U + \Delta W \tag{8.3}$$

The CHPV instrumentation installed on the lysimeter facilities has been reported to accurately measure T (Tfwala et al., 2018), which renders T a reliable measure in the system. The total water use therefore, in this case T, was expressed as the sum of U (T_{gw}- from the supply bucket) and ΔW in the top soil (T_{sw} - measured with the HS capacitance probes), resulting in Equation 8.3 to be re-written as:

$$T = T_{gw} + T_{sw} \tag{8.4}$$

8.2.6 Statistics analysis

The Wilmott index of agreement (D) between T and the sum of T_{gw} and T_{sw} was computed to ascertain the measurement accuracies of the latter two. The accuracy of summing T_{gw} and T_{sw} to estimate T was established from computing the mean absolute error (MAE). The deviation of the sum from the CHPV measured T was determined by the mean bias error (MBE). An important assumption which was made here is that the transition of water between the capillary fringe and the overlying soil profiles become negligible after 24 hours following an irrigation

event and throughout the drying cycle. D, MAE, and MBE were calculated as (Willmott, 1982; Abbas et al., 2012):

$$D = 1 - \frac{\sum_{i=1}^{n}(E_i - O_i)^2}{\sum_{i=1}^{n}(|E_i - \bar{O}| + |E_i - \bar{O}|)^2} \quad (8.4)$$

$$MAE = \frac{1}{n}\sum_{i=1}^{n}(E_i - O_i) \quad (8.5)$$

$$MBE = \sum_{i=1}^{n}(E_i - O_i)/n \quad (8.6)$$

where n is the number of observations, E_i, O_i and $\bar{O}$ are the estimated transpiration (T_{gw} + T_{sw}), observed or measured transpiration (T) and mean values for T, respectively. A D -index close to 1 and MAE close to 0 indicates good agreement between measured and estimated values. (Willmott, 1982). A negative MBE indicates that the sum of T_{gw} and T_{sw} is underestimating the total T while a positive value indicates an overestimation (Abbas et al., 2012).

8.3 Results

8.3.1 Total transpiration and water sources

The results of total tree T as well as the contributions of T_{sw} and T_{gw} are depicted in Figure 8.2. The total T for sweet thorn was relatively steady and ranged between 7 and 9 L day^{-1}. The contribution of T_{gw} seemed to increase from 3 to 9 L day^{-1} along the ten days drying cycle period. Contrary, the contribution of T_{sw} decreased from 6.9 L day^{-1} after irrigating the top soil to 0.2 L day^{-1} towards the end of the drying cycle.

For buffalo thorn, T ranged from 25 L day^{-1} when the soil was wet, to 11 L day^{-1} when the top soil was drying. The daily contribution of T_{gw} towards total T ranged from 7 L when the top soil was wet to 15 L as the top soil was drying. Similar to the case of sweet thorn, the daily

contribution of T_{sw} towards total T was decreasing with the drying cycle. This decrease ranged from 20 L when the top soil was wet to 0.2 L when the soil was dry.

On black karee, total T decreased from about 10 L day^{-1} when the soil was wet to 8 L day^{-1} as the soil was drying. The contribution of T_{gw} on total T increased from 4 L day^{-1} when the soil was wet to 8 L day^{-1} as the top soil got dry. The daily contribution of T_{sw} decreased from 8 to 0.2 L across the drying cycle period.

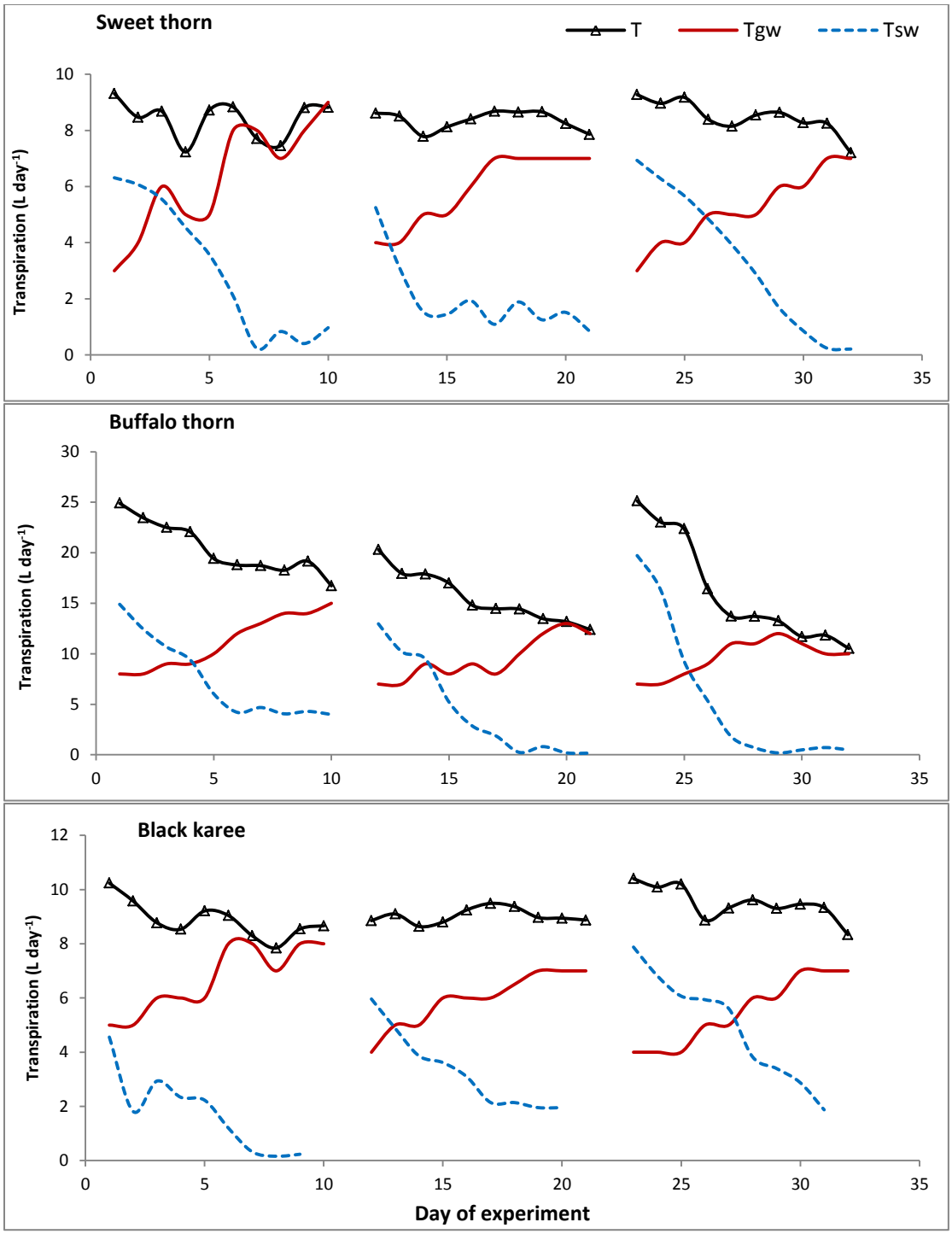

Figure 8.2: Contributions of soil water (T_{sw}) and groundwater (T_{gw}) towards total transpiration (T) of selected indigenous trees measured over three drying cycles (Cycle I - day 1-10, Cycle II - 12-21 and Cycle III - 23-32).

8.3.2 Accuracy of groundwater and soil water measurements

A summary of statistical parameters including the agreement indices between CHPV measured T and the sum of the two sources of water supply ($T_{gw} + T_{sw}$) to the trees, whose measurements are being tested, is presented in Table 1. The Wilmott index of agreement (D) ranged from 0.859 to 1.000. The mean absolute error ranged from 0.855 L day^{-1} on black karee to 1.816 L day^{-1} on buffalo thorn. The MBE values ranged from 0.013 to 0.029 L day^{-1}.

Table 8.1: Statistical parameters (Wilmott index of agreement (D), mean absolute error (MAE) and mean bias error (MBE)) on using the sum of groundwater and soil water to estimate total transpiration of sweet thorn, buffalo thorn and black karee, in comparison with using the compensation heat pulse velocity technique.

Tree species	D-index	MAE (L day^{-1})	MBE (L day^{-1})	N
Sweet thorn	0.859	0.877	0.013	30
Buffalo thorn	0.999	1.816	0.029	30
Black karee	1.000	0.855	0.013	30

8.4 Discussion

8.4.1 Total tree transpiration and water source

The daily tree water use rates reported here (4 – 25 L day^{-1}) are in line with other studies reported under field conditions elsewhere, which means the trees were transpiring normally, considering their sizes. Bréda et al. (1993) reported daily water use of 10 L on a 90 mm stem diameter *Ouercus petraea* tree investigation conducted in Nacny, France. Daily transpiration rates of 6 L were reported by Dierick and Hölscher (2009) on a *Hopea plagata* tree with stem diameter of 80 mm in Patag, Philippines. Morris et al. (2004) investigated transpiration of

Eucalyptus urophylla with stem dimeter of 100 mm in China, and reported transpiration of up to 27 L day^{-1}.

The total T reported here was generally decreasing as the top soil was drying despite the continuous presence of the water table. This was attributed to limited availability of water in the proximity of the superficial roots. Other studies have also reported that tree water use increase with increased availability of water and vice versa, to cope with situations such as droughts. Nasr and Mechlia (2007) reported that sap flow from irrigated apple trees was 50% greater than that of their counterparts under deficit irrigation. Similarly, long leaf pine trees with water table at 1 m below the soil surface recorded tree water use which was 30% greater than those where the water table was 6 m from the soil surface (Ford et al., 2008).

The average contribution of T_{gw} towards total T of sweet thorn over the three drying cycles increased from 36% versus 64% contributed by T_{sw} when the top 0.8 m soil profile was wet, to 97% compared to 3% when the top soil was dry. For buffalo thorn, the average contribution of T_{gw} increased from 31% to 93% as the top soil was drying. The contribution of T_{sw} in this case was as high as 69% after irrigation from the top to almost nothing as the top soil got dry. A similar trend was observed for black karee, where on average T_{gw} contributed 44% of total tree water use when the top soil was wet, and increased to about 93% as the soil was drying. These observations suggested that trees have the ability to switch to access water from different sources depending on the availability. If the top soil is wet, the bulk of transpiration requirements are met by T_{sw} and once the superficial soil profiles get dry, the deeper roots are used to source water from underlying soil layers.

Similar results to the findings presented above, though the investigation was conducted in the field, were reported by Dawson and Pate (1996) on their investigation using stable isotope

analysis to determine the water source for *Banksia prionotes*, where they reported that the trees depended on groundwater during dry conditions and derived water from the top soil layers using the lateral roots after rainfall events. The dominance of T_{gw} contribution towards T during the dry periods was also reported on *Quercus suber* trees of the Mediterranean region in Iberian Peninsula, where it was 73.2% (Pinto et al., 2014). This dimorphic root structure of trees makes them to adapt easily to dynamic soil water availability conditions such as droughts.

8.4.2 Accuracy implication for field application

The good agreement indices (D values close to 1) and high accuracy without biasness (MAE and MBE close to 0) of summing T_{gw} and T_{sw} to estimate T qualifies the water balance approach as a good candidate for quantifying the contributions of different water pools in the total T of trees, especially between the unsaturated and saturated zones. However this requires that at least one of the sources, say the unsaturated (T_{sw}) be accurately measured alongside sap flow measurements. The contribution of the other source can then be determined by subtraction from the reliably measured T. The other factors which were eliminated in this study such as drainage, surface runoff and precipitation should also be accounted for in the field where they cannot be ruled out. The results presented here can also be useful input into models that predict hydrological processes in the field to inform appropriate water resources management and budgeting.

8.5 Conclusions

Tree T of selected indigenous trees grown in lysimeters was measured with the CHPV technique and partitioned into T_{gw} and T_{sw}. It was concluded that the total T decrease as the θv of the upper 0.8 m soil water decreases. After an irrigation event, which is similar to after a rainfall event, the selected trees rely almost entirely on the supply of soil water sourced by the superficial lateral roots. As the upper soil layers get dry, the trees rely mainly on the supply from the saturated zone (T_{gw}) accessed by deeper growing roots. This setup was an imitation of the real field situation where there are roots within the unsaturated zone and in most cases some, especially the tap roots in contact with the saturated zone. If this contact is terminated the survival of the trees may be threatened particulary during dry periods. Measurement of the different sources of water was proven to be accurate (high *D*-indices, *MAE* and *MBE* close to 0), which suggests the water balance approach's good candidature for estimating tree T water sources. The results of this study can also serve as good basis for modelling of hydrological processes of forested areas and aid in water resources management.

References

Abbas, F., Fares, A., Fares, S., 2011. Filed calibration of soil moisture sensors in a forested watershed. Sensors 11, 6354-6369.

Barbeta, A., Peñuelas, J., 2017. Relative contribution of groundwater to plant transpiration estimated with stable isotopes. Scientific reports 7(1), 10580.

Bello, Z.A. and Van Rensburg, L.D., 2017. Development, calibration and testing of a low-cost small lysimeter for monitoring evaporation and transpiration. Irrig. and Drain. 66(2), 263-272.

Bréda, N., Cochard, H., Dreyer, E., Granier, A., 1993. Water transfer in a mature oak stand (*Quercus petraea*): seasonal evolution and effects of a severe drought. Can. J. Forest Res. 23(6), 1136-1143.

Canadell, J., Jackson, R.B., Ehleringer, J.B., Mooney, H.A., Sala, O.E. and Schulze, E.D., 1996. Maximum rooting depth of vegetation types at the global scale. Oecologia 108(4), 583-595.

Dawson, T.E., 1996. Determining water use by trees and forests from isotorpic, energy balance and transpiration analyses: the roles of tree size and hydraulic lift. Tree Physiol. 16, 263-272.

Dawson, T.E., Ehleringer, J.R. 1991. Stream side trees do not use stream water. Nature 350(6316), 335-337.

Dawson, T.E., Pate, J.S., 1996. Seasonal water uptake and movement in root systems of Australian phraeatophytic plants of dimorphic root morphology: a stable isotope investigation. Oecologia 107(1), 13-20.

Dierick, D., Hölscher, D., 2009. Species-specific tree water use characteristics in reforestation stands in the Philippines. Agr. Forest Meteorol. 149(8), 1317-1326.

Dlamini, P., Ukoh, IB., van Rensburg, L.D., du Preez, C.C., 2016. Reduction of evaporation from bare soil using plastic and gravel mulches and assessment of gravel mulch for partitioning evapotranspiration under irrigated canola. Soil Res. 55(3), 222-233.

Dye, P.J., Soko, S., Poulter, A.G., 1996. Evaluation of the heat pulse velocity method for measuring sap flow in *Pinus patula*. J. Exp. Bot. 47(7), 975-981.

Edwards, W.R.N., Warwick, N.W.M., 1984. Transpiration from a kiwifruit vine as estimated by the heat-pulse technique and the Penman-Monteith equation. N.Z. J. Agric. Res. 27, 537–543.

Evett, S.R., Schwartz, R.C., Casanova, J.J., Heng, L.K., 2012. Soil water sensing for water balance, ET and WUE. Agric. Water Manage. 104, 1-9.

Fernández, J.E., Durán, P.J., Palomo, M.J., Diaz-Espejo, A., Chamorro, V., Girón, I.F., 2006. Calibration of sap flow estimated by the compensation heat pulse method in olive, plum and orange trees: relationships with xylem anatomy. Tree Physiol. 26(6), 719-728.

Ford, C.R., Mitchell, R.J., Teskey, R.O., 2008. Water table depth affects productivity, water use, and the response to nitrogen addition in a savanna system. Can. J. Forest Res. 38(8), 2118-2127.

Green, S.R., Clothier, B.E., 1988. Water use of kwiwifruit vines and apple trees by the heat pulse technique. J. Exp. Bot. 39 (198), 115-123.

Green, S.R., Clothier, B.E., Jardine, B., 2003. Theory and practical application of heat pulse to measure sap flow. Agron. J. 95, 1371-1379.

Gush, M.B., 2008. Measurement of water-use by *Jatropha curcus* L. using the heat pulse velocity technique. Water SA 34(5), 1-5.

Hensley, M., Bennie, A.T.P., Van Rensburg, L.D., Botha, J.J., 2011. Review of 'plant available water' aspects of water use efficiency under irrigated and dryland conditions. Water SA, 37(5), 771-779.

Hillel, D., 1998. Environmental Soil Physics, Academic Press, San Diego, USA.

Huber, B., 1932. Beobachtung und messung pflanzicher saftstrome. Dtsch. Bot. Ges. 50, 89-109.

Johnson, R.S., Williams, L.E., Ayars, J.E., Trout, T.J., 2005. Weighing lysimeters aid study of water relations in tree and vine crops. Calif. Agric. 59(2), 133-136.

Liu, C., Du, T., Li, F., Kang, S., Li, S., Tong, L., 2012. Trunk sap flow characteristics during two growth stages of apple tree and its relationship with affecting factors in an arid region of northwest China. Agric. Water Manage. 104, 193-202.

Lubczynski, M.W., 2009. The hydrological role of trees in water-limited environments. Hydrogeol. J. 17, 247-259.

Marshall, D.C., 1958. Measurement of sap flow in conifers by heat transport. Plant physiol. 33, 385-396.

Marshall, T.J., Holmes, J.W., Rose, C.W., 1996. *Soil physics*. Cambridge University Press.

Morris, J., Ningnan, Z., Zengjiang, Y., Collopy, J., Daping, X., 2004. Water use by fast-growing *Eucalyptus urophylla* plantations in southern China. Tree physiol. 24(9), 1035-1044.

Nasr, X., Mechlia, N.B., 2007. Measurements of sap flow for apple trees in relation to climatic and watering conditions. Mediterranean Options 56, 91-98.

Newman, B.D., Wilcox, B.P., Archer, S.R., Breshears, D.D., Dahm, C.N., Duffy C.J., McDowell, N.G., Phillips, F.M., 2006. Ecohydrology of water-limited environments: A scientific vision. Water Resour. Res. 42, 1-15.

Pinto, C.A., Nadezhidina, N., David, J.S., Kurz-Besson, C., Caldeira, M.C., Henriques M.O., Monteeiro, F.G., Pereira, J.S., David, T.S., 2014. Transpiration in *Quercus suber* trees under shallow water table conditions: the role of soil and groundwater. Hydrol. Process. 28, 6067-6079.

Ratliff, L.F., Ritchie, J.T., Cassel, D.K., 1983. Field-Measured Limits of Soil Water Availability as Related to Laboratory-Measured Properties 1. Soil Sci. Soc. Am. J. 47(4), 770-775.

Reyes-Acosta, J.L., Lubczynski, M.W., 2011. Spatial assessment of transpiration, groundwater and soil-water uptake by oak trees in dry season at a semi-arid open-forest in Samanca, Spain. Stud. Unsat. Soil Zone 10, 65-70.

Reyes-Acosta, J.L., Lubczynski, M.W., 2013. Mapping dry-season tree transpiration of an oak woodland at the catchment scale, using object attributes derived from satellite imagery and sap flow measurements. Agr. Forest Meteorol. 174, 184-201.

Roets, N.J.R., Cronje, R.B., Schoeman, S.P., Murovhi, N.R., Ratlapane, I.M., 2013. Calibrating avocado irrigation through the use of continuous soil moisture monitoring and plant physiological parameters, South African Avacado Growers Association Year Book 36, ARC – ITSC, Neilspriut, South Africa.

Roberts, J.M., 2009. The role of trees in the hydrological cycle, *In* Owens, J.N., Lunday, H.G., (Eds) Forests and Forest Plants, Vol 3, Encyclopedia of life support systems, UNESCO. 42-76.

Robinson, D.A., Campbell, C.S., Hopmans, J.W., Hornbuckle, B.K., Jones, S.B., Knight, R., Ogden, F., Selker, J., Wendroth, O., 2008. Soil moisture measurement for ecological and hydrological watershed-scale observatories: A review. Vadose Zone J. **7**(1), 358-389.

Swanson, R.H., Whitfield, D.W.A., 1981. A numerical analysis of heat pulse velocity theory and practice. J. Exp. Bot. 32(126), 221-239.

Tfwala, C.M., van Rensburg, L.D., Bello, Z.A., Green, S.R., 2018. Calibration of compensation heat pulse velocity technique for measuring transpiration of selected indigenous trees using weighing lysimeters. Agric. Water Manage. 200, 27-33.

Ungar, E.D., Roternberg, E., Raz-Yaseef, N., Cohen, S., Yakir, D., Schiller, G., 2013. Transpiration and annual water balance of Aleppo pine in a semiarid region: Implications for forest management. Forest Ecol. Manag. 298, 39-51.

Willmott, C.J., 1982. On the validation of models. Phys. Geogr. 2, 184-194.

Wullschleger, S., Meinzer, F.C., Vertessy, R.A., 1998. A review of whole-plant water use studies in trees. Tree Physiol. 18, 499-512.

9. Transpiration dynamics and water sources for selected indigenous trees under varying soil water content

Abstract

The major route through which water from the earth's surface re-enters the hydrologic cycle in forested ecosystems is via tree transpiration (T). It is therefore important to have detailed understanding of the quantity and source of water transpired by different tree species. The aims of this study were to i) assess the trends of T for selected tree species (camel thorn, sweet thorn, shepherd's tree and buffalo thorn) across a range of soil water content conditions and ii) partition the total T of the selected tree species growing in arid environments dominated by open cast mining activities into soil water and groundwater. Tree T was measured using the compensation heat pulse velocity (CHPV) method, while soil water content was monitored using DFM capacitance probes. The soil water content within the upper 0.5 m soil profile ranged from 11 mm during the dry season to 20 mm during the wet season. The deeper soil layer (0.5-1.2 m) was generally wetter compared to the top layer with water content was up to >30 mm during the wet season. The measured tree T ranged from 6 L day^{-1} on buffalo thorn during the dry season to 125 L day^{-1} on camel thorn in summer. It was also revealed that T of large (diameter at breast height = 460 mm) camel thorn trees is not responsive to seasonal variations of soil water availability and remained constant at approximately 80 L day^{-1}. Diurnal patterns of T did not effect changes on the soil water depletions within the top 1.2 m soil profile, which indicated that the trees sourced water beyond this zone. Signs of daytime redistribution were observed within the canopy areas of the investigated trees during very limited soil water conditions of the dry season. It was concluded that the water use of trees is inclined to the seasonal variations, which however is not the case in old trees. Close to 100% of the water transpired by trees in the study area is sourced

from groundwater reserves. We recommended investigation of daytime redistribution among the indigenous tree species of the study area. We also recommended extension of tree water use studies to other species for comprehensive catchment tree water use calculations to inform water budgets.

Keywords: Tree water use, indigenous trees, Soil water content, arid environments, Kolomela Mine

9.1 Introduction

The principal components of the terrestrial hydrosphere that govern freshwater fluxes are plant transpiration (T) (45,000 km^3 yr^{-1} (Schlesinger and Jasechko, 2014) to 62,000 km^3 yr^{-1} (Jasechko, S. et al., 2013)), streamflow (37,000 km^3 yr^{-1} to 40,000 km^3 yr^{-1} (Dai and Trenberth, 2002; Oki and Kanae, 2006)) and groundwater recharge (12,000 km^3 yr^{-1} to 16,200 km^3 yr^{-1} (Wada et al., 2013)). To accurately predict the impacts of global changes on water scarcity and ecosystem services, it is essential to establish insights on the sources of water and the processes governing the flow channels in each of the components (Oki and Kiane, 2006; Evaristo et al., 2015). Amongst these components, T is the largest water flux from the earth's surface, accounting for 80 to 90 per cent of terrestrial evapotranspiration (ET), and using almost half of the total solar energy absorbed by the earth's surface (Jasechko et al., 2013).

The dominance of T in global water fluxes warrants prioritization of investigations in biological water fluxes from plants for optimal management of water resources. T is one of the principal factors affecting ecosystem water balance and productivity. This is especially so in forested (Roberts, 2009) and water limited environments, where there are prolonged dry periods of inactivity punctuated by highly active periods of water and carbon exchange succeeding precipitation events (Williams et al., 2004; Lubczynski, 2009). Forests which cover approximately 33 per cent of the earth's land surface area (Bond et al., 2008) contribute substantially to the global water fluxes via T (Dawson, 1996; Meiresonne et al., 2003; Shimizu et al., 2015). Extensive research on tree T for commercial forest species (Morris et al., 2004; Wildy et al., 2004; Gush, 2008) and orchard trees (Fernández et al., 2001; Ortuño et al., 2004; Nicolas et al., 2005) has been done globally and even in the South African context. There is still an acute need to quantify T for the native tree species (Dye et al., 2008).

Arrays of techniques have been developed to estimate ET in forested areas. At the stand level, the Eddy covariance and Bowen ratio methods are the most widely used (Clulow et al., 2015; Soubie et al., 2016). These methods estimate mainly ET, while the main focus here is on the T component of ET at the tree level. Thermal based methods of sap flow measurement are also wildly used to quantify whole tree water use (Granier, 1987; Smith and Allen, 1996; Green et al., 2003). These techniques are however unable to detect where the tree sources the water. Tree physiologists have for several decades used the variations of stable isotopes of hydrogen and/or oxygen between plant tissue and different water pools to identify water sources for trees (Graig, 1961; Dawson, 1996, 1998; Gazis and Feng, 2004). The isotope analysis is however limited by its requirements of costly equipment and complicated laboratory procedures.

A combination of the different techniques can provide a comprehensive understanding of the hydrological processes including the amount and sources of water from a single tree, to the forest and ecosystem levels. The continuous measurements of sap flow and soil water content were simultaneously employed in our experiment. The aim of the study was to estimate the transpiration of selected indigenous trees and partition it into soil water and groundwater across seasons.

9.2 Materials and Methods

9.2.1 Study site description

The study was conducted at Wolhaarkop Farm within the Kolomela Mine property. The property is situated 22 km south west of Postmasburg in the Northern Cape Province of South Africa (latitude: -28.385, longitude: 22.985 and elevation of 1220 m). The experiment was carried out from November 2016 to August 2017. The topography in the greater study area is characterized

mostly by undulating hills with moderate slopes and flat plains. The average precipitation is 241 mm per year and most of the rainfall events are found between November and April (Mucina and Rutherford, 2006). The peak precipitation month is March, and July is the driest, normally with no precipitation at all. The mean maximum temperatures are 32°C and 17°C in January and June, respectively. The region experiences its coldest temperatures during June and July, with a mean cold temperature of 0°C (Tfwala et al., 2017). The vegetation type is predominantly the Savana Biome, comprised mainly of the Kuruman Mountain Bushveld and Postmasburg Thornveld (Acocks, 1988; Mucina and Rutherford 2006). The soils in the study area are of the Hutton form with red Aeolian sand of the Kalahari Group overlying the volcanic rock and sediments of the Griqualand West Supergroup, which outcrops in some places (Mucina and Rutherford 2006). The main economic activity within the study area is open cast mining, which primarily depends on groundwater resources. Agriculture and nature conservation come second and third, respectively. Three stations with the target trees within the farm were selected for tree transpiration measurement and soil water content monitoring for a period of 10 months, covering both the wet and dry seasons. The geographical positions were -28.345, 22.868 and elevation of 1 243 m for station 1, -28.388, 22.839 and elevation of 1 208 m for station 2 and -28.345, 22.867 at elevation of 1 230 m for station 3.

The physical and chemical properties of the soils in the three experimental stations are presented in Table 9.1. The soil in all the three stations was of the fine sand textural class; with clay content ranging from 1.3% – 8.3%, silt content ranging between 0.7% and 7.3%, and sand contents of 88.8% – 95%. The concentration of Ca among the soils ranged from 260 mg kg^{-1} to 824 mg kg^{-1}. For Mg, the soils contained 42-159 mg kg^{-1}. The concentrations of K and Na ranged

from 76-214 mg kg^{-1} and 6-13 mg kg^{-1}, respectively. The Sodiun Adsorbtion Ratio (SAR) ranged from 4.8 to 15.5. Lastly, the soil pH was between 7.2 and 8.2.

Table 9.1: Physical and chemical properties of the soil in the three stations in the experimental site.

Station	Depth	Physical properties				Exchangeable cations					
		clay (%)	Silt (%)	Sand (%)	Class	Ca (mg/kg)	Mg (mg/kg)	K (mg/kg)	Na (mg/kg)	pH	SAR
1	0.1 m	2.7	3.3	93.5	Fine sand	260	42	205	11	7.6	15.5
1	0.2 m	4.7	2.0	92.8	Fine sand	348	67	190	7	7.7	12.8
1	0.4 m	4.0	4.0	91.8	Fine sand	387	72	129	8	7.7	8.3
1	0.6 m	8.3	0.7	91.4	Fine sand	382	74	146	7	7.4	9.5
1	0.8 m	6.0	2.3	90.7	Fine sand	338	75	111	6	7.7	7.6
1	1.0 m	5.0	3.0	91.3	Fine sand	396	93	89	6	7.8	5.7
1	1.2 m	7.0	1.0	91.5	Fine sand	414	112	76	9	7.8	4.8
2	0.1 m	1.3	2.7	95.5	Fine sand	614	69	185	7	7.2	9.8
2	0.2 m	3.3	5.3	91.9	Fine sand	456	74	192	6	7.6	11.6
2	0.4 m	4.7	4.0	90.7	Fine sand	543	119	126	6	7.2	7.1
2	0.6 m	6.7	4.0	89.2	Fine sand	528	143	104	12	7.6	5.9
2	0.8 m	6.3	3.0	89.9	Fine sand	503	135	105	11	7.5	6.1
2	1.0 m	6.3	3.7	89.4	Fine sand	580	159	103	12	7.4	5.6
2	1.2 m	6.0	4.0	89.5	Fine sand	570	149	100	12	7.8	5.5
3	0.1 m	7.7	2.7	89.1	Fine sand	659	119	214	6	8.2	11.0
3	0.2 m	3.7	6.3	89.1	Fine sand	649	126	165	10	7.8	8.6
3	0.4 m	5.7	4.7	88.9	Fine sand	698	90	92	12	7.7	4.6
3	0.6 m	3.0	7.3	88.8	Fine sand	824	117	132	13	8.0	6.2

Note: SAR = sodium adsorption ratio.

9.2.2 Meteorological data

Meteorological data were sourced from the South African Weather Services, acquired through an automatic weather station at Postmasburg.

9.2.3 Tree selection

A total of eight trees comprising of three camel thorn (*Vachellia erioloba*) trees, one sweet thorn (*Vachelia karoo*), three shepherd's trees (*Boscia albitrunca*) and a buffalo thorn tree (*Ziziphus mucronata*) were selected for this investigation. These trees were identified and selected across three stations (Table 9.2). The selection of trees was based on; (i) canopy size (representative), (ii) appearance of stems (symmetrical shape), and iii) verification that there were no signs of decay, hollow stems and/or disease. Another factor considered was the distance from each other as they had to be connected to a central point with a data logger and power system. Biometric characteristics of the selected trees are also presented in Table 9.2. Where there was more than one stem, their stem diameters at breast height (DBH) are all presented.

Table 9.2: Biometric characteristics of trees selected for transpiration investigation at Kolomela Mine from November 2016 to August 2017. Tree code is a representation of the station and the tree species.

Station	Tree	Tree code	Stem diameter (mm)	Tree height (m)	Crown radius (m)
1	Camel thorn	ST1Ct	230, 210, 180	5.6	4.5
	Shepherd's tree	ST1Sht	180, 160, 250	3.6	3.7
2	Camel thorn	ST2Ct	460	7.4	5
	Shepherd's tree	ST2Sht	320	4	5
3	Camel thorn	ST3Ct	490	7.1	4.5
	Shepherd's tree	ST3Sht	180,150,240	3.8	3
	Sweet thorn	ST3St	320	7.3	4.5
	Buffalo thorn	ST3Bt	110, 140, 90	4.2	3

9.2.4 Soil water content measurements

DFM capacitance probe (DFM Software Solutions, South Africa) sensors which use the principle of measuring the dielectric permittivity of the mineral soil particles, water and other constituents contained in the soil around the probe (Dean et al. 1987; Zerizghy et al., 2013), were employed to monitor soil water content. Water has a higher dielectric constant than soil components and air, therefore the dielectric permittivity within a soil profile is a function of the volumetric soil water content (θv) (Dean et al., 1987; Evett et al., 2006).

Five probes were installed under the canopy area of each tree to form a line from the south-east (SE) to north-west (NW) direction and programmed to store average soil water content readings hourly. The probes were positioned to ensure a good representation of the soil water content under canopy areas of each tree (Figure 9.1). From November 2016 to August 2017, θv was continuously monitored at the depths of 0.2, 0.4, 0.6, 0.8, 1 and 1.2 m. The DFM probes were covered by metal caps to protect them against damage by animals. DFM sensor readings were converted to θv using calibration equations derived from the relationships (data not presented here) between the gravimetrically determined soil water content. For the calibration, three soil cores were taken on site, with each sensor next to the sample spots when the soil was wet (in March), moderately dry (in June) and relatively dry (in August). The θv measurements were finally expressed in mm of water depth. The top 0.5 m, where the soil water content was observed to be changing more frequently was presented separately from the deeper 0.5 to 1.20 m of the soil profile which was comparatively more stable.

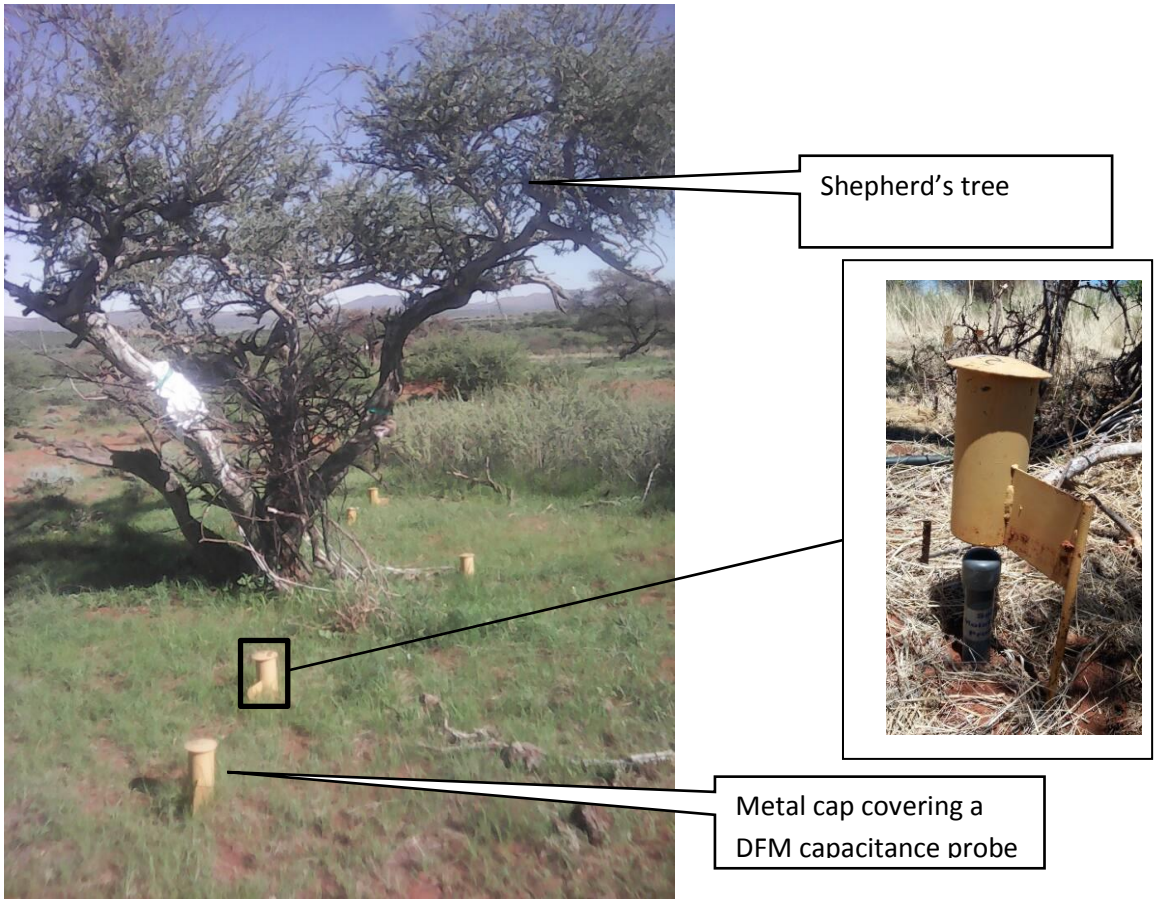

Figure 9.1: Shows the setup of DFM capacitance probes covered by metal protective caps under the canopy area of a shepherd's tree in station 1 at Wolhaarkop Farm at Kolomela Mine.

9.2.5 Sap flow measurements

Tree stem sap flow was continuously monitored over a period of ten months (November 2016 to August 2017) using the compensation heat pulse velocity (CHPV) method (Swanson and Whitfield, 1981; Green 2003). Two sensor probes were installed 5 mm upstream and 10 mm downstream of a heater to measure sap flow at various depths across the sapwood of the trees (Figure 9.2). The heater and sensor units were installed into holes drilled horizontally into the sapwood and then covered by aluminium foil to eliminate external environmental effects. In case where a tree had more than one stem, all stems were instrumented separately. Measurements were collected every 30 minutes through a CR 1000 data logger (Campell

Scientific, Inc, Logan, UT, USA) and converted into sap flux rates (L hr^{-1}) according to the procedures outlined in Edwards and Warwick (1984), Green and Clothier (1988) and Green et al. (2003). Empirical correction factor of 2.8 for the 2 mm drill bits used to account for the wounding effects was adapted from Green et al. (2003). The half hourly T rates over 24 hours were summed to compute daily water use per tree throughout the experiment. The volumetric water use by each tree was divided by the projected canopy area to convert it into mm.

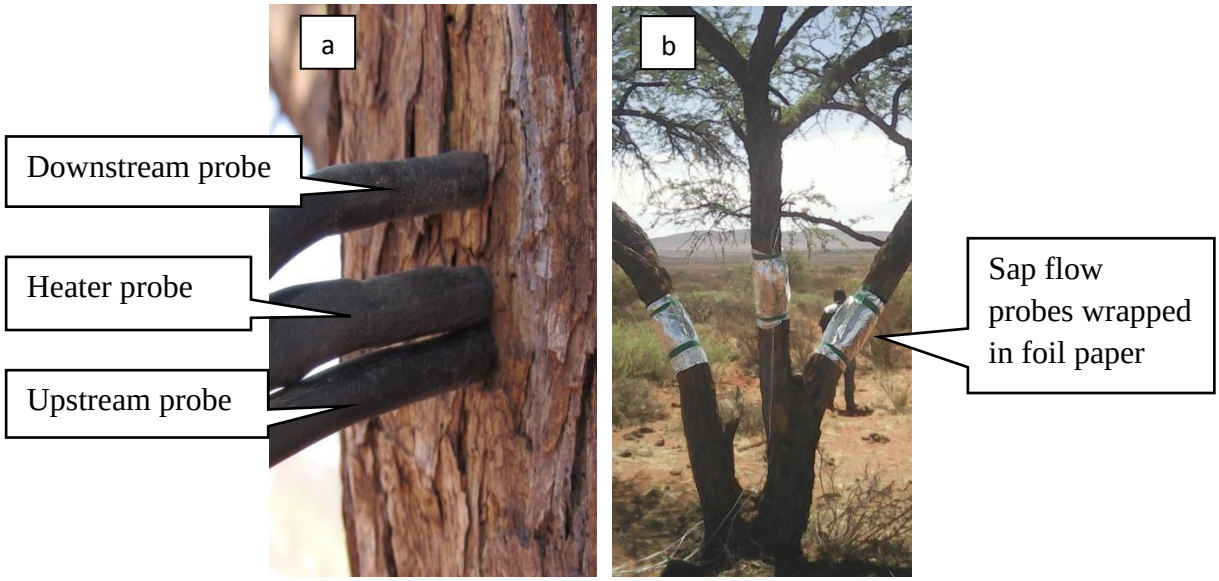

Figure 9.2: Shows a) heat pulse velocity sap flow probes installed on camel thorn tree and b) wrapped with aluminium foil paper at Wolhaarkop Farm at Kolomela Mine.

9.2.6 Estimating water sources

The wet and dry seasons during the experimental period were treated separately in estimating the source of water for the trees. Diurnal cycles of T and soil water content for two days representing the wet and dry seasons were assessed for each tree. These days were chosen because they had climatic parameters which were deemed typical for the majority of days in the respective seasons. The summer day (17 February 2017) had minimum and maximum air temperatures of 21.4°C and 33.4°C, respectively. The average relative humidity was 70% and the reference evapotranspiration (ETo) was 5.8 mm. On the winter day, the minimum and

maximum air temperatures were respectively -0.3°C and 23.9°C. The relative humidity on this day was 46% and the ETo was 3.2 mm. The changes in soil water content within the top 1.2 m and the tree T was assessed to give an indication of the water source for tree transpiration. The T measurements over the 24-hr period were converted from L hr^{-1} to mm hr^{-1} based on the canopy area of an individual tree. The change in soil water content (mm hr^{-1}) (soil water depletion) was taken as the difference between the measured soil water content (mm) in a particular time (hr) and the soil water content measured in the previous hour. The difference between the tree T and the observed change in soil water content was taken to be water depth sourced by the trees from beyond the soil zone. The soil zone was taken as 1.2 m in the present study following definition of Fetter (2001) who suggested that the agricultural definition of soil water is confined to a depth of 1 m to 2 m below the ground surface.

9.3 Results

9.3.1 Meteorological conditions

The coldest temperatures were experienced in June and July while November, December and January were the hottest months (Figure 9.3). Typical for the region, the rainy season was very brief. The majority of rainfall events were in January and February, with a few occurring in November, December, March and April. The ETo was at its lowest around coldest periods and peaked during the hottest months. These confirm that this is a region with low rainfall and high temperature.

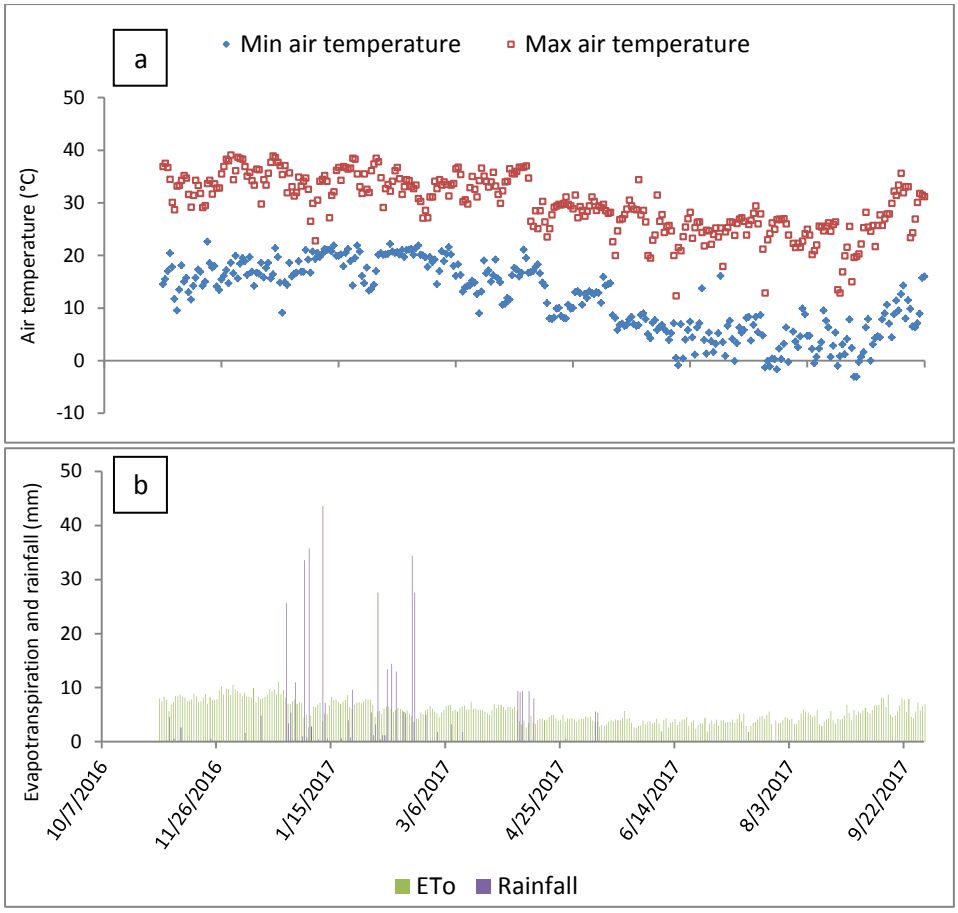

Figure 9.3: Meteorological conditions at Wolhaarkop Farm at Kolomela Mine (a) daily minimum and maximum air temperatures; (b) reference evapotranspiration (ETo) and rainfall during the experimental period.

9.3.2 Seasonal trends of soil water content and tree transpiration

The soil water content trends under the canopy areas for the selected trees and sap measured across the experimental period are presented in Figure 9.4. The soil water content within the top 0.5 m layer of the soil profile was up to about 20 mm depth of water under the canopy area of the trees in station 2 during the rainy season (12/27/2016). This was however highly fluctuating; soil was wet immediately after rainfall events and dropped quickly during dry spells. In the dry season (8/13/2017), the water content within this profile dropped to generally constant levels between 11 mm and 15 mm for all the trees. A similar trend was observed for the deeper (0.5-1.2 m) soil profile, but in this case the fluctuation was not as high as in the top layer. Also, the water content was relatively higher (up to > 30 mm) within

the deeper soil layers than in the top soil layers. For camel thorn trees, sap flow rates were low at the beginning of the measurements in November, which was before the onset of the rainy season. Tree ST1Ct recorded 57 L day^{-1}, 98 L day^{-1} and 40 L day^{-1} in spring, summer and winter, respectively. A similar trend was observed for tree ST2Ct which peaked at approximately 125 L day^{-1} in summer and dropped to approximately 60 L day^{-1} during the winter season. The biggest (DBH = 460 mm) camel thorn tree, and certainly the eldest, (ST3Ct) displayed an average water use pattern of approximately 80 L day^{-1} across seasons.

All three shepherd's trees displayed a seasonally inclined pattern of water use peaking during the peak of the rainy season between February and March and lowest water use values during the winter season until the onset of the rainy season. For Tree ST1Sht, the highest rate of water consumption was 50 L day^{-1} and lowest values (33 L day^{-1}) was found during the lengthy dry season. For tree ST2Sht, which was the biggest tree of this species, sap flow rate was 100 L day^{-1} in summer, and this declined by more than 50% during winter. Sap flow rates for tree ST3Sht started from 30 L day^{-1} before the start of the rainy season to the peaks of 70 L day^{-1} in summer.

The only buffalo thorn tree (ST3Zm) under investigation showed a distinctly seasonal pattern on the sap flow rate measurements. The peak sap flow rate was 35 L day^{-1} in summer and the lowest daily sap flow rate measured in winter was 6 L day^{-1}. On the last tree under investigation (ST3St), the sap flow rate pattern also showed an increase of up to 55 L day^{-1} during the peak of the rainy season and stayed at 30 L day^{-1} during winter.

9.3.3 Diurnal transpiration and water sources

The rates of T for the investigated trees and the corresponding soil water depletion in the top 1.2 m soil layer within their crown areas during sunny days in summer (17 February, 2017) and winter (25 July, 2017) are respectively presented in Figures 9.5 and 9.6. The focus was

on the summer and winter seasons because they were considered to be having the extremes, with the autumn and spring seasons generally expected to be intermediate of the two. In both days the T was typically close to zero during the night, started slow with the day to peak just after midday and declined again towards end of the day, for all the trees in both summer and winter. The soil water depletion on the other hand showed different patterns between the summer and winter days. Negative soil water depletion meant that the soil profile was gaining water from somewhere.

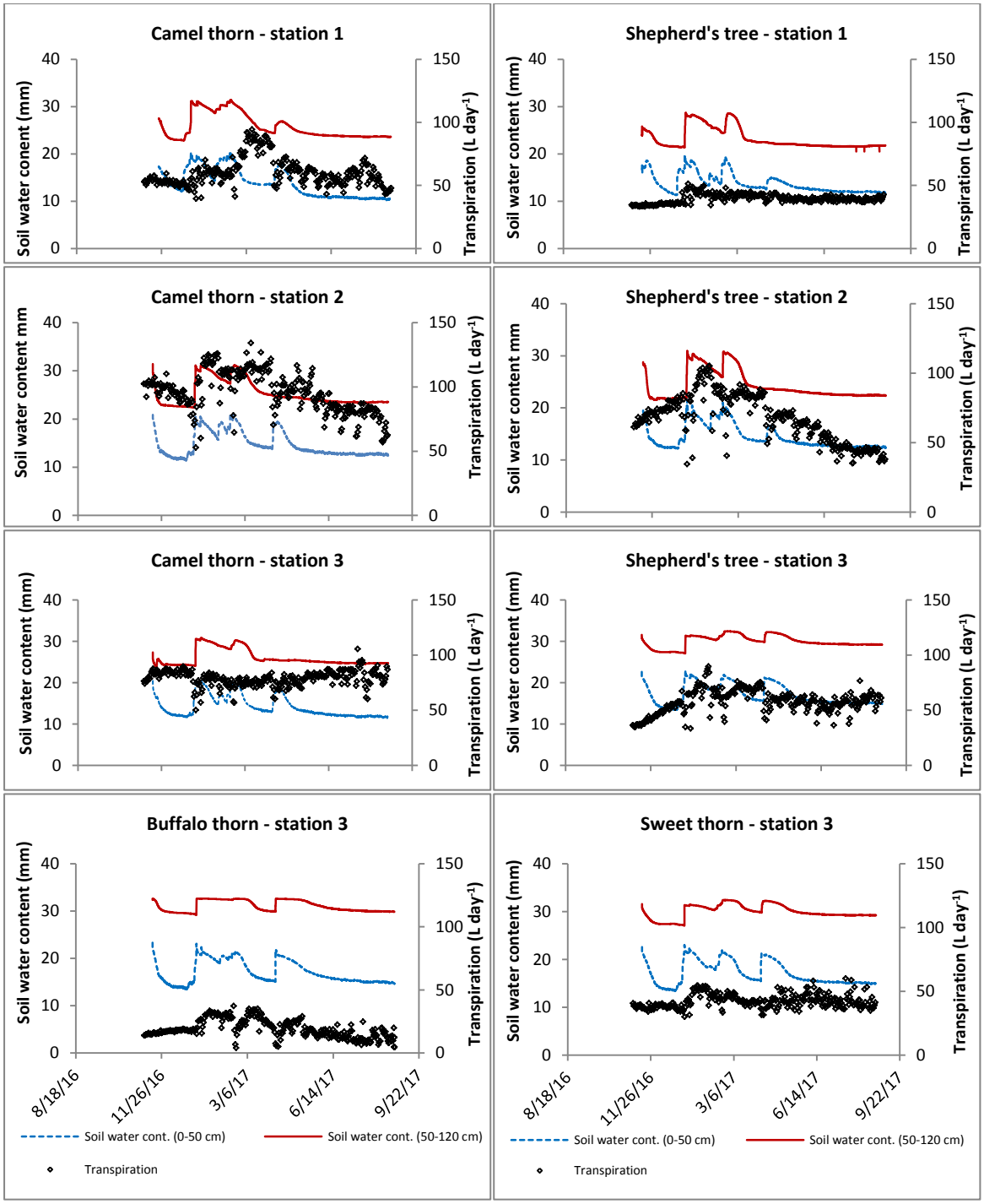

Figure 9.4: Transpiration of eight selected indigenous trees and soil water content measured at 0-0.5 m and 0.5-1.2 m depths, monitored continuously over a period of twelve months (November 2016 to October 2017), at Wolhaarkop Farm of the Kolomela Mine.

Based on the canopy area, the T rate for trees ST1Ct, ST2Ct and ST3Ct ranged from 0.03 mm hr^{-1} to 0.1 mm hr^{-1}. The soil water depletion within the top 0.5 m soil profile under these trees

was generally constant at 0.01 mm hr^{-1} or less over a 24-hr period. The lower lying soil layer (0.5-1.2 m) typically showed no water depletion over a 24-hr, instead a gain of water was observed in a few instances (Figure 9.5). For the Shepherd's trees (ST1Sht, ST2Sht and ST3Sht) the T rate peaked at a range between 0.08 mm hr^{-1} to 0.1 mm hr^{-1}. Again a constant rate of soil water depletion of 0.02 mm hr^{-1} in the top 0.5 m soil layer was observed under ST2Sht, while the lower lying layer showed insignificant soil water depletion. Under the canopies of ST1Sht and ST3Sht, the soil water depletion was generally zero regardless of the soil depth. The peak T rate for tree ST3St was 0.06 mm hr^{-1} and the highest soil water depletion observed was approximately 0.02 mm hr^{-1}. This depletion however did not seem to be following the diurnal trend of tree T. Tree ST3Bt showed peak transpiration rate of 0.1 mm hr^{-1} and the soil water content within its canopy area did not show changes over a 24-hr period.

During the winter sunny day, there was a consistent trend of negative soil water depletion (gain of soil water) especially during the daytime hours (Figure 9.6). Even though following a similar trend, the peak T rate was generally smaller on this day compared to the summer sunny day in all the investigated trees. Sap flow measured on trees ST3St and ST3Bt were the only exceptions with no clear diurnal pattern and very minimal flows (close to zero). In both the summer and winter diurnal water use, there was a considerable amount of nocturnal sap flow (Figures 9.5 and 9.6).

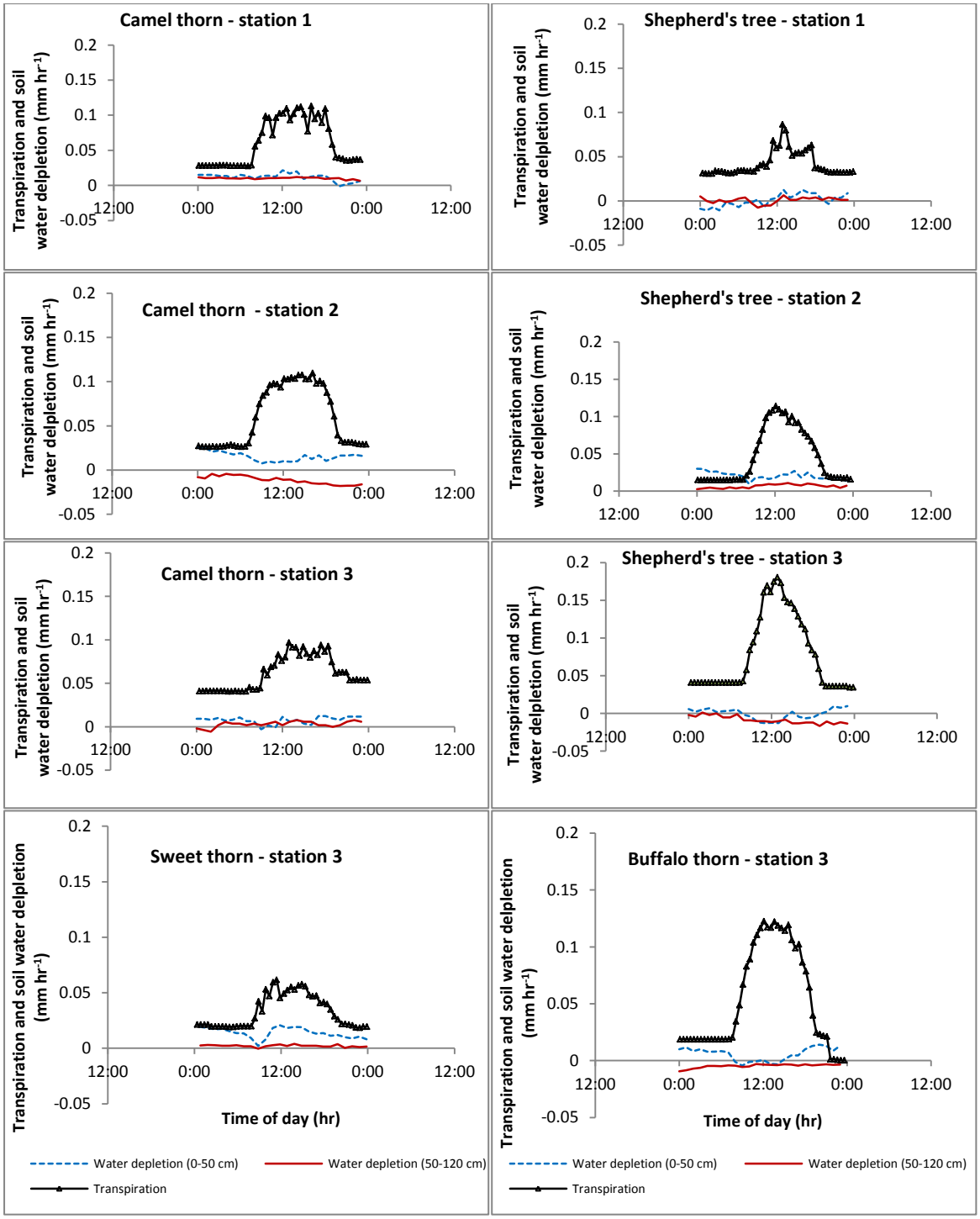

Figure 9.5: Diurnal variation of tree transpiration for selected indigenous trees and soil water depletion during the rainy season in February, at Wolhaarkop Farm of the Kolomela Mine.

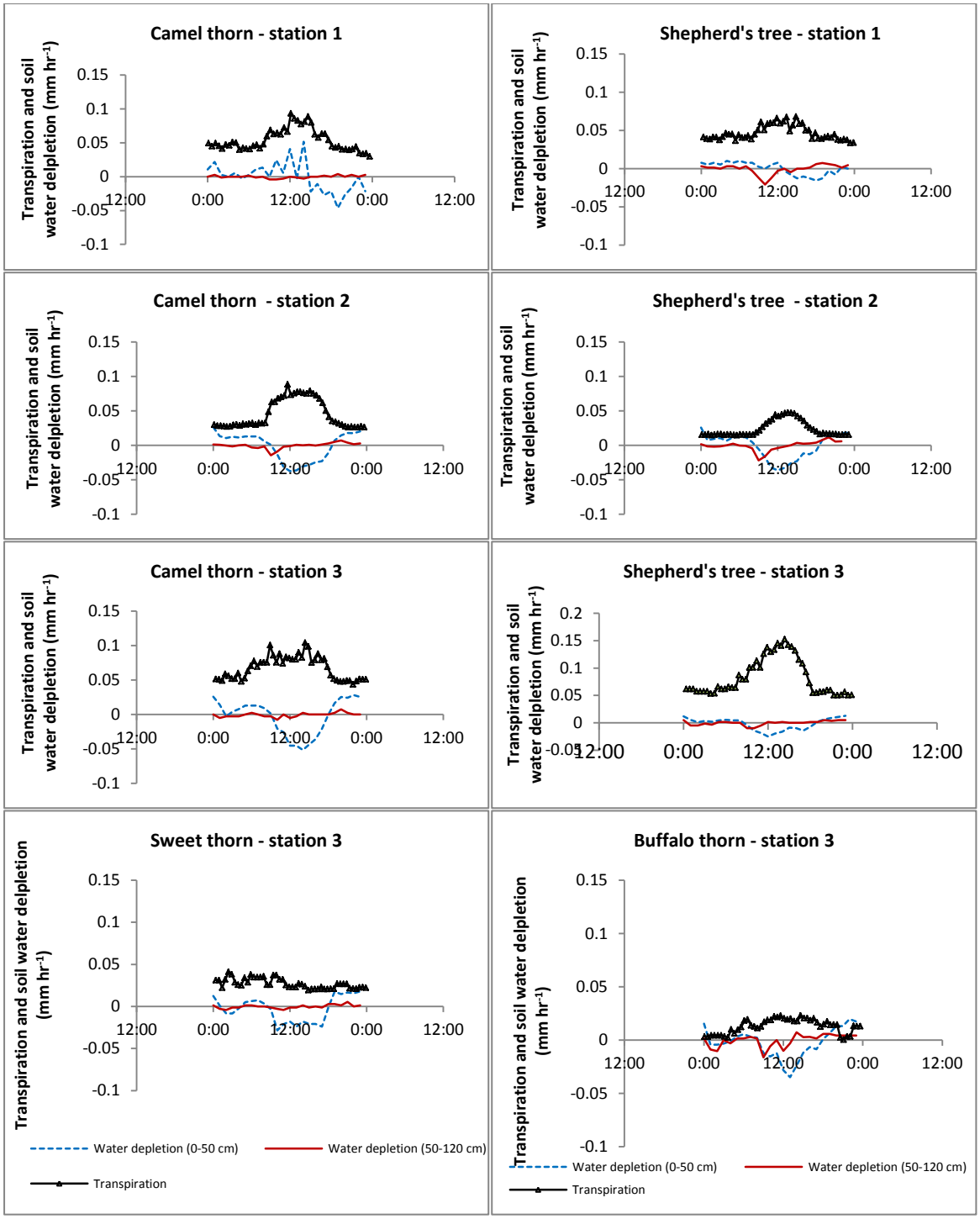

Figure 9.6: Diurnal variation of tree transpiration for selected indigenous trees and soil water depletion during the dry season in July, at Wolhaarkop Farm of the Kolomela Mine.

9.4 Discussion

9.4.1 Transpiration in relation to soil water availability

Between the dry and wet seasons, tree T for camel thorn ranged from 40 L day^{-1} on tree ST1Ct to 125 L day^{-1} on tree ST2Ct. Based on the projected canopy area, this range corresponds to 0.63 mm day^{-1} to 1.59 mm day^{-1}. On shepherd's tree, the measured T ranged from 30 L day^{-1} (1.06 mm day^{-1}) on tree ST3Sht in winter to 100 L day^{-1} (1.27 mm day^{-1}) on tree ST2Sht in summer. The T of sweet thorn was approximately 30 L day^{-1} (0.38 mm day^{-1}) during the dry season and peaked at about 55 L day^{-1} (0.70 mm day^{-1}) in summer. The last tree, (ST3Bt) showed a peak of 35 L day^{-1} during the wet season and 6 L day^{-1} under water limited conditions during winter.

Daily T rates similar to those obtained here have been reported in other studies conducted in relatively similar environmental conditions (arid and semi-arid). The increase of sap flow in trees with increasing water availability has been reported by numerous researchers previously. Do et al. (2008) monitored the T of an *Acacia tortilis* tree (DBH = 170 mm) growing in arid conditions in Souilene, Senegal, and reported minimum water use of 8.8 L day^{-1} during the dry season and maximum of 40 L day^{-1} towards the end of the rainy season. Ford et al. (2004) studied the T of trees in a 32-year old loblolly pine plantation in northern Georgia, US from May through September and reported water use ranging from 30 to 130 L day^{-1}. Čermák et al. (1982) measured up to 400 L day^{-1} of water use on a 33 m tall *Quercus robur* tree growing in a semi-arid environment in Lednice, South Moravia. Studying yellow poplar tree with DBH between 150 and 690 mm in Tennessee, US, Wullchelger and King (2000) reported sap flow rates ranging from 28 to 675 L day^{-1} $tree^{-1}$.

Another observation made was that generally the water use increased with DBH. This has also been reported by previous researchers. Bosch et al. (2014) reported a nonlinearly increase of water use with DBH on tree in a riparian forest in the Southern Plain Region of

the US which was primarily composed of *Pinus elliottii*, *Pinus palustris* and *Liriodendron tulipifera*. Previously, Vertessy et al. (1995; 1997) conducted experiments on *Eucalyptus regnans* trees and reported coefficients of determination (R^2 values) between 0.86 and 0.89 between DBH and water use. Meinzer et al. (2004) also reported a strong positive correlation between DBH and tree water use on a variety of different tree species.

Age effects were revealed on the biggest camel thorn tree (ST3Ct, DBH = 460 mm), which was because of the size assumed to be the eldest among the camel thorn trees. This tree did not record the highest rate of water use despite its stem size. Instead, it recorded a constant rate of water use across seasons. This result concurs with findings of Moore et al. (2003) where the water use of a 40-year-old forest of Douglas fir was found to use 3.3 times more water than a 450-year-old forest of the same species, yet both forests were growing in the H.J. Andrews Forests of the western Cascade Range of Oregon. Jassal et al. (2009) also conducted a study on Douglas fir in Pacific Northwest and found that a 58-year-old stand exhibited less variability in water use rates and was less sensitive to seasonal water availability changes in comparison with younger (7 and 19-year-old) stands. These differences are attributed to the fact that as trees age their sapwood "living wood" through which sap flows becomes less and less and the heartwood "dead wood" becomes more proportionally dominant. Also, with age comes greater height which in turn comes with greater pressure gradient due to gravity resulting in greater resistance to water flow. The extension of these investigations to a wide range of tree sizes and inclusion of all dominant tree species can be crucial to establish comprehensive information on total tree water use at the catchment level and hence appropriate water use allocation decisions be taken.

9.4.2 Diurnal tree transpiration pattern and water source

Corresponding to the observed high daily water use during the wet season compared to the dry season, the diurnal patterns also reached higher peak hourly water use in the summer day than the winter day. The soil water depletion did not change simultaneously with the water use across the day, especially in summer. The observed soil water depletion was constantly about 0.01 mm hr^{-1} (Figure 9.5), which is at most 10% of the peak T rates of up 0.1 mm hr^{-1} or more recorded for most of the trees. Understory vegetation and evaporation also contribute significantly (up to 50%) to total ecosystem evapotranspiration (Wilson et al., 2001). The marginal soil water depletion (0.01 mm hr^{-1}) is likely to be completely lost through the understory T and surface evaporation. This therefore suggests that the trees are almost entirely dependent on water sources beyond the top 1.2 m soil layer, and inferring that their roots are constantly connected to ground water reserves.

With the water table depth constantly fluctuating between 20 and 25 m in the Kolomela Mine (data not presented here), and some of the investigated trees with a potential to grow roots systems to depths of up to 60 m (Canadell et al., 1996), it is undoubtable that the mature trees within the study area, including the ones under investigation here are accessing water from the saturated zone. The reliance of trees on groundwater increases with a decrease in the soil water content (Lubczynski, 2009). In environments such as the study area, where rainfall events are very few and the rate of evapotranspiration very high, the soil dries quickly such that it is almost always dry even during the "wet season". The trees are therefore bound to adapt to a permanent limited soil water content mode and extend their roots into the saturated zone.

As mentioned earlier, the main economic activity in the study area is open cast mining, which involves a continuous drawdown of the water table by pumping it out of the mining hole. Thus impacts on the hydrological cycle are inevitable. The extent of this pumping on the

water table depths in the surroundings of the mine areas must be monitored closely as it is bound to affect the vegetation which rely heavily on groundwater. The Kolomela Mine is already implementing groundwater recharge programs, and these have to be intensified in order to minimize alterations in groundwater reserves and hence prevent its adverse effects especially on the sustainability of the environment.

The diurnal pattern during the winter revealed a rather unexpected phenomenon where there was negative soil water depletion (water gain) within the canopy areas of the trees investigated. Since there was no precipitation prior to this day, the likely possibility is hydraulic redistribution of water by the tree roots. This phenomenon has been previously reported to be nocturnal (Burgess et al., 1998: Lubczynski, 2009; Nadezhdina et al., 2010), however there is a need to investigate its possibility during the day amongst the investigated tree species, particularly in arid environments.

9.5 Conclusions

This study investigated the water use of selected indigenous trees growing in arid conditions dominated by open cast mining activities. The aims were to determine the response of tree water use to seasonal variation of soil water availability and to estimate the dominant water source(s) contributing to tree T. It was concluded that the water use of the selected tree species varies with seasonal variations of soil water content. It was also concluded that in old trees, the water use declines and is less responsive to seasonal variations of soil water availability. The diurnal patterns of T peaked at higher rates during summer compared to during water limited conditions in winter. It was established that the trees are close to 100% reliant on groundwater and therefore changes on groundwater reserves should be monitored closely and effects thereof be mitigated. Artificial groundwater recharge should be intensified to counter the effects of the continuous water table drawdown during mining operations. It was also recommended that the possibility of daytime water redistribution by tree roots should be investigated. Future studies should extend to other tree species and then scale up tree water use at the catchment level in order to inform appropriate calculations and budgeting with regards to water resources.

References

Acocks, J.P.H., 1988. *Veld types of South Africa* (No. 57, Ed. 3).

Allison, G.B., Barnes, C.J. and Hughes, M.W., 1983. The distribution of deuterium and 18O in dry soils 2. Experimental. J. Hydrol. 64(1-4), 377-397.

Bond, B.J., Meinzer, F.C., Brooks, J.R., 2008. How trees influence the hydrological cycle in forest ecosystems. Hydroecology and ecohydrology: Past, present and future, pp.7-28.

Bosch, D.D., Marshall, L.K., Teskey, R., 2014. Forest transpiration from sap flux density measurements in a southeastern Coastal Plain riparian buffer system. Agr. Forest Meteorol. 187, 72-82.

Burgess, S.S.O., Adams, M.A., Turner, N.C., Ong, C.K., 1998. The redistribution of soil water by tree root systems. Oecologia 115, 306-311.

Canadell, J., Jackson, R.B., Ehleringer, J.R., Mooney, H.A., Sala, O.E., Schulze, E.D., 1996. Maximum rooting depth of vegetation types at the global scale. Oecologia 108, 583-595.

Čermák, J., Ulehla, J., Kučera, J., Penka, M., 1982. Sap flow rate and transpiration dynamics in the full-grown oak (*Quercus robus* L.) in floodplain forest exposed to seasonal floods as related to potential evapotranspiration and tree dimensions. Biol. Plantarum 24(6), 446-460.

Clulow, A. D., C. S. Everson, M. G. Mengistu, J. S. Price, A. Nickless, and G. P. W. Jewitt. "Extending periodic eddy covariance latent heat fluxes through tree sapflow measurements to estimate long-term total evaporation in a peat swamp forest." *Hydrology and Earth System Sciences Discussions* 11, no. 12 (2014): 13607-13661.

Dai, A., Trenberth, K.E., 2002. Estimates of freshwater discharge from continents: latitudinal and seasonal variations. J. Hydrometeorol. 3, 660-687.

Dawson, T.E., 1996. Determining water use by trees and forests from isotopic, energy balance and transpiration analyses: the roles of tree size and hydraulic lift. Tree Physiol. 16, 263-272.

Dawson, T.E., 1998. Fog in the California redwood forest: ecosystem inputs and use by plants. Oecologia 117(4), 476-485.

Dean, T.J., Bell, J.P., Baty, A.J.B., 1987. Soil moisture measurement by an improved capacitance technique, Part 1. Senor Design and performance. J. Hydrol. 930, 67-78.

Do, F.C., Rocheteau, A., Diagne, A.L., Goudiaby, V., Granier, A., Lhomme, J., 2008. Stable annual pattern of water use by *Acacia tortilis* in Sahelian Africa. Tree Physiol. 28(1), 95-104.

Dye, P.J., Gush, M.B., Everson, C.S., Jarmain, C., Clulow, A., Mengistu, M., Geldenhuys, C.J., Wise, R., Scholes, R.J., Archibald, S., Savage, M.J., 2008. Water-use in relation to biomass of indigenous tree species in woodland, forest and/or plantation conditions. WRC Report TT 361/08, Water Research Commission, Pretoria, South Africa.

Edwards, W.R.N., Warwick, N.W.M., 1984. Transpiration from a kiwifruit vine as estimated by the heat-pulse technique and the Penman-Monteith equation. N.Z. J. Agric. Res. 27, 537-543.

Evaristo, J., Jasechko, S., McDonnell, J.J., 2015. Global separation of plant transpiration from groundwater and streamflow. Nature 525(7567), 91-101.

Evett, S.R., Tolk, J.A., Howell, T.A., 2006. Soil profile water content determination: sensor accuracy, axial response, calibration, temperature dependence, and precision. Vadose Zone J. 5, 894-907.

Fernández, J.E., Palomo, M.J., Díaz-Espejo, A., Clothier, B.E., Green, S.R., Girón, I.F., Moreno, F., 2001. Heat-pulse measurements of sap flow in olives for automating irrigation: tests, root flow and diagnostics of water stress. Agric. Water Manage. 51, 99–123.

Fetter, C.W., 2001. Applied Hydrogeology, 4th ed. New Jersey: Prentice Hall.

Ford, C.R., Goranson, C.E., Mitchell, R.J., Will, R.W., Teskey, R.O., 2004. Diurnal and seasonal variability in the radial distribution of sap flow: predicting total stem flow in Pinus taeda trees. Tree Physiol. 24, 951–960.

Gazis, C., Feng, X., 2004. A stable isotope study of soil water: evidence for mixing and preferential flow paths. Geoderma 119(1), 97-111.

Craig, H., 1961. Isotopic variations in meteoric waters. Science 133(3465), 1702-1703.

Granier A (1987) Evaluation of transpiration in a Douglas-fir stand by means of sap flow measurements. Tree Physiol. 3, 309-320.

Green, S., Clothier, B., Jardine, B., 2003. Theory and practical application of heat pulse to measure sap flow. Agron. J. 95, 1371-1379.

Green, S.R., Clothier, B.E., 1988. Water use of kwiwifruit vines and apple trees by the heat pulse technique. J. Exp. Bot 39 (198), 115-123.

Gush, M.B., 2008. Measurement of water-use by Jatropha curcus L. using ther heat pulse velocity technique. Water SA 34(5), 1-5.

Jasechko, S., Sharp, Z.D., Gibson, J.J., Birks, S.J., Yi, Y., Fawcett, P.J., 2013. Terrestrial water fluxes dominated by transpiration. Nature, 496(7445), 347-350.

Jassal, R.S., Black, A., Spittlehouse, D.L., Brummer, C., Nesic, Z., 2009. Evapotranspiration and water use efficiency in different-aged Pacific Northwest Douglas-fir stands. Agr. Forest Meteorol. 149, 1168-1178.

Lubczynski, M.W., 2009. The hydrological role of trees in water-limited environments. Hydrogeol. J. 17, 247-259.

Meinzer, F.C., James, S.A., Goldstein, G., 2004. Dynamics of transpiration, sap flow and use of stored water in tropical forest canopy trees. Tree Physiol. 24, 901-909.

Meiresonne, L., Sampson, D.A., Kowalski, A.S., Janssens, I.A., Nadezhdina, N., Čermák, J., Van Slycken, J., Ceulemans, R., 2003. Water flux estimates from a Belgian Scots pine stand: a comparison of different approaches. J. Hydrol. 270(3), 230-252.

Moore, G.W., Bond, B.J., Jones, J.A., Phillips, N., Meinzer, F.C., 2003. Structural and compositional controls on transpiration in the 40- and 450-year-old riparian forests in western Oregon, USA. Tree Physiol. 24, 481-491.

Morris, J., Ningnan, Z., Zengjiang, Y., Collopy, J., Daping, X., 2004. Water use by fast-growing Eucalyptus urophylla plantations in southern China. Tree physiol. 24(9), 1035-1044.

Mucina, L., Rutherford, M.C., 2006. The Vegetation of South Africa Lesotho and Swaziland. South African National Biodiversity Institute, Pretoria, South Africa.

Nadezhdina, N., David, T.S., David, J.S., Ferreira, M.A., Dohnal, M., Tesar, M., Gartner, K., Leitgeb, E., Nadezhdin, V., Cermak, J., 2010. Trees never rest: the multiple facets of hydraulic redistribution. Ecohydrol. 3, 431-444.

Nicolas, E., Torrecillas, A., Ortuno, M.F., Domingo, R., Alarcón, J.J., 2005. Evaluation of transpiration in adult apricot trees from sap flow measurements. Agr. Water Manage. 72(2), 131-145.

Oki, T., Kanae, S., 2006. Global hydrological cycles and world water resources. Science 313, 1068-1072.

Orlowski, N., Frede, H.G., Brüggemann, N., Breuer, L., 2013. Validation and application of a cryogenic vacuum extraction system for soil and plant water extraction for isotope analysis. Journal of Sensors and Sensor Systems 2(2), 179-193.

Ortuño, M.F., Alarcón, J.J., Nicolás, E., Torrecillas, A., 2004. Interpreting trunk diameter changes in young lemon trees under deficit irrigation. Plant Sci. 167, 275-280.

Roberts, J.M., 2009. The role of trees in the hydrological cycle, *In* Owens, J.N., Lunday, H.G., (Eds) Forests and Forest Plants, Vol 3, Encyclopedia of life support systems, UNESCO. 42-76.

Schlesinger,W. H., Jasechko, S., 2014. Transpiration in the global water cycle. Agric. For. Meteorol. 189, 115-117.

Shadwell, E., February, E., 2017. Effects of groundwater abstraction on two keystone tree species in an arid savanna national park. PeerJ *5*, e2923.

Shimizu, T., Kumagai, T.O., Kobayashi, M., Tamai, K., Iida, S.I., Kabeya, N., Ikawa, R., Tateishi, M., Miyazawa, Y. and Shimizu, A., 2015. Estimation of annual forest evapotranspiration from a coniferous plantation watershed in Japan (2): Comparison of eddy covariance, water budget and sap-flow plus interception loss. J. Hydrol. 522, 250-264.

Smith, D.M., Allen, S.J., 1996. Measurement of sap flow in plant stems. J. Exp. Bot. 47, 1833-1844.

Soubie, R., Heinesch, B., Granier, A., Aubinet, M., Vincke, C., 2016. Evapotranspiration assessment of a mixed temperate forest by four methods: Eddy covariance, soil water budget, analytical and model. Agr. Forest Meteorol. 228, 191-204.

Swanson, R.H., Whitfield, D.W.A., 1981. A numerical analysis of heat pulse velocity theory and practice. J. Exp. Bot. 32(126), 221-239.

Tfwala, C.M., van Rensburg, L.D., Schall, R., Mosea, S.M., Dlamini, P., 2017. Precipitation intensity duration frequency curves and their uncertainties for the Ghaap Plateau, Clim. Risk Manage. 16, 1-9.

Vertessy, R.A., Benyon, R.G., O'Sullivan, S.K., Gribben, P.R., 1995. Relationships between stem diameter, sapwood area, leaf area and transpiration in a young mountain ash forest. Tree Physiol. 15, 559-567.

Vertessy, R.A., Hatton, T.J., Reece, P., O'Sullivan, S.K., Benyon, R.G., 1997. Estimating stand water use of large mountain ash trees and validation of the sap flow measurement technique. Tree Physiol. 17, 747-756.

Wada, Y., Van Beek, L.P.H., Wanders, N., Bierkens, M.F.P., 2013. Human water consumption intensifies hydrological drought worldwide. Environ. Res. Lett. 8, 034036.

Wildy, D.T., Pate, J.S., Bartle, J.R., 2004. Budgets of water use by *Eucalyptus kochii* tree belts in the semi-arid wheat belt of Western Australia. Plant Soil 262(1), 129-149.

Williams, D.G., Cable, W., Hultine, K., Hoedjes, J.C.B., Yepez, E.A., Simonneaux, V., Er-Raki, S., Boulet, G., De Bruin, H.A.R., Chehbouni, A., Hartogensis, O.K., 2004. Evapotranspiration components determined by stable isotope, sap flow and eddy covariance techniques. Agr. Forest Meteorol. 125(3), 241-258.

Wilson, K.B., Hanson, P.J., Mulholland, P.J., Baldocchi, D.D., Wullchleger, S.D., 2001. A comparison of methods for determining forest evapotranspiration and its components: sap flow, soil water budget, eddy covariance and catchment water balance. Agr. Forest Meteorol. 106, 153-168.

Wullschleger, S.D., King, A.W., 2000. Radial variation in sap velocity as a function of stem diameter and sapwood thickness in yellow-poplar trees. Tree Physiol. 20, 511-518.

Zerizghy, M.G., van Rensburg, L.D., Anderson, J.J., 2013. Comparison of neutron scattering and DFM capacitance instruments in measuring soil evaporation. Water SA 39(2), 183-190.

10. Synthesis and Recommendations

10.1 Synthesis

The global importance of water and investigations of components driving the hydrologic cycle thereof cannot be overemphasised. Transpiration (T) from vegetation, especially trees, together with streamflow and groundwater recharge forms one of the three major freshwater fluxes of the terrestrial hydrosphere. With forests covering about a third of the earth's land area, and their T representing the major route through which water re-enters the atmosphere in the hydrologic cycle, it is crucial to unpack this process from the global scale to the tree level. To achieve a realistic and accurate reflection of the involvement of trees in the hydrologic cycle; it is crucial to get an insight of the climatic trends where the trees are growing and also to ensure reliable instruments and methods are employed for data acquisition. This thesis involved an overview of whole tree T subject at the global scale, an analysis of precipitation patterns, a series of methods and instruments calibration experiments and lastly, laboratory (lysimeter) and field tree T studies.

To gain an insight of the factors driving whole tree T at the global scale; a literature search was conducted, and a total of 94 published studies, which were conducted on 130 different tree species in sites distributed across the world, were identified (Chapter 2). Tree morphological traits; tree height (H) and diameter at breast height (DBH) were in this study reaveled as the principal drivers of tree T. These parameters respectively showed positive Spearman correlations (r_s) of 0.55 and 0.62 with T. With regard to environmental factors (mean annual precipitation (MAP), mean annual air temperature (MAT) and altitude (Z)), only MAP showed a weak positive correlation (r_s = 0.16) with T, otherwise MAP and Z were not correlated with T. The investigation also revealed that thermodynamic based methods of measuring tree T, especially heat pulse velocity and thermal heat dissipation methods, are the most commonly used.

Prior to conducting field experiments on tree water use at the Kolomela Mine; an analysis of the rainfall pattern within the region was conducted (Chapters 3 and 4). Chapter 3 focussed on the occurrence, severity and duration of droughts, as well as the trends of precipitation patterns over the years. Using long-term data (1918-2014) from the nearest and surrounding meteorological stations, it was revealed that droughts became more frequent after the year 1990. All the droughts that occurred during the data record period, except for the 1992 drought which was severe, were moderate and no drought lasted for more than 2 consecutive years during the precipitation data record period. The total annual rainfall was found to follow a secular pattern of fluctuations over the years, while the number of rainfall days and extreme rainfall events were essentially stable. Chapter 4 was aimed at predicting the intensities of precipitation for durations of 0.125, 0.25, 0.5, 1, 2, 4 and 6 hours and return periods of 2, 10, 25, 50 and 100 years, and establish the uncertainty of the predictions for the study area. The predicted precipitation intensity ranged from 4.2 mm hr^{-1} for a 6-hr storm duration to 55.8 mm hr^{-1} for 0.125 hrs at the return period of 2 years. For the longest return period of 100 years, the predicted intensity ranged between 13.3 mm hr^{-1} for a 6 hr duration storm and 175 mm hr^{-1} for the duration of 0.125 hrs. The uncertainty of prediction ranged from 11.7% to 58.4%.

The need for conducting intensive studies on trees under controlled environments such as lysimeters has mainly been limited by the lack of equipment and methods to transplant grown trees into such facilities. A mechanical sampler and a procedure were developed and implemented on four selected indigenous trees of the semi-arid Free State of South Africa (Chapter 5). The trees were sampled with a soil volume of 1.2 m^3 and transplanted into weighing lysimeters. Tested 3 years after the transplanting exercise, the water use of the trees ranged from 7 to 14 L day^{-1}, which was within the water use range of trees of similar sizes

under natural conditions. The conclusion was therefore made that the procedure is appropriate for tree – soil monolith sampling.

Accurate volumetric soil water content (θv) measurement is crucial for efficient soil water management. A newly developed HydraSCOUT (HS) capacitance probe (Hydra Sensor Technologies International Ltd) was calibrated to develop calibration equations in the field and laboratory, and then compare their level of accuracy in estimating θv for the Plinthosol (Bainsvlei) and Ferralsol (Bloemdal) soil types (Chapter 6). Laboratory equations estimated θv better (RMSE=0.001 m^3 m^{-3} - 0.015 m^3 m^{-3}) than field calibration equations (RMSE=0.004 m^3 m^{-3} - 0.026 m^3 m^{-3}).

The compensation heat pulse velocity (CHPV) method is among the most commonly used methods to measure sap flow in trees. This method was calibrated against pre-calibrated loadcells to determine its accuracy to estimate T of selected South African indigenous tree species (Chapter 7). Good agreements were observed between the CHPV technique and the loadcells across tree species (D = 0.778-1.000, RMSE = 0.001-0.017 L hr^{-1}, MAE < 0.001 L hr^{-1} and MBE = -0.0007-0.0008 L hr^{-1}). It was concluded that the CHPV method can accurately measure tree water use to the investigated indigenous trees and others with similar wood characteristics.

A lysimeter experiment was conducted at Kenilworth Experiment Farm of the University of the Free State, Bloemfontein, South Arica. The objective of this experiment was to partition total tree T for selected indigenous trees into groundwater and soil water (Chapter 8). Total tree T was measured using the CHPV technique, soil water depletion was measured using the HS capacitance probes and, groundwater use was monitored using an automated water supply bucket system. The bulk of water transpired by trees (up to 97%) was found to be from groundwater supply when the top 0.8 m soil layers were dry, while only 31% came from this source when the top soil had just been irrigated. The trees sourced up to 69% of their T

requirements from the superficial soil layers after an irrigation event, which decreased to a mere 3% as the top soil was drying. The conclusion was that the investigated trees have dimorphic root structures, which enabled them to switch to different water pools of water depending on availability. The results of this investigation also suggested that the water balance approach can be used to partition tree T into groundwater and soil water.

Finally, a field investigation seeking to have detailed understanding of the quantity and source of water transpired by camel thorn, sweet thorn, shepherd tree and buffalo thorn trees was conductcted at Wolhaarkop Farm of the Kolomela Mine in the arid Northern Cape province of South Africa. The study focussed on i) assessing the trends of T for the selected tree species across a range of soil water content conditions and ii) partition the total T of these tree species into soil water and groundwater. The soil water content within the top 0.5 m layer, measured through the use of DFM capacitance probe, ranged from 11 mm in winter to 20 mm in summer. The deeper (0.5-1.2 m) soil layer was wetter (up to 30 mm) during the wet season. Overall, tree water use ranged from 6 L day^{-1} for buffalo thorn in winter to 125 L day^{-1} for camel thorn in summer. The water use for a camel thorn tree with DBH of 460 mm was found to be constant regardless of the season of the year. Diurnal tree water use did not seem to effect any diurnal changes in the soil water content within the top 1.2 m soil profile, suggesting that the trees source their water beyond this profile, and most likely from the saturated zone. There was an observed daytime gain in soil water content under the canopies of the investigated trees. This observation probed the need to investigate daytime redistribution of water by the investigated tree species.

10.2 Recommendations

- The morphological traits of trees in the form of H and DBH should be incorporated into global scale modelling of tree T in forested ecosystems.
- Analysis of long-term precipitation data can form a good basis for predicting future catastrophic events such as droughts and floods.
- The prediction of precipitation intensities should be integrated into the formulation of policies that govern the design of stormwater and flood management infrastructures, especially for rapidly developing municipalities such as mining towns.
- Laboratory calibration of the HS capacitance probe was recommended for more accurate estimations of θv.
- The use of the CHPV technique was recommended for measuring tree water use of the investigated indigenous tree species as well as other species with similar wood characteristics.
- The water balance approach can be used to partition total tree transpiration into groundwater and soil water.
- Investigation of daytime water redistribution by the investigated trees and other trees of the arid study area was recommended.
- Extension of the species specific tree water use investigations to other trees species within the study area was recommended in order to comprehensively inform water managers on the involvement of trees in the hydrology at the catchment level.

APPENDICES

Appendix 2.1: Database used in the paper

Author	Country	Location	Latitude	Longitude	Elevation	MAP	MAT	*Species*	Height (m)	DBH (mm)	Method	Transpiration (l/d)
Alcorn et al., 2013	Australia	Nana Glen	-30.02	153.13	165	1437	11.6	*Eucalyptus cloeziana*	12	160	HB	25
Alcorn et al., 2013	Australia	Nana Glen	-30.02	153.13	165	1437	11.6	*Eucalyptus pilularis*	11	140	HB	18
Andrade et al., 1998	Panama	Panama	8.97	-79.57	50	1800	20	*Cecropia longipes*	18	200	TD	47
Andrade et al., 1998	Panama	Panama	8.97	-79.57	50	1800	20	*Spondias mombin*	23	330	TD	80
Ansley et al., 1991	USA	Throckmorton	33.33	-99.23	450	624	21	*Prosopis glandosa*	3.7	200	HB	75
Ansley et al., 1994	USA	Vernon	33.87	-99.28	368	665	10.4	*Prosopis glandosa*			HB	108
Ansley et al., 1994	USA	Vernon	33.87	-99.28	368	665	10.4	*Populus trichocarpa x*	4		TD	108
Arneth et al., 1996	Russia	Siberia	61	128	300	442	5	*Larix gmelinii*	20	250	TD	67
Becker, 1996	Borneo	Brunei	4.66	114. 52	37	3000	27.1	*Dryobalanops*	60	750	TD	310
Bleby et al., 2012	Australia	Jarrahdale	-32.65	116.02	250	1250	16.6	*Eucalyptus marginata*	10		HRM	6
Bosch et al., 2014	USA	Geogia	31.43	-83.58	836	1271	17	*Pinus palustris*	24	390	TD	142
Bréda et al., 1993a	France	Nancy	48.73	6.23	204	731	9.7	*Quercus robur*			TD	10
Bréda et al., 1993a	France	Nancy	48.7424	6.3485	237	731	9.7	*Quercus petraea*			TD	12
Bréda et al., 1993b	France	Nancy	48.7424	6.3485	237	731	9.7	*Quercus petraea*	15	90	TD	10
Bréda et al., 1995	France	Nancy	48.7424	6.3485	237	731	9.7	*Quercus petraea*			TD	11
Čermák and Kucera, 1987	Czech	Brno	49.0889	18.6372	620	683	6.6	*Picea abies*			HB	130
Čermák et al., 1995	Sweden	Norunda	60.05	17.48	45	527	5.5	*Picea abies*			TD	23
Čermák et al., 1982	South Moravia	Lednice	48.7883	16.8039	160	493	8.8	*Quercus robur*	33		TD	400
Čermák et al., 1984	Czech	Mokré Louky	49.8083	15.4504	285	713	8	*Salix fragilis*			TD	103
Čermák et al., 1993	Switzerland	Zurich,	8.78	47.5	764	1086	8.8	*Fagus sylvatica*	35	540	TD	137
Čermák et al., 1995	Sweden	Norunda	60.08	17.48	45	527	5.5	*Pinus sylvestris*			TD	13
Cienciala et al., 1992	Sweden	Skogaby	56.57	13.23	100	1100	7	*Picea abies*	15	190	TD	49
Cienciala et al., 2002	Sweden	Vindeln	64.23	19.77	175	600	1	*Pinus sylvestris*	11	120	HB	25
Dang et al., 2014	China	Gansu	38.63	103.08	1539	487	9.2	*Populus alba*	15	310	TD	85
Dierick and Hölscher, 2009	Philippines	Marcos	10.4555	124.4725	11	2753	27.5	*Durio zibethinus*	17	270	TD	33
Dierick and Hölscher, 2009	Philippines	Marcos	10.4555	124.4725	11	2753	27.5	*Gmelina arborea*	21	260	TD	20
Dierick and Hölscher, 2009	Philippines	Patag	10.441	124.4816	11	2753	27.5	*Hopea malibato*	15	140	TD	13
Dierick and Hölscher, 2009	Philippines	Patag	10.441	124.4816	11	2753	27.5	*Hopea plagata*	11	80	TD	6
Dierick and Hölscher, 2009	Philippines	Marcos	10.4555	124.4725	11	2753	27.5	*Myrica javanica*	12	260	TD	43
Dierick and Hölscher, 2009	Philippines	Patag	10.441	124.4816	11	2753	27.5	*Parashorea*	15	120	TD	15
Dierick and Hölscher, 2009	Philippines	Marcos	10.4555	124.4725	11	2753	27.5	*Sandoricum koetjape*	14	190	TD	23
Dierick and Hölscher, 2009	Philippines	Patag	10.441	124.4816	11	2753	27.5	*Shorea contorta*	20	250	TD	26
Dierick and Hölscher, 2009	Philippines	Patag	10.441	124.4816	11	2753	27.5	*Swietenia macrophylla*	16	160	TD	34
Dierick and Hölscher, 2009	Philippines	Marcos	10.4555	124.4725	11	2753	27.5	*Vitex parviflora*	14	260	TD	21
Do et al., 2008	Senegal	Souilene	16.33	15.42	10	280	28.7	*Acacia tortilis*	7	170	TD	48
Dragoni et al., 2005	USA	Geneva	41.8875	-88.3054	186	850	8.6	*Malus domestica*	3	70	HPV	40
Dye et al., 1992	South Africa	Frankfort	-25.5547	30.5	1572	1240	15	*Eucalypus grandis*	23	180	RSI	94
Dye et al., 1996	South Africa	Mpumalanga	-25.2734	28.5225	1459	748	20.3	*Eucalypus grandis*	43	300	TD	141
Dzikiti et al., 2013	South Africa	Simonsberg Mountain	-33.8504	18.9073	409	812	17.5	*Pinus spp*		270	HRM	33
Fernández et al, 2007	New Zealand	Blenheim	-41.5134	173.9612	1	711	12.6	*Malus domestica*			TD	55
Fernández et al., 2006	Spain	La Hampa	37.28	6.05	30	607	18.2	*Olea europaea*			TD	84
Fritschen et al., 1973	USA	Seatle	47.6062	-122.3321	158	866	11.1	*Pseudotsuga menziesii*	28	380	LP	64
Glenn, 2016	USA	Kearneysville	39.3882	-77.8856	159	965	18	*Malus domestica*			LP	48

Goldstein et al., 1998	Panama	Panama	8.97	-79.57	50	1800	20	*Ficus insipida*	30	540	TD	164
Goldstein et al., 1998	Panama	Panama	8.97	-79.57	50	1800	20	*Luehea seemannii*	29	370	TD	129
Goldstein et al., 1998	Panama	Panama	8.97	-79.57	50	1800	20	*Anacardium excelsum*	35	1020	TD	379
Gonzalez-Benecke et al., 2011	USA	Florida	29.73	-82.15	14	1504	19.8	*Pinus elliottii*			TD	55
Gonzalez-Benecke et al., 2011	USA	Florida	29.73	-82.15	14	1504	19.8	*Pinus palustris*			TD	37
Goodwin, 2006	Australia	Tatura	-36.43	146.25	242	524	15.2	Prunus persica	4		HPV	40
Granier et al., 1990	France	Estampon	44.5	-0.5	146	839	13.6	*Pinus pinaster*	20	340	TD	161
Granier et al., 1996	French Guiana	Saint Elie	5.2	-53.3	56	1046	4.2	*Caryocar glabrum*	27	260	TD	48
Granier et al., 1996	French Guiana	Saint Elie	5.2	-53.3	56	1046	4.2	*Vouacapoua americana*	28	490	TD	29
Granier et al., 1996	French Guiana	Saint Elie	5.2	-52.3	56	1046	4.2	*Eperua grandifolia*	33	550	TD	151
Granier et al., 1996	French Guiana	Saint Elie	5.2	-53.3	56	1046	4.2	*Hirtella glandulosa*	31	320	TD	62
Granier et al., 1996	French Guiana	Saint Elie	5.2	-53.3	56	1046	4.2	*Lecythis idatimon*	34	390	TD	94
Granier et al., 1996	French Guiana	Paracou	5.2	-52.7	7	3041	26	*Carapa procera*	37	380	TD	52
Granier et al., 1996	French Guiana	Paracou	5.2	-52.7	7	3041	26	*Dicorynia guianensis*	44	570	TD	212
Granier et al., 1996	French Guiana	Paracou	5.2	-52.7	8	3041	26	*Eperua falcata*	35	450	TD	166
Granier, 1987	France	Nancy	48.73	6.23	250	731	9.7	*Pseudotsuga menziesii*	18	200	TD	22
Green and Clothier, 1999	New Zealand	Palmerston North	-40.2	175.4	58	960	17	*Malus domestica*	5		HPV	40
Green et al., 2002	New Zealand	Hastings	-39.65	176.8	9	750	14.1	*Vitis vinifera*	1.5		HPV	56
Green et al., 2002	New Zealand	Marlborough	-41.5	173.87	146	1200	17	*Olea europaea*			HPV	33
Green et al., 2002	New Zealand	Motueka	-41.6	173	56	1308	12.7	*Malus domestica(dwarf)*			HPV	14
Green et al., 2003	New Zealand	Palmerston North	-40.2	175.4	58	960	17	*Malus domestica*	5		HPV	70
Greenwood and Beresford, 1979	Australia	Popanyinning	-32.661	117.1363	305	420	16.4	*Eucalyptus camaldulensis*			VC	22
Greenwood and Beresford, 1979	Australia	Popanyinning	-32.661	117.1363	305	420	16.4	*Eucalyptus cladocalyx*			VC	26
Greenwood and Beresford, 1979	Australia	Popanyinning	-32.661	117.1363	305	420	16.4	*Eucalyptus kondininensis*			VC	21
Greenwood and Beresford, 1979	Australia	Popanyinning	-32.661	117.1363	305	420	16.4	*Eucalyptus loxophleba*			VC	21
Greenwood and Beresford, 1979	Australia	Popanyinning	-32.661	117.1363	305	420	16.4	*Eucalyptus occidentalis*			VC	21
Greenwood and Beresford, 1979	Australia	Popanyinning	-32.661	117.1363	305	420	16.4	*Eucalyptus platypus*			VC	1
Greenwood and Beresford, 1979	Australia	Popanyinning	-32.661	117.1363	305	420	16.4	*Eucalyptus wandoo*			VC	23
Greenwood and Beresford, 1979	Australia	Dryandra	-32.7235	116.9281	304	500	18.3	*Eucalyptus camaldulensis*			VC	36
Greenwood and Beresford, 1979	Australia	Dryandra	-32.7235	116.9281	304	500	18.3	*Eucalyptus cladocalyx*			VC	32
Greenwood and Beresford, 1979	Australia	Dryandra	-32.7235	116.9281	304	500	18.3	*Eucalyptus leucoxylon*			VC	25
Greenwood and Beresford, 1979	Australia	Dryandra	-32.7235	116.9281	304	500	18.3	*Eucalyptus platypus*			VC	33
Greenwood and Beresford, 1979	Australia	Dryandra	-32.7235	116.9281	304	500	18.3	*Eucalyptus sargentii*			VC	30
Greenwood and Beresford, 1979	Australia	Dryandra	-32.7235	116.9281	304	500	18.3	*Eucalyptus wandoo*			VC	31
Greenwood and Beresford, 1979	Australia	Bannister	-34.5943	149.4883	847	850	7.5	*Eucalyptus camaldulensis*			VC	29
Greenwood and Beresford, 1979	Australia	Bannister	-34.5943	149.4883	847	850	7.5	*Eucalyptus cladocalyx*			VC	21
Greenwood and Beresford, 1979	Australia	Bannister	-34.5943	149.4883	847	850	7.5	*Eucalyptus globulus*			VC	49
Greenwood and Beresford, 1979	Australia	Bannister	-34.5943	149.4883	847	850	7.5	*Eucalyptus leucoxylon*			VC	16
Greenwood and Beresford, 1979	Australia	Bannister	-34.5943	149.4883	847	850	7.5	*Eucalyptus robusta*			VC	22
Greenwood and Beresford, 1979	Australia	Bannister	-34.5943	149.4883	847	850	7.5	*Eucalyptus saligna*			VC	29
Greenwood and Beresford, 1979	Australia	Bannister	-34.5943	149.4883	847	850	7.5	*Eucalyptus sargentii*			VC	29
Greenwood and Beresford, 1979	Australia	Bannister	-34.5943	149.4883	847	850	7.5	*Eucalyptus wandoo*			VC	14
Greenwood et al., 1981	Australia	Colie	-33	116.3	184	923	15.8	*Pinus radiata*	16	220	VC	179
Greenwood et al., 1982	Australia	Colie	-33	116.5	185	877	15.1	*Eucalyptus wandoo*			VC	150
Greenwood et al., 1985	Australia	Dwellingup	-32.7098	116.2063	267	1250	15.6	*Banksia grandis*			VC	101
Greenwood et al., 1985	Australia	Dwellingup	-32.7098	116.2063	267	1250	15.6	*Banksia grandis*			VC	36
Guevara-Escobar et al., 2000	New Zealand	Pohangina Valley	-40.13	175.88	225	1065	12.9	*Populus deltoides*	30	790	HPV	417
Gush, 2008	South Africa	Makhathini	-27.4	32.18	75	720	21	*Jatropha curcas*	6		HPV	80
Herzog et al., 1995	Switzerland	Davos	46.8027	9.836	1639	1000	3.9	*Picea abies*	25	360	TD	175
Hinckley et al., 1994	USA	Sumner	47.2032	-122.2404	23	1016	10.6	*Populus trichocarpa x*	15	150	TD	51
Hunt and Beadle, 1998	Australia	Wyena	-41.2	147.26	130	1000	12.9	*Acacia dealbata*		130	HPV	8
Hunt and Beadle, 1998	Australia	Wyena	-41.2	147.26	130	1000	12.9	*Eucalyptus nitens*		21	HPV	104

Jordan and Kline, 1977	Venezuela	San Carlos	2	-67	115	3500	17.4	*Ocotea sp.*			RSI	396
Jordan and Kline, 1977	Venezuela	San Carlos	2	-67	154	3500	17.4	*Licania sp.*			RSI	34
Jordan and Kline, 1977	Venezuela	San Carlos	2	-67	154	3500	17.4	*Protium sp.*			RSI	41
Jordan and Kline, 1977	Venezuela	San Carlos	2	-67	156	3500	17.4	*Micranda spruceana*			RSI	140
Jordan and Kline, 1977	Venezuela	San Carlos	2	-67	154	3500	17.4	*Aspidosperma album*			RSI	40
Jordan and Kline, 1977	Venezuela	San Carlos	2	-67	154	3500	17.4	*Aspidosperma*			RSI	179
Jordan and Kline, 1977	Venezuela	San Carlos	2	-67	154	3500	17.4	*Eperua leucantha*			RSI	91
Jordan and Kline, 1977	Venezuela	San Carlos	2	-67	154	3500	17.4	*Eperua purpurea*			RSI	1 180
Jung et al., 2011	South Korea	Mt. Gyebangsa	37.4441	128.2646	960	1453	12.4	*Acer mono*	14	220	TD	9
Jung et al., 2011	South Korea	Mt. Gyebangsa	37.4441	128.2646	960	1453	12.4	*Cornus controvera*	15	250	TD	20
Jung et al., 2011	South Korea	Mt. Gyebangsa	37.4441	128.2646	960	1453	12.4	*Quercus mongolica*	12	130	TD	96
Jung et al., 2011	South Korea	Mt. Gyebangsa	37.4441	128.2646	960	1453	12.4	*Tilia amurensis*	17	290	TD	30
Jung et al., 2011	South Korea	Mt. Gyebangsa	37.4441	128.2646	960	1453	12.4	*Ulmus davidiana*	16	290	TD	30
Kelliher et al., 1992	New Zealand	Maruia	-42.22	172.25	400	2367	11.6	*Nothofagus fusca*	34	600	TD	110
Kline et al., 1970	Puerto Rico	Montane	18.32	-65.83	350	3500	26	*Sloanea berteriana*	18	270	RSI	140
Kline et al., 1970	Puerto Rico	Montane	18.32	-65.83	350	3500	26	*Dacryodes excelsa*	20	550	RSI	372
Kline et al., 1976	USA	Andrews	32.3187	-102.5457	218	384	17.8	*Pseudotsuga menziesii*	76	1340	RSI	530
Knight, 1981	China	Wyoming	43.076	107.2903	2850	600	8	*Pinus contorta*		260	LP	44
Köstner et al., 1992	New Zealand	South Island	-42.22	172.25	400	2054	9.4	*Nothofagus spp.*	36		TD	84
Köstner et al., 1998	Germany	Oberwarmensteinach	50.0006	11.4726	632	757	6.7	*Picea abies*	17	150	TD	66
Krauss et al., 2007	USA	Florida	26.05	-81.701	14	1300	19.8	*Laguncularia racemosa*		240	TD	31
Krauss et al., 2007	USA	Florida	27.7081	-81.4035	14	1300	19.8	*Rhizophora mangle*		60	TD	7
Krauss et al., 2007	USA	Florida	26.05	-81.701	30	1300	19.8	*Avicennia germinans*		120	TD	18
Kunert et al., 2010	Panama	Sardinilla	9.32	-79.63	70	2350	26.2	*Acacia mangium*	21	390	TD	94
Kunert et al., 2010	Panama	Sardinilla	9.32	-79.63	70	2350	26.2	*Anacardium excelsum*	7	110	TD	32
Kunert et al., 2010	Panama	Sardinilla	9.32	-79.63	70	2350	26.2	*Cedrela odorata*	13	130	TD	14
Kunert et al., 2010	Panama	Sardinilla	9.32	-79.63	70	2350	26.2	*Gmelina arborea*	21	160	TD	42
Kunert et al., 2010	Panama	Sardinilla	9.32	-79.63	70	2350	26.2	*Hura crepitans*	6	200	TD	39
Kunert et al., 2010	Panama	Sardinilla	9.32	-79.63	70	2350	26.2	*Luehea seemannii*	10	140	TD	29
Kunert et al., 2010	Panama	Sardinilla	9.32	-79.63	70	2350	26.2	*Tabebuia rosea*	8	130	TD	19
Kunert et al., 2010	Panama	Sardinilla	9.32	-79.63	70	2350	26.2	*Tectona grandis*	13	190	TD	50
Kunert et al., 2010	Panama	Sardinilla	9.32	-79.63	70	2350	26.2	*Terminalia amazonia*	23	270	TD	59
Köcher et al., 2013	Germany	Hainich	51.07	10.5	352	600	7.5	*Acer pseudoplatanus*	27	380	TD	45
Köcher et al., 2013	Germany	Hainich	51.07	10.5	352	600	7.5	*Carpinus betulus*	27	460	TD	71
Köcher et al., 2013	Germany	Hainich	51.07	10.5	352	600	7.5	*Fagus excelsior*	28	500	TD	54
Köcher et al., 2013	Germany	Hainich	51.07	10.5	352	600	7.5	*Fraxinus sylvatica*	28	410	TD	13
Köcher et al., 2013	Germany	Hainich	51.07	10.5	352	600	7.5	*Tilia cordata*	28	410	TD	65
Loranty et al., 2008	USA	Wisconsin	45.94	-90.27	65	860	8.8	*Thuja occidentalis*			TD	22
Loranty et al., 2008	USA	Wisconsin	45.94	-90.27	312	860	8.8	*Populus tremuloides*			TD	8
Loranty et al., 2008	USA	Wisconsin	45.94	-90.27	473	860	8.8	*Alnus incana*			TD	6
Lott et al., 1996	Kenya	Machakos	-1.55	37.23	1660	650	19.4	*Grevillea robusta*			TD	12
Loustau et al., 1996	Portugal	Carrasqueira	38.83	-8.85	24	550	17.1	*Pinus pinaster*	26	350	TD	125
Luvall and Murphy, 1982	USA	Aiken	33.5604	-81.9176	157	1331	17.9	*Pinus taeda*	5	80	RSI	40
Martin et al., 1997	USA	Cedar	41.4823	-82.6835	1300	870	11.1	*Abies amabilis*	18	400	TD	98
Medhurst et al., 2002	Australia	Creekton	-43.35	146.9	120	1175	13	*Eucalyptus nitens*		200	HPV	95
Meinzer et al., 2004	Panama	Panama	9.02	-79.85	50	1800	20	*Anacardium excelsum*	38	980	TD	890
Meinzer et al., 2004	Panama	Panama	9.02	-79.85	50	1800	20	*Cordia alliodora*	26	340	TD	60
Meinzer et al., 2004	Panama	Panama	9.02	-79.85	50	1800	20	*Ficus insipida*	28	650	TD	400
Meinzer et al., 2004	Panama	Panama	9.16	-79.85	50	1800	20	*Schefflera morototoni*	22	470	TD	158
Miyazawa et al., 2014	Cambodia	Svay Bakav	11.592	104.4427	76	1500	25	*Dipterocarpus obtusifolius*		120	TD	19
Miyazawa et al., 2014	Cambodia	Svay Bakav	11.592	104.4427	76	1500	25	*Eucalyptus camaldulensis*		240	TD	38
Miyazawa et al., 2014	Cambodia	Svay Bakav	11.592	104.4427	76	1500	25	*Shorea roxburghii*		12	TD	15

Morris et al., 2004	China	Hetou	21.08	109.9	25	546	6.9	*Eucalyptus urophylla*	19	100	HPV	49
Morris et al., 2004	China	Hetou	20.9	109.87	70	546	6.9	*Eucalyptus urophylla*	18	100	HPV	27
Nicolas et al., 2005	Spain	Mula	37.87	-1.05	340	339	16.3	*Prunus spp*			TD	100
Otieno et al., 2005	Kenya	Kibwezi	2.35	37.88	914	450	24	*Acacia tortilis*	7	220	TD	13
Otieno et al., 2014	Kenya	Kibwezi	2.35	37.88	914	450	24	*Acacia xanthophloea*	13	370	TD	47
Owens and Moore, 2007	USA	Percos Texas	31.4021	-102.4803	783	870	21	*Tamarix spp*			TD	121
Owston et al., 1972	USA	Califonia	38.3052	-119.6213	1901	1270	13.8	*Pinus contorta*	20	250	RSI	25
Pataki et al., 2011	USA	Los Angeles	33.6839	-117.7947	17	380	18.3	*Pinus canariensis*		680	TD	98
Pataki et al., 2011	USA	Los Angeles	33.6839	-117.7947	17	380	18.3	*Platatus racemosa*		600	TD	94
Pataki et al., 2011	USA	Los Angeles	34.1391	-118.2805	71	380	18.3	*Malosma laurina*		150	TD	3
Pataki et al., 2011	USA	Los Angeles	34.0522	-118.2427	87	380	18.3	*Platatus hybrida*		690	TD	327
Pataki et al., 2011	USA	Los Angeles	34.0522	-118.2427	87	380	18.3	*Platatus racemosa*		390	TD	157
Pataki et al., 2011	USA	Los Angeles	34.1391	-118.2805	150	380	18.3	*Jacaranda mimosifolia*		180	TD	18
Pataki et al., 2011	USA	Los Angeles	34.1391	-118.2805	150	380	18.3	*Pinus canariensis*		510	TD	9
Pataki et al., 2011	USA	Los Angeles	34.136	-118.0518	165	380	18.3	*Brachychiton discolor*		720	TD	54
Pataki et al., 2011	USA	Los Angeles	34.136	-118.0518	165	380	18.3	*Brachychiton populneus*		480	TD	44
Pataki et al., 2011	USA	Los Angeles	34.136	-118.0518	165	380	18.3	*Eucalyptus grandis*		780	TD	104
Pataki et al., 2011	USA	Los Angeles	34.136	-118.0518	165	380	18.3	*Ficus microcarpa*		360	TD	121
Pataki et al., 2011	USA	Los Angeles	34.136	118.0518	165	380	18.3	*Gleditsia tricanthos*		550	TD	131
Pataki et al., 2011	USA	Los Angeles	34.136	-118.0518	165	380	18.3	*Jacaranda chelonia*		370	TD	129
Pataki et al., 2011	USA	Los Angeles	34.136	-118.0518	165	380	18.3	*Koelreuteria paniculata*		370	TD	83
Pataki et al., 2011	USA	Los Angeles	34.136	-118.0518	165	380	18.3	*Lagerstroemia indica*		210	TD	83
Pataki et al., 2011	USA	Los Angeles	34.0692	-118.2348	185	380	18.3	*Pinus canariensis*		720	TD	109
Pataki et al., 2011	USA	Los Angeles	34.0692	118.2348	185	380	18.3	*Sequoia sempervirens*		550	TD	24
Pataki et al., 2011	USA	Los Angeles	34.0692	118.2348	185	380	18.3	*Ulmus parvifolia*		350	TD	182
Pfautsch and Adams, 2013	Australia	Britannia Range	-33.49	140.79	595	1700	12	*Eucalyptus regnans*	30	430	HRM	70
Pfautsch et al., 2010	Australia	Britannia Creek	-37.49	145.41	470	1740	10	*Eucalyptus regnans*	57	940	HRM	190
Pinto et al., 2013	Portugal	Lisbon	38.83	-9.82	46	753	16.8	*Quercus suber L*	12.82	730	HFD	42
Roberts, 1977	UK	Thetford Chase	52.42	0.74	27	584	9.5	*Pinus sylvestris*			LP	13
Roccuzzo et al., 2014	Spain	Cordoba	37.8	-4.8	140	606	17.5	*Citrus sinensis*			HPV	10
Sansigolo and Ferraz, 1982	Brazil	University of São	-22.72	-47.63	580	1454	22.5	*Pinus caribaea*	7	130	RSI	100
Santos et al., 2007	Portugal	Safara	38.08	7.27	75	1081	27.4	*Olea europaea*			HPV	145
Schiller and Cohen, 1995	Israel	Ramat ha'Nadiv	32.38	34.93	125	600	19	*Pinus halepensis*	9		TD	49
Schiller et al., 2003	Israel	Ramat ha'Nadiv	32.38	34.93	125	600	19	*Quercus calliprinos*		190	HPV	35
Schiller et al., 2003	Israel	Ramat ha'Nadiv	32.38	34.93	125	600	19	*Phillyrea latifolia*	4		HPV	11
Schulze et al., 1985	Czech Republic	Brno	49.1951	16.6068	620	683	6.6	*Picea abies*	25		TD	63
Schulze et al., 1985	Germany	Bayreuth	49.9456	11.5713	450	702	7.8	*Larix sp.*	20		TD	74
Steinberg et al., 1990	USA	Stephenville	32.12	98.13	4595	802	17.6	*Carya illinoensis*	4	80	LP	150
Sun et al., 2014	Japan	Mt. Karasawa	36.37	139.6	198	1265	14.1	*Chamaecyparis obtusa*		190	TD	21
Teskey and Sheriff, 1996	Australia	Wandilo	-37.7379	140.728	66	714	16.1	*Pinus radiata*	25	420	TD	349
Tognetti et al., 1998	Italy	Rapolano Terme	43.28	11.58	350	777	13.4	*Quercus ilex*		120	HPV	30
Tricker et al., 2009	Italy	Tuscania	42.3704	11.8087	150	683	15	*Populus x euramericana*		200	HB	7
Vandegehuchte and Steppe,	Tunisia	Enfidha	36.38	10.22	128	429	18.2	*Olea europaea*	3.5	180	TD	34
Verbeeck et al., 2007	Belgium	Brasschaat	51.1833	4.3114	16	750	9.8	*Pinus sylvestris*	21	290	HFD	28
Vertessy et al., 1995	Australia	North Maroondah	-37.8053	145.8203	890	1713	15	*Eucalyptus regnans*		370	TD	151
Vertessy et al., 1995	Australia	North Maroondah	-37.8053	145.8203	890	1713	15	*Acacia dealbata*		250	TD	59
Vertessy et al., 1997	Australia	Yarra Ranges	-37.57	145.63	750	1660	15	*Eucalyptus regnans*	58	890	TD	285
Waring and Roberts, 1979	Scotland	Moray Firth	58	-4	123	660	9.5	*Pinus sylvestris*	15		RSI	29
Wildy et al., 2004	Australia	Kalannie	-30.09	117.12	290	319	20	*Eucalyptus kochii*			HPV	28

Reference list for database table

Alcorn, P.J., Forrester, D.I., Thomas, D.S., James, R., Smith, R.G.B., Nicotra, A.B., Bauhus, J., 2013. Changes in whole-tree water use following live-crown pruning in young plantation-grown *Eucalyptus pilularis* and *Eucalyptus cloeziana*. Forests 4(1), 106-121.

Andrade, J.L., Meinzer, F.C., Goldstein, G., Holbrook, N.M., Cavelier, J., Jackson, P., Silvera, K., 1998. Regulation of water flux through trunks, branches, and leaves in trees of a lowland tropical forest. Oecologia 115(4), 463-471.

Ansley, R.J., Dugas, W.A., Heuer, M.L., Trevini, B.A., 1994. Stem flow and porometer measurements of transpiration from honey mosque (*Prosopis glandulosa*). J. Exp. Bot. 45(275), 847-856.

Ansley, R.J., Jacoby, P.W., Hicks, R.A., 1991. Leaf and whole plant transpiration in honey mesquite following severing of lateral roots. J. Range Manage. 44 (6)577-583.

Aranda, I., Forner, A., Cuesta, B., Valladares, F., 2012. Species-specific water use by forest tree species: From the tree to the stand. Agr. Water Manage. 114, 72-82.

Arneth, A., Kelliher, F.M., Bauer, G., Hollinger, D.Y., Byers, J.N., Hunt, J.E., McSeveny, T.M., Ziegler, W., Vygodskaya, N.N., Milukova, I., Sogachov, A., 1996. Environmental regulation of xylem sap flow and total conductance of *Larix gmelinii* trees in eastern Siberia. Tree Physiol. 16(1), 247-255.

Barkataky, S., Morgan, K.T., Ebel, R.C., 2012. Plant water requirement of Hamlin' sweet orange in cold temperature conditions. Irrigation Sci. 31, 431-443.

Becker, P., 1996. Sap flow in Bornean heath and dipterocarp forest trees during wet and dry periods. Tree Physiol. 16, 295-299.

Bleby, T.M., Colquhoun, I.J., Adams, M.A., 2012. Hydraulic traits and water use of Eucalyptus on restored versus natural sites in a seasonally dry forest in south western Australia. Forest Ecol. Manag. 274, 58-66.

Bosch, D.D., Marshall, L.K., Teskey, R., 2014. Forest transpiration from sap flux density measurements in a southeastern Coastal Plain riparian buffer system. Agr. Forest Meteorol. 187, 72-82.

Bréda, N., Cochard, H., Dreyer, E., Granier, A., 1993. Field comparison of transpiration, stomatal conductance and vulnerability to cavitation of *Quercus petraea* and *Quercus robur* under water stress. Ann. Sci. Forest. 50(6), 571-582).

Bréda, N., Cochard, H., Dreyer, E., Granier, A., 1993. Water transfer in a mature oak stand (*Quercus petraea*): seasonal evolution and effects of a severe drought. Can. J. Forest Res. 23(6), 1136-1143.

Bréda, N., Granier, A., Aussenac, G., 1995. Effects of thinning on soil and tree water relations, transpiration and growth in an oak forest (*Quercus petraea* (Matt.) Liebl.). Tree physiol. 15(5), 295-306.

Čermák, J., Cienciala, E., Kučera, J., Lindroth, A., Bednářová, E., 1995. Individual variation of sap-flow rate in large pine and spruce trees and stand transpiration: a pilot study at the central NOPEX site. J. Hydrol. 168(1-4), 17-27.

Čermák, J., Kučera, J., 1987. Transpiration of mature stands of spruce (*Picea abies* (L.) Karst.) as estimated by the tree-trunk heat balance method. IAHS Publ. 167, 311-317.

Čermák, J., Matyssek, R., Kučera, J., 1993. Rapid response of large, drought-stressed beech trees to irrigation. Tree Physiol. 12(3), 281-290.

Čermák, J., Ulehla, J., Kučera, J., Penka, M., 1982. Sap flow rate and transpiration dynamics in the full-grown oak (*Quercus robus* L.) in floodplain forest exposed to seasonal floods as related to potential evapotranspiration and tree dimensions. Biol. Plantarum 24(6), 446-460.

Cienciala, E., Lindroth, A., Čermák, J., Hällgren, J.E., Kučera, J., 1992. Assessment of transpiration estimates for *Picea abies* trees during a growing season. Trees 6(3), 121-127.

Cienciala, E., Mellander, P.E., Kučera, J., Oplu-tilová, M., Ottosson-Löfvenius, M., Bishop, K., 2002. The effect of a north-facing forest edge on tree water use in a boreal Scots pine stand. Can. J. Forest Res. 32(4), 693-702.

Dang, H., Zha, T., Zhang, J., Li, W., Liu, S., 2014. Radial profile of sap flow velocity in mature Xinjiang poplar (*Populus alba* L. var. pyramidalis) in Northwest China. J. Arid Land 6(5), 612-627.

Dierick, D., Hölscher, D., 2009. Species-specific tree water use characteristics in reforestation stands in the Philippines. Agr. Forest Meteorol. 149(8), 1317-1326.

Do, F.C., Rocheteau, A., Diagne, A.L., Goudiaby, V., Granier, A., Lhomme, J., 2008. Stable annual pattern of water use by *Acacia tortilis* in Sahelian Africa. Tree Physiol. 28(1), 95-104.

Dragoni, D., Lakso, A.N., Piccioni, R.M., 2005. Transpiration of apple trees in a humid climate using heat pulse sap flow gauges calibrated with whole-canopy gas exchange chambers. Agr. Forest Meteorol. 130(1), 85-94.

Dye, P.J., 1996. Response of *Eucalyptus grandis* trees to soil water deficits. Tree Physiol. 16, 233-238.

Dye, P.J., Olbrich, B.W., Calder, I.R., 1992. A comparison of the heat pulse method and deuterium tracing method for measuring transpiration from *Eucalyptus grandis* trees. J. Exp. Bot. 43, 337-343.

Dzikiti, S., Schachtschneider, K., Naiken, V., Gush, M., Le Maitre, D., 2013. Comparison of water-use by alien invasive pine trees growing in riparian and non-riparian zones in the Western Cape Province, South Africa. Forest Ecol. Manag. 293, 92-102.

Fernández, J.E., Díaz-Espejo, A., Infante, J.M., Durán, P., Palomo, M.J., Chamorro, V., Girón, I.F., Villagarcía, L., 2006. Water relations and gas exchange in olive trees under regulated deficit irrigation and partial rootzone drying. Plant Soil 284, 273-291.

Fritschen, L.J., Cox, L., Kinerson, R., 1973. A 28-meter Douglas-fir in a weighing lysimeter. Forest Sci. 19(4), 256-261.

Glenn, D.M., 2016. Effect of highly processed calcined kaolin residues on apple water use efficiency. Sci. Hortic. - Amsterdam 205, 127-132.

Goldstein, G., Andrade, J.L., Meinzer, F.C., Holbrook, N.M., Cavelier, J., Jackson, P., Celis, A., 1998. Stem water storage and diurnal patterns of water use in tropical forest canopy trees. Plant Cell Environ. 21(4), 397-406.

Gonzalez-Benecke, C.A., Martin, T.A., Cropper, W.P., 2011. Whole-tree water relations of co-occurring mature *Pinus palustris* and *Pinus elliottii* var. elliottii. Can. J. Forest Res. 41(3), 509-523.

Goodwin, I., Whitfield, D.M., Connor, D.J., 2006. Effects of tree size on water use of peach (*Prunus persica* L. Batsch). Irrigation Sci. 24(2), 59-68.

Granier, A., 1987. Evaluation of transpiration in a Douglas-fir stand by means of sap flow measurements. Tree Physiol. 3, 309-320.

Granier, A., Bobay, V., Gash, J.H.C., Gelpe, J., Saugier, B., Shuttleworth, W.J., 1990. Vapour flux density and transpiration rate comparisons in a stand of Maritime pine (*Pinus pinaster* Ait.) in Les Landes forest. Agr. Forest Meteorol. 51, 309-319.

Granier, A., Huc, R., Barigah, S.T., 1996. Transpiration of natural rain forest and its dependence on climatic factors. Agr. Forest Meteorol. 78, 19-29.

Green, S., Clothier, B., Jardine, B., 2003. Theory and practical application of heat pulse to measure sap flow. Agron. J. 95, 1371-1379.

Green, S.R., Clothier, B., Caspari, H., Neal, S., 2002. Root-zone processes, tree water use and equitable allocation of irrigation water to olives. Geophys. Monogr. 129, 337-345.

Greenwood, E.A.N., Beresford, J.D., 1979. Evaporation from vegetation in landscapes developing secondary salinity using the ventilated- chamber technique. I. Comparative transpiration from juvenile Eucalyptus above saline ground-water seeps. J. Hydrol. 42, 369-382.

Greenwood, E.A.N., Beresford, J.D., Bartle, J.R., 1981. Evaporation from vegetation in landscapes developing secondary salinity using the ventilated-chamber technique: III. Evaporation from a *Pinus radiata* tree and the surrounding pasture in an agroforestry plantation. J. Hydrol. 50**,** 155-166.

Greenwood, E.A.N., Beresford, J.D., Bartle, J.R., Barron, R.J.W., 1982. Evaporation from vegetation in landscapes developing secondary salinity using the ventilated-chamber technique: IV. Evaporation from a regenerating forest of *Eucalyptus wandoo* on land formerly cleared for agriculture. J. Hydrol. 58, 357-366.

Greenwood, E.A.N., Klein, L., Beresford, J.D., Watson, G.D., 1985. Differences in annual evaporation between grazed pasture and Eucalyptus species in plantations on a saline farm catchment. J. Hydrol. 78, 261-278.

Guevara-Escobar, A., Edwards, W.R.N., Morton, R.H., Kemp, P.D., Mackay, A.D., 2000. Tree water use and rainfall partitioning in a mature poplar-pasture system. Tree Physiol. 20(2), 97-106.

Gush, M.B., 2008. Measurement of water-use by *Jatropha curcas* L. using the heat-pulse velocity technique. Water SA 34(5), 1-5.

Herzog, K.M., Häsler, R., Thum, R., 1995. Diurnal changes in the radius of a subalpine Norway spruce stem: their relation to the sap flow and their use to estimate transpiration. Trees 10(2), 94-101.

Hinckley, T.M., Brooks, J.R., Cermak, J., Ceulemans, R., Kucera, J., Meinzer, F.C., Roberts, D.A., 1994. Water flux in a hybrid poplar stand. Tree physiol. 14(7), 1005-1018.

Hunt, M.A., Beadle, C.L., 1998. Whole-tree transpiration and water-use partitioning between *Eucalyptus nitens* and *Acacia dealbata* weeds in a short-rotation plantation in northeastern Tasmania. Tree Physiol. 18(8), 557-563.

Jordan, C.F., Kline, J.R., 1977. Transpiration of trees in a tropical rainforest. J. Appl. Ecolol. 14, 853-860.

Jung, E.Y., Otieno, D., Lee, B., Lim, J.H., Kang, S.K., Schmidt, M.W.T., Tenhunen, J., 2011. Up-scaling to stand transpiration of an Asian temperate mixed-deciduous forest from single tree sap flow measurements. Plant Ecol. 212(3), 383-395.

Kelliher, F.M., Köstner, B.M.M., Hollinger, D.Y., Byers, J.N., Hunt, J.E., McSeveny, T.M., Meserth, R., Weir, P.L. and Schulze, E.D., 1992. Evaporation, xylem sap

flow, and tree transpiration in a New Zealand broad-leaved forest. Agr. Forest Meteorol. 62, 53-73.

Kline, J.R., Martin, J.R., Jordan, C.F., Koranda, J.J., 1970. Measurement of transpiration in tropical trees with tritiated water. Ecology 51(6), 1068-1073.

Kline, J.R., Reed, K.L., Waring, R.H., Stewart, M.L., 1976. Field measurement of transpiration in Douglas-fir. J. Appl. Ecol. 13, 272-283.

Knight, D.H., Fahey, T.J., Running, S.W., Harrison, A.T., Wallace, L.L. 1981. Transpiration from 100-year-old lodgepole pine forests estimated with whole-tree potometers. Ecology 62, 717-726.

Köstner, B., Schupp, R., Schulze, E.D., Rennenberg, H., 1998. Organic and inorganic sulfur transport in the xylem sap and the sulfur budget of *Picea abies* trees. Tree physiol. 18(1), 1-9.

Köstner, B.M.M., Schulze, E.D., Kelliher, F.M., Hollinger, D.Y., Byers, J.N., Hunt, J.E., McSeveny, T.M., Meserth, R., Weir, P.L., 1992. Transpiration and canopy conductance in a pristine broad-leaved forest of Nothofagus: an analysis of xylem sap flow and eddy correlation measurements. Oecologia 91(3), 350-359.

Krauss, K.W., Young, P.J., Chambers, J.L., Doyle, T.W., Twilley, R.R., 2007. Sap flow characteristics of neotropical mangroves in flooded and drained soils. Tree physiol. 27(5), 775-783.

Kunert, N., Schwendenmann, L., Hölscher, D., 2010. Seasonal dynamics of tree sap flux and water use in nine species in Panamanian forest plantations. Agr. Forest Meteorol. 150(3), 411-419.

Köcher, P., Horna, V., Leuschner, C., 2013. Stem water storage in five coexisting temperate broad-leaved tree species: significance temporal dynamics and dependence on tree functional traits. Tree Physiol. 33, 817-832.

Loranty, M.M., Mackay, D.S., Ewers, B.E., Adelman, J.D., Kruger, E.L., 2008. Environmental drivers of spatial variation in whole-tree transpiration in an aspen-dominated upland-to-wetland forest gradient. Water Resour. Res. 44, 1-15.

Lott, J.E., Khan, A.A.H., Ong, C.K., Black, C.R., 1996. Sap flow measurements of lateral tree roots in agroforestry systems. Tree Physiol. 16, 995-1002.

Loustau, D., Berbigier, P., Roumagnac, P., Arruda-Pacheco, C., David, J.S., Ferreira, M.I., Pereira, J.S., Tavares, R., 1996. Transpiration of a 64-year-old maritime pine stand in Portugal. Oecologia 107(1), 33-42.

Luvall, J.C., Murphy, C.E., 1982. Evaluation of the tritiated water method for measurement of transpiration in young *Pinus taeda* L. Forest Sci. 28(1), 5-16.

Martin, T.A., Brown, K.J., Cermak, J., Ceulemans, R., Kucera, J., Meinzer, F.C., Rombold, J.S., Sprugel, D.G., Hinckley, T.M., 1997. Crown conductance and tree and stand transpiration in a second-growth *Abies amabilis* forest. Can. J. Forest Res. 27(6), 797-808.

Medhurst, J., Parsby, J.A.N., Linder, S., Wallin, G., Ceschia, E., Slaney, M., 2006. A whole-tree chamber system for examining tree-level physiological responses of field-grown trees to environmental variation and climate change. Plant, Cell Environ. 29(9), 1853-1869.

Meinzer, F.C., Bond, B.J., Warren, J.M., Woodruff, D.R., 2005. Does water transport scale universally with tree size? Funct. Ecol. 19, 558-565.

Meinzer, F.C., James, S.A., Goldstein, G., 2004. Dynamics of transpiration, sap flow and use of stored water in tropical forest canopy trees. Tree Physiol. 24(8), 901-909.

Miyazawa, Y., Tateishi, M., Komatsu, H., Ma, V., Kajisa, T., Sokh, H., Mizoue, N., Kumagai, T.O., 2014. Tropical tree water use under seasonal waterlogging and drought in central Cambodia. J. Hydrol. 515, 81-89.

Morris, J., Ningnan, Z., Zengjiang, Y., Collopy, J., Daping, X., 2004. Water use by fast-growing *Eucalyptus urophylla* plantations in southern China. Tree physiol. 24(9), 1035-1044.

Nicolas, E., Torrecillas, A., Ortuno, M.F., Domingo, R., Alarcón, J.J., 2005. Evaluation of transpiration in adult apricot trees from sap flow measurements. Agr. Water Manage. 72(2), 131-145.

Otieno, D.O., Schmidt, M.W.T., Kinyamario, J.I., Tenhunen, J., 2005. Responses of *Acacia tortilis* and *Acacia xanthophloea* to seasonal changes in soil water availability in the savanna region of Kenya. J. Arid Environ. 62(3), 377-400.

Owens, M.K., Moore, G.W., 2007. Saltcedar water use: realistic and unrealistic expectations. Range. Ecol. Manage. 60(5), 553-557.

Owston, P.W., Smith, J.L., Halverson, H.G., 1972. Seasonal water movement in tree stems. Forest Sci. 18(4), 266-272.

Pataki, D.E., McCarthy, H.R., Litvak, E., Pincetl, S., 2011. Transpiration of urban forests in the Los Angeles metropolitan area. Ecol. Appl. 21(3), 661-677.

Pfautsch, S., Adams, M.A., 2013. Water flux of Eucalyptus regnans: defying summer drought and a record heatwave in 2009. Oecologia 172(2), 317-326.

Pfautsch, S., Bleby, T.M., Rennenberg, H., Adams, M.A., 2010. Sap flow measurements reveal influence of temperature and stand structure on water use of *Eucalyptus regnans* forests. Forest Ecol. Manag. 259, 1190-1199.

Pinto, C.A., Nadezhdina, N., David, J.S., Kurz-Besson, C., Caldeira, M.C., Henriques, M.O., Monteiro, F.G., Pereira, J.S., David, T.S., 2014. Transpiration in Quercus suber trees under shallow water table conditions: the role of soil and groundwater. Hydrol. Process. 28(25), 6067-6079.

Roberts, J., 1977. The use of tree-cutting techniques in the study of the water relations of mature *Pinus sylvestris* LI The technique and survey of the results. J. Exp. Bot. 28(3), 751-767.

Roccuzzo, G., Villalobos, F.J., Testi, L., Fereres, E., 2014. Effects of water deficits on whole tree water use efficiency of orange. Agr. Water Manage. 140, 61-68.

Sansigolo, C.A., Ferraz, E.S.B., 1982. Measurement of transpiration and biomass in a tropical *Pinus caribaea* plantation with tritiated water. Agr. Meteorol. 26(1), 25-33.

Santos, F.L., Valverde, P.C., Ramos, A.F., Reis, J.L., Castanheira, N.L., 2007. Water use and response of a dry-farmed olive orchard recently converted to irrigation. Biosyst. Eng. 98(1), 102-114.

Schiller, G., Cohen, Y., 1995. Water regime of a pine forest under a Mediterranean climate. Agr. Forest Meteorol. 74(3), 181-193.

Schiller, G., Unger, E.D., Moshe, Y., Cohen, S., Cohen, Y., 2003. Estimating water use by sclerophyllous species under east Mediterranean climate: II. The transpiration of *Quercus calliprinos* Webb. in response to silvicultural treatments. Agr. Forest Meteorol. 179(1), 483-495.

Schulze, E.D., Čermák, J., Matyssek, M., Penka, M., Zimmermann, R., Vasicek, F., Gries, W. and Kučera, J., 1985. Canopy transpiration and water fluxes in the xylem of the trunk of Larix and Picea trees - a comparison of xylem flow, porometer and cuvette measurements. Oecologia 66(4), 475-483.

Steinberg, S.L., McFarland, M.J., Worthington, J.W., 1990. Comparison of trunk and branch sap flow with canopy transpiration in pecan. J. Exp. Bot. 41(6), 653-659.

Sun, X., Onda, Y., Otsuki, K., Kato, H., Hirata, A., Gomi, T., 2014. The effect of strip thinning on tree transpiration in a Japanese cypress (*Chamaecyparis obtusa* Endl.) plantation. Agr. Forest Meteorol. 197, 123-135.

Teskey, R.O., Sheriff, D.W., 1996. Water use by *Pinus radiata* trees in a plantation. Tree Physiol. 16, 273-279.

Tognetti, R., Longobucco, A., Miglietta, F., Raschi, A., 1998. Transpiration and stomatal behaviour of *Quercus ilex* plants during the summer in a Mediterranean carbon dioxide spring. Plant Cell Environ. 21(6), 613-622.

Tricker, P.J., Pecchiari, M., Bunn, S.M., Vaccari, F.P., Peressotti, A., Miglietta, F., Taylor, G., 2009. Water use of a bioenergy plantation increases in a future high CO 2 world. Biomass Bioenerg. 33(2), 200-208.

Vandegehuchte, M.W., Steppe, K., 2012. Use of the correct heat conduction–convection equation as basis for heat-pulse sap flow methods in anisotropic wood. J. Exp. Bot. 63(8), 2833-2839.

Verbeeck, H., Steppe, K., Nadezhdina, N., de Beeck, M.O., Deckmyn, G., Meiresonne, L., Lemeur, R., Čermák, J., Ceulemans, R. and Janssens, I.A., 2007. Stored water use and transpiration in Scots pine: a modeling analysis with ANAFORE. Tree Physiol. 27(12), 1671-1685.

Vertessy, R.A., Benyon, R.G., O'Sullivan, S.K., Gribben, P.R., 1995. Relationships between stem diameter, sapwood area, leaf area and transpiration in a young mountain ash forest. Tree Physiol. 15, 559-567.

Vertessy, R.A., Hatton, T.J., Reece, P., O'Sullivan, S.K., Benyon, R.G., 1997. Estimating stand water use of large mountain ash trees and validation of the sap flow measurement technique. Tree Physiol. 17, 747-756.

Waring, R.H., Roberts, J.M., 1979. Estimating water flux through stems of Scots pine with tritiated water and phosphorus-32. J. Exp. Bot. 30(3), 459-471.

Wildy, D.T., Pate, J.S., Bartle, J.R., 2004. Budgets of water use by *Eucalyptus kochii* tree belts in the semi-arid wheatbelt of Western Australia. Plant Soil 262(1), 129-149.

Appendix 4.1: SAS code for analysis

```
proc mcmc stats=all nbi=10000 nmc=1000000 thin=10 monitor=(theta1 theta2 theta3 q50 q80
q90 q96 q98 q99);

* Specify parameter vector: theta[1]=mu theta[2]=sigma theta[3]=xi;

array theta[3] theta1 theta2 theta3;

* Specify initial values for parameters;

parms theta1 33 theta2 14 theta3 0.1;

* Specify log-likelihood of data y for GEV distribution;

llike=-log(theta[2])-((1/theta[3])+1)*log(1+theta[3]*(y-theta[1])/theta[2])

-(1+theta[3]*(y-theta[1])/theta[2])**(-1/theta[3]);

model y ~ general(llike);

beginnodata;

* Specify Maximal Data Information prior;

pll=log((1/theta[2])*exp(-1.57722*(1+theta[3])));

prior theta: ~ general(pll, lower=-1);

* Calculate quantiles for p=0.5, p=0.8, p=0.9, p=0.96 and p=0.99

corresponding to return periods of T=2, T=5, T=10, T=25, T=50 and T=100 years;

q50=theta[1]+(theta[2]/theta[3])*((-1/log(0.5))**theta[3]-1);

q80=theta[1]+(theta[2]/theta[3])*((-1/log(0.8))**theta[3]-1);

q90=theta[1]+(theta[2]/theta[3])*((-1/log(0.9))**theta[3]-1);

q96=theta[1]+(theta[2]/theta[3])*((-1/log(0.96))**theta[3]-1);

q98=theta[1]+(theta[2]/theta[3])*((-1/log(0.98))**theta[3]-1);

q99=theta[1]+(theta[2]/theta[3])*((-1/log(0.99))**theta[3]-1);

endnodata;

* Output point and interval estimates for parameters and quantiles;

ods output PostSummaries=estimate;

ods output PostIntervals=quantile;

run;
```

Appendix 5: Supplementary material (monolith experiment)

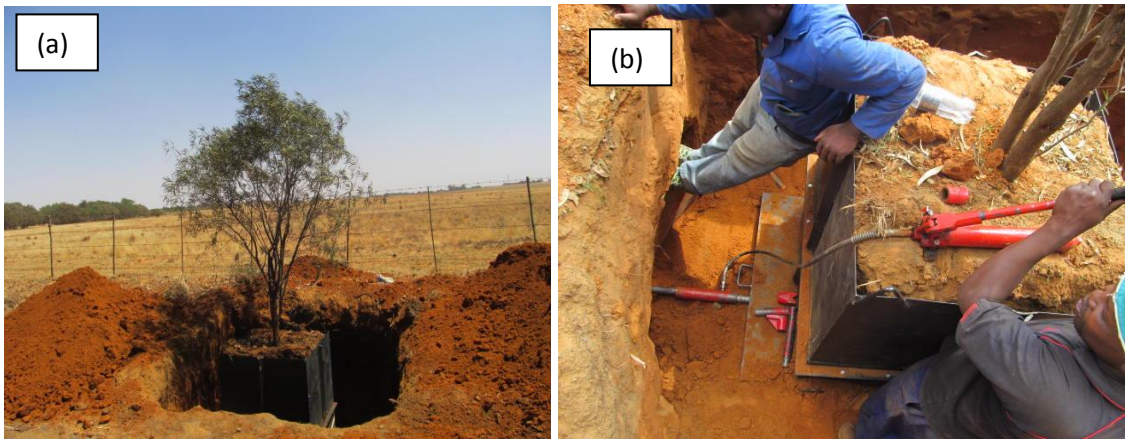

Appendix 5.1: (a) Fully excavated *Sersia lancea* tree and (b) metal base plate at driven by hydraulic jack.

Appendix 5.2: a) Lifting soil monolith with *Olea africana* tree using a chain block supported by a due-pod stand to a lowbed trailer before b) transporting it to Kenilworth farm

Appendix 5.3: *Ziziphus mucronata* tree being transplanted into a lysimeter container.